~~CONFIDENTIAL~~

~~SECRET~~

~~SECURITY INFORMATION~~

UNCLASSIFIED

~~RESTRICTED DATA~~

~~This document contains restricted data as defined in the Atomic Energy Act of 1946. Its transmittal or the disclosure of its contents in any manner to an unauthorized person is prohibited.~~

NEPA PROJECT

Quarterly Progress Report
for the Period
April 1 – June 30
1950

~~CONFIDENTIAL~~

~~Classification cancelled or changed to~~ [illegible]
~~by authority of~~ [illegible] 12-5-61
~~by~~ [illegible], date 12-14-61

Submitted by:
NEPA DIVISION
Fairchild Engine & Airplane Corporation

Ia Sims
General Manager

UNCLASSIFIED

Accepted:
James P. Steele Major USAF
Contracting Officer

REPORT NO. NEPA 1484

~~SECRET~~

R-2861

~~SECURITY INFORMATION~~ ~~CONFIDENTIAL~~

UNCLASSIFIED

~~SECRET~~ ~~CONFIDENTIAL~~

[redacted] FOURTH QUARTER, FISCAL YEAR 1950

~~RESTRICTED DATA~~

~~ATOMIC ENERGY ACT OF 1946~~

~~SPECIFIC RESTRICTED DATA CLEARANCE REQUIRED~~

FOREWORD

This report summarizes the activities of NEPA Division, Fairchild Engine and Airplane Corporation, for the period April 1 – June 30, 1950. It is a technical review showing the current status of the NEPA Project.

DISCLAIMER

UNCLASSIFIED

~~SECRET~~

~~CONFIDENTIAL~~

DISCLAIMER

Portions of this document may be illegible in electronic image products. Images are produced from the best available original document.

CONTENTS

0. SUMMARY

0.1 TECHNICAL STATUS OF NEPA PROJECT

Exploration of various types of power plant cycles for nuclear propelled aircraft has been continued during this quarter. The principal current objective of the project is the development of information which will make an intelligent choice of the basic power plant cycle possible. It is still hoped that this choice can be made late in 1950. The survey studies which have been under way for several months continued during the quarter. These consist of analyses and rough preliminary layouts for various types of aircraft, using each of the several basic cycles which have been seriously considered for each of the three phases of development. The phases of development, the cycles under consideration, and their present status are shown in Table 1.

Although it is still extremely premature to discuss the relative merits of the various cycles, the information so far developed discloses some cycle differences which may, if confirmed by additional work, be significant. In this respect, there have been no recent major changes in the comparative standings of the cycles.

The air cycle continues to enjoy the outstanding advantage of general simplicity. The principal questions about it are those of radiation damage to materials for the reactor, the leakage of neutrons through ducts, and performance (which, on paper, is somewhat poorer than that of the other cycles). There have been no major developments in any of these respects during the quarter.

The liquid-metal cycle has received the most

Table I

STATUS OF SURVEY STUDIES AT CLOSE OF QUARTER

Phase	Air Cycle	Liquid-Metal Cycle	Helium Cycle
I XB-52 airplane, modified, M = 0.8, 45,000 ft. altitude	Analysis nearly complete; maximum feasible altitude 35,000 ft., 350,000 lb. gross weight; extensive modification of XB-52 airframe would be necessary	Analysis complete for 45,000 ft., 305,000 lb., 6 XJ-53 engines; will be revised for more conservative reactor design and 40,000 ft.; nuclear-plus-chemical test aircraft service ceiling 37,500 ft., max. speed 480 knots at 27,000 ft.; analysis complete for present	Analysis complete; maximum feasible altitude 40,000 ft.; major modification of XB-52 would be necessary; 340,000 lb.
II M = 0.9 - 1.5; altitude = 60,000 - 45,000 ft.; or M = 0.9 at sea level	M = 0.9 sea-level airplane being worked on; gross weight less than 350,000 lb.; study reported two quarters ago now obsolete, being repeated; may be unable to attain 45,000 ft. at M = 1.5 using Phase II assumptions	Analysis under way on M = 0.9, 60,000 ft. airplane; have dropped two-reactor idea; analysis under way on M = 1.5, 45,000 ft. airplane; gross weight 400,000 lb., 475,000-kw. reactor power	Study reported two quarters ago obsolete, to be revised; showed 600,000 lb. gross weight for M = 1.5, 45,000 ft. altitude
III As fast as possible at 45,000 ft. and at 60,000 ft.; as high as possible at M = 0.9	No results available	No results available	No results available

attention during the quarter. The possibility that two reactors might be installed on an aircraft using the liquid-metal cycle now seems very remote, since the uranium content of the application would be prohibitively high. New information on the neutron absorption cross-section of molybdenum makes molybdenum seem less attractive than formerly as structural material for the reactor. This factor may result in an increase in uranium content of the reactor of the liquid-metal type. Molybdenum is still, however, better than any other metal, disregarding the fabrication problem. Liquid-metal corrosion experiments seem at present to indicate the necessity of canning the moderator as well as the fuel. This also is likely to increase the uranium content of the liquid-metal reactor.

The circulating fuel cycle may turn out to be easier to control than has been thought previously, but its uranium inventory is certainly greater than that of the liquid-metal cycle as now envisioned. Its other characteristics are similar to those of the liquid-metal cycle, with the exception that it is essentially unaffected by the recent changes in ideas of the cross-section of molybdenum.

Work on the helium cycle continues to show up the problems of vulnerability of the aircraft to enemy action or accidental damage. These problems are magnified by the high operating pressures of this cycle.

In general, it still seems that the air cycle and the liquid-metal cycle have distinctly more favorable positions than the helium and circulating fuel cycles. During the quarter, members of the Reactor Development Division of the Atomic Energy Commission in Washington proposed a high-pressure water reactor, operating at pressures of 5,000 to 10,000 pounds per square inch in the supercritical range. Further work on this cycle will be necessary, however, before an evaluation of it is possible.

0.2 IMPORTANT DEVELOPMENTS OF THIS QUARTER

Work continued throughout the quarter on all three of the major cycles.

The General Electric group reported that the neutron capture cross-section of molybdenum at 2000 electron volts is approximately thirty times as great as that predicted on the grounds of the simple theory used in previous reactor calculations at Oak Ridge. This factor, while not ruling out molybdenum as a reactor material, makes it less attractive, and makes more desirable than ever a serious investigation of the possibility of producing molybdenum^{92} (which is known to have a low capture cross-section). Tactical considerations emphasize the importance of low uranium inventories in the reactor. In the circulating fuel reactor, these can be achieved only by the use of a hydrogenous solution such as sodium hydroxide. The problems of radiation damage to sodium hydroxide and of corrosion by sodium hydroxide are essentially unsolved, however. Further investigation of fast-spectrum reactors shows that these require too much uranium investment for serious consideration. An investigation of the optimum reflector thickness problem (the balance between the high peak power density and a large shielded volume) seems to show that a 2- to 3-inch-thick reflector (beryllium carbide) for a 3 1/2-foot reactor is near the optimum. It was found in other work that, contrary to general impression, age theory can be applied to hydrogenous reactors with little error. This was confirmed by comparison with experiment.

Preparations for critical experiments continued. The joint Carbide-NEPA criticality building will be ready during the month of July. Responsibility for these experiments has been assumed by ORNL, with NEPA supplying most of the workers. The first experiments will be done on a simulated liquid-metal—cooled reactor. The movable half of the assembly table has been operated, as have prototypes of the safety and control rods. Control and indicating equipment is being tested and mounted on instrument panels.

FOURTH QUARTER, FISCAL YEAR 1950

During the quarter, a fairly detailed study was made, comparing sodium and bismuth as coolants in the core circuit of the liquid-metal–cooled reactor. Of the two materials, sodium appears to be slightly the better, its main disadvantages being its low boiling point (enough pressure can be held on it to overcome this), and the radioactivity induced in it which makes the heat exchanger extremely radioactive. Its main advantage is that it permits lower power plant weight. $Lithium^7$ would of course be even better than sodium, if it were available and cheap. Fairly intensive design studies were carried out on the configuration of the reactor proper for the liquid-metal cycle. The currently preferred configuration consists of a framework of molybdenum, containing a number of cells. The fuel and moderator elements in the form of plates or rods are supported by this framework and arranged in bundles in the cells. End-supported rods running from one end of the reactor to the other were found impractical, since the rod diameters and wall thicknesses required to prevent undue sagging of the rods were inconsistent with the nuclear and heat transfer requirements of the reactor.

A great amount of effort continued to be expended on reactor and engine materials. Work on air cycle materials has shown that the shift from 88-12 to 70-30 beryllium carbide–graphite mixtures has not produced as large a change in the coefficient of thermal expansion of the mixture as anticipated. Coatings developed for the 88-12 mixture are therefore usable for the 70-30 mixture also. It was feared that new coatings might have to be developed. A eutectic of uranium, beryllium, and carbon, melting below 3630°F, seems to have been found. Thermal cycling of beryllium carbide–graphite mixtures has been found to lower the modulus of elasticity, the strength, and the electrical resistance. It has been found that the application of a load to measure elasticity does not in itself alter the modulus of elasticity. A new technique of molding holes in beryllium carbide–graphite mixtures, involving the use of combustible molds, has been developed. Air cycle material coating work continued without outstanding development, although considerable progress was made. The application of molybdenum silicide to beryllium carbide has turned out to be more difficult than anticipated. The best beryllium carbide coating now seems to be the high melting glaze developed by NEPA and A. O. Smith Corporation, consisting mainly of silica plus oxides of titanium, lithium, barium, sodium, and aluminum. The best coatings are obtained if the material is first impregnated with silicones.

The molybdenum-UO_2 mixtures discussed in the previous report have been worked on further. It is found that mixtures of 80 per cent molybdenum and 20 per cent UO_2 can be fabricated in much the same way as the 90-10 mixture previously used. Experiments on the bismuth corrosion of metals and ceramics show that the addition of aluminum and magnesium to deoxidize bismuth is not successful and does not markedly influence the corrosion of metals by bismuth. Beryllium carbide was found to be slightly attacked by bismuth at 1850°F. It cannot now be said whether beryllium carbide or any satisfactory moderator material can be used without canning. Molybdenum continues to be the most corrosion-resistant metallic material in all liquid metals. Tests seem to show that several days may be required to reach solubility equilibrium in liquid-metal corrosion tests.

Radiation damage testing was carried out in the ORNL reactor and in the cyclotrons at Washington University, Ohio State University, and the University of California at Berkeley. The pile and cyclotron bombardments produce qualitatively the same effects on beryllium carbide. The modulus of elasticity was decreased (in one case by a factor of ten) and the electrical resistance was greatly increased (in some cases by several orders of magnitude). The results have not yet been interpreted. Some of the effect on electrical conductivity may be due to oxidation, but the changes in elastic modulus are probably due to the effects of radiation. Experiments on radiation damage to lubricants continued with the test operation of six dynamic rigs, under simulated service conditions, in the Oak Ridge National Laboratory pile. The tests are complete but the data have not been interpreted as yet.

There were no new major developments in the bulk shielding experiments in which NEPA participates at the Oak Ridge National Laboratory. At ORNL's request, NEPA will continue to work on a beta-ray spectrometer, a Compton recoil coincidence counter, a multiple crystal spectrometer, and a proton-recoil neutron spectrometer for use in shielding experiments. These instruments are at present in various stages of development. Experiments on the measurement of scattering cross-sections for neutrons at high energies continued at Bartol Research Foundation and the University of Kentucky, and are being suspended at Westinghouse Electric Corporation.

Calculations of the weight of an idealized shield were extended to include the factors of sidewalls around the crew and plenum chamber volume within the shielded volume of the reactor. Indications from these somewhat oversimplified calculations are that the lowest total weight of the divided shield is obtainable with no sidewalls. Only a shadow disk at the end of the crew compartment is necessary. It is also thought possible that heavy materials may be put only on the side of the reactor nearest the crew, thus further lightening the shield around the reactor. The proposal to use sodium as the core coolant, coupled with the fact that the intermediate heat exchanger is in present designs essentially exposed (but aft of the reactor), led to an examination of the radioactivity of the sodium coolant. It has been shown to be no worse than the gamma activity that passes through the shield of the reactor proper. New developments in the shield material fabrication include the successful welding together of thin sheets of wolfram and the fabrication of slabs of boron carbide for tests in the ORNL lid tank.

Engine design studies included a study of the XJ-57 engine. It will be 15 per cent heavier for nuclear power than for chemical applications. The Westinghouse study of the J-34 adaptation to nuclear power is complete. The result indicates that this engine could be used in test work, but since other work of this kind is already going on in Oak Ridge on a small scale, no further action will be taken. Design and fabrication of heat exchangers are going on at A. O. Smith Corporation and Harrison Radiator Division, in order to supply heat exchangers for testing, at Oak Ridge, in the liquid-metal cycles. One of the main problems is that of joining the parts by brazing with a high-temperature brazing alloy or welding.

Wright Aeronautical Corporation has spent considerable time in the design of a suitable compressor and turbine for the helium cycle during the quarter.

This quarter's experimental work on engine components included study of the handling (on a small scale) of liquid bismuth at temperatures up to 1660°F. The maximum temperature reached during the previous quarter was 1150°F. No special trouble was encountered. Tests on liquid lithium at high temperatures show that it readily attacks mica, asbestos, Superex, and other siliceous insulators. A 1/16-inch aluminum sheet was pierced in five seconds by a 1000°F lithium stream. A small model of a lithium radiator was made to leak lithium through a small hole into an air stream, at 1375°F and 100 pounds per square inch. Although there were copious fumes and a local raising of the temperature, there was no explosion. A stream of liquid lithium 1/16-inch in diameter at 1510°F ate 1/8-inch into a concrete slab in 3 seconds, producing a very bright light, many fumes, and explosive scattering of solid particles. It is found that lithium reacts with many valve packings, forming high-melting solids which sometimes cause the valves to jam.

Heat-transfer and fluid-flow experimentation continued at NEPA with the initial operation of the air heat-transfer rig. Some difficulties were encountered.

A short study was carried out on the possibility of using airplane structure as shielding. It was found that since the optimum structural configuration is that of a hollow shell with a minimum of interior structure, there are many paths from the reactor to the crew which can transmit radiation directly. The average amount of material in the radiation path was approximately 1 inch of aluminum. An investigation of crew shield weights as a function of crew compartment shape and size and number of reactors is under way. Some consideration was given during the quarter to the use of areas other than the Arco and adjacent areas for the flight test base. Of these other areas, several locations in Florida look best.

During the quarter, the NEPA Medical Advisory Committee was dissolved. In its place, a small Research Guidance Committee was appointed. The Naval Radiological Defense Laboratory at Hunter's Point, California, is about to start work on studies of physical fitness following irradiation, using funds assigned by NEPA.

During the quarter, the ANP Technical Advisory Board started work with headquarters in the Y-12 area. A group of approximately twenty-five engineers and scientists, some of whom were previously associated with the Lexington Project, is at work. As yet, the group has reached no conclusions.

The Oak Ridge National Laboratory has commenced the planning of a small reactor to be built as a replica (in all respects except power level) of a possible aircraft reactor. ORNL assumes for the purpose of planning that this will be a metal-cooled reactor, although if the cycle chosen should not be the liquid-metal cycle, it is anticipated that this planning would be changed, and the ARE (Aircraft Reactor Experiment, as it has been named) would be redesigned to use the cycle chosen.

• • • • •

1. STUDIES OF PERFORMANCE OF AIRFRAME-POWER PLANT COMBINATIONS

Studies of the performance and characteristics of complete airframe-engine-reactor-shield combinations bring together the results of more detailed studies of aircraft components. By pointing out directions in which further analysis or experimentation will be profitable, they summarize and guide the work of the project to a great extent.

In more specific terms, these studies result in the establishment of relationships among speed, altitude, gross weight, uranium content, and general engineering practicality. They map out regions of optimum compromise between conflicting design requirements, and provide mutually compatible specifications for the airframe, engine, reactor, and shield.

1.1 THE SURVEY STUDIES (5.2 Man-months)

A very large fraction of the effort of the project, during the quarter just completed, has gone, directly or indirectly, into a continuation of the survey studies undertaken several months ago. The objective of these studies is a fairly rapid appraisal of the relative merits of several possible power plant cycles under serious consideration at present.

The main cycles under study continue to be the following three:

1) The open, or air cycle;

2) The compound liquid-metal cycle (ternary);

3) The compound helium cycle (binary).

The circulating fuel cycle may be considered in most respects a variation of the compound liquid-metal cycle. It, too, is being given some consideration.

Each cycle is being evaluated for a range of performance conditions. Fig. 1 shows the design

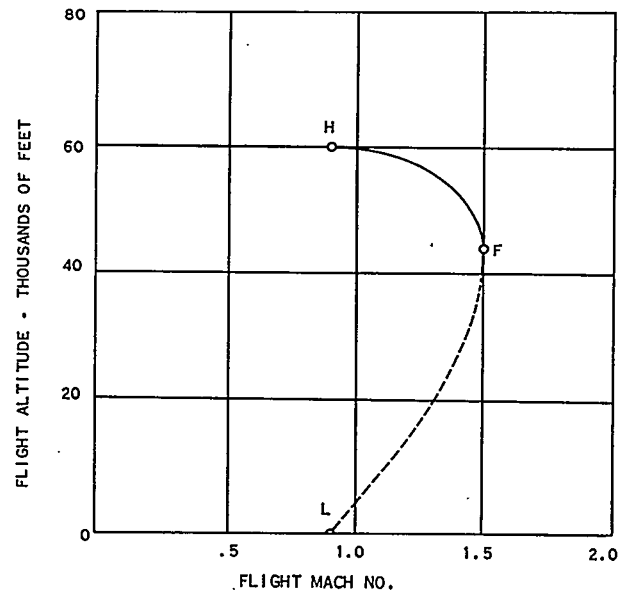

Fig. 1 - MINIMUM FLIGHT PERFORMANCE REQUIREMENTS FOR TACTICAL NUCLEAR-POWERED AIRCRAFT

speeds and altitudes currently believed to define the minimum performance acceptable for a nuclear powered aircraft. With this curve as a guide, the survey studies are divided into three phases. Each cycle is being evaluated at most of the following conditions:

Phase I. - Adaptation of nuclear power plants to the XB-52 aircraft, with a design flight Mach number of 0.8 and altitudes of 35,000 - 45,000 feet. The nuclear powered XB-52 is considered as a test vehicle only, or at best, perhaps as an interim tactical aircraft. Conservative assumptions, consistent with early development, are used. A very similar adaptation could be made using a swept-wing B-36 aircraft.

Phase II. - Tactical aircraft with the following design points on the minimum acceptable line: 60,000 feet at Mach 0.9, 45,000 feet at Mach 1.5, and sea level at Mach 0.9. Somewhat more optimistic assumptions are used than in Phase I, consistent with developments that may be expected in the next 10 years.

Phase III.- Tactical aircraft with maximum performance for each cycle. The design points are: 1) the maximum altitude which can be attained at Mach 0.9; 2) the maximum speed which can be attained at 60,000 feet; and 3) the maximum speed which can be attained at 45,000 feet. More optimistic assumptions are used in Phase III, consistent with what may be possible after a number of years of development beyond Phase II.

1.2 CURRENT RESULTS OF SURVEY STUDIES

Data are listed below giving the results of all studies which are still of current interest, including studies completed prior to the report period.

The survey studies have now reached the point where it is possible to use the results obtained to date in selecting Phase II and III airplanes which show promise of feasibility. Aircraft of little promise will be studied only briefly or not at all. These may be replaced by other aircraft.

Some of the results of these studies have already been submitted for evaluation by the Weapons Systems Evaluation Group. Their results to date are very preliminary, but two general conclusions seem likely to emerge from them. First, it is important to hold the uranium investment to a practical minimum, and second, the general standards of minimum acceptable performance, which have been adopted by NEPA, probably cannot be lowered without raising serious questions as to the military usefulness of the aircraft.

The following paragraphs contain a brief description of each aircraft under consideration and give some of its characteristics. In addition, a list of design assumptions, similar to that presented last quarter, is given in this report. Many items not listed in the tabulated data may be found in the standard assumptions.

a. Open Cycle

Aircraft No. 10 2.- During the report period, analytical work approached completion on the Phase I adaptation of the open cycle to the XB-52 aircraft. A tabulation of design point data is given below under "Design Data" (open cycle).

The aircraft is designed to fly at a Mach number of 0.8 at 35,000 feet. This altitude is lower than that of either the liquid-coolant cycle or the helium cycle Phase I aircraft. Its gross weight is 350,000 pounds. The chemically fueled XB-52 has a take-off gross weight of 390,000 pounds and a maximum allowable landing gross weight of 240,000 pounds. The XB-52 airframe must be greatly modified. Since the turbo-jets cannot be mounted in the wing, the wing must be redesigned structurally. The installation of the turbo-jets and shield in the fuselage requires a specially redesigned fuselage.

It continues to appear that the air cycle is better adapted to low-altitude high-speed flight than to high-altitude low-speed flight, for the reasons given last quarter.

Six modified XJ-57 turbo-jets are used. A landing condition cycle analysis has been completed, but the results have not been listed, since it is felt that they incorporate an unnecessary limitation on engine speed. In any case, there is good assurance that the landing thrust will be adequate.

The aircraft uses a split-flow reactor with a core diameter of 3.45 feet. The landing condition reactor power, maximum power density, maximum tube-wall heat flux, and thermal response may be approximated by multiplying the design point values by a factor of 2. It may be seen that the maximum power density and the thermal response are low by comparison with those of the liquid-coolant cycle and the helium cycle. The total flow area of the inlet plus outlet ducts through the shield may be as high as 18.8 square feet. This makes duct leakage an important problem on which essentially no good experimental data exist.

Aircraft No. IIOL 7.- This aircraft is designed to fly at a Mach number of 0.9 at sea level, using the open cycle. Such an aircraft is of interest tactically, since it is difficult to detect with early warning radar, difficult to attack with fighter aircraft, and relatively invulnerable to large-caliber ground defenses. It is a flight condition in which the merits of open cycle should show up to best advantage. No data are listed on this aircraft, since the analysis is still incomplete.

Considerable progress was made on this aircraft during the report period. It seems likely that its gross weight will be less than 350,000 pounds. There is some possibility that a straight-through-flow reactor may be used, leading to a low uranium investment.

The XJ-57 turbo-jet is being considered for this aircraft, and it seems likely that six or fewer units will be required. Chemical fuel burners are being incorporated ahead of the turbines to provide standby power in the event of reactor failure.

Aircraft No. IIOF P.- This study represents the application of the open cycle to a high-speed Phase II aircraft. The same data were presented in the previous quarterly report. The data are the result of an incomplete and now somewhat obsolete study. The aircraft is now being reinvestigated in the survey studies. There is some question as to whether an altitude of 45,000 feet at Mach 1.5 will be feasible, using Phase II assumptions.

b. Compound Liquid-Coolant Cycle

Aircraft No. IL 1.- All work was completed on the first study of the Phase I adaptation of the liquid-coolant cycle to the XB-52 aircraft. The data on this aircraft, listed below, were presented in the previous quarterly report.

Although the first study is completed, work continued on many modifications of the aircraft which will be incorporated in the second study. One modification which is being studied is the use of sodium instead of bismuth as the reactor coolant. Some advantages of using sodium are: lower weight of coolant; lower pressure drops (hence lower pumping power and pressure forces on the reactor); lower melting point; and a large body of available data on sodium. Although the reactor temperatures are above the normal boiling point of sodium, cavitation can be avoided by moderate pressurization. A serious problem arises from gamma activity induced in the sodium, particularly with respect to the maintenance crew. Measures must be taken to solve this problem in conjunction with the already existing maintenance problem due to gamma activity from the reactor.

A second modification which was studied during the report period is an increase in the core diameter from 1.99 to 2.5 feet. This was felt to be necessary to reduce the thermal response and thermal stresses to more reasonable values. This increase in core diameter would require an increase in airplane gross weight to roughly 350,000 pounds, and a reduction in design-point altitude to 40,000 feet.

A third proposed modification is the use of a metallic reactor for the liquid-coolant cycle, in order to improve resistance to radiation damage and thermal stress.

A fourth modification, which is applicable to all cycles, and promises considerable weight reduction, is the use of shadow shielding in the primary gamma shield.

The proper use of chemical fuel for boost and for standby is also being studied and may affect this airplane.

Aircraft No. IILH 5.- Analytical work continued on a Phase II liquid-coolant cycle aircraft designed to fly at 60,000 feet and Mach 0.9. No data are listed on this airplane.

During the report period, it became increasingly evident that the uranium investment per tactical aircraft should be held to a practical minimum. It is now felt that 200 pounds per aircraft is an excessive amount, and that it is highly desirable to hold the investment below 100 pounds per aircraft. These considerations led to the suspension of work on two-reactor aircraft, since such applications generally require more than twice the uranium investment of the equivalent one-reactor aircraft. It is now proposed that all aircraft use chemical fuel as standby in the event of reactor failure. It may also be advantageous to use chemical boost routinely at take-off and landing. Three schemes are under study:

1. Putting burners behind the radiators of all engines. This entails a considerable weight penalty, but enables the aircraft to fly at its design point on chemical fuel.

2. Putting burners behind the radiators of part of the engines. This entails a lower weight penalty but adds the control problems of dissimilar engines, and lowers the performance on chemical fuel.

3. Installing a small number of separate chemically fueled engines. This entails a moderate weight penalty and reduced performance, but gives a simpler control problem and a simpler engine modification problem.

The nuclear power plant will be designed to be capable of flying the aircraft throughout the full range of altitudes from sea level to the design point (although it may not be capable of meeting the landing and take-off requirements without chemical assistance). It may be necessary to shut down as many as two-thirds of the turbo-jets at sea level to avoid an excessive power demand on the reactor.

Aircraft No. IILF 6.- During the report period, considerable progress was made on the study of a liquid-coolant cycle aircraft designed to fly at 45,000 feet and Mach 1.5. Preliminary results of this work are tabulated below, under "Design Data" (compound liquid-coolant cycle). Design-point and landing-approach cycle analyses were completed. Aerodynamic and structural studies were completed for a typical straight-wing aircraft and are now being revised. Similar studies are in progress for a swept-wing aircraft.

When these studies are completed, a design analysis will be made for the reactor and liquid-metal circulating system.

The data listed apply to the straight-wing aircraft. The study indicated that this aircraft would be feasible at a gross weight of 400,000 pounds. It would use nine turbo-jets, each having a sea-level static equivalent air flow of 400 pounds per second, as recommended in NEPA Report No. 7. A compressor pressure ratio of 7/1 is used to reduce the radiator frontal area to a size that can be installed within the turbo-jet case diameter.

The reactor power per unit volume is lower than that of the Phase I aircraft as listed, and is consistent with that of the proposed 2.5-foot Phase reactor.

c. Compound Helium Cycle

Aircraft No. IH 3.- During the report period, work was completed on the Phase I adaptation of the compound helium cycle to the XB-52 aircraft. Data are listed below (see "Design Data," compound helium cycle). As a result of necessary revision, the design altitude had to be reduced to 40,000 feet. Thus the latest revisions of the liquid-coolant cycle and helium cycle Phase I aircraft indicate a feasible altitude only 5000 feet above that of the open cycle at the same gross weight.

Revisions made on this aircraft during the report period stemmed mainly from difficulties in radiator design. After the investigation of several configurations, it was decided that it would be necessary to double the pressure throughout the helium system and use a round tube-and-shell radiator design. In order to reduce the weight of helium lines, the turbo-jets were placed in the fuselage. As in the case of aircraft No. IO 2, this requires a structurally redesigned wing and a new fuselage. The high-pressure cycle leads to a low reactor free-flow area of 1.21 square feet, which in turn leads to a low uranium investment of approximately 80 pounds.

The mechanical problems and vulnerability of the helium cycle are still regarded as severe limitations.

Aircraft No. IIHF P.- Data are presented below on a Phase II helium cycle aircraft designed to fly at 45,000 feet and Mach 1.5. The same data were listed in the preceding quarterly report. These are the results of an incomplete and now somewhat obsolete study, which, however, has not yet been revised.

DESIGN DATA

Open Cycle

Phase	Phase I	Phase II
Aircraft	Aircraft No. IO 2	Aircraft No. IIOF P (preliminary data)
Design flight Mach No.	0.8	1.5
Design altitude (ft.)	35,000	45,000
Aircraft type	XB-52	
Design point L/D	18.9/1	6.5/1
Component Weights (lb.)		
Turbo-jets, air valves, ducts to and from shield	43,000	140,000
Reactor-shield assembly and crew shield	154,000	265,000
Airframe and equipment	143,000	235,000
Payload	10,000	10,000
Gross weight	350,000	650,000
	Design Point	
Turbo-jets	6 XJ-57's	12 turbo-jets
Frontal area per engine (ft.^{2})	10.1	13.75
Equivalent sea-level static air flow per engine (lb./sec.)	150	383
Total thrust available (lb.)	18,500	100,000
Specific impulse (sec.)	47.0	46.6
Air flow per engine (lb./sec.)	65.6	179
Compressor		
Inlet temperature (°F)	−17	110
Inlet pressure (lb./in.^{2})	5.16	7.2
Pressure ratio	14/1	20/1
Efficiency	0.817	0.82

Turbine

Inlet temperature (°F)	1685	2100
Inlet pressure (lb./in.^{2})	43.7	93.8
Pressure ratio	0.250/1	0.155/1
Efficiency	0.85	0.85
Outlet temperature (°F)	1151	1303

Reactor

Type	split-flow	split-flow
Core diameter (ft.)	3.45	5.93
Reflector thickness (in.)	3.3	3.1
Reflector outside diameter (ft.)	4.0	6.45
Free-flow ratio	0.35/1	0.40/1
Free-flow area (ft.^{2})	6.55	22
Tube hydraulic diameter (in.)	0.14	0.17
Heat transfer area (ft.^{2})	3366	15,700
Uranium investment (lb.)	160	180
Atomic ratio	325/1	900/1
Median energy for fission (ev.)	9	0.2
Max./avg. power, longitudinal	1.32/1	1.32/1
Max./avg. power, radial	1.07/1	1.0/1
Min./avg. flow, radial	0.85/1	1.0/1
Power (Btu./sec.)	115,300	690,000
Virgin flux (n./cm.^{2}/sec.)		8.3×10^{13}
Max. power density in fuel element (Btu./sec./ in.^{3})	6.26	6.0
Max. tube wall heat flux (Btu./ft.^{2}/hr.)	174,100	198,000
Inlet temperature (°F)	586	1003
Avg. outlet temperature (°F)	1685	2100
Max. wall temperature (°F)	2500	2500
Inlet pressure (lb./in.^{2})	67.3	134
Total pressure ratio	0.694/1	0.752/1
Inlet Mach No.	0.225	0.177
Outlet Mach No.	0.547	0.372
Avg. Reynolds' No.	27,270	45,500
Avg. heat-transfer coeff. (Btu./hr./ft.^{2}/°F)	171	250
Thermal response (°F/sec.)	94	131

Shield

Type	divided	divided
Reactor-crew separation (ft.)	50	150
Reactor-shield diameter (ft.)	15	17.5
Weight of reactor-shield assembly (lb.)	106,000	193,000
Crew shield weight (lb.)	45,000	40,000
Shield cooling radiator weight (lb.)	3,000	8,000

Water pressure in shield (lb./in.^{2})	~90
Water inlet temperature (°F)	~265
Water outlet temperature (°F)	~285
Water flow (lb./sec.)	~185

Compound Liquid-coolant Cycle

Phase . . . . Phase I

Aircraft . . . . Aircraft No. IL 1

Design flight Mach No.	0.8
Design altitude (ft.)	45,000
Aircraft type	XB-52
Design point L/D	19.0/1

Component Weights (lb.)

Turbo-jets	36,800
Radiators	6,200
Lithium pumps and lines plus auxiliary power supply	14,500
Reactor-shield assembly plus crew shield	110,000
Airframe and equipment	127,500
Payload	10,000
Gross weight	305,000

	Landing Approach	Design Point
Flight Condition		
Speed	175 knots	M =0.8
Altitude (ft.)	0	45,000
Turbo-jets	6 XJ-53's	
Frontal area per engine (ft.^{2})	12.35	
Equivalent sea-level static air flow per engine (lb./sec.)	258	
Total thrust available (lb.)	32,000	17,200
Specific impulse (sec.)	26.8	48.0
Air flow per engine (lb./sec.)	199	59.5
Rpm	5,110	5,550
Turbo-jet Compressor		
Inlet temperature (°F)	64	−17
Inlet pressure (lb./in.^{2})	15.4	3.20

Pressure ratio	3/1		5/1
Efficiency	0.81		0.85
Turbo-jet Radiator			
Type		plate-and-fin	
Frontal area per engine (ft.^{2})		12.35	
Air side free-flow area per engine (ft.^{2})		7.78	
Air side tube length (in.)		12	
Air side plate spacing (in.)		0.150	
Air side fin thickness (in.)		0.007	
Air side fin pitch (fins/in.)		11.1	
Plate thickness (in.)		0.010	
Lithium side plate spacing (in.)		0.050	
Air inlet temperature (°F)	303		289
Air inlet pressure (lb./in.^{2})	45.7		15.8
Air inlet Mach No.	0.122		0.104
Air total pressure ratio	0.925/1		0.909/1
Lithium flow in radiators per engine (lb./sec.)	37.0		37.0
Lithium flow by-passing radiators per engine (lb./sec.)	3.7		3.7
Lithium inlet temperature (°F)	1581		1600
Lithium outlet temperature (°F)	616		1140
Turbo-jet Turbine			
Inlet temperature (°F)	1019		1400
Inlet pressure (lb./in.^{2})	41.9		14.2
Pressure ratio	0.482/1		0.479/1
Efficiency	0.87		0.88
Intermediate Heat Exchanger		shell-and-tube	
Frontal area (ft.^{2})		5.13	
Length (in.)		36	
Lithium flow (lb./sec.)	252		252
Lithium inlet temperature (°F)	712		1186
Lithium outlet temperature (°F)	1581		1600
Bismuth flow (lb./sec.)	6974		6974
Bismuth inlet temperature (°F)	1671		1643
Bismuth outlet temperature (°F)	802		1229
Lithium Pumps		2 centrifugal pumps	
Tip diameter (in.)		5.9	
Scroll max. diameter (in.)		13.0	
Rpm	7830		7830

Flow per pump (gal./min.)	1920		1920
Head (ft.)	620		620
Pressure rise (lb./in.^{2})	126.5		126.5
Shaft power per pump (h.p.)	174		174
Bismuth Pumps		2 centrifugal pumps	
Tip diameter (in.)		17.16	
Scroll max. diameter (in.)		37.5	
Rpm	668		668
Flow per pump (gal./min.)	2565		2565
Head (ft.)	34		34
Pressure rise (lb./in.^{2})	144		144
Shaft power per pump (h.p.)	263		263
Auxiliary Power Supply		2 T-38's	
Total max. available power (h.p.)			1400
Total air flow at MAP* (lb./sec.)			14
Total lithium flow at MAP (lb./sec.)			8
Flight drag (lb.)			24
Reactor		straight-through flow	
Core diameter (ft.)		1.98	
Reflector thickness (in.)		2.5	
Reflector outside diameter (ft.)		2.4	
Free-flow ratio		0.35/1	
Free-flow area (ft.^{2})		1.08	
Tube hydraulic diameter (in.)		0.14	
Heat transfer area (ft.^{2})		734	
Uranium investment (lb.)		$\sim$200	
Atomic ratio		70/1	
Median energy for fission (ev)		10^3	
Max./avg. power, longitudinal		1.25/1	
Max./avg. power, radial		1.07/1	
Avg./min. flow		1.18/1	
Power (Btu./sec.)	220,000		105,000
Virgin flux (n./cm.^{2}/sec.)	4.8×10^{14}		2.3×10^{14}
Max. power density in fuel element (Btu./sec./in.^{3})	43.0		20.6
Max. tube wall heat flux (Btu./hr./ft.^{2})	1,450,000		692,000
Bismuth inlet temperature (°F)	802		1229
Bismuth outlet temperature (°F)	1671		1643
Max. tube wall temperature (°F)	1960		1781
Avg. heat transfer coeff. (Btu./hr./ft.^{2}/°F)		10,280	

*MAP = maximum available power.

Thermal response of core plus coolant in core (°F/sec.)	770		370
Bismuth velocity (ft./sec.)	10.6		10.6
Header-to-header pressure drop (lb./in.^{2})	40		40
Shield		divided	
Reactor-crew separation (ft.)		46	
Reactor shield diameter (ft.)		10.5	
Weight of reactor-shield assembly (lb.)		82,000	
Crew shield weight (lb.)		25,000	
Shield cooling radiator weight (lb.)		3000	
Water pressure in shield (lb./in.^{2})			70
Water inlet temperature (°F)			110
Water outlet temperature (°F)			265
Water flow (lb./sec)			20
Performance *			
Take-off distance (ft.)	16,400		
Take-off distance with ATO (16,000 lb. thrust for 31 sec.) (ft.)	10,400		
Rate of climb at sea level (ft./min.)	1300 (at 250 knots)		
Max. speed at sea level (knots)	385		
Rate of climb at 45,000 ft., M = 0.8 (ft./min.)	130		
Max. rate of climb at 45,000 ft. (ft./min.)	240 (at 420 knots)		
Landing speed (knots)	140		
Nuclear-plus-Chemical Test Aircraft	Aircraft No. IL 4		
Aircraft type	XB-52		
Four nuclear turbo-jets; operating at gross weight of 335,000 lb.			
Rate of climb at sea level (ft./min.)	1150 (at 260 knots)		
Maximum speed (knots)	480 (at 27,500 ft.)		
Service ceiling (ft.)	37,500		
Two chemical turbo-jets; operating at gross weight of 335,000 lb.			
Rate of climb at sea level MC**(ft./min.)	540 (at 230 knots)		
Maximum speed, MC (knots)	340 (at 12,500 ft.)		
Service ceiling, MC (ft.)	17,500		
Fuel load (lb.)	30,000		
Endurance at 5000 feet and 230 knots (hr.)	2		

* No ATO (assisted take-off) unless specified.

**MC = maximum continuous power.

Sinking speed at landing, MC (ft./sec.)	6.5 (at 140 knots)
Landing speed (knots)	140

Four nuclear and two chemical turbo-jets; operating at gross weight of 335,000 lb.

Take-off distance (ft.)	7900
Rate of climb at sea level (ft./min.)	3500 (at 305 knots)

Compound Liquid-Coolant Cycle

Aircraft	Aircraft No. IILF 6
Design flight Mach No.	1.5
Design altitude (ft.)	45,000
Design point L/D	6.6/1

Component Weights (lb.)

Turbo-jets Radiators Lithium pumps and lines plus auxiliary power supply	110,500
Reactor-shield assembly plus crew shield .	121,700
Airframe and equipment	157,800
Payload	10,000
Gross weight	400,000

	Landing Approach		Design Point
Flight Condition			
Speed	175 knots		M = 1.5
Altitude (ft.)	0		45,000
Turbo-jets		9 engines	
Frontal area per engine ($ft.^2$)		14.35	
Equivalent sea level static air flow per engine (lb./sec.)		400	
Total thrust available (lb.)	70,500		60,500
Specific impulse (sec.)	21.3		37.2
Air flow per engine (lb./sec.)	363		181
Turbo-jet Compressor			
Inlet temperature (°F)	66		109
Inlet pressure ($lb./in.^2$)	15.4		7.23
Pressure ratio	5.6/1		7/1
Efficiency	0.84		0.85

Turbo-jet Radiator		plate-and-fin	
Frontal area per engine ($ft.^2$)		10	
Air side free-flow area per engine ($ft.^2$)		6.4	
Air side tube length (ft.)		1.72	
Air side plate spacing (in.)		0.150	
Air side fin thickness (in.)		0.006	
Air side fin pitch (fins/in.)		11	
Plate thickness (in.)		0.010	
Lithium side plate spacing (in.)		0.050	
Air inlet temperature (°F)	457		597
Air inlet pressure ($lb./in.^2$)	86		50
Air inlet Mach No.	0.153		0.142
Air total pressure ratio	0.823/1		0.81/1
Lithium flow in radiator per engine (lb./sec.)	137		137
Lithium flow by-passing radiators per engine (lb./sec.)	17		17
Lithium inlet temperature (°F)	1260		1650
Lithium outlet temperature (°F)	742		1200
Turbo-jet Turbine			
Inlet temperature (°F)	995		1500
Inlet pressure ($lb./in.^2$)	70.7		40.9
Pressure ratio	0.274/1		0.307/1
Efficiency	0.87		0.87
Outlet temperature (°F)	625		1060
Intermediate Heat Exchanger		shell-and-tube	
Lithium inlet temperature (°F)	794		1245
Lithium outlet temperature (°F)	1260		1650
Reactor		straight-through flow	
Core diameter (ft.)		3.04	
Reflector thickness (in.)		5.8	
Reflector outside diameter (ft.)		4.00	
Atomic ratio		110/1	110/1
Power (Btu./sec.)	447,000		389,000
Shield			
Type		divided	
Reactor-crew separation (ft.)		100	
Reactor shield diameter		~11	
Reactor shield weight (lb.)		93,000	

Crew shield weight (lb.)	23,700
Shield cooling radiator weight (lb)	5000

Compound Helium Cycle

Phase	Phase I	Phase II
Aircraft	Aircraft No. IH 3 (preliminary data)	Aircraft No. IIHF P (preliminary data)
Design flight Mach No.	0.8	1.5
Design altitude (ft.)	40,000	45,000
Aircraft type	XB-52	
Design point L/D	20.2/1	6.5/1
Component Weights (lb.)		
Turbo-jets	40,800	94,000
Radiators	19,900	96,000
Helium machinery and lines	15,800	11,000
Reactor-shield assembly plus crew shield	120,000	176,000
Airframe and equipment	133,500	213,000
Payload	10,000	10,000
Gross weight	340,000	600,000

	Landing Approach	Design Point	Design Point
Flight Condition			
Speed	175 knots	M = 0.8	M = 1.5
Altitude (ft.)	0	40,000	45,000
Turbo-jets	6 XJ-53's		14 turbo-jets
Frontal area per engine (ft.^{2}).	12.35		13.5
Equivalent sea-level static air flow per engine (lb./sec.)	258		378
Total thrust available (lb.)	30,000	17,000	92,300
Specific impulse (sec.)	21.6	36.6	37.4
Air flow per engine (lb./sec.)	231	77.4	169
Rpm	5500	5550	

Turbo-jet Compressor

Inlet temperature (°F)	65	−17	110
Inlet pressure (lb./in.^{2})	15.4	4.1	7.2
Pressure ratio	4.4/1	6.0/1	4.0/1
Efficiency	0.83	0.84	0.85

Turbo-jet Radiator	shell-and-tube		snell-and-tube
Frontal area per engine (ft.^{2})	12.35		27.4
Air side flow area per engine (ft.^{2})	4.57		10.6
Length (in.)	28.8		32
Tube inside diameter (in.)	0.145		
Tube thickness (in)	0.012		
Air inlet temperature (°F)	394	333	430
Air outlet temperature (°F)	1000	1170	1500
Air inlet pressure (lb./in.^{2})	66.7	24.2	28.5
Air inlet Mach No.	0.10	0.089	
Air total pressure ratio	0.86/1	0.85/1	0.73/1
Helium inlet temperature (°F)	1540	1650	1753
Helium outlet temperature (°F)	566	546	590
Helium inlet pressure (lb./in.^{2})	650		345
Helium total pressure ratio	0.95/1		0.95/1

Turbo-jet Turbine

Inlet temperature (°F)	1000	1170	1500
Inlet pressure (lb./in.^{2})	57.1	20.3	20.8
Pressure ratio	0.34/1	0.37/1	0.48/1
Efficiency	0.84	0.86	0.86

Helium Compressor

Frontal area (ft.^{2})	8		
Inlet temperature (°F)	566	546	590
Inlet pressure (lb./in.^{2})	605		330
Pressure ratio	2.24/1	1.23/1	1.82/1
Efficiency	0.85	0.80	0.85
Helium flow (lb./sec.)	176	72	476
Quantity of helium in system (lb.)	20	15	~65

Helium Turbine

Inlet temperature (°F)	2000	1760	2090
Inlet pressure (lb./in.^{2})	1220		522
Pressure ratio	0.54/1	0.86/1	0.67/1
Efficiency	0.86	0.84	0.88

Reactor			split-flow
Core diameter (ft.)	2.48		3.2
Reflector thickness (in.)	4.7		6.0
Reflector outside diameter (ft.)	3.27		4.2
Free-flow ratio	0.25/1		0.3/1
Free-flow area ($ft.^2$)	1.21		4.97
Tube hydraulic diameter (in.)	0.18		0.105
Heat-transfer area ($ft.^2$)	760		2910
Uranium investment (lb.)	80		75
Atomic ratio	370/1		600/1
Median energy for fission (ev)	8		0.7
Max./avg. power, longitudinal	1.3/1		1.3/1
Max./avg. power, radial	1.07/1		1.0/1
Min./avg. flow, radial	0.85/1		
Power (Btu./sec.)	215,000	99,300	691,000
Virgin flux ($n./cm.^2/sec.$)	3×10^{14}	1×10^{14}	2×10^{14}
Max. power density in fuel element ($Btu./sec./in.^3$)	16	7.3	35.2
Max. tube wall heat flux ($Btu./ft.^2/hr.$)	1,410,000	651,000	1,110,000
Helium inlet temperature (°F)	1026	656	926
Avg. helium outlet temperature (°F)	2000	1760	2090
Max. tube wall temperature (°F)	2500	2200	2500
Avg. Reynolds' No.	74,100	33,500	22,600
Avg. heat-transfer coeff. ($Btu./hr./ft.^2/°F$)	1630	790	1000
Inlet pressure ($lb./in.^2$)	1320		581
Total pressure ratio	0.95/1		0.92/1
Avg. exit velocity (ft./sec.)	790		1230
Thermal response (°F/sec.)	410	190	750

Shield			
Type	divided		divided
Reactor-crew separation (ft.)	50		100
Reactor shield diameter (ft.)	14		15
Weight of reactor-shield assembly (lb.)	75,000		123,000
Crew shield weight (lb.)	42,000		45,000
Shield radiator weight (lb.)	3000		8000
Water pressure in shield ($lb./in.^2$)		~90	
Water inlet temperature (°F)		~265	
Water outlet temperature (°F)		~285	
Water flow (lb./sec.)		~160	

c23

STANDARD DESIGN ASSUMPTIONS

The following is a list of assumptions which are generally adhered to in the analytical work of preliminary design studies. All of these assumptions are subject to change. Those listed here have either been used for some time, or are expected to be used for some time. In some cases, ranges of values have been listed rather than a fixed value. There were no significant changes made in the standard assumptions during this quarter.

Atmosphere

NACA standard.

Diffuser

Flight Mach No.: 0.9; 1.5; 2.0.

Design-point diffuser efficiency:[1] 0.95; 0.92; 0.90.

These efficiencies apply to nose inlets or undisturbed nacelle inlets. They may be decreased for side inlets and some other configurations.

Jet Nozzle

Design-point jet efficiency: 0.96.

Complete expansion to atmospheric pressure.

Turbo-jets

In adaptation studies, data on specific engines are used.

In generalized studies, the following assumptions are used:

For air cycle: Weight (pounds) of turbo-jets plus ducting to and from reactor = corrected air flow (in pounds per second) x 12 x (1 + 0.52 ln compressor pressure ratio). (The corrected air flow is the air flow corrected to sea-level static conditions.)

For binary and ternary turbo-jets: Weight (pounds) of turbo-jet (without radiator) = corrected air flow (in pounds per second) x 10 x (1 + 0.52 ln compressor pressure ratio).

Compressor: Design-point corrected air flow: 2.79 pounds per square foot of case area per second. For compressor pressure ratios less than 23/1, design-point over-all efficiency: 0.85. For compressor pressure ratios greater than 23/1, design-point stage efficiency: 0.90.

Air turbine: Maximum allowable inlet temperature: 1900° - 2200°F. Design-point turbine efficiency: 0.85 - 0.87.

[1] All efficiencies are energy efficiencies.

Helium turbine: Maximum allowable inlet temperature: 2000° - 2100°F.

Ducting

For air cycle: Loss in total pressure from compressor outlet to reactor inlet: 7 per cent. Loss in total pressure from reactor outlet to turbine inlet: 7 per cent.

For compound cycles: Loss in total pressure from compressor outlet to radiator inlet: 1 per cent. Loss in total pressure from radiator outlet to turbine inlet: 1 per cent.

Radiator

Plate-and-fin, tube-and-fin, or shell-and-tube construction.

Thermal conductivity of radiator metal: 15.7 Btu./hr./ft./°F.

For plate and fin, air side ϕ (defined as $\frac{h}{c_p G} \div \frac{f}{2}$) = 0.8;

where:

h is heat transfer coefficient (Btu./hr./ft.^{2}/°F);
c_p is the specific heat at constant pressure (Btu./lb./°F);
G is the mass velocity (lb./hr./ft.^{2});
f = friction factor.

Helium cycle radiator: Maximum allowable inlet temperature: 1650° - 1750°F.

Intermediate Heat Exchanger

Maximum heat exchanger material temperature: less than 1700°F.

Reactor

Moderator and reflector material: beryllium carbide (Be_2C + 1/3C).

Uranium: 90 per cent enriched.

In reactivity calculations, depletion and poisoning are based on 100 hours of operation at 600,000 kw.

Reactor must be restartable up to 1 hour after shutdown, and after 48 hours after shutdown.

End reflector thickness = jacket reflector thickness ÷ (1 - free flow ratio).

Longitudinal maximum-to-average power ratio: 1.3 to 1.4.

Radial maximum-to-average power ratio: 1.0 to 1.25.

Item	Gas-cooled Reactors	Liquid-Metal-cooled Reactors
Coating material (per cent by weight)	44.8 Fe, 41 Cr, 7.1 Al, 3.4 Si, 3.3 Mn, 0.4 Ti	75 Fe, 25 Cr
Coating thickness	0.005-inch	0.008-inch
Flow arrangement	Split or straight through	Straight through
Maximum allowable wall temperature	2500°F	2000°F
Average temperature used in reactivity calculations	2200°F	1600°F
Core length-to-diameter ratio	0.9 split flow; 1.0 straight through	1.0

Shield

Crew tolerance: 1 roentgen per hour (for a maximum of 25 hours).

Average of 2.5 gammas per fission with an average energy of 2 Mev.

One-tenth of all neutrons leaking from reactor are fast.

For gas-cooled reactors: Inlet duct total free-flow area = core total free-flow area. Outlet duct free-flow area = 1.88 x core total free-flow area.

High-density unit shield: Specific gravity of shield material: 8. Improvement factor (see NEPA 1079-EAR-T1): 0.9. Weight correction for shadow shielding: -15 per cent.

Divided shield: Five inches of lead around the reactor attenuate gammas by a factor of 50.

Five inches of lead plus 43 inches of water and/or hydrocarbon attenuate neutrons by a factor of 5×10^7.

Gamma relaxation length in water or hydrocarbon is 24 centimeters.

Rear face of crew shield based on 2-Mev gammas.

Fluxes calculated by inverse square law.

Side and front faces of crew shield based on 1-Mev gammas.

All scattering due to air; none by the aircraft.

Aircraft

Maximum allowable landing speed: 175 knots.

Maximum allowable sinking speed during normal landing: 10 feet per second.

Rate of climb at rated altitude: 500 feet per minute.

• • • • •

2. REACTOR

Work continued throughout the quarter on all of the three main types of reactors, with some attention given to the circulating fuel reactor as in the previous quarter.

2.1 REACTOR NUCLEAR STUDIES AND DESIGN (40.0 Man-hours)

2.11 Calculations on Particular Reactors. - Nearly 30 per cent of the reactor calculations made during the quarter were on isolated cases contributing to the design of the liquid-metal-cooled and helium-cooled reactors. This design work is discussed in sections 2.2 and 6.1 of this report.

The large-scale mapping of critical masses as a function of size and composition was concluded last quarter. However, new data have been obtained from General Electric Company on the cross-sections of many elements at 2000 ev. An effort is being made to obtain information as complete as possible on cross-section data for use in future calculations. Future results for reactors containing diluents or poisons in the form of coatings or structural material may differ appreciably from those reported, since, in existing maps, if nothing better was available, assumptions of 1/v extrapolation from thermal capture cross-sections were made. In particular, General Electric reports a molybdenum cross-section of 0.27 barn at 2000 ev., which indicates a much higher intermediate energy absorption than that previously assumed for this proposed structural material. However, additional data are being sought for the region from above thermal to the neighborhood of the General Electric measurement. It is felt that the use of molybdenum as a structural material may be more limited than previously expected, but that additional measurements of the epithermal cross-section should be made.[2]

[2] Further information, received as this report was being edited, indicates that the cross-section of molybdenum at intermediate energies, while higher than heretofore assumed, is still low enough to make molybdenum a very desirable reactor structural material.

Circulating fuel reactors. - Considerable work was done during the quarter on the determination of uranium weights necessary for circulating fuel type reactors. Each reactor was considered to consist of a cylindrical pot containing the molten solvent and fissionable material. Various assumptions were made regarding the necessary fluid volume outside the core. The solvents considered were lithium hydride plus lithium and sodium hydroxide.

Table 2 presents estimates of the core uranium weights with the lithium hydride–lithium solvent. The lithium is assumed to be 99.93 per cent lithium^7 isotope. The mean temperature is 1500°F, the fission-product poisons are taken at equilibrium density, and the given cores are surrounded by a a 6-inch beryllium carbide reflector.

TABLE 2

URANIUM INVENTORY (LB.) IN LITHIUM HYDRIDE-LITHIUM FUEL REACTORS WITH 6-INCH Be_2C + 1/3C REFLECTORS

Core Diameter (feet)	Volume of Coolant Outside Core (cubic feet)			
	0	10	20	30
3.25	190	295	400	505
3.50	115	170	225	275
4.0	105	140	170	195
4.5	130	160	185	210
5.5	210	230	255	290

Thus, in the lithium hydride–lithium circulating fuel reactor with a 6-inch beryllium carbide reflector, and 20 cubic feet of coolant in the heat exchanger and lines, the minimum total uranium weight is approximately 170 pounds. The core size at this minimum is approximately 4 feet.

Table 3 presents estimates of the uranium weights with an assumed sodium hydroxide solvent. The mean temperature is 1500°F, the fission-product

TABLE 3

URANIUM INVENTORY (LB.) IN SODIUM HYDROXIDE

CIRCULATING FUEL REACTORS - NO REFLECTOR

Core Diameter (feet)	Volume of Coolant Outside Core (cubic feet)			
	0	10	20	30
2.0	28	68	124	145
2.5	26	47	69	90
3.0	33	48	64	80
3.5	41	54	66	78
4.0	52	62	72	83

poisons are taken at equilibrium density, and the reactors are bare. Reflector calculations have not yet been made.

Thus, in a sodium hydroxide circulating fuel reactor with no reflector and 20 cubic feet of coolant outside the core, the minimum weight is approximately 64 pounds. The core size at this minimum weight is approximately 3 feet, but little penalty is incurred in decreasing it to 2.5 feet or increasing it to 4 feet. From a nuclear standpoint, it is clear that sodium hydroxide is much the better solvent.

Reactors with moderating coolant. - A study was made to determine a type of aircraft reactor design that would have a minimum uranium weight. A A sodium hydroxide—graphite—uranium dicarbide system seems to provide the best possibility from the nuclear standpoint. The sodium hydroxide would act in the dual role of moderator and coolant, and the fuel elements would be composed of uranium-impregnated graphite. A coating of silicon carbide was considered necessary to protect the graphite from attack by the sodium hydroxide.

Table 4 presents the results of critical mass calculations on these sodium hydroxide—graphite—uranium dicarbide systems. The mean reactor temperature in this case is 1500°F, the power level is 100,000 kw., and the fission-product poisoning is determined for the 1-hour-after-shutdown condition. Uranium depletion of 1 pound is included. The absorbing effect of coatings is not yet included, but it is estimated this would add only a few pounds to the critical mass, since silicon carbide has a very low capture cross-section.

TABLE 4

CRITICAL MASSES FOR A SODIUM-HYDROXIDE-GRAPHITE-URANIUM CARBIDE SYSTEM

Volume Fraction NaOH	Atomic Ratio H/U-235	Reflector Thickness Graphite (inches)	Core Diameter (feet)	Critical Mass (lb.)
0.35	100	0	3.45	67
0.35	100	6	2.88	40
0.35	200	0	4.33	66
0.35	200	6	3.70	41
0.50	100	0	2.88	56
0.50	100	6	2.32	30
0.50	200	0	3.19	37
0.50	200	6	3.00	22

The weights given in Table 4 are low in comparison to any proposed liquid-metal—cooled beryllium—moderated design with ferro-chrome coatings.

Fast reactors. - Critical mass calculations were made for some fast all-metal reactors, using the matrix multiplication method reported on last quarter. These reactors have a molybdenum core matrix with 40 per cent of the core volume occupied by coolant. A 12-inch wolfram carbide reflector surrounds the given core in each case. Operating effects are included. Table 5 reports these results for various core sizes.

Thus, it seems clear that unmoderated cores having diameters greater than 1.5 feet are impractical from the critical-mass standpoint. Even with a 1.5-foot core diameter, the uranium content is high enough to make such reactors unattractive.

TABLE 5

CRITICAL MASSES (LB.) IN FAST, MOLYBDENUM CORE (40 PER CENT COOLANT) WITH 12-INCH WOLFRAM CARBIDE REFLECTORS

Coolant	Core Diameter (feet)		
	1.5	2.0	3.0
Lithium	275	435	810
Bismuth	240	360	620
Zinc	215	315	515

Reflector comparison. - Calculations are continuing on the comparison of different reflectors in regard to critical-mass savings. The reactor thus far considered has a beryllium carbide-graphite (Be_2C + 1/3C) moderated bismuth-cooled core with a moderator-to-uranium molecular ratio of 30/1. The usual effects of temperature and equilibrium poisons are included, and the fraction of core volume that is attributed to coolant is 0.30. Coatings 0.010-inch thick of iron and chromium alloy are present on the heat-transfer surface.

Table 6 presents the preliminary results of this investigation.

TABLE 6

COMPARISON OF REFLECTORS ON (BERYLLIUM CARBIDE + 1/3C): UC_2 CORE OF MOLECULAR RATIO 30/1

Reflector	U-235 Weight (lb.)	Reflector Outside Diameter (ft.)	Free-Flow Area (sq. ft.)
None	219	2.44	1.40
2 1/2-inch Be_2C + 1/3C	118	3.06	0.92
6 1/2-inch Pb (inelastic scattering neglected)	127	3.11	0.97
2 1/2-inch Be_2C + 1/3C inside a 4-inch layer of Pb	76	2.79	0.70
6 1/2-inch Be_2C + 1/3C	54	2.61	0.55

A graph of these results indicates that, for the core considered, the 6 1/2-inch reflector combination composed of 2 1/2 inches of beryllium carbide plus graphite mixture (Be_2C + 1/3C) inside of 4 inches of lead achieves the same uranium savings as a 4 3/4-inch beryllium carbide plus one-third graphite reflector. Inelastic scattering in the lead was neglected in this work, hence the results for the case in which the lead is adjacent to the core may be quite pessimistic. Further investigation of this factor will be made. Calculations are in process using other molecular ratios, and it is planned to map the results, so that the critical masses can be compared from the standpoint of constant core size, constant reflector outside diameter, etc.

Optimum reflector thickness. - Work continued on the study of the optimum thickness of the moderating reflector. The problem is one of choosing a reflector that effects a good power distribution in the core and low uranium weight, but does not result in increased shield weight. Current thinking is that the moderating reflector can be counted as neutron shielding material (it is probably not quite as effective as water). The use of moderating reflector tends to increase the weight of the heavy-element primary gamma layer, because in this case, the gamma layer would be located on a larger radius. However, if this heavy layer need be only on the side towards the crew compartment (as a shadow gamma shield), then this penalty should be slight. In any event, it seems advisable, from these results, to use at least 2 or 3 inches of moderating reflector inside of the heavy-element reflector, from the standpoints of critical mass and core power distribution. If it is necessary to borate the heavy layer to reduce secondary gamma production, then the moderating reflector layer should be thicker (5 or 6 inches).

In particular, an investigation was made of the optimum thickness of a moderating end reflector, in the case in which the end reflector has the same free-flow ratio as the core. The problem was considered to be one of compromise between low peak power density on the one hand, and low shield weight on the other. If the moderating reflector is effective as shielding, then its thickness should be extended to the point at which additional thickness does not significantly improve the core peak-to-average power ratio. This would require a thickness of 6 to 8 inches, depending upon the core energy spectrum. However, the moderating reflector may not be the best shield material. Assuming, as a limit, that the moderating reflector provides no shielding whatsoever, it follows that the shield weight could be held constant only by decreasing the core length 1 inch for each inch of moderating end reflector.

This leads to an increased peak power density for given total power, because the improvement in longitudinal peak-to-average power ratio does not make up for the loss of core volume. From this viewpoint, then, the moderating end reflector should be of zero thickness. An intermediate and perhaps more realistic assumption is to consider that if, say, 2 inches of moderating end reflector were used, the core size must be reduced only 1 inch to keep the shield weight the same. This leads to an optimum thickness for minimum peak power density. The results show the optimum range to be approximately 1 to 2 inches for a 2-foot reactor, 1 1/2 to 2 1/2 inches for 2.5-foot and 3-foot reactors, and 2 to 3 inches for a 3.5-foot reactor. Because of the approximate nature of the assumption made above, these results must be regarded as very tentative.

Table 7 gives some indication of the longitudinal peak-to-average power ratios that can be expected for typical reactor cores with end reflectors. The free-flow ratio is 0.3/1 in both the core and end reflector.

TABLE 7

LONGITUDINAL PEAK-TO-AVERAGE POWER RATIOS

Core Length (feet)	End Reflector Thickness (inches)			
	0	2	4	6
2	1.4	1.3	1.3	1.2
2.5	1.5	1.3	1.3	1.3
3	1.5	1.4	1.3	1.3
3.5	1.5	1.4	1.4	1.3

2.12 Theory and Methods of Calculation

Hydrogen-moderated reactors. - A circulating fuel reactor, because of the material outside the core, requires low uranium concentration, which in turn requires a thermal energy spectrum. Because of its moderating power, hydrogen in the form of a metal hydride or hydroxide provides the most effective means of lowering the neutron energy spectrum.

In order to evaluate the feasibility of this type of reactor in terms of uranium investment, it is necessary to compute critical masses for a wide range of moderator-coolant-fuel combinations. It is therefore desirable to use age theory, since the age equation takes a very simple form for a thermal or nearly thermal reactor.

The usual derivation of the age equation does not apply to reactors containing hydrogen, and it is well known that age theory does not give the correct slowing-down distance for a point source of neutrons in a hydrogenous medium. The problem of a spatially independent source in an absorbing medium has, however a simple solution (cf. Marshak, *Review of Modern Physics*, 19, 189 (1947)). Using the fact that, for the special case of a bare critical reactor, leakage is formally the same as absorption, a solution for the slowing-down density can still be obtained, which to a first approximation is identical with age theory.

Let $(n(E)dE) \equiv$ (the number of neutrons leaving the energy interval dE about E per unit time and volume), and

$(a(E')dE) \equiv$ (the probability that a neutron leaving energy E' will be scattered into the interval dE about E).

The continuity equation can be written

$$n(E) = \int_E^{E_f} a(E')\,n(E')\,dE' , \qquad (1)$$

where E_f is the energy of fission neutrons, which are assumed to be monoenergetic. Differentiating with respect to E and solving the resulting differential equation leads to

$$n(E) = n(E_f) \exp \int_E^{E_f} a(E')\,dE' . \qquad (2)$$

Assuming that moderation is due to hydrogen only, the scattering probability depends only on the energy of the neutron prior to scattering, and can be written

$$a(E') = \frac{\Sigma_{SH}(E')}{\Sigma_{SH}(E') + \Sigma_a(E') + \frac{\lambda_{tr}}{3} K^2} \cdot \frac{1}{E'} , \qquad (3)$$

where $(\Sigma_{SH}) \equiv$ (macroscopic scattering cross-section of hydrogen);
$(\Sigma_a) \equiv$ (total absorption cross-section);
$(\lambda_{tr}) \equiv$ (total transport mean free path);
and
$(K^2) \equiv$ (material buckling).

The integral in equation (2) can be expanded as

$$\int_E^{E_f} \frac{1}{1 + \left(\frac{\Sigma_a}{\Sigma_{SH}} + K^2 \frac{\lambda_{tr}\,\lambda_{SH}}{3}\right)} \cdot \frac{dE}{E}$$

$$= \int_E^{E_f} \left[1 - \left(\frac{\Sigma_a}{\Sigma_{SH}} + K^2 \frac{\lambda_{tr}\lambda_{SH}}{3}\right) + \ldots\right] \frac{dE}{E} , \qquad (4)$$

where higher terms are neglected, since the quantity in parentheses is small compared to unity, being of the order of the mean free path divided by a characteristic dimension of the reactor, squared. Since Σ_{SH} can be written as $\xi\Sigma_S$ (ξ is the average mean log energy loss, taken as 1 for hydrogen and zero for the other, nonmoderating elements present), equation (2) becomes

$$\left.\begin{aligned} n(E)E &= n(E_f)E_f \exp - \int_E^{E_f} \frac{\Sigma_a}{\Sigma_S} \frac{dE}{\delta E} \\ &\cdot \exp - K^2 \int_E^{E_f} \frac{\lambda_{tr}\,\lambda_S}{3} \frac{dE}{\xi E} . \end{aligned}\right\} \qquad (5)$$

It remains to be shown that $n(E)E$ is the slowing-down density $q(E)$, defined as the number of neutrons slowing past the energy E per unit time and volume. Since neutrons which do not slow down past a given energy have either been absorbed or have leaked out of the volume under consideration, one can write

$$\frac{dq}{dE} = n(E) \left(\frac{\Sigma_a + \frac{\lambda_{tr}}{3} K^2}{\Sigma_a + \frac{\lambda_{tr}}{3} K^2 + \Sigma_{SH}} \right) . \qquad (6)$$

Using equations (2) and (3), it can be verified by direct substitution that $q(E) = n(E)E$.

Taking $q(E_f) = 1$, equation (5) becomes

$$q(E) = p(E) \ \exp - K^2 \tau(E), \qquad (7)$$

where $p(E) \equiv \exp - \int_E^{E_f} \frac{\Sigma_a}{\Sigma_S} \frac{dE}{\xi E}$

can be identified with the probability of escaping absorption in slowing to energy E,

$$\tau(E) \equiv \int_{E}^{E_f} \frac{\lambda_s \lambda_{tr}}{3} \frac{dE}{\xi E}$$

is the symbolic age of neutrons at energy E, and $\exp -K^2 \tau(E)$ is the probability of escaping leakage in slowing to energy E.

Equation (7) leads directly to the Fermi pile equation in the usual way (cf. Soodak, AECD 2201, p. 30). It should be noted that the age in a hydrogenous medium as defined above has no simple relation to the experimentally determined slowing-down area. The two quantities coincide only for comparatively heavy elements, where the slowing-down follows a Gaussian distribution; for water they differ by a factor of 2.

In view of the assumptions made in this derivation, the usefulness of the age equation can be judged only by the accuracy with which it checks experimental results. Accordingly, the critical masses of a series of water-moderated reactors were computed for a range of atomic ratios. These results are given below. Experimental data were taken from K-343, *Critical Mass Studies*, Part III, by Beck, Callihan, Morfitt, and Murray.

TABLE 8

COMPARISON OF CALCULATED AND EXPERIMENTAL CRITICAL MASSES FOR BARE CYLINDRICAL H_2O-U(235) O_2F_2 REACTORS

Atomic Ratio H/U-235	Diameter (cm.)	Calculated Height (cm.)	Experimental Height (cm.)	Difference in Critical Mass (per cent)
43.9	25.4	33.2	32.3	3
86.4	25.4	35.6	31.9	12
174	30.5	25.4	24.7	3
320	30.5	31.3	30.3	3
499	38.1	27.2	27.0	1
755	38.1	38.7	41.7	-7
999	50.8	34.3	36*	-5

* Estimated from 29.5 cm.

The accuracy of the method is surprisingly high, and its use in the circulating fuel hydrogen-moderated reactor is warranted.

Reflector calculations. - In the comparison of different reflectors described in section 2.11 of this report, the Garabedian-Householder matrix technique was used to advantage. It reduces the computation required to find the critical core radius of a spherical reactor with two reflectors (two-group theory) from trial and error on an 8th order determinant to trial and error on a 4th order determinant.

2.13 **Critical Experiments.** - Preparing for and executing those critical experiments which give information necessary for the proper design of ANP reactors are now a joint ORNL-NEPA program. The Oak Ridge National Laboratory has been given the over-all responsibility for critical experiments. Dr. A. D. Callihan has been designated the person responsible. The only other personnel at present actively engaged in preparing for critical experiments are NEPA personnel. The extensive preparations and planning which were already under way at NEPA have been accepted without essential change by the ORNL, and are being continued.

During this quarter, it has been decided that the first ANP critical experiments will be on a simulated liquid-metal reactor, in agreement with the idea that the ARE (described elsewhere in this report) is at present envisioned as a liquid-metal type.

The joint laboratory building which is being built to accommodate both Carbide and Carbon Chemicals Division process safety critical experiments and ANP reactor critical experiments is nearly 70 per cent complete--approximately 10 per cent behind schedule. It should be finished in August 1950. (It was originally scheduled to be completed July 15, 1950.) See Figs. 2 and 3 for sketches of the building.

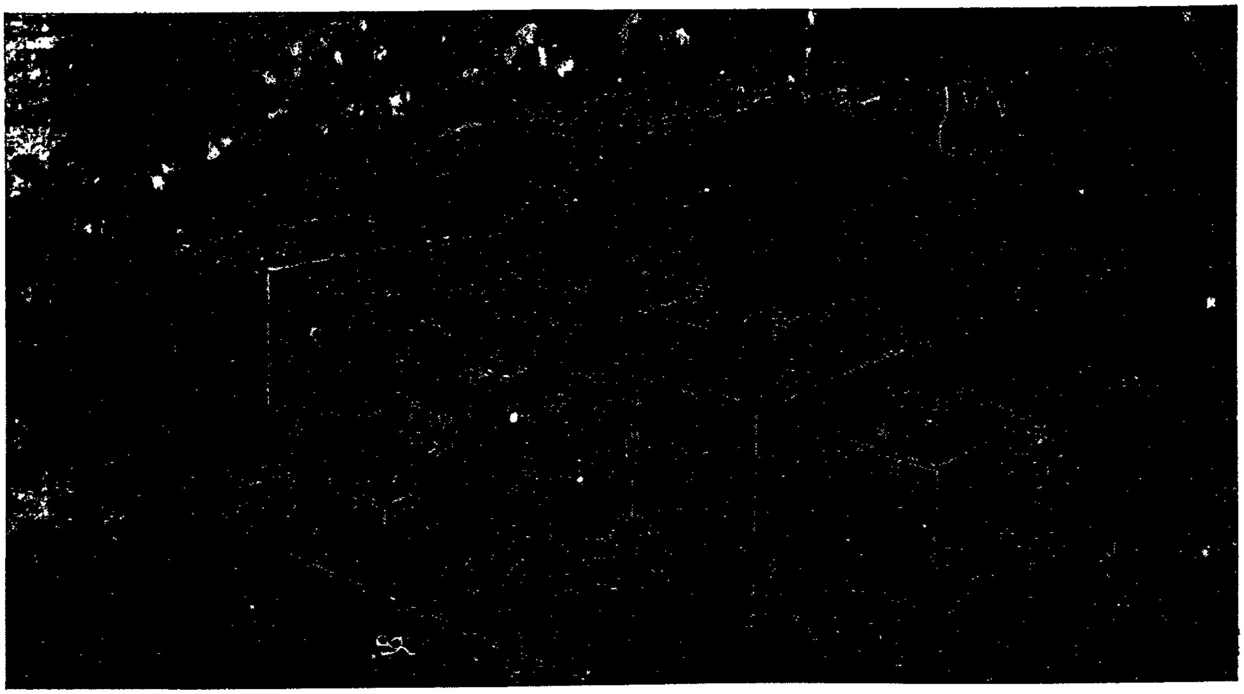

Fig. 2 - ARTIST'S CONCEPTION OF CRITICAL EXPERIMENTS FACILITY

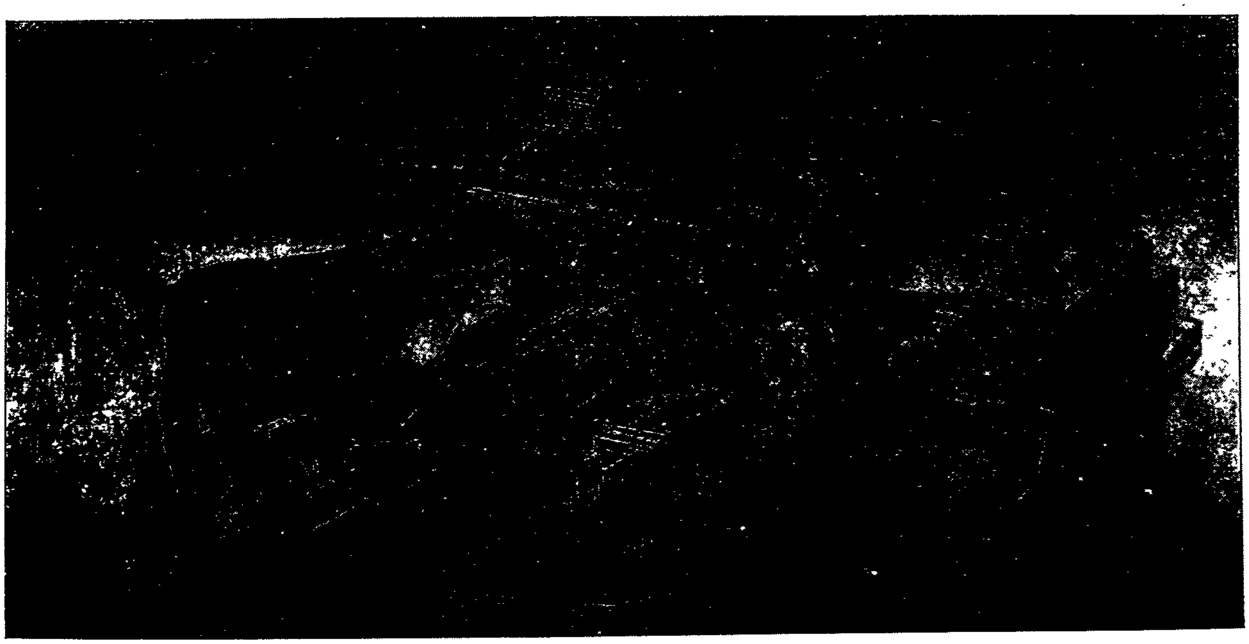

Fig. 3 - ARTIST'S CONCEPTION OF CRITICAL EXPERIMENTS FACILITY (CUTAWAY OF ANP PORTION)

All other phases of preparation for critical experimentation, except that of core material procurement, are proceeding according to schedule. Probably the greatest delay in starting critical experiments will be met in the procurement of a beryllium or beryllium-bearing moderator material in sufficient quantity and purity to be used in the assembly core and reflector. A maximum in experimental flexibility is obtained by the use of the metal itself. Since it is also easiest to handle, it is preferred. Present sources of the purified beryllium metal are insufficient to supply the needs of the critical experiment program in sufficient time to keep up with the procurement of other equipment. A delay of several months in construction of a beryllium-moderated core will be encountered unless some major source of beryllium can be found. A request for an allotment of beryllium metal for the ANP critical experiments has been placed with the AEC by the ORNL. A request for an allotment of uranium^{235} has also been placed by the ORNL. High-density graphite for use in the core, either alone or in conjunction with the beryllium, has been ordered by NEPA.

Fig. 4 shows the method of assembling an experimental fuel rod which closely duplicates a nuclear composition which might occur in a metal-cooled aircraft reactor. The moderator and diluents are simulated by fabricating blocks of the material and placing them on the rod in a suitable arrangement. The uranium is present in the form of disks which can be placed to provide the desired uranium distribution. If lithium or sodium is used as coolant, it will be placed in stainless steel cans with central holes to permit stringing on the retainer rod (as in the case of graphite or bismuth blocks).

The general arrangement of the assembly equipment is shown by artist's sketch in Fig. 5. During the quarter, the operation of the assembly table, which is now set up at NEPA, was tested with a 20,000-pound static load on the movable half. The movable half is driven by a controlled-speed electric motor. Limit switches are located at intervals to reduce the speed in increments as the movable half approaches a closed position. No difficulty was experienced in the mechanical or electrical operation.

Tests were started on prototype safety and control rods mounted on the assembly table. Deflection tests were performed on the square aluminum tubing to be used in the honeycomb. This was done by loading a bank of tubes with lead bricks. The load simulated in weight a 5-foot bismuth-cooled reactor with a 0.3/1 free-flow ratio. This was considered to be equal in weight to the maximum load which the honeycomb would experience in any likely criticality experiment. The observed deflection in the bottom row of tubes was only 0.005-inch, which is considered satisfactory. There was no apparent buckling of the tube walls.

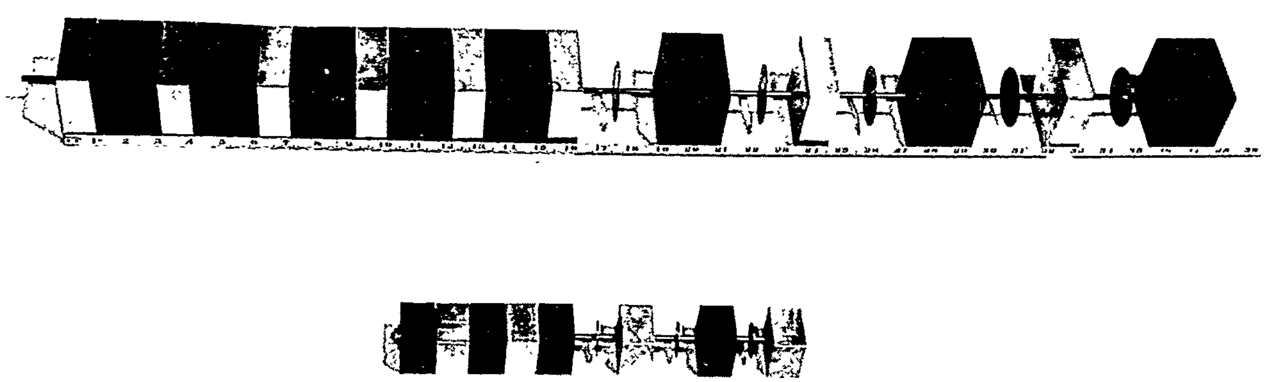

Fig. 4 - EXPERIMENTAL FUEL ROD ASSEMBLIES

153 C35

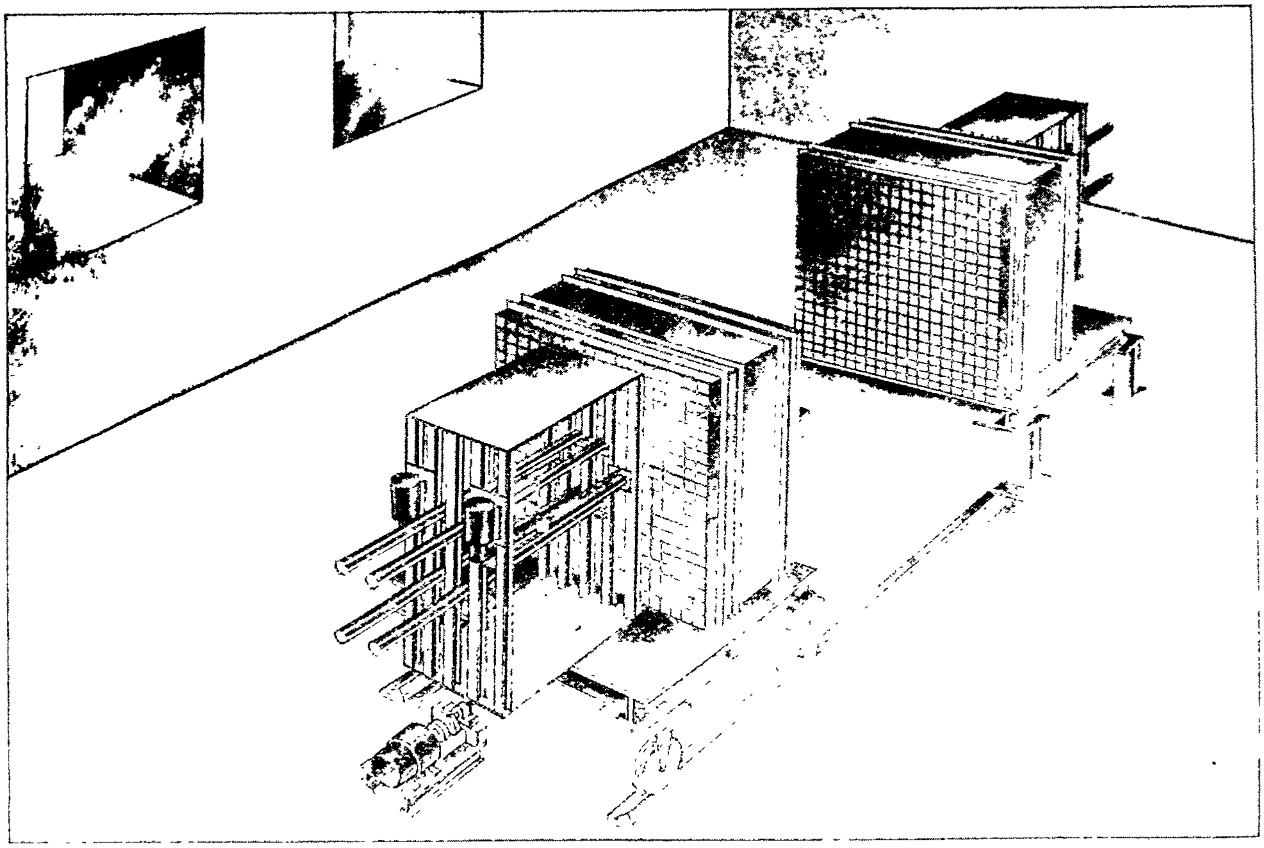

Fig. 5 - ARTIST'S CONCEPTION OF CRITICAL EXPERIMENTS RIG

An order was placed for fabrication of a sample section of the aluminum honeycomb.

The over-all system for electrical control and interlock of the assembly table and control and safety rods has been worked out and tested in part. Control room equipment is being assembled in a mock-up of the control panels.

Training of the operating crew is proceeding satisfactorily. Of the five NEPA men currently designated for the operating crew, four have had experience at other sites. During the quarter, two of these men spent some time at the General Electric criticality site at Sacandaga, New York.

2.2 GENERAL REACTOR STUDIES AND DESIGN (6.3 Man-months)

2.21 **Open Cycle.** - No general design work was done on the open-cycle reactor during this quarter.

2.22 **Compound Liquid-Coolant Cycle.**

Choice of core-circuit liquid-metal coolant. - During the quarter, the choice of bismuth as the core-circuit coolant was re-examined in the light of the change from the unit shield to the divided shield as the basis for design studies. This change has been discussed in section 3.5, page 78, of the preceding quarterly report, NEPA 1374-IPR-52. In spite of its relatively poor characteristics as a heat-transfer medium, bismuth was

TABLE 9

DESIGN DATA, SODIUM-COOLED AND BISMUTH-COOLED REACTORS: PHASE I

Item	Design Point		Landing	
	Bi	Na	Bi	Na
Weight flow rate, lb./sec.	6,974	845	6,974	845
Velocity through reactor, ft./sec.	10.6	15.6	10.6	15.6
Average coolant entrance temp., °F	1229	1229	802	802
Average coolant exit temp., °F	1643	1643	1671	1671
Max. coolant exit temp., °F	1747	1747	1888	1888
Max. reactor wall temp., °F	1769	1755	1933	1905
Absolute pressure at reactor entrance, psi.	118	107	118	107
Absolute pressure at reactor exit, psi.	78	100	78	100
Pressure drop through reactor core, psi. (including entrance and exit losses of flow passages)	40	7	40	7
Thrust force due to core pressure drop, lb.	28,800	5,000	28,800	5,000
Flow passage Reynolds No.	210,000	470,000	210,000	470,000
Uranium investment (all effects plus radial flattened power distribution), lb.	~ 250	~ 250	~ 250	~ 250

selected originally because of its very good gamma shielding characteristics. Bismuth itself does not become gamma active, its high density enables it to retain radiation from gamma-active impurities within it, and its circulating system can be designed to provide shielding against gamma activity in the reactor core.

In the more recent divided shield concept, the crew compartment and reactor are separated as much as possible, and gamma shielding is provided by a combination of shadow shielding at both of these locations. In this arrangement, the gamma activity and shielding characteristics of the core coolant are no longer the controlling factors; therefore, heat-transfer characteristics become an important consideration in the selection of the coolant.

On this basis, both lithium^7 and sodium are being considered. Lithium^7 is outstanding in almost all respects except the almost prohibitive cost (currently estimated) of producing a sufficiently pure isotope. Sodium is also an excellent heat-transfer fluid and is being given preferred consideration as a substitute for bismuth in the Phase II application for the following reasons:

1. A great amount of experimental and development work has already been done on sodium

systems for other nuclear and commercial applications, although this work has been limited to relatively low temperature ranges.

2. A lithium[7] system, which may eventually prove to be feasible and desirable for at least the more advanced applications, is probably more closely simulated by a sodium system than by a bismuth system.

Table 9 compares sodium-cooled and bismuth-cooled reactors for the Phase I XB-52 aircraft.

This table is based on the same average entrance and exit temperatures for both coolants. The advantage of sodium therefore appears here in the form of lower pressure drop through the reactor and, consequently, the lower thrust force imposed on the reactor structure (see section 4.11).

A comparative weight estimate of the two core-circuit systems, including all components, was made on the basis of layouts illustrated in Figs. 6 and 7. The layouts show the primary gamma shield heavy layer, equivalent to 5 inches of lead,

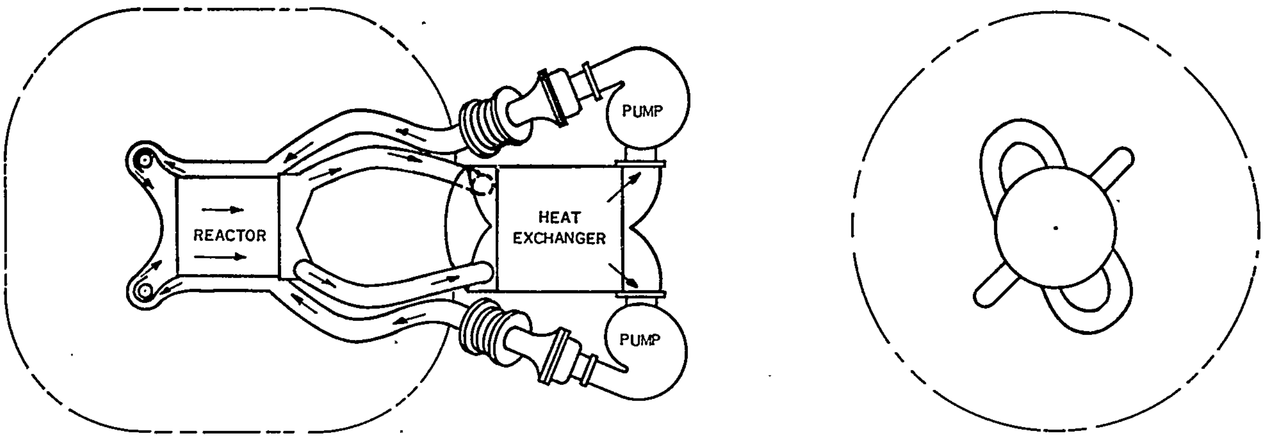

Fig. 6 - PHASE I BISMUTH CORE CIRCUIT, SCHEMATIC

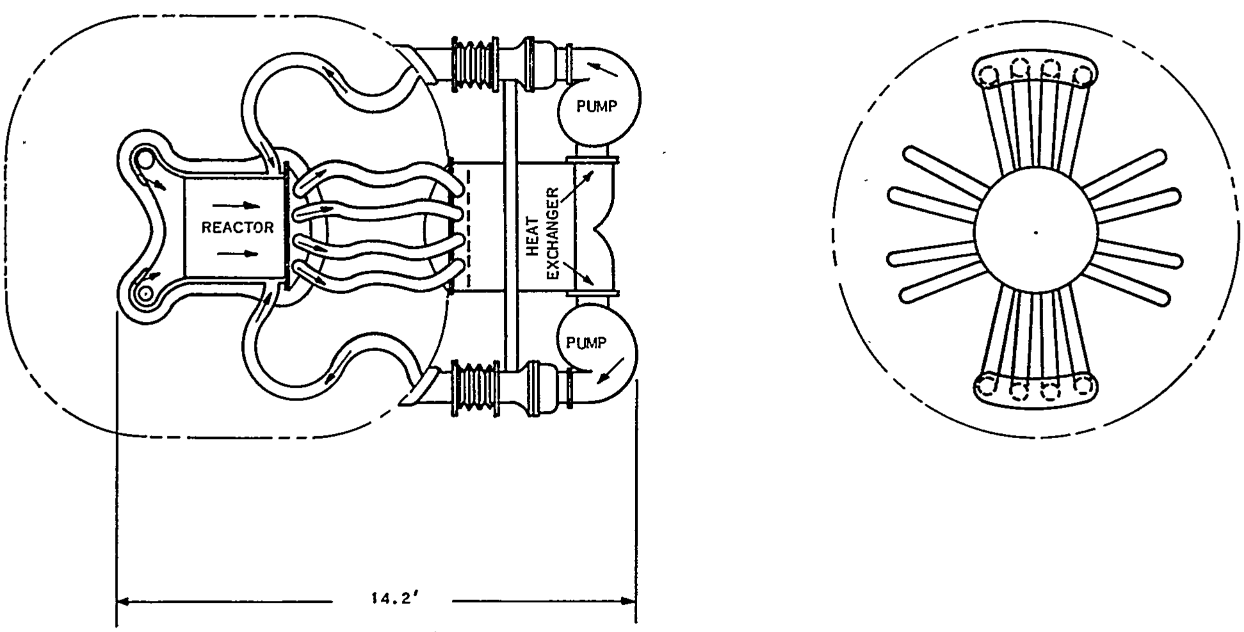

Fig. 7 - PHASE I SODIUM CORE CIRCUIT, SCHEMATIC

wrapped closely around the reactor core and reflector. This arrangement favors the bismuth system, since the bismuth coolant in the core header spaces and in the annular flow area around the core serves the purpose of the heavy layer. In the sodium system, the equivalent weight of this gamma shield layer, in the form of wolfram carbide, is greater, because the layer is located around the outside of the core mounting mechanism and header volumes. The core-mounting mechanism is described in section 2.22, page 35, of the preceding quarterly report, NEPA 1374-IPR-52.

These layouts result in an over-all weight of 93,000 pounds for the sodium system, compared to 105,000 pounds for the bismuth system. In both systems, the weight of the shielded reactor assembly, including the coolant contained therein, is approximately the same: ~ 85,000 pounds. This occurs because the greater weight of bismuth, in the bismuth system, is balanced by the greater weight of the gamma shield layer in the sodium system. In both systems, the combined structural weights of heat exchanger, pumps, and ducts are also very nearly equal: ~ 8,500 pounds. The 12,000-pound difference in over-all weight results primarily from the high density of the bismuth in these components outside the shield.

This estimate of weight difference is in itself not decisive in view of the uncertainty of some of the layout details on which the comparison is based. However, it seems likely that refinement of designs will further favor the sodium system for the following reasons:

1. Optimum shield configurations currently being studied do not utilize a gamma shield heavy layer close to and surrounding the reflected reactor core (see section 3.5). The bismuth system may therefore lose some of the advantage of the dual function of the bismuth in this capacity.

2. The use of sodium permits more flexibility in the design of the circulating system. Pressure-drop calculations are currently based on idealized flow conditions and smooth flow passages throughout the system. With a heavy liquid such as bismuth, pressure drops are appreciable, even for these conditions. Therefore, refinements in the design of the circulating system are more likely to incur serious pressure drop penalties (and consequently structural weight penalties) with the bismuth system than with the sodium system. This might be a critical item within the reactor core, where increase in structural weight probably means increase in uranium investment.

Metallic reactor. - During this quarter, an intensive investigation of reactor designs based on the use of metallic structure and fuel element canning was undertaken. The use of metal is considered for the liquid-coolant cycle reactor, because in this case, the maximum wall surface temperature can probably be kept below 2000°F. The object of these studies is to determine whether a metallic reactor core structure can be designed to withstand the temperature distortions and acceleration loads of aircraft application better than the ceramic moderator type of structure. The basic requirement in these studies is that a minimum amount of structural and canning metal be used in the core to prevent uranium investment from becoming excessive.

Molybdenum has been selected as the initial fuel element canning material and basic structural material within the core for the following reasons:

1. High-temperature strength: Wall temperature may approach 2000°F in some parts of the reactor core. Molybdenum has some structural strength at these temperatures, and has a very high melting point (~4700°F).

2. Corrosion resistance: Preliminary corrosion tests indicate that molybdenum probably will not react with liquid-metal coolants such as sodium, lithium^7, or bismuth, if the coolants are sufficiently free of impurities such as oxides, carbides, and nitrides.

3. Nuclear properties: At the start of this investigation, available data gave only a

thermal absorption cross-section of 2.6 barns for natural molybdenum. From a 1/v extrapolation, it appeared that molybdenum could be used in a liquid-metal–cooled reactor of 2.5 to 3 feet diameter with an investment of less than 200 pounds of uranium[235] provided that: (1) the molybdenum occupied only about 15 per cent by volume of core; (2) the reflector was 5 inches thick; and (3) the moderator was essentially beryllium. However, the additional cross-section data received during this quarter, and discussed in section 2.11 of this report, indicate somewhat less favorable values. Therefore, the permissible volume of molybdenum in the core may be less than 15 per cent (see section 2.11). Further investigation is necessary before the over-all effect of these new data can be evaluated. However, two alternative can be immediately suggested:

a. Molybdenum[92] is known to have a much lower thermal cross-section than natural molybdenum. The separation of isotopes is a very costly process and may not be feasible.

b. Metals (such as stainless steel) which have satisfactory resistance to corrosion and better nuclear properties may be substituted for molybdenum in the cooler portions of the of the pile, where temperatures are not excessive.

From the above considerations, the following modification of the specifications for the IL1 aircraft under landing approach conditions were selected as the basis for these design studies:

Reactor coolant	sodium
Core diameter (ft.)	2.5
Reflector thickness (in.)	5
Reflector outside diameter (ft.)	3.33
Max./avg. power, longitudinal	1.25
Max./avg. power, radial	1.07
Avg./min. flow	1.18
Power (Btu./sec.)	250,000
Sodium inlet temperature, °F.	800
Sodium outlet temperature, °F, average	1670
Sodium outlet temperature, °F, maximum	1900
Sodium flow, lb./sec.	950

The investigation thus far has developed the following alternate approaches to three basic aspects of the design:

1. Flow-tank versus flow-channel core configuration: Reactor designs based on the use of ceramic moderator as the structural material within the core generally confine the coolant flow within continuous channels through the fuel-bearing moderator, as illustrated in Fig. 8. This ceramic type reactor is discussed in detail in the preceding quarterly report, NEPA 1374-IPR-52.

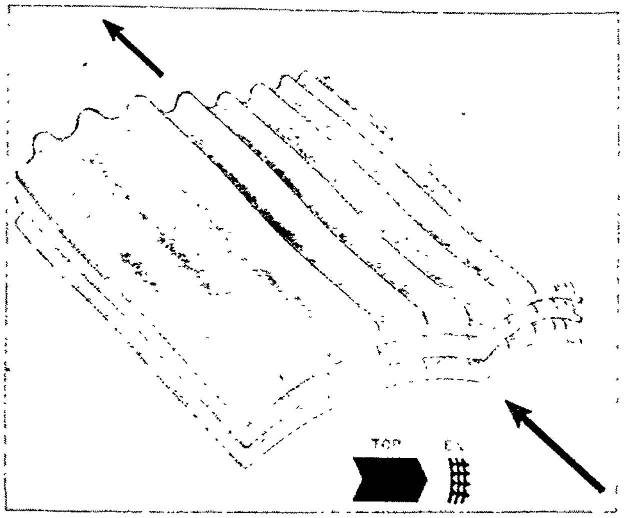

Fig. 8 - CERAMIC FUEL ELEMENTS

The use of metal for canning fuel elements suggests the possibility of spanning lengths of the coolant-filled reactor shell with the canned fuel elements, so that they are surrounded and separated by the flowing coolant. Fig. 9 illustrates this with the fuel elements in the form of canned rods.

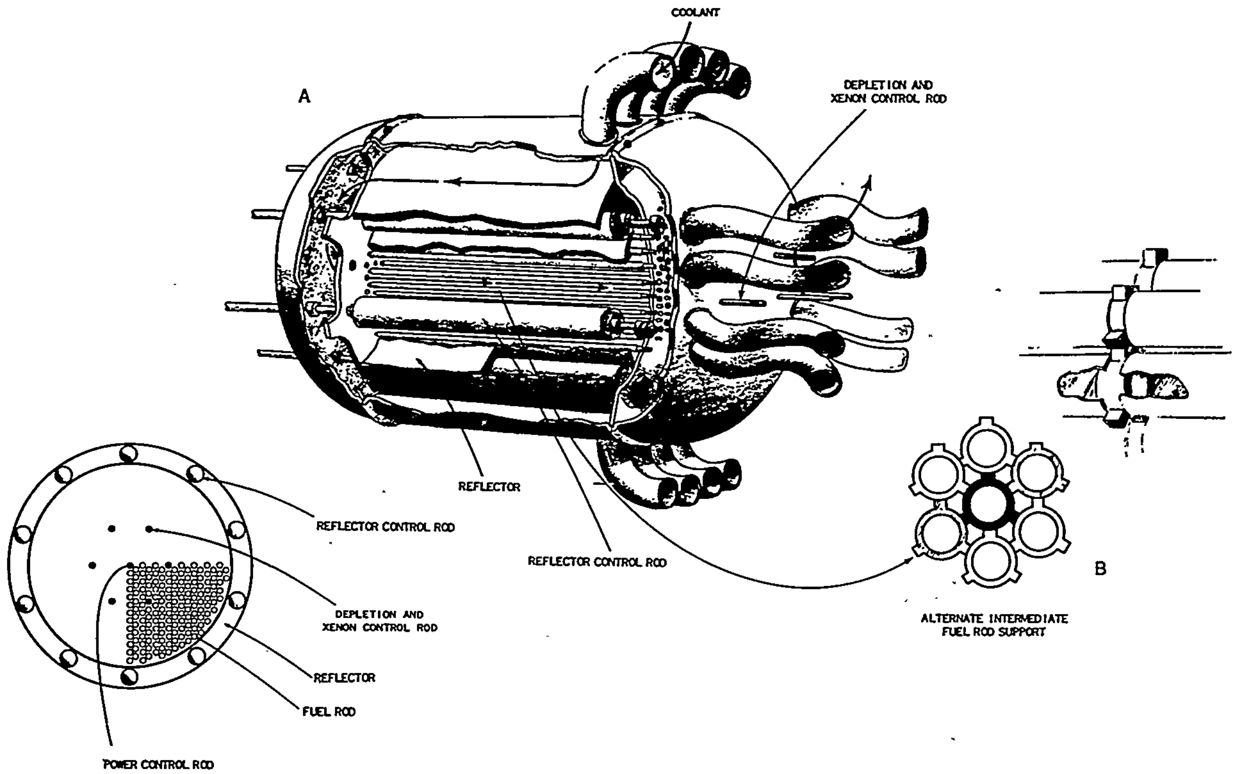

Fig. 9 - FUEL-ROD TYPE REACTOR DESIGN

Several features of this approach are of interest. Thermal expansions and distortions can occur locally to some extent without affecting the rest of the structure. Cross-current circulation of the coolant across the fuel elements can occur, possibly preventing major local hot spots from forming in the core. In comparison to a tubular channel configuration, the rod arrangement gives the same flow and heat transfer surface areas with a coarser configuration; i.e., a smaller number of larger fuel elements. This is desirable in order to reduce the weight of metal canning material.

2. The use of special metallic structure within the core to supplement or replace the fuel element cans as load-bearing structure: Fig. 9 illustrates an approach to the one extreme of using only the fuel element can for structure within the core. Fig. 12 shows an approach to the opposite extreme, using a metallic box grid within the core to support groups of fuel and moderator elements. The principal advantage in this case is that the box grid metal does not contain heat-producing fuel, and therefore will operate at lower temperature than the metal in the fuel element cans. These designs are discussed in detail later.

3. Canning of fuel and moderator together versus separate fuel and moderator elements: Fig. 10 illustrates a fuel element rod consisting of uranium-bearing moderator contained within the metal can. A small amount of liquid

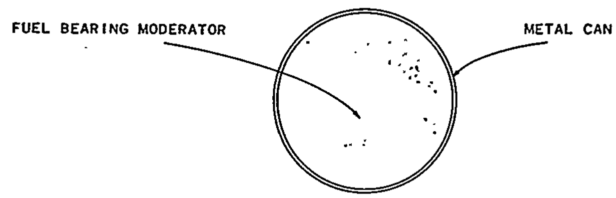

Fig. 10 - METALLIC FUEL ROD (FUEL IN MODERATOR)

metal is included within the can as a heat-transfer agent in the interface between the moderator and can. The requirement to minimize the amount of metal in the core can best be met by using a small number of large-diameter fuel rods. However, the temperature at the center of the rod increases rapidly as rod diameter is increased. One way to minimize this temperature effect is to sandwich the fuel, in the form of a uranium dioxide–molybdenum metal-ceramic, between the double walls of the can, as shown in Fig. 11. This

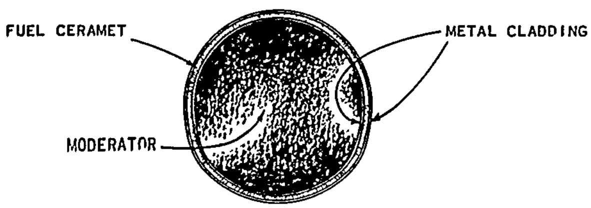

Fig. 11 - METALLIC FUEL ROD (FUEL SANDWICH WALL)

design does not use the metal in the can efficiently from the heat-transfer standpoint, since only one of the double walls of the can is in contact with the coolant. Therefore, as an alternative, consideration is being given to configurations in which alternate layers of fuel sandwich and moderator are separated by coolant streams. Fig. 14 shows one such arrangement for use in the box grid design of Fig. 7.

The designs discussed in this report are of an exploratory nature. The final reactor design will probably represent some compromise among the extreme design alternatives discussed above.

Beam and column loading are basic characteristics of the open structure of the designs discussed below. Therefore, deflection, buckling, and creep at high temperature are critical stress problems. Some preliminary work has already been

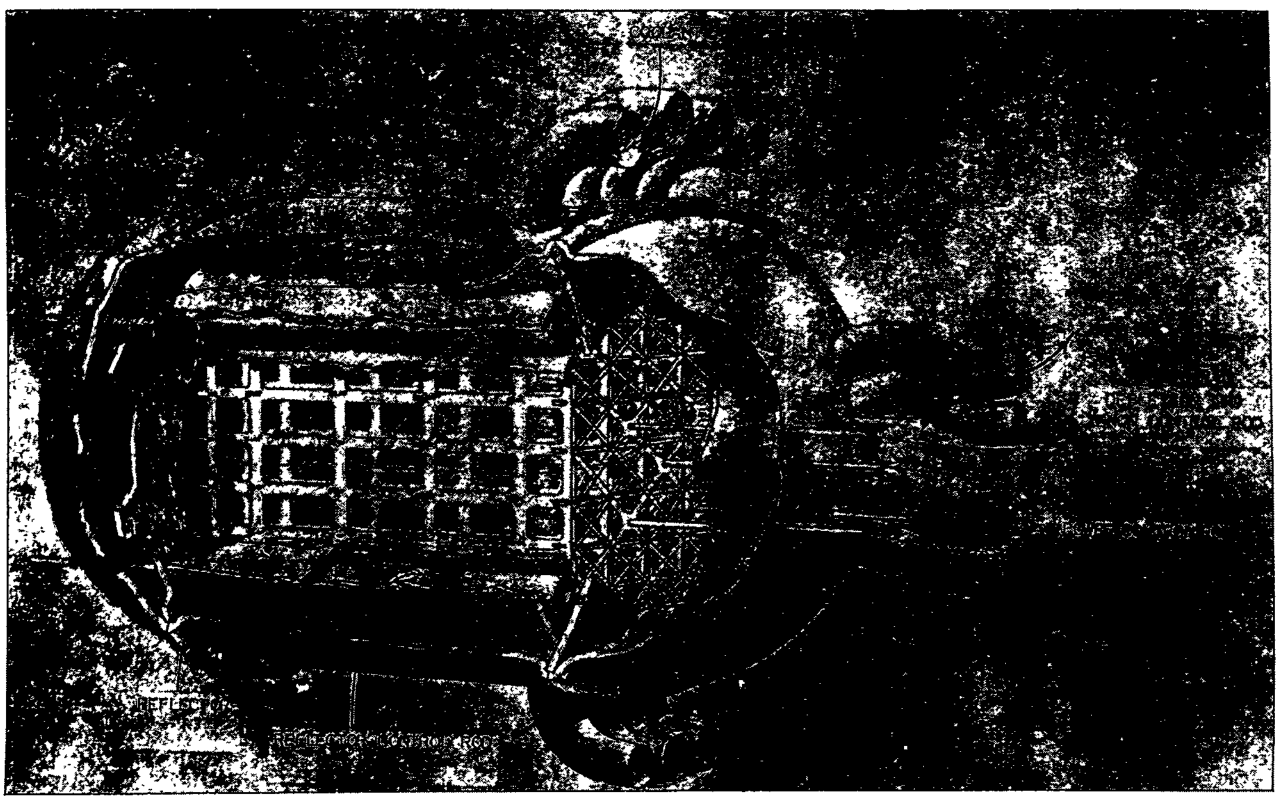

Fig. 12 - PHASE I SODIUM CIRCUIT REACTOR; METALLIC BOX-GRID CORE

done, but, as a basis for more refined stress analysis, a careful study is being made of the direction, magnitude, and duration of aircraft maneuver and gust loads, and the safety factors with which they must be applied to the reactor structure. A study is also being made of analytical procedures for calculating combined elastic, creep, and temperature stresses and deformations.

Reactor fuel rod design. - The first proposal (shown in Fig. 9 (a)) consists of a round tube design utilizing combination fuel and moderator elements canned with molybdenum and supported at each end in tube sheets. In addition to the specifications listed above, the following conditions prevail:

Tube diameter (in.)	1.05
Tube spacing (in.)	0.106
Tube arrangement	Triangular
Coolant flow-area ratio	0.25/1
Core pressure drop (psi.) . . .	10
Core velocity (ft./sec.)	20
Maximum fuel-rod surface temperature (°F)	2000
Tube wall thickness (in.) . . .	0.020

In this proposal, there are approximately 600 tubes with a maximum length of 45 inches. The 30-inch center sections of the tubes contain fuel, while the end sections are reflector only. Seven of the tubes are replaced with control rods. The ends of the tubes are necked down to 0.25-inch to fit into tube sheets so that each tube is a simple beam freely supported at each end. There are no intermediate supports or spacers in this configuration. Provision must be made to provide stops and clearance for lengthwise expansion of the rods.

The tube sheets are curved to reduce stresses induced by coolant pressure drop across the reactor core from inlet to outlet. With proper stiffening, a plate thickness of approximately 2 inches would probably be required to keep stresses to an allowable maximum of 5,000 pounds per square inch. This plate will have holes for both the coolant flow and the fuel rods. If the number of fuel rods increased appreciably, it might be difficult to maintain the 0.25/1 free-flow ratio in the tube sheet. Since the tube sheet is not subjected to maximum temperatures approaching 2000°F (as in the fuel elements) it is reasonable to assume that it can be made from a stainless steel such as type 310 (25 Cr - 20 Ni) rather than from molybdenum. The tube sheets have radial extensions or spokes which engage radial slots in the outer structure and provide mounting and centering for the reactor core. This arrangement permits expansion of the core relative to the container without loss of centering.

Stress analysis of the basic rod design in the horizontal position shows that total deflection is marginal when using a single span. For a 1.05-inch diameter tube with 0.020-inch wall thickness, 45 inches long, filled with beryllium moderator contributing weight but no strength, the calculated results are as follows:

Load (g's)	Elastic Deflection (in.)	Max. Stress (p.s.i.)	Estimated Additional Deflection Due to Creep at 2000°F	
1	0.0192	1420	4×10^{-5}(in.)/hr.	0.004(in.)/100 hr.
1.5	0.0288	2130	28×10^{-5}(in.)/hr.	
3	0.0576	4260	0.01(in.)/hr.	0.10(in.)/10 hr.
6	0.1152	8520	0.28(in.)/hr.	
12	0.2304	17040		
18	0.3456	25560		

Since molybdenum has an anticipated 1000-hour stress, for rupture, of 5000 pounds per square inch and an ultimate strength of approximately 30,000 pounds per square inch at 2000°F, the stresses are not considered unreasonable. The extreme maximum stress would probably be encountered under crash-landing conditions—a load of approximately 12 g. The deflections, however, become so large that intermediate supports are desirable, if not wholly essential. During the life of a reactor (100 hours) a total deflection of 0.220-inch would occur. This deflection would consist of an elastic deflection at 6 g of 0.115-inch, plus a 10-hour creep deflection at 3 g of 0.101-inch plus a 100-hour creep deflection at 1 g of 0.004-inch. If smaller outside diameter fuel tubes are used to reduce the internal tube temperature (this is desirable), deflections are larger and intermediate supports are probably essential.

Alternate fuel rod design. - An arrangement with a single intermediate support is also shown in Fig. 9 (b). Based on the 1.05-inch tube size of the first proposal, the stresses in the table above would be reduced by a factor of 4. This would reduce the estimated additional deflection due to creep to more acceptable values. The elastic deflection would be reduced by a factor of 16, and thus would not be a serious problem.

Several methods of intermediate support are possible and have been laid out. Only one, considered the best, is shown in Fig. 9 (b). Heavy-wall machined connectors are welded to the open ends of each section of tube. Lugs attached to these connectors rest against adjacent tubes and provide proper spacing. The connectors are also heavy-walled enough to carry a load through the middle section of the reactor. The lugs do not appreciably interrupt the coolant flow, and no additional tube sheet is necessary.

In criticism of either of the tubular proposals it can be said that:

a. Apparently, too much metal is required. Calculations show weights of 460 pounds for 1.05-inch tubes with 0.020-inch walls, and 744 pounds for 1/2-inch tubes within the core. This is enough material to cause serious poisoning, particularly if molybdenum is used. Weights could be halved by the use of 0.010-inch-wall tubing.

b. The metallic walls of the fuel elements running at the maximum temperatures of the entire cycle (approximately 2000°F locally) are subjected to serious structural loads.

A more detailed temperature and stress analysis is under way. Further results will be reported during the next quarter.

Box grid reactor design. - In view of the magnitude of the element-wall structural loads noted above, another proposal has been laid out. This configuration (Fig. 12), which shows promise, is a metallic grid structure that supports the fuel elements and the moderator. The structure is surrounded by coolant. The design uses five supports, each having a 4-inch-square section, to reduce the maximum span for a fuel element or moderator section to 10 inches. The design can be adapted to various types of fuel elements which can be made up in 4-inch-square bundles and inserted in the sections. Round rods can be used (Fig. 13) or flat-plate type "sandwich" fuel elements can be inserted with moderator in between (Fig. 14).

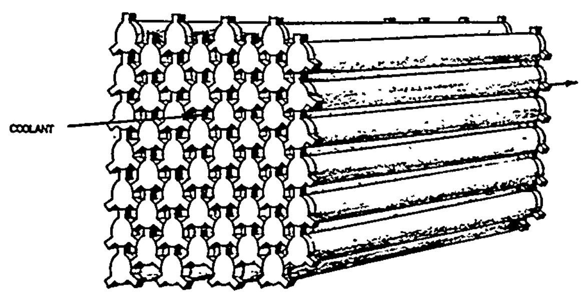

Fig. 13 - METALLIC FUEL RODS (4-INCH-SQUARE BUNDLE)

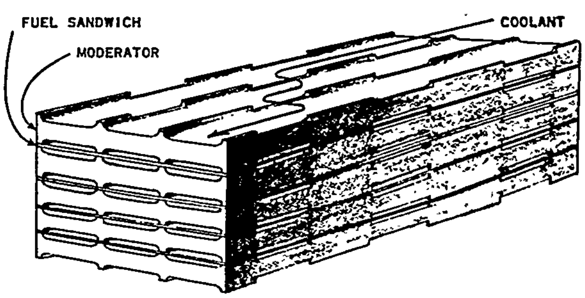

Fig. 14 - SANDWICH TYPE FUEL ELEMENTS (4-INCH-SQUARE BUNDLE)

The structure can be made of sheet-metal sections welded together. The vertical members are 0.100-inch thick. The horizontal members have a thickness of 0.150-inch. This configuration results in a metal (molybdenum) weight of only 50 pounds inside the core, with an additional 13 pounds between the core and the reflector. In this design, the fuel elements do not have to provide much structural strength. They merely rest on a cooler structure already provided. Heavy tube sheets at the ends are not needed; thus, pressure drop through the tube sheets is eliminated. Coarse screens or strips are provided at the ends to retain the fuel elements. The supports are located so that the fuel elements can be made up in convenient short lengths to allow easy assembly or replacement. Nonuniform longitudinal or radial distribution of uranium can be accomplished easily. The fuel is relatively easily removed without destroying the entire reactor. This makes for ease in testing and fuel recovery.

The entire core-and-reflector assembly is mounted internally on the pressure shell by means of front and rear rings with a radial spline arrangement similar to that described for the tubular design. Since the front and rear rings were held together through the grid, it is possible to remove the entire core and reflector as a unit for servicing.

Reactor control rods and actuators. - Present ideas about control rod configuration have been influenced mainly by the effects of the rods on density distribution, reactor design, and safety. Two types of rods are now proposed:

1. Rods, situated longitudinally in the reactor reflector, which rotate through 180° and position absorbing material either close to the core or approximately the reflector thickness away from the core.

2. Rods moved axially into or out of the reactor core proper.

A total of seventeen rods is currently assumed. There are ten reflector type rods, whose diameter is approximately equal to the reflector thickness, with the absorber material introduced as a section of the periphery. Seven core rods are assumed. One of these is centrally located in the core; the other six are equally spaced on the circumference of a circle having a radius of four-tenths that of the core. Fig. 15 shows some of the mechanical details of reflector and core rods and their installation in the reactor.

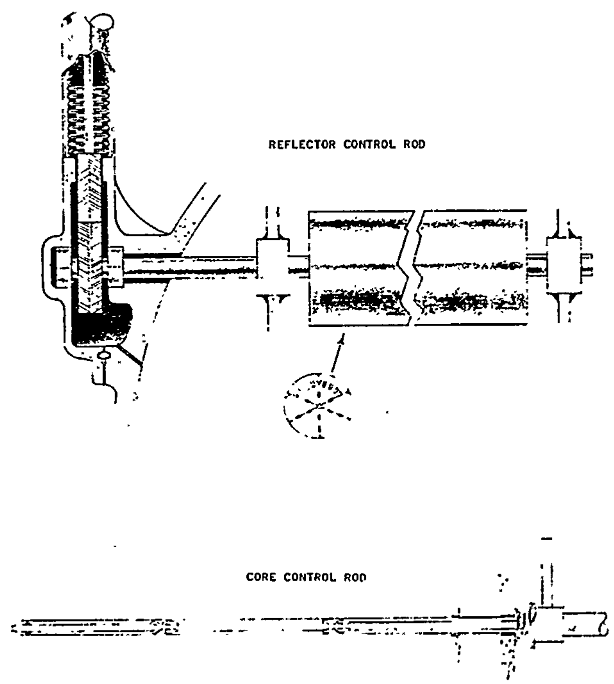

Fig. 15 - CONTROL ROD DETAILS

Actuation methods for both types of rods are being investigated. Methods of interest include the use of the magnetic clutch and mechanical movement, hydraulic, pneumatic, or solenoid actuators, or hybrid types embodying desirable features of all. These classes are named in order of choice at present, but all are being thoroughly investigated.

The control rods are intended to operate as follows:

1. Reflector rods are designed to control temperature-reactivity effects, and will be rotated from the "in" position to the "out" position as the reactor temperature is changed from cold to the operating range. These rods will be individually actuated for safety purposes and may be used as shutdown controls with very short operation times.

2. The six core rods positioned concentrically at four-tenths of the core radius will be used to compensate for reactivity changes caused by depletion, xenon poisoning, etc. These rods also will be individually actuated for safety use.

3. The center rod will be used to make dynamic power control changes and will be constructed with only enough reactivity effect to make these changes within the times needed to meet transient demands. The center rod is desirable for power control because the power distribution is not radically disturbed by movement of the rod, provided that the fuel is properly distributed in the core.

All rods but the center one will be stepped individually through predetermined distances. Movement of the outer rods will occur when the center rod reaches a certain displacement from its central position. This method of control has the advantage of extreme positioning accuracy for the greater number of rods, and the positioning accuracy of the dynamic control rod is given greater latitude. The outer rod motion will be insensitive to small, rapid oscillations of the central rod.

The reflector control rod mechanical design shows a thin-tube shell with welded end pieces (used to decrease the diameter to that of the bearing journal). The core coolant will be allowed to flow inside this tube and around the reflector and absorber material for cooling. Coolant flow metering may be obtained by a metering orifice within the angle drive and trunnion shaft. Longitudinal strengthening ribs are to be welded to the tube interior; these form positioning stops for the material segments. The reflector material may be fabricated in sectors to fit closely (but not attached) to the tube. Sectors are used so that needed coolant passages may be grooves on the sector faces. The absorbing material covers a 120° arc on the rod periphery with sufficient thickness to provide the desired absorption.

The core rods will be inserted into the core and pressure-shell assembly with a canning tube around each rod. This tube can is sealed from the core coolant, and the actuator end is sealed to the pressure shell. An auxiliary coolant fills the space between the tube can and the absorber rod. The absorber rod is supported within the tube can by a roller and universal linkage. This linkage breaks the rod into three pieces, allowing deflections within the core without binding of the control rod.

Present estimates indicate that each reflector and core rod (with exception of the center rod) should supply approximately 1 per cent reactivity change. The center rod reactivity effect can be made smaller than 1 per cent--probably small enough to insure that the reactor does not become supercritical by an amount greater than the delayed neutron contribution. This would prevent the dynamic control rod from being capable of making the reactor prompt critical. The servo-actuator specifications are tentatively set to control the power within plus or minus 3 per cent, and to have frequency response well above expected power fluctuation frequencies, which are assumed to be 10 cycles per second or less.

Fig. 16 shows schematically a shielded reactor assembly with an arrangement of mechanical drives between the control rods and servo actuators. Since the type of servo actuator has not yet

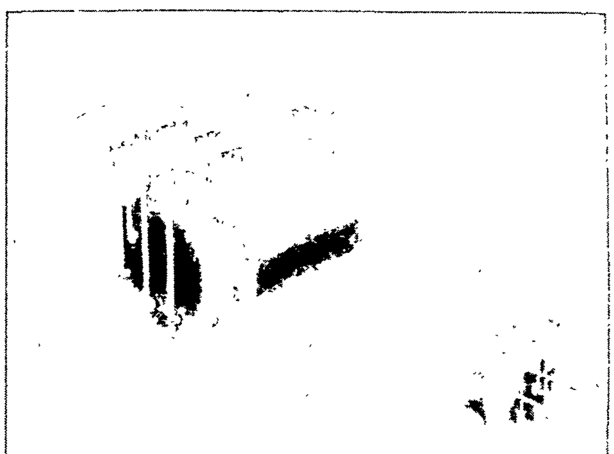

Fig. 16 - CONTROL ROD DRIVE TAKE-OFFS

been selected, only the general locations are indicated here. While a multiplicity of actuators introduces undesirable complexity, individual actuators for each rod have been used for safety reasons. The actuators may be arranged radially around the reactor, but this drawing shows them staggered and brought to the top (to facilitate gas sealing and prevent the escape of liquid coolant or core fluid in case of mechanical seal failure).

2.23 **Compound Helium Cycle.** - No general design work was done on the compound helium cycle during this quarter.

2.24 **The ARE.** - The Oak Ridge National Laboratory has started planning a small experimental reactor as a part of its share of the ANP program. This reactor is to be as nearly as possible a replica of the reactor finally selected for the first nuclear powered aircraft, except that its power level will be of the order of 1000 kilowatts instead of a few hundred thousand kilowatts. It has been decided that the planning of this reactor (the ARE, aircraft reactor experiment) will be based on the assumption that it will be of the liquid-metal–cooled type. Since the ARE is supposed to be of the same type as the final aircraft reactor, and since the type of the latter has not yet been chosen, it is evident that the planning of the ARE at this time is somewhat general. Accordingly, the ORNL has turned to an exploration of the problems of high-powered metal-cooled aircraft reactors in an effort to arrive at the design which the ARE is to simulate. NEPA also is engaged in this work, and is assisting the ORNL in other parts of the ARE programs, including reactivity analyses and reactor control.

If the cycle finally chosen for the ARE is not the liquid-metal cycle, the planning of the ARE will shift to the cycle chosen.

2.3 REACTOR MATERIALS
(219.4 Man-months)

During this quarter, increased emphasis has been placed on investigations of metallic materials for both the reactor proper and the heat exchanger. The work on molybdenum–uranium oxide has been expanded. Creep testing of this system should start during the coming quarter. Other compositions involving beryllium and its alloys are being given a cursory examination. Testing of possible heat exchanger materials has been extended to include sodium as a coolant. In addition to the agitator tests on various materials, creep testing of type 347 stainless steel in sodium has been begun. It is expected that there will be reportable data on solubility and creep during the coming quarter.

As a result of the 5th coatings conference held at Battelle Memorial Institute, the coatings testing committee convened at Oak Ridge for a special meeting. It was decided that the time for testing a prototype element under simulated operating conditions had arrived, as any further real progress on coatings will be dependent upon a better understanding of the operational problems.

Thermal stress studies have resulted in shifting the emphasis on beryllium carbide matrix bodies from the 88 per cent beryllium carbide – 12 per cent carbon composition to one of 70 per cent beryllium carbide – 30 per cent carbon. The latter composition appears to retain a sufficient amount of self-healing (as evidenced by the formation of a beryllia film) upon exposure to air. Coating studies now in progress will aid in further evaluating this composition.

2.31 **Air-Cycle Materials.**

Synthesis of beryllium carbide. - A total of approximately 150 pounds of nominal grade beryllium carbide powder was prepared for NEPA by the Fansteel Metallurgical Corporation. This significant increase in quantity is due primarily to the setting up of production schedules and the use of highly compacted mixtures of the reactants. Yields of from 75 to 88 per cent of theoretical are now being attained. Be_2C content is being maintained above 94 per cent; in several instances batches analyzing 96 per cent Be_2C have been made. The following is a typical analysis:

Be_2C	94.82 per cent
BeO	1.13
Be_3N_2	2.94
$BeO \cdot H_2O$	0.10
Free C	0.96
Free H_2O	0.06
SiO_2	0.05
Total	100.06 per cent

As reported last quarter, the difficulty of obtaining pure beryllium carbide is related to the presence of nitrogen. The nature of the solid solution of beryllium nitride (Be_3N_2) in beryllium carbide is now evolving. Beryllium carbide and beryllium nitride are considered to be ionic structures, with beryllium carbide being referred to a face-centered (anti - CaF_2) structure, and beryllium nitride to a body-centered (Mn_2O_3) structure. The latter structure may be thought of as a distorted calcium fluoride structure, with one-quarter of the beryllium atom sites vacant. As nitrogen atoms displace carbon atoms in the structure (with distortion and shrinkage of the lattice), beryllium atoms are also displaced, and these are reconstituted with nitrogen atoms to form additional beryllium nitride in solid solution. The system then consists of beryllium nitride in solid solution in beryllium carbide, beryllium carbide in solid solution in beryllium nitride, and carbon set free to form graphite. It is now thought that nitrogen-free material may be produced, and a determined effort will be made during the coming quarter to do this.

Fabrication studies of beryllium carbide–base bodies. - In an attempt to improve the thermal stress resistance of beryllium carbide–graphite bodies with the least sacrifice in the moderating power of the body, thermal stress specimens containing 70 per cent grade 46 beryllium carbide and 30 per cent graphite have been fabricated by hot-pressing techniques. Densities of 2.3 to 2.35 grams per cubic centimeter were achieved. The variations in density were apparently a function of the initial grain size of the beryllium carbide. The two mesh sizes studied were minus 200 and minus 325. Higher densities were obtained with the finer carbide particle size. These densities are as high as those of previously fabricated bodies containing higher carbide percentages. Fabrication of the 70-30 composition thermal-stress tubes presented no major difficulties.

The incorporation of uranium in fuel element bodies may significantly influence the thermal stress resistance of the element. A number of beryllium carbide–base bodies containing normal uranium carbide additions have therefore been prepared for thermal stress testing. A powder mixture containing 78 per cent of an 88 per cent beryllium carbide – 12 per cent graphite mixture and 22 per cent uranium carbide was hot pressed into a high-density tube at 2000°C (3630°F). However, a liquid constituent, presumably rich in a beryllium–carbon–uranium eutectic, was exuded from the compact during pressing. A representative photomicrograph of the body is presented in Fig. 17. This structure consists of massive beryllium carbide grains (gray) in a network of uranium dicarbide (white) and contains free graphite. This structure is generally similar to those observed by Battelle for sintered beryllium carbide–uranium carbide specimens containing no free carbon.

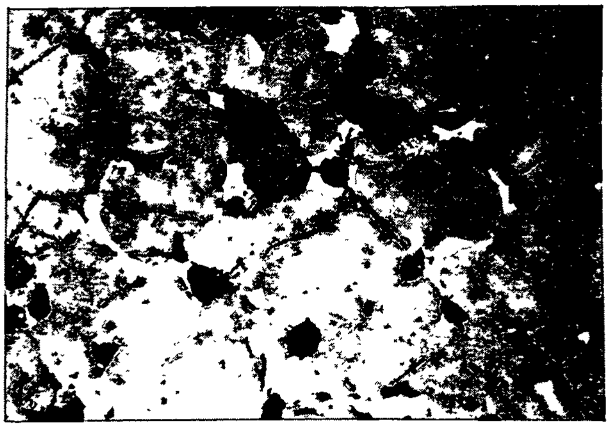

Fig. 17 - PHOTOMICROGRAPH OF HOT-PRESSED BERYLLIUM CARBIDE–GRAPHITE–URANIUM CARBIDE BODY (500X)

Recent information indicates that the eutectic composition contains approximately 5 per cent beryllium by weight.

Thermal cycling. - Of interest to the matrix materials program is the influence of repeated thermal cycling on various physical properties of reactor components. Standard modulus-of-rupture bars (2 1/4 inches by 1/4 inch by 1/8 inch) of hot pressed 88 per cent grade 46 beryllium carbide–12 per cent graphite (atomic composition: Be_2C + 1/3C) were heated from room temperature to 2500°F in 1 1/2 minutes in a protective hydrogen atmosphere. After soaking at 2500°F for 3 minutes, the samples were cooled to within a few hundred degrees of room temperature in approximately 2 minutes. This procedure was repeated for each cycle. Specimens were tested after two, five, ten, and twenty-five cycles. The specimens were loaded to failure in the standard flexure test to obtain the modulus of rupture and modulus of elasticity. The specific electrical resistance of both halves of each broken specimen was then measured. The resulting data are plotted in Fig. 18.

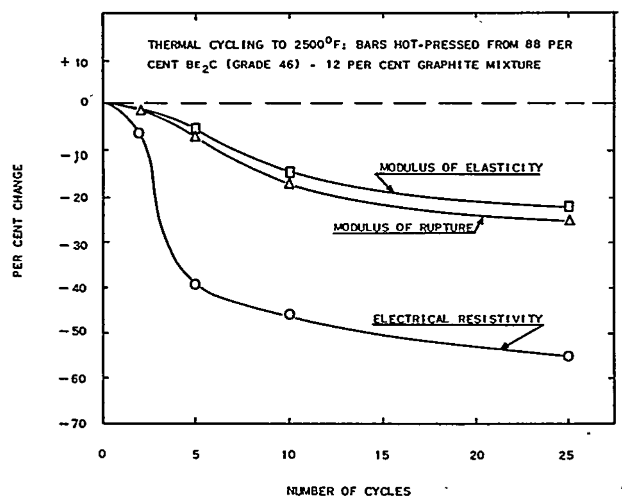

Fig. 18 - EFFECT OF THERMAL CYCLING ON THE CHARACTERISTICS OF Be_2C–GRAPHITE BARS

Thermal cycling is seen to decrease the modulus of elasticity, the strength, and the electrical resistance of the mixture. The effects are most pronounced during the first ten cycles. In this region, approximately two-thirds of the total decrease in the strength and stiffness occurs, along with over three-quarters of the total electrical resistivity decrease. There is a further decrease up to twenty-five cycles, but the curves tend to flatten in this region.

This experiment was of an exploratory nature, and certain limitations are evident. The relatively thin bars may not be as susceptible to thermally induced stresses as other more complex or larger shapes. Contaminants in the hydrogen atmosphere may have reacted with the specimens and contributed to the observed changes. Carbonaceous decomposition products from the graphite cover also may have had a similar influence, especially on the electrical resistivity values. Analysis of these specimens (now in process) and further cycling tests should provide additional information.

The thermal expansion of 100 per cent beryllium carbide (grade 46), beryllium carbide–graphite, and graphite is shown in Fig. 19. The beryllium carbide–base bodies were prepared by hot pressing. It is significant to note that a 12 per cent graphite addition has no effect on the expansion of beryllium carbide, and that as much as 50 per cent graphite addition lowers the expansion but slightly. The average expansion of the KS graphite is seen to be much lower than that of beryllium carbide with or without the graphite addition. A series of resistance measurements were conducted to investigate heating methods to be used

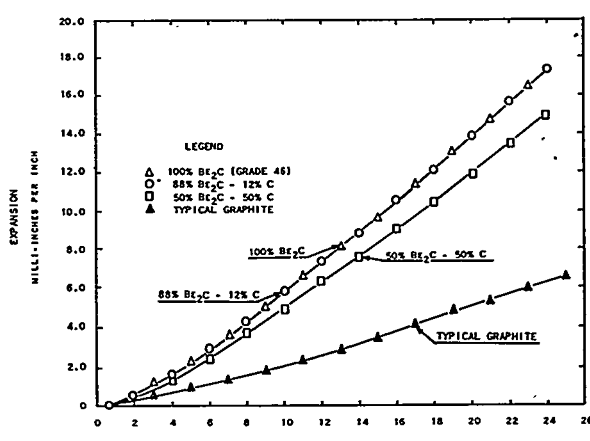

Fig. 19 - EXPANSION OF BERYLLIUM CARBIDE, GRAPHITE, AND BERYLLIUM CARBIDE-GRAPHITE MIXTURES

in coating experiments, and also for correlation of the "before-and-after" tests of the radiation damage program.

The specific electrical resistance of 100 per cent grade 46 beryllium carbide was observed during repeated heatings to temperatures in excess of 2000°F. All tests were conducted in a vacuum to minimize oxidation and nitriding of specimens. The following trends were noted:

1. Data on virgin specimens agree over the entire temperature range.

2. During the second runs, the specific resistance is generally higher than during the initial runs.

3. After the first run, the specific resistance values do not agree quantitatively, although the curves all have the same general shape. At higher temperatures, the curves converge and are similar. The specific resistance is dependent upon the highest temperature reached in the previous tests.

4. The resistivity decreases sharply above room temperature, reaching a minimum between 100° and 150°F, and rising to a maximum near 500°F. Between 500°F and 1000°F, the resistivity decreases rapidly, followed by a gradual decrease as the temperature increases to 2500°F.

In Fig. 20, data are plotted for two consecutive runs on duplicate specimens. These are typical of the many tests of which have been conducted.

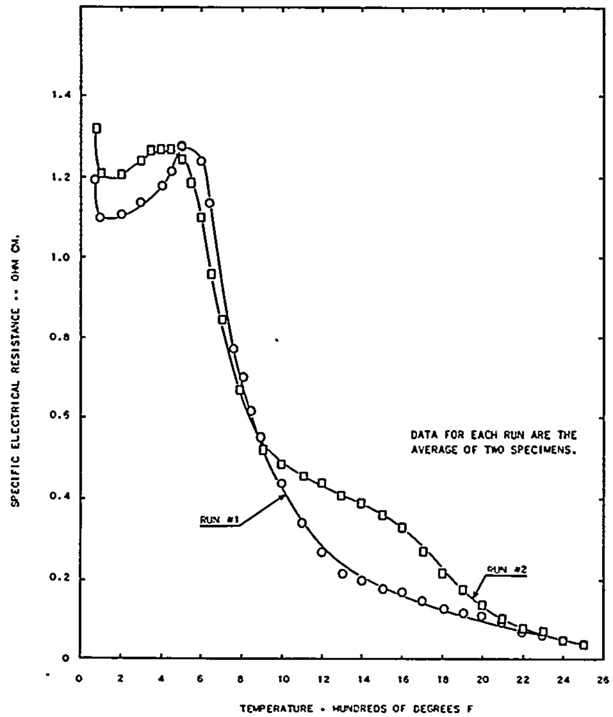

Fig. 20 - EFFECT OF TEMPERATURE ON THE SPECIFIC ELECTRICAL RESISTANCE OF GRADE 46 BERYLLIUM CARBIDE

Thermal emf of beryllium carbide. - During the course of the electrical resistance experiments, some anomalous results were obtained. A surprisingly high thermal emf was developed by a beryllium carbide–molybdenum differential thermocouple formed by the molybdenum potential leads and the beryllium carbide specimens. The emf's developed at each end of the specimen are in opposition and should tend to nullify each other. However, the beryllium carbide–molybdenum thermocouple was so effective that an appreciable emf was generated by the relatively small thermal gradient along the length of the specimen.

Tests were conducted with platinum as a reference leg to determine the magnitude of this emf output. Since, at present, beryllium carbide bodies cannot be fabricated into wire form, it was necessary to measure emf as a function of the temperature differential caused by heating one end of a rod. With a relatively short rod of 100 per cent grade 46 beryllium carbide, the emf generated was 65 millivolts for a differential of 250°F. Using a longer rod of 90 per cent beryllium carbide–10 per cent graphite, the emf generated was 175 millivolts for a differential of 2000°F.

From Fig. 21, it may be seen that the beryllium carbide–versus–platinum emf output is many times greater than the output of conventional thermocouples such as chromel versus alumel or platinum

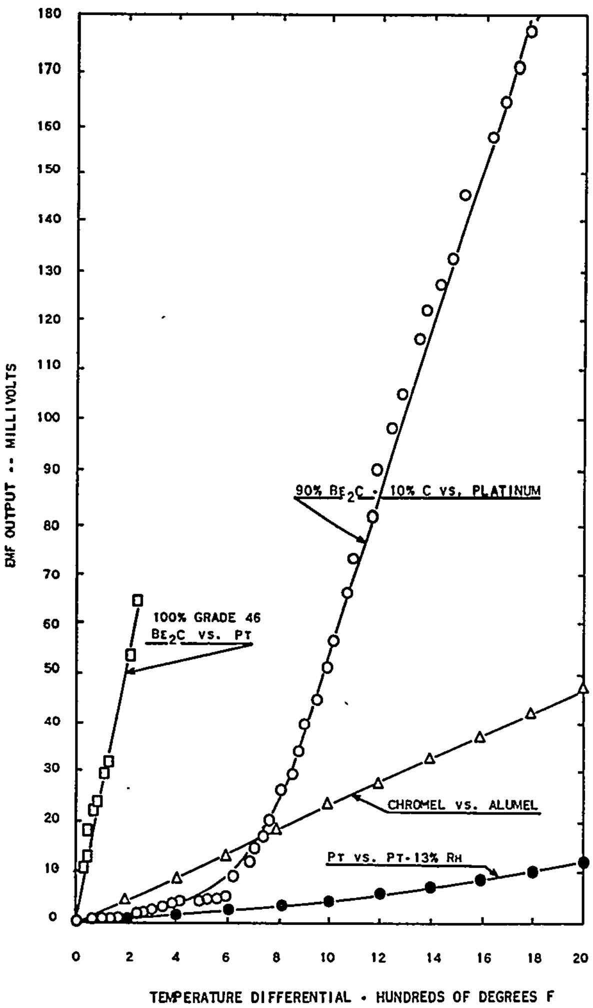

Fig. 21 - THERMAL EMF OUTPUT OF BERYLLIUM CARBIDE-CARBON BODIES VS. PLATINUM AS A FUNCTION OF TEMPERATURE DIFFERENTIAL

versus platinum-rhodium. It is also significant that the addition of 10 per cent graphite to grade 46 beryllium carbide greatly diminishes the emf output below 600°F. Above this temperature, the slopes of the curves are similar. Near 600°F, the electrical resistivity of beryllium carbide drops sharply as the temperature is increased.

Although platinum wire was chosen as one leg of the thermocouple because it is a usual standard, a much higher emf output can be attained using molybdenum with the beryllium carbide.

Since the "cold" ends of the beryllium carbide rods in these tests were heated by conduction from the "hot" ends, the curves may be displaced somewhat from those obtained using a "cold" end at constant temperature.

Beryllium carbide shows promise for accurate temperature determinations to a fraction of a degree over a small temperature range as a constituent of a high-emf-output high-temperature thermocouple, and as a self-contained specimen with a minimum of lead wire in which the change in emf output may be a measure of radiation damage.

Flexure testing of beryllium carbide. - The results of a series of flexure tests conducted on microspecimens of beryllium carbide are presented below, with previously obtained data on larger specimens. The specimens were machined from grade 46 beryllium carbide hot pressed at 3632°F and 2500 pounds per square inch. It may be seen that the specimen size and shape do not greatly influence the values obtained.

To determine the effect of previous strain history upon the modulus of elasticity in flexure, a cyclotron specimen was loaded and unloaded four times to a maximum outer-fibre stress of 6500 pounds per square inch. A trend toward stiffening of the material was noted, but at the higher stresses the slopes of the deflection curves were similar. Thus it appears that the load applied to determine elasticity before irradiation will not in itself appreciably affect the modulus of elasticity after irradiation.

The Battelle Memorial Institute program on sintering of beryllium carbide–base bodies has been de-emphasized. Some of the specimens of beryllium carbide–matrix bodies prepared containing uranium carbide have exhibited more strength than others. One specimen in particular, fired in the usual manner, showed a modulus of rupture value of 22,200 pounds per square inch. Photomicrographs of this specimen are shown in Fig. 22. The rounding of the beryllium carbide grains is attributed to limited solubility at the sintering

TABLE 10

FLEXURE TEST DATA, Be_2C MICROSPECIMENS

Type Specimen	Span Length (in.)	Specimen Width (in.)	Specimen Thickness (in.)	Breaking Load (lb.)	Modulus of Rupture (psi.)	Modulus of Elasticity (10^6 psi.)
Be_2C cyclotron	0.375	0.275	0.025	3.1	10,300	10.2
Be_2C cyclotron	0.375	0.275	0.025	3.8	12,400	16.9
Be_2C cyclotron	0.375	0.275	0.025	3.1	10,100	15.6
Be_2C cyclotron	0.375	0.200	0.036	4.6	10,000	10.1
Be_2C flexure	1.0	0.252	0.127	28.5	10,400	
Be_2C flexure	1.0	0.266	0.126	19.1	10,200	12.5
Be_2C flexure	1.0	0.243	0.125	20.3	12,000	18.2
Be_2C flexure	1.0	0.244	0.125	19,9	11,700	23.6

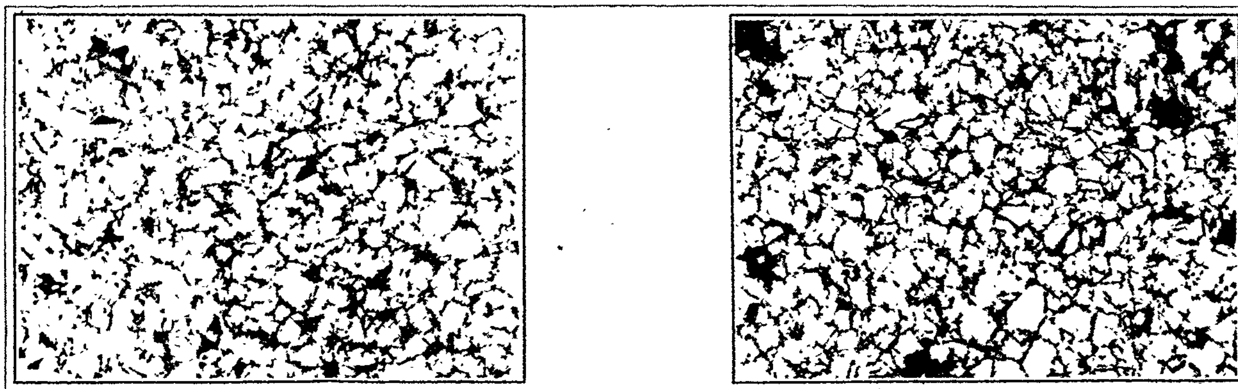

SPECIMEN A 100X SPECIMEN B 100X

PHASES	APPEARANCE
URANIUM-BEARING MATERIAL	BRIGHT WHITE
BERYLLIUM CARBIDE	LIGHT GRAY
BERYLLIUM OXIDE	DARK GRAY
VOIDS AND CRACKS	BLACK

Fig. 22 - PHOTOMICROGRAPHS OF POLISHED SECTIONS OF SPECIMEN HUM-77

temperature, with formation of a liquid phase of beryllium carbide in uranium dicarbide. The uranium compounds were reported to have a significantly expanded lattice.

Beryllium carbide–beryllium body fabrication. - Experimental hot pressings were made of a 50 per cent minus 200 mesh beryllium carbide, 50 per cent minus 200 mesh beryllium metal (by volume) mixture. Temperatures from 1175°C to 1250°C (2150°F to 2280°F) and pressures of 1800 pounds per square inch to 2300 pounds per square inch were used. Hot pressing was conducted in a hydrogen atmosphere. Densities 92 per cent to 95 per cent of theoretical were obtained. Fig. 23 is a photomicrograph of the 95-per-cent dense specimen. The excess of voids resulted from dislodging beryllium carbide particles during polishing. Fig. 23 also shows a 2500X photomicrograph which indicates the absence of any noticeable reaction zone between beryllium (white) and beryllium carbide (gray). These compacts were pressed within a molybdenum liner to avoid reaction between beryllium and the graphite dies. Under these conditions, beryllium reacted with the molybdenum. A similar reaction was observed in experiments conducted for the liquid-metal cycle, and is discussed under section 2.32.

Beryllium carbide–beryllia bodies. - An investigation of the effect of carbide particle size on the thermal-stress resistance of beryllium carbide–beryllia matrix bodies has been continued. Thermal-stress tubes have been machined from massive hot-pressed bodies containing 40 per cent minus 325 mesh beryllia mixed with 60 per cent nominal grade beryllium carbide powder.

Physical tests of these specimens are not yet complete. From a fabrication standpoint, little difference has been noted (other than a minor increase in compact density) with reduced carbide particle size. Thermal stress specimens of beryllia containing no carbide additions were hot pressed using minus 325 mesh beryllia, and were submitted for comparative purposes. The average density for these bodies was 2.9 grams per cubic centimeter.

Severe difficulties have been experienced in coring or drilling holes through massive sections of hot-pressed beryllium carbide or beryllium oxide bodies during the machining of thermal-stress specimens. If graphite core rods are used to mold the bores directly during the hot-pressing operation, subsequent shrinkage of the body invariably results in cracking due to differential thermal contractions. A successful method for overcoming this condition was developed. Graphite powders were tamped into a thin-walled combustible tube which served as a compressible core rod with a compression modulus matching the compression modulus of the material being hot pressed. Fig. 24 shows a beryllium carbide-base

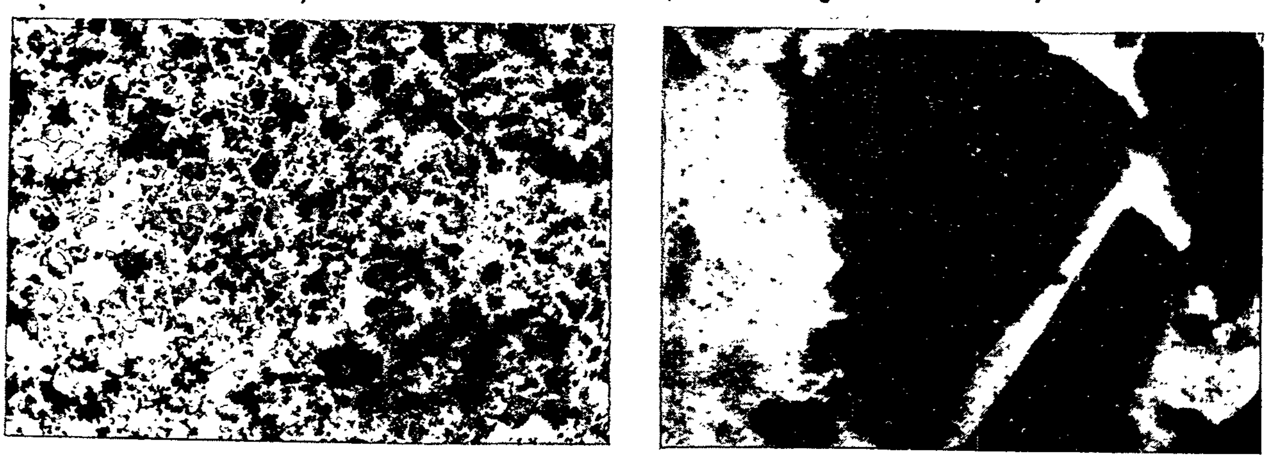

Fig. 23 - MICROSTRUCTURE OF HOT-PRESSED BERYLLIUM CARBIDE–BERYLLIUM METAL BODY. (A) UNETCHED (100X), (B) UNETCHED (2500X)

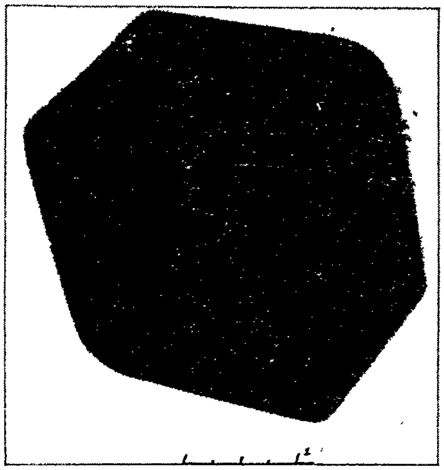

Fig. 24 - MOLDED BERYLLIUM CARBIDE BASE BODY USING NEW TECHNIQUE

body with nine holes molded in this fashion. A photograph of the die and paper tubes preparatory to loading is shown in Fig. 25. This method lends itself to the molding of intricate bores, and is also advantageous in that it provides a more uniform over-all density of the final body.

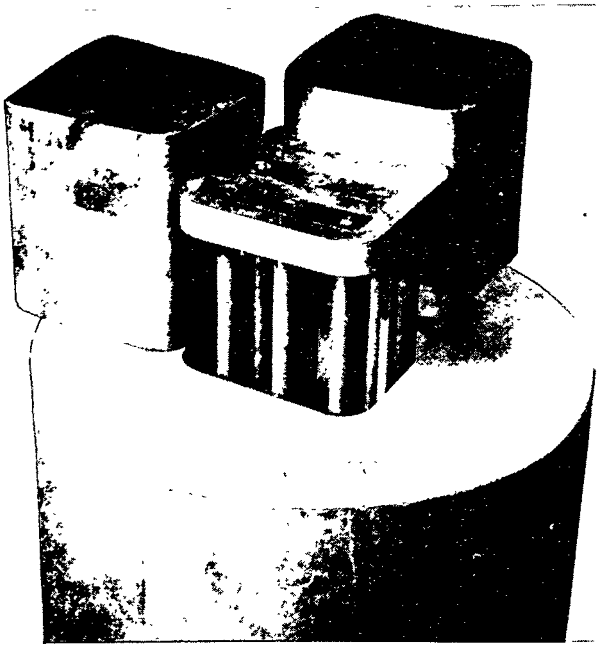

Fig. 25 - DIE ASSEMBLY FOR MOLDING NINE-HOLE SPECIMENS

The effect of sintering beryllium carbide-base bodies under gas pressure is being investigated with Battelle's new pressure-sintering furnace. Since Battelle's usual method of sintering employed temperatures in the beryllium carbide decomposition range, some beryllium was lost through vaporization. The new equipment has lowered the effective sintering temperature by more than 200°F, and provides a sounder body, since the beryllium is retained.

Three-component-system oxide additions (such as barium carbonate–titania-silica) to beryllium carbide–matrix bodies have given an improvement in specimen resistance to oxidation. The resistance to hydration is greater when minus 100 plus 200 mesh oxides are used than when the specimens are prepared from material of finer size.

Thermal-stress testing of beryllium carbide. - Thermal–stress testing was continued during the quarter, using the small apparatus described in a previously quarterly progress report (NEPA 1281).

Tests were run on beryllium carbide mixtures in order to determine their relative resistance to thermal rupture. These specimens were of a standard tubular shape, externally heated by radiation, and internally cooled by radiation to a tube containing an air-water mixture. Temperatures were maintained between 2500°F and 1500°F. One set of samples ranged from pure beryllium carbide through a graduated mixture with beryllia to pure beryllia. The other set of samples ranged from pure beryllium carbide through a graduated mixture with graphite. Mixtures with more than 30 per cent graphite had such a high resistance to thermal stress that it was not possible to maintain temperatures within the 2500°F - 1500°F range and obtain rupture. Fig. 26 is a plot showing the relative resistance to thermal rupture as a function of composition.

In an attempt to break the 50 per cent beryllium carbide–50 per cent graphite mixture, very high power densities were used. As a result, the outer surface of the cylindrical specimen was raised above the decomposition temperature. Smaller

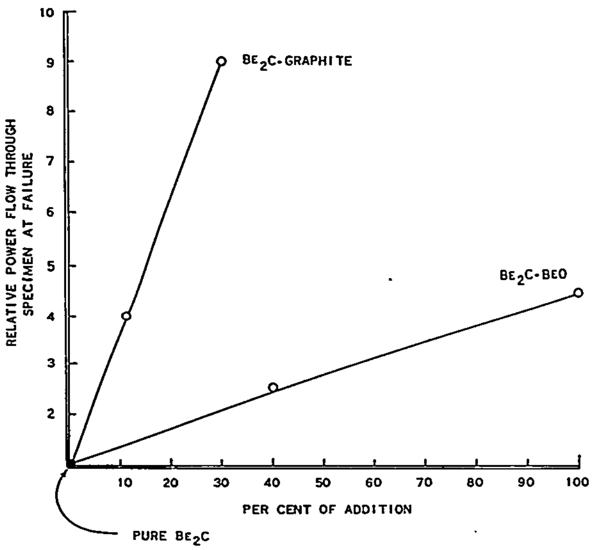

Fig. 26 - RUPTURE RESISTANCE OF STANDARD TUBULAR SPECIMENS; TEMPERATURES 1500° - 2500°F

specimens were used and a heat flow through the specimens of 40 Btu. per cubic inch per second was obtained without indication of thermal rupture. Inasmuch as disassociation was expected at higher power inputs due to excessive temperatures, the test was discontinued.

Additional theoretical work was conducted on calculations of stresses in tubular fuel elements having uniform power generation and internal cooling, with external insulation. The effective thermal stress is represented by:

$$\sigma = \frac{E_{\alpha} W_o}{6\,k} \left(2r_o^2 - r_o r_1 - r_1^2\right),$$

where

w_o = power generated,

r_o = external radius,

r_1 = internal radius,

σ = effective stress, and

k = thermal conductivity.

The small NEPA thermal stress rig will be duplicated by Battelle and used as a screening test mechanism for their body development program. Specimens of alumina–titanium carbide were exchanged with Battelle. The results obtained agreed substantially with the values reported by NEPA.

Coating development. - The underbodies used in coating development studies during the quarter were beryllium carbide with and without uranium carbide, beryllium oxide, and graphite. Graphite bodies are frequently used in preliminary work because they provide a convenient means of evaluating coating conditions, especially where new techniques or new coating compositions are concerned.

In addition to conventional ceramic methods and vapor decomposition methods of applying coats, studies have been made with two new techniques of coating deposition: (1) decomposition of metals by cathodic sputtering; and (2) impregnation by liquid coating materials.

Work has been continued during the quarter on several coating compositions, including silicon carbide, molybdenum silicide, metallic coats, vitrified ceramic enamels, refractory oxide combinations, and metal-ceramic compositions.

Coating with silicon carbide. - In order to complete the evaluation of silicon carbide as a coating material for graphite, Battelle Memorial Institute coated a number of samples and subjected them to oxidation testing. From incomplete data on these tests, which are still in progress, the average life of the coated specimens is 670 hours at 2500°F in slowly moving air. One sample has been protected for 1400 hours; others have failed due to defects at various periods up to 500 hours. When the thickness of the coat exceeds 15 mils, a long life may be expected; when the coat is less than 15 mils thick, it may contain defects leading to early failure. The cause of these defects has not yet been determined, but they may be occasioned by improper application of the coats.

Coating with metals. - Platinum precipitate coatings brushed onto Be_2C-matrix specimens and sintered in air at 2550°F yielded apparently uniform coatings, which, however, permitted the formation of an interfacial layer of beryllium oxide between the platinum coating and the underbody. This layer, shown in Figs. 27 and 28, "grew" from approximately 0.0003 inch, as sintered, to approximately 0.002 inch after 250 hours of exposure at air at 2500°F. An increase in the original firing temperature increased the metallic appearance of the coats, but they had relatively poor oxidation and thermal shock resistance. The best specimen exhibited no visible creaks at a magnification of 12X after thermal shocking through fifteen heating and cooling cycles.

A new approach has been made to coating underbodies with metals through the use of cathodic sputtering. Instead of trying to meet all the necessary requirements in a single coating, this procedure may permit the use of a prime coat as an intermediate layer between the body and the cover coat to relieve stresses set up by poor fits and provide good anchorage for cover coats. The equipment built for this application is shown in Fig. 29.

During the preliminary work, the importance of experimental variables, such as spacing between electrodes and symmetry of electrodes, was determined. Thin uniform layers of platinum on

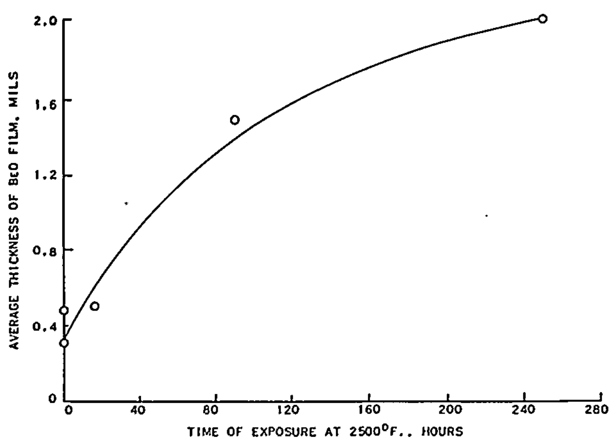

Fig. 27 - GROWTH OF THE BERYLLIA INTERFACE DURING EXPOSURE OF PLATINUM-COATED BERYLLIUM CARBIDE SPECIMENS AT 2500°F

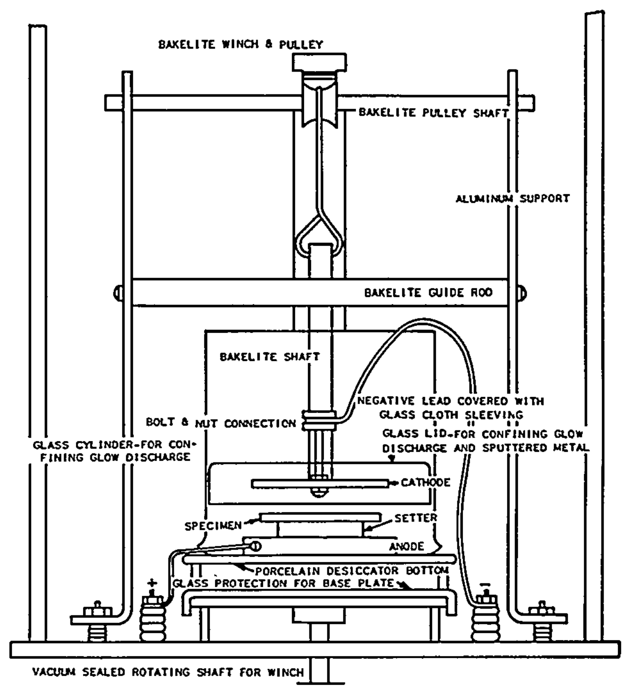

Fig. 29 - APPARATUS FOR CATHODIC SPUTTERING

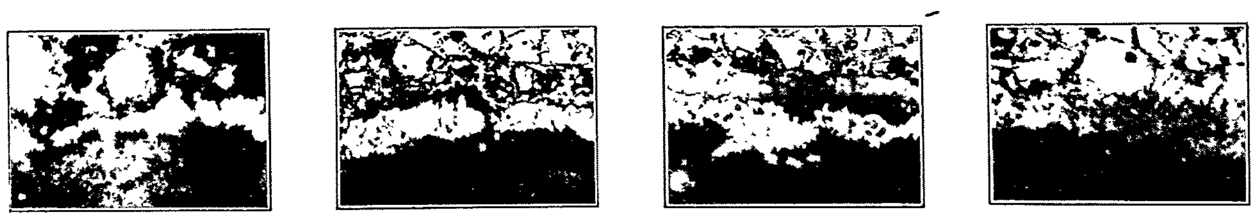

500X AS SINTERED.

250X AFTER 17½ HOURS' EXPOSURE.

250X AFTER 90 HOURS' EXPOSURE.

250X AFTER 250 HOURS' EXPOSURE.

Fig. 28 - PHOTOMICROGRAPHS OF BERYLLIUM OXIDE INTERFACE AFTER EXPOSURE OF PLATINUM-COATED SPECIMENS AT 2500°F

graphite have been obtained. Beryllium carbide bodies were also successfully coated with platinum. Coating with molybdenum offers more experimental difficulties, as sputtering characteristics vary from one metal to another. The next step will be the evaluation of the layers obtained in comparison with coatings deposited by other methods.

Molybdenum silicide coatings. - Vapor-decomposition methods of applying molybdenum coatings onto beryllium carbide have thus far been unsuccessful. In attempts to coat with molybdenum by the vapor-deposition method, using molybdenum carbonyl as source of the metal, it was found that instead of the expected pure molybdenum, the coatings formed consisted of a mixture of the oxides of molybdenum, molybdenum carbide, and molybdenum metal. When molybdenum pentachloride was used for the deposition of the molybdenum layer, oxide and carbide were also found in the coating. Attempts to form molybdenum silicide by overcoating these mixtures with silicon followed by heat treatment to produce a diffusion alloy resulted in spalling or destructive side reactions. The presence of free carbon in the beryllium carbide body makes the deposition of pure molybdenum and its subsequent reaction with silicon very difficult. Reports by other laboratories on the successful use of molybdenum carbonyl, in spite of the $CO \rightleftharpoons CO_2$ equilibrium, are puzzling.

Vitrified ceramic enamels. - To date, the high melting glazes (mainly silica, with smaller amounts of titanium, lithium, barium, sodium, and aluminum oxides) appear to offer one of the best approaches for protecting beryllium carbide—matrix bodies. The cooperative work between the A.O. Smith Corporation and NEPA laboratories has yielded ceramic coatings of uniform appearance, free from bubbles, which have withstood over 800 hours exposure at 2500°F in an oxidizing atmosphere. Failure of the test furnace has prevented continuing the test. Preliminary tests of coated beryllium carbide specimens in a cyclotron with a flux of 10^{15} deuterons per square centimeter per second at 1000°C (1832°F) showed no apparent deterioration of the coat or underbody, and no impairment of adherence between coat and underbody (Table 14, section 2.4).

The impregnation method of coating consists of dipping the specimen in a liquid silicone to impregnate the surface pores of the specimen and to wet the outer surface uniformly. The wetted specimen is then fired in a controlled atmosphere to decompose the silicone or organic silicon compound to vitreous silica. Coats of vitreous silica applied to beryllium carbide by this method are thin (1 mil and less), impervious to air at 2500°F for 350 hours, and have shown no perceptible devitrification during this time.

Firing the coatings in a hydrogen atmosphere was found to be definitely superior to firing in air; this procedure has been adopted as standard practice in the NEPA laboratory. The impregnation coatings, originated at A. O. Smith, form an excellent anchor coating for an overcoat, and form a satisfactory diffusion barrier. They are being investigated further for use as ultimate coats.

Refractory oxide coatings. - Beryllium carbide—matrix specimens coated with a 1-to-1 mixture of strontium carbonate and silica showed considerable resistance to attack by oxidation and water vapor at 2500°F. Precalcined coatings were smoother than their uncalcined counterparts, but their adherence, oxidation resistance, and spalling properties were comparable. Zirconia, in combination with alumina, calcium hydroxide, silica, or barium carbonate, was generally ineffective as a coating for beryllium carbide—matrix bodies. No improvement was obtained by substituting stabilized zirconia for the chemically pure material. Good adherence was obtained with coatings consisting of calcined mixtures of beryllium oxide and silica or magnesia; these are being investigated further.

The mechanism whereby most of the mixed oxide coatings protect beryllium carbide from oxidation at elevated temperatures may be explained by the observations made upon platinum-coated specimens, which have also been duplicated qualitatively for some of the mixed oxide coatings. This mechanism postulates a filtering action for the coating, whereby a limited amount of oxygen penetrates the interstices of the coating oxides to attack the beryllium carbide and form beryllia. The growing beryllia layer progressively plugs itself up until the rate of attack by oxygen is reduced to a negligible amount (see Figs. 27 and 28). From analytical and X-ray data, the beryllia that is formed in place on the beryllium carbide is chemically and structurally no different than other beryllia. As could be expected, it contains segregations of various impurities. Its behavior as a coating material, however, is significantly different from that of normal beryllia. The product that is formed in place is not appreciably attacked by water vapor, has better adherence to beryllium carbide, and is more inert to reaction with other compounds.

Metal-ceramic combinations. - Surface energy calculations continued at the Massachusetts Institute of Technology, using results obtained through the previously described sessile-drop method, with copper metal and lead metal on plaques of alumina, zirconia, and graphite. Wetting tests were made both in hydrogen and in vacuum. Copper shows a slight tendency to wet alumina and zirconia; the different contact angles obtained in vacuum and in hydrogen show that the furnace atmosphere is an important variable.

At Ohio State University, the effect of firing atmospheres on metal-ceramic coatings in the system silicon-zirconia on beryllia bodies was investigated. Firing in nitrogen resulted in soft, porous, nonadherent coatings. It is believed that silicon was converted into its nitride, while the zirconia remained unchanged. This coating oxidized rapidly in the air at 2500°F. Firing the coatings in a mixture of 5 per cent oxygen and 95 per cent nitrogen resulted in the complete oxidation of the silicon. Helium atmospheres caused beading, indicative of poor wetting. On the other hand, coatings fired in oxygen and in dry air retained a large proportion of unoxidized silicon, and were found to be continuous and uniform.

In the NEPA laboratories, attempts were made to determine the wetting of ceramics by titanium metal. Mixtures of titanium metal powder heated with the compounds beryllia, alumina, beryllium carbide, zirconia, and titania above the melting point of the metal show more or less wetting and reaction, but the results obtained have not yet been evaluated.

2.32 **Liquid-Coolant-Cycle Materials.** - Work on the liquid-coolant-cycle materials during the past quarter has continued to emphasize materials for the intermediate heat exchanger, although the alloys and pure elements studied would, in general, be suitable for use in the reactor proper as well. The solubility and high-temperature properties of these materials appear essentially to meet both needs, and there are no decisive differences in their nuclear properties which would lead to their being automatically excluded from the reactor.

The use of all-metal fuel elements poses special problems if a thermal reactor is desired, as was pointed out in last quarter's report. A major factor in this respect is the small number of good moderator elements. It may be that incorporation of the fuel in the structure and the use of separate moderator bodies that do not carry loads will prove to be a workable method. Bodies of molybdenum and uranium dioxide may also prove to be of use.

Fabrication of molybdenum-base bodies. - Continued work on the fabrication of 90 per cent molybdenum—10 per cent uranium dioxide bodies has established the necessary procedures for forming simple shapes. Powdered materials are consolidated with powder metallurgical techniques by hydrostatic or mechanical pressing operations at pressures between 60,000 and 100,000 pounds per square inch. The green compacts are then sintered by heating to 2000°C (3630°F). Such sintered bodies have an average porosity of 8 per cent, and must be hot worked to effect consolidation and to obtain densities of better than 99 per cent theoretical. It is only after consolidation and subsequent hot working that the bodies may be expected to develop optimum properties.

Fabrication of rods 3/8 inch in diameter and 5 inches long by hot swaging sintered compacts 1/2 inch in diameter by 2 3/4 inches long is being undertaken to provide bodies for evaluation of tensile and creep properties. The rod elements are fabricated by encasing the sintered body in a molybdenum tube with a wall thickness of 1/16 inch. Three reductions in 10-per cent steps are made by swaging from 1800°C (3270°F) to consolidate the body. Further reductions are made at temperatures between 1100°C (2000°F) and 1400°C (2550°F) for grain refinement.

Sintered bodies have been formed from an 80 per cent molybdenum—20 per cent uranium dioxide composition. Such bodies are roughly 8 to 10 per cent porous. This composition is not as readily worked as the 90 per cent molybdenum—10 per cent uranium dioxide, but initial tests have indicated that the material may be hot swaged under conditions similar to those required for working the 10 per cent uranium dioxide composition.

Twelve sintered bodies of the 90 per cent molybdenum—10 per cent uranium dioxide composition were fabricated in the form of rectangular bars and sent to Battelle. These bodies are being hot rolled into sheets in a cooperative program designed to demonstrate the feasibility of rolling this material and to evaluate the mechanical properties of the resultant sheet stock. Preliminary work has indicated that this composition may be hot rolled at temperatures possibly as low as 1200°C (2190°F) after consolidation at 1800°C (3270°F). Fig. 30 is a photomicrograph of a cross-section of rolled material showing the longitudinal structure. The large gray areas represent uranium dioxide grains. The lighter area is the molybdenum phase etched to show grain boundaries and flow texture.

Fig. 31 illustrates the rolled 90 per cent molybdenum—10 per cent uranium dioxide body from which the photomicrograph was taken.

The specific electrical resistance of a swaged rod of 90 per cent molybdenum—10 per cent uranium dioxide was measured so that calculations could be made to determine whether such a body could be resistance-heated for thermal stress tests. Since molybdenum oxidizes readily in air, these tests were conducted in vacuum. Data obtained up to 2500°F are plotted in Fig. 32. For comparison, a curve based on literature values for pure molybdenum is included. It may be seen that the resistivity of the body containing 10 per cent uranium dioxide is slightly higher than that of the molybdenum at all temperatures. This is to be expected, since uranium dioxide is a very poor conductor compared to molybdenum.

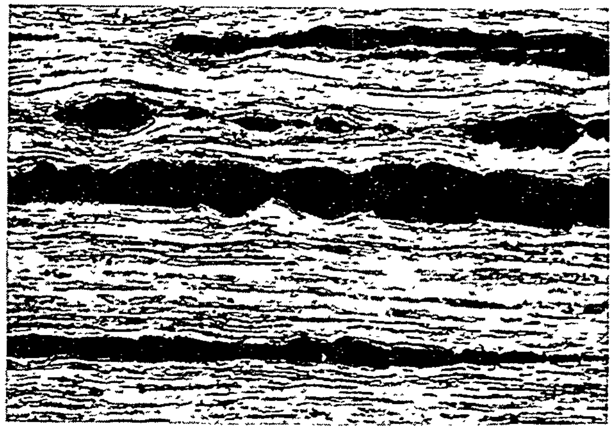

Fig. 30 - PHOTOMICROGRAPH OF LONGITUDINAL CROSS-SECTION; 90 PER CENT MOLYBDENUM-10 PER CENT URANIUM OXIDF SPECIMEN (500X; ETCHED IN ALKALINE POTASSIUM FERROCYANIDE)

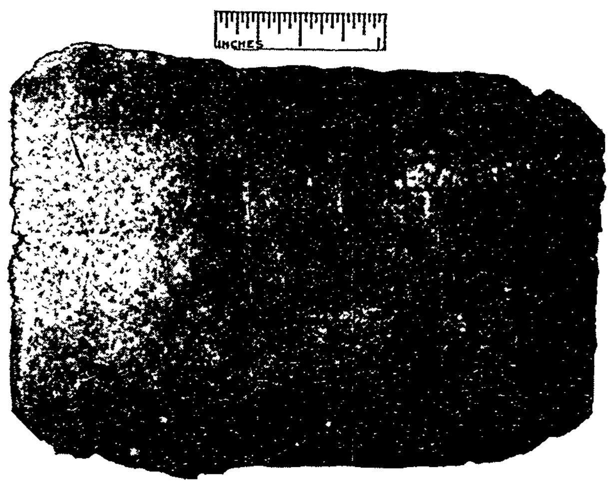

Fig. 31 - ROLLED SHEET OF MOLYBDENUM BASE BODY

SECRET

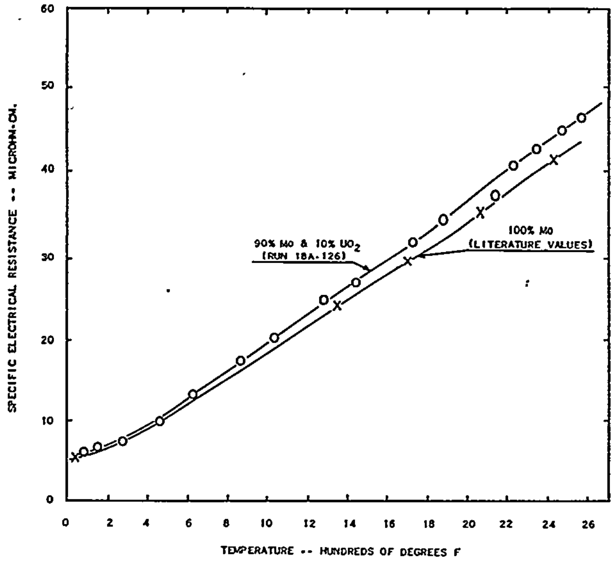

Fig. 32 - EFFECT OF TEMPERATURE ON THE RESISTIVITY OF MOLYBDENUM-URANIUM OXIDE AND MOLYBDENUM SPECIMENS

Liquid-metal container materials. - The liquid-metal container program uses four main testing techniques. These are: (1) static tests; (2) agitator tests; (3) spinner tests; and (4) circulation tests. The program, which was at first designed to develop suitable container and auxiliary materials for the coolants bismuth, lithium, and lead-bismuth eutectic, was modified during the quarter to include sodium. The reasons for this modification are outlined in sections 2.22 and 4.11 of this report. The results of the present quarter will be presented according to the coolant being tested.

All the results now available are from the static and agitator types of tests. The agitator test rig was described in a previous quarterly progress report (NEPA 1281, p. 23). In addition to the corrosion results reported in this section, section 4.2 contains reports of larger-scale experiments in the handling of high-temperature liquid metals.

Bismuth. - The test program on bismuth has been made inactive awaiting completion of outstanding chemical analyses. A total of 232 capsules have been submitted for chemical analyses. The work is complete on 162 of these. A statistical analysis is under way on available data but the trends are not apparent at this stage of the investigation.

Because of the possible importance of oxygen content in corrosion testing, deoxygenation of bismuth by addition of aluminum and magnesium was attempted. The capsules made up with additions were tested at 1350°F and 1850°F. The oxygen content was erratic and the general trend did not change from that normally found. A tendency toward higher total solubility of the container material was noted in those cases in which aluminum or magnesium had been added. A possible explanation for the higher solubilities noted may be that the aluminum and magnesium act as wetting agents. Wetting of surfaces usually results in higher reaction rates.

Static testing of beryllia at temperatures near 1350°F produces no noticeable change in the dimensions of the test specimens. Test conducted in a dynamic system show very slight dimensional changes at this temperature for periods to 100 hours.

The data obtained in a series of tests to determine the effect of bismuth on beryllium carbide are presented in Table 11. These tests show that beryllium carbide is not attacked markedly by bismuth at 1850°F in 50 hours.

The status of work on the bismuth circulation rig changed during the quarter due to the curtailment of work on bismuth. The reasons for this change are given in sections 2.22 and 4.11. It is now planned to check out the circulation rig with lithium. In order to put the system into operation as soon as possible, it was decided not to make changes in materials or design for the preliminary tests. A few revisions which were necessary from safety and other considerations were made in the original design. The rig was designed to handle bismuth at flow rates up to 50 feet per second in a 1/4-inch inside diameter test section with a temperature differential of 1000°F in the system,

SECRET

TABLE 11

RESULTS OF TESTS ON Be_2C VS. BISMUTH*

Specimen No.	Temperature °F	Time (hours)	Type	Weight Before Run (grams)	Weight After (grams)	Distance Between Flats Before (inches)	Distance Between Flats After (inches)
328	1350	92	Static	0.852	0.845	0.190 - 0.194	0.190 - 0.194
329	1350	76	Dynamic	0.903	0.892	0.210 - 0.195	0.202 - 0.209
330	1500	92	Static	0.717	0.713	0.184 - 0.186	0.182 - 0.187
331	1500	92	Dynamic	0.802	0.788	0.202 - 0.206	0.200 - 0.211
332	1850	25	Static	0.722	0.848	0.189 - 0.208	0.184 - 0.207
333	1850	25	Dynamic	0.852	0.914	0.199 - 0.203	0.196 - 0.201
334	1850	50	Static	0.830	0.952	0.191 - 0.206	0.192 - 0.207
335	1850	50	Dynamic	0.725	0.750	0.205 - 0.210	0.195 - 0.206

* Obtained from static and dynamic tests on beryllium carbide samples. (There were 20 grams bismuth charge in each capsule.)

and a maximum temperature to 2000°F at the test section. The use of induction heating as a source of heat is one of the factors which remain to be proved.

Three thermal harps using liquid bismuth as the circulating medium were constructed. Harp No. 1 was constructed of types 316 and 310 stainless steels. It developed a leak in one of the welds after a short period of operation. Harp No. 2 was constructed entirely of type 310 stainless steel. It was operated continuously for a period of 65 hours with a temperature differential of 350° - 400°F at a maximum temperature of 1350°F. A vacuum was maintained throughout the test. Operation was halted due to burn-out of the heating elements. The cooling and freezing of the bismuth resulted in rupture of one of the welds. Fig. 33 shows the fractured joint. Harp No. 3 was constructed entirely of type 347 stainless steel. The harp was operated for 150 hours, during which time there was evidence of thermal circulation for 78 hours. Maximum temperature level varied from 1250° to 1550°F, with a thermal differential of 200°F. The circulation of this harp was stopped by the formation of an obstruction at the top of the hot leg. The harp was allowed to freeze and

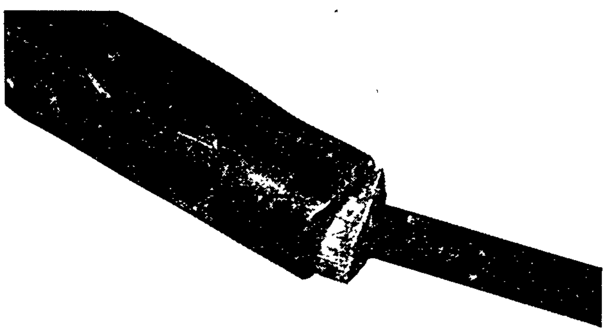

Fig. 33 - RUPTURE OF WELD IN THERMAL HARP NO. 2

was then sectioned longitudinally. A high-melting-phase material was found to be scattered throughout the system, and some segregation was noted. It is suspected that the material which caused plugging of the harp is composed of the more soluble elements in the structural material of the harp.

The elements are probably nickel, manganese, and iron. The mechanism causing the plugging is believed to be one involving solution at higher temperatures and redeposition at lower temperatures. The fact that the plugs developed on the hot side is not explainable at this time. A sketch showing the locations of the material which finally caused plugging is given in Fig. 34.

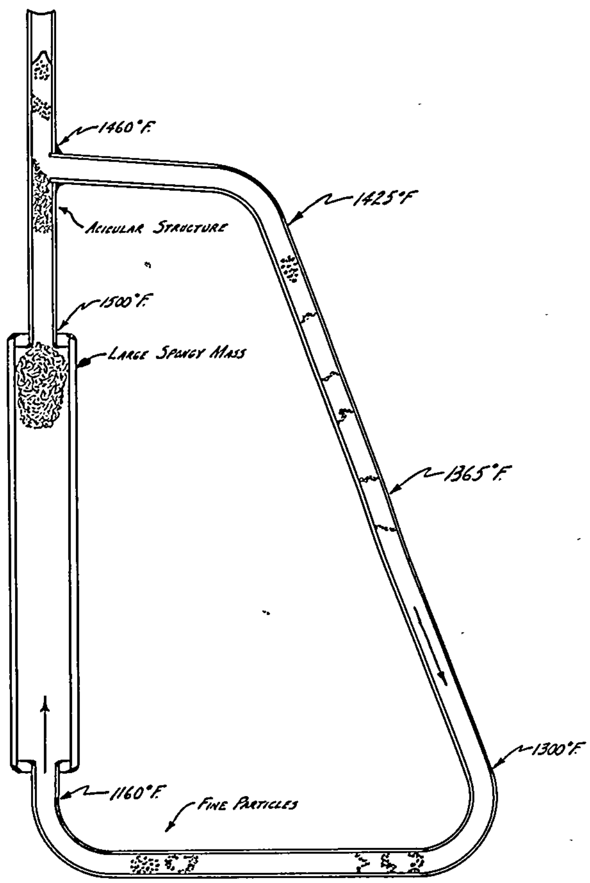

Fig. 34 - SKETCH OF THERMAL HARP NO. 3 CROSS-SECTION SHOWING ACCUMULATION OF MATERIAL OBSTRUCTING BISMUTH FLOW

A series of capsules fabricated from type 347 and type 310 stainless steels containing bismuth and having welded wall sections were tested to study the effect of liquid bismuth on welds. Half of the welds were solution-treated at 1900°F for 30 minutes and air-cooled, while the rest were not treated. Three of the seven untreated welds failed, although no treated welds failed. A microexamination of the weld areas is being made to determine the difference in structure and amount of attack by the bismuth.

Lithium. - The lithium program continued with duration of tests being increased to 500 hours at temperatures to 1850°F. Higher temperatures present a problem which has not been solved satisfactorily to date for these long-term tests. The main difficulty experienced has been that of locating suitable canning materials to protect the test capsule from oxidation. An obvious solution would be the use of an inert atmosphere furnace, but this solution is not entirely satisfactory due to the cost and long procurement time of a suitable type furnace. The short-time tests used earlier in this program were discontinued. The test program now involves testing at 1350°F, 1500°F, 2000°F, and 2200°F, for relatively long periods. Test hours spent on this program during the quarter totaled 14,900.

A series of tests were run using aluminum and magnesium as "getters" to determine the effect of these materials on the oxygen and nitrogen present. The conclusion drawn from these tests is that magnesium and aluminum are not good "getters" for either nitrogen or oxygen in lithium. The additions made no significant change in the solubility trends.

It has been suggested that one of the major factors in the corrosion of metals by lithium may be lithium nitride dissolved in the lithium. Lithium nitride (Li_3N) is known to be a very corrosive material and is present in the purest lithium commercially available to the extent of 0.25 per cent maximum. In order to determine the effect of lithium nitride, it has been proposed to test a series of capsules identical to those being run, using, however, lithium metal which has been vacuum-distilled to remove the nitride.

Data obtained during the quarter on pure elements yielded the trends shown in Figs. 35, 36, and 37 for nickel, zirconium, niobium, and molybdenum. The figures show the trend in solubility as a function of time. It should be pointed out that the saturation values are not known for these elements. The figures as given are not intended to convey the idea that solubility increases logarithmically with time; one would expect the curves to

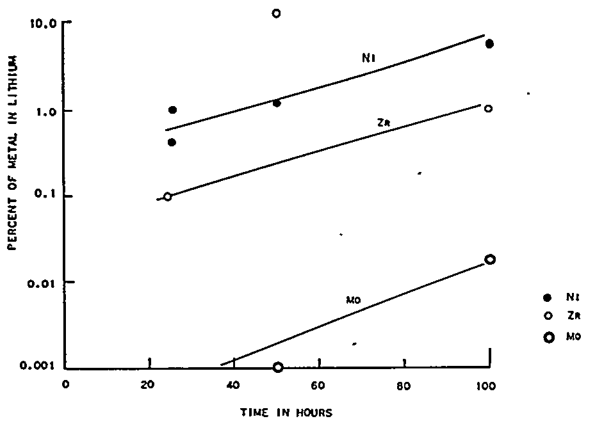

Fig. 35 - TRENDS IN THE SOLUBILITIES OF METALS IN LITHIUM AT 1350°F

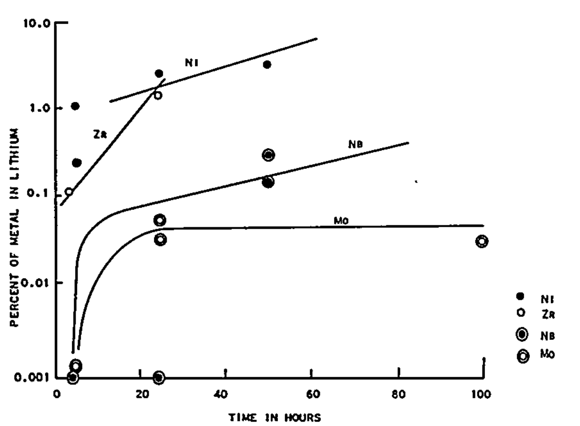

Fig. 36 - TRENDS IN THE SOLUBILITIES OF METALS IN LITHIUM AT 1850°F

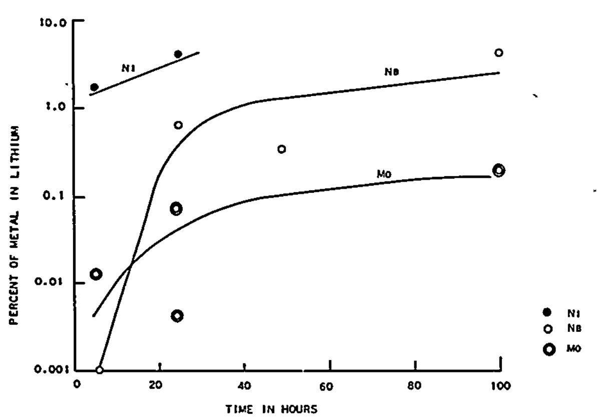

Fig. 37 - TRENDS IN THE SOLUBILITIES OF METALS IN LITHIUM AT 2000°F

level out as saturation is approached. However, the data available at this time are in most cases insufficient to determine that point.

The Babcock and Wilcox Company has settled on a design for the lithium erosion test apparatus being set up in its laboratories. An electromagnetic pump was developed and tested. This pump developed 4 pounds per square inch at 1/3 gallon per minute. A second, improved pump is being built. An isothermal loop operating at 1000°F was built, charged, and run. A leak developed in the tubing, causing a minor fire. The loop is being repaired. Suitable flow meters have been developed for the preliminary tests.

Lead-bismuth. - No further test work was done on lead-bismuth during the period of this report. Microexamination of the container materials, after previous tests, revealed that this coolant appears to have more effect on microstructure than bismuth. A limited number of analytical results indicate a lower total solubility in this coolant than that noted with bismuth.

Sodium. - A program for the development of container materials for liquid sodium was outlined tentatively during the quarter. Preliminary solubility tests have been run at 1850°F and 2000°F. The materials tested were beryllium, niobium, molybdenum, and molybdenum-uranium dioxide. Duration of the tests completed to date was 100 hours; tests of longer duration are still in progress. Microexamination of the container materials is being made, as is chemical analysis of the sodium from these runs.

Miscellaneous. - It is known that, in certain cases, self welding occurs when two metallic surfaces are placed in contact in suitable mediums, provided that the temperature is favorable. A series of tests were performed using the coolants lithium and bismuth with stainless steel in order to see whether this phenomenon might occur in their presence. Type 347 stainless steel was used for the tests. Test procedure consisted of packing small hexagonal or circular tubes into a 1/2-inch diameter tube and immersing the contact surfaces in moving or static coolant. No evidence of self welding was noted in the case of lithium. Bismuth tended to act as a welding medium. The results of the tests are presented in Figs. 38 and 39.

The gold-brazed joint used in making up the hexagonal tube bundle illustrated in last quarter's report was tested in both lithium and bismuth. The joint failed in both coolants. It is not known whether other heat treatments resulting in more

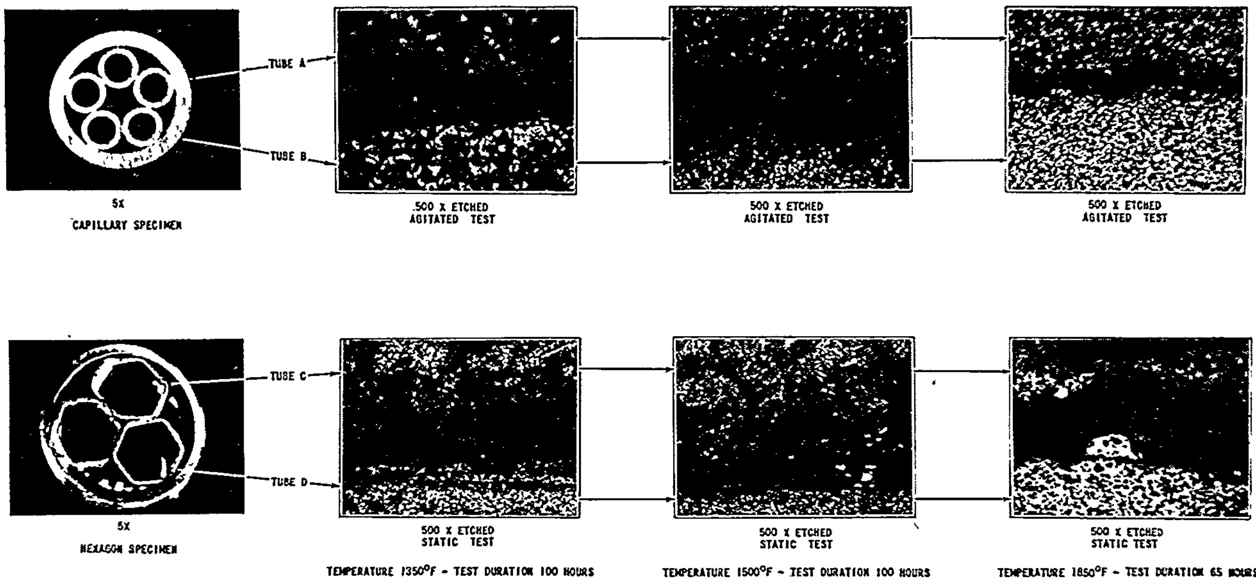

Fig. 38 - CONTACT WELDING TEST IN LITHIUM

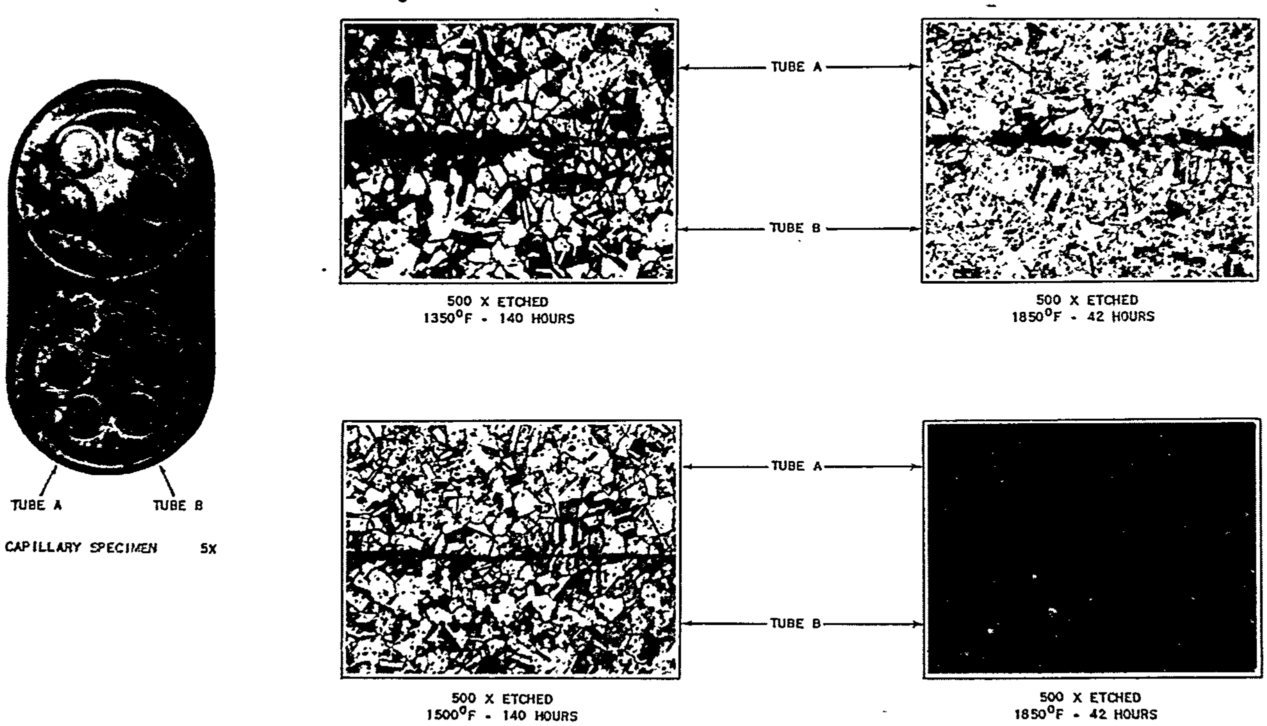

Fig. 39 - CONTACT WELDING TEST IN BISMUTH

complete diffusion of the gold would result in similar behavior.

A cursory diffusion study of the beryllium-molybdenum system was carried out in both the solid and liquid states. Tests were made at 2000°F and 2350°F for 100 hours. Fig. 40 presents the microphotographs obtained. The spaces present in some cases between the phases are believed to be due to differential thermal expansion. Two phases were noted on the specimens. It was impossible to determine the extent of the second phase at the latter test temperature, due to shrinkage and break up of the cast beryllium.

Properties of coolants.

Viscosity. - A subcontract with the University of Cincinnati was initiated to determine the high-temperature viscosities of the coolants of interest. A literature survey on the subject is under way.

Thermal conductivity. - A subcontract was activated with Ohio State University under which work will be done on the development of methods for determination of the thermal conductivity of liquid metals. Work also continued at NEPA on both the radial and longitudinal methods for determining thermal conductivity of liquid metals at elevated temperatures.

Features of the apparatus were being investigated to assure desired accuracy. There has been no change in the data presented in the last report.

Density. - Preliminary measurements of the density of liquid bismuth and lead-bismuth eutectic were obtained for the temperature range 400°F to 1850°F. The composition of the eutectic was 43.5 per cent (by weight) lead and 56.5 per cent (by weight) bismuth. Estimated accuracy of the density values determined was plus or minus 5 per cent.

Tables 12 and 13 show the experimental values obtained.

2.4 RADIATION DAMAGE
(43.8 Man-months)

2.41 Radiation Damage

Physical Tests. - Engineering evaluation of ANP reactor materials is being pursued under a joint NEPA - ORNL program coordinated by Dr. D. S. Billington, of the Oak Ridge National Laboratory. The investigations have been primarily concerned with the ceramic type moderator and fuel element bodies.

A slug containing a 1/4-inch x 1/4-inch x 5-inch specimen of beryllium carbide containing 2.5 per

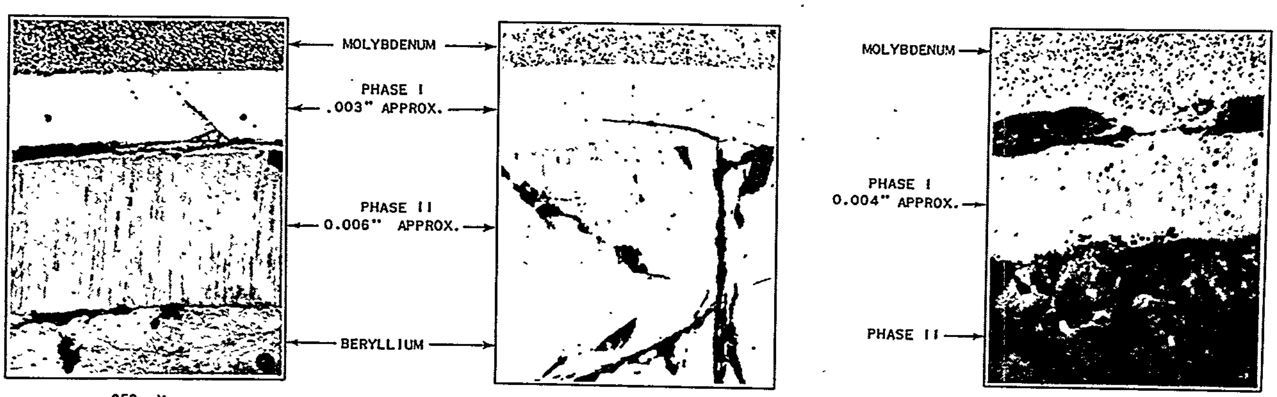

250 X
UNETCHED
SPECIMEN 1.
2000°F. 100 HOURS

250 X
UNETCHED
SPECIMEN 2.
2000°F. 100 HOURS

250 X
UNETCHED
2350° - 2400°F. 100 HOURS

Fig. 40 - DIFFUSION STUDIES, MOLYBDENUM AND BISMUTH

TABLE 12

DENSITY OF LIQUID BISMUTH BY MAXIMUM BUBBLE PRESSURE METHOD

Temperature (degrees)		Density	
C	F	gm./cu. cm.	lb./cu. in.
358	676	(10.31)*	(0.373)
364	687	9.92	0.358
393	739	(10.14)	(0.366)
619	1146	9.81	0.354
621	1150	9.54	0.345
835	1535	9.50	0.343
841	1546	9.47	0.342
1008	1846	9.41	0.340
1019	1866	9.37	0.339

* Values in parentheses are of doubtful accuracy.

TABLE 13

DENSITY OF LIQUID LEAD-BISMUTH EUTECTIC MIXTURE* BY MAXIMUM BUBBLE PRESSURE METHOD

Temperature (degrees)		Density	
C	F	gm./cu. cm.	lb./cu. in.
208	406	10.50	0.379
391	736	10.22	0.369
588	1090	10.03	0.362
790	1454	9.76	0.353
995	1823	9.57	0.346

* 43.5 per cent lead, by weight.

cent uranium carbide was irradiated in the ORNL reactor for an integrated dosage of approximately 5×10^{18} nvt. A transverse crack was discovered after irradiation which may have resulted when the capsule was discharged from the fuel channel. Therefore, only a 3-inch-long specimen was used for post-irradiation tests. No change in appearance or density of the specimen was noted. The modulus of elasticity decreased from 30×10^6 pounds per square inch (as reported by Battelle) to 22×10^6 pounds per square inch. Electrical resistivity changed greatly. Before irradiation, it was 0.16 ohm-cm., while after irradiation it appeared to be as high as 1 megohm-cm. If this observation is confirmed, it means that the material changes during bombardment from a fair electrical conductor to a near insulator. The modulus of rupture after irradiation was 11,200 pounds per square inch. When compared with the modulus of rupture of two control specimens, the differences in values obtained were accounted for by experimental error of the apparatus or slight variations between samples.

Five groups of specimens have been prepared for irradiation at Hanford. These include beryllium carbide samples with varying amounts of carbon, some with additions of 2.5 per cent uranium carbide, and some with coatings; and an assortment of sintered ceramic specimens – tubular alumina, Norton alundum, zircon, and beryllia-alumina.

Apparatus for testing an enriched fuel element has been designed (see Fig. 41). Preliminary tests are to be made in the ORNL reactor which has a low neutron flux. Consequently, an auxiliary electric heater has been incorporated in the central portion of the element to boost the temperature of the specimen to 1800°F. Stability of the prototype element (beryllium carbide plus graphite plus uranium carbide) and coating (refractory oxide) is to be determined. Activity in the exit gas stream will indicate that fission products have escaped through the coating by diffusion or through fissures.

After the completion of the final design of the "in pile" stress deformation apparatus, two units were started on the bench, using type 321 stainless steel specimens under 5000 pounds per square inch stress at a temperature of 1400°F. Results obtained are comparable to literature data for 1000-hour tests. Additional units are being assembled for 7500 pounds per square inch stress and 1800°F operation.

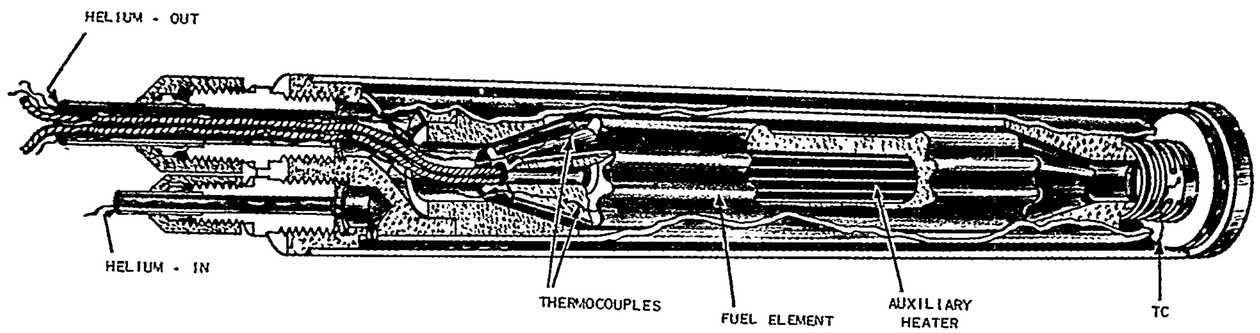

Fig. 41 - PROTOTYPE FUEL ELEMENT TEST RIG

Both creep and stress-rupture test rigs for ceramic and metal specimens will be developed using the same basic unit. Arrangements have been completed for insertion of one such unit, with a stainless steel specimen, in the ORNL reactor.

Cyclotron bombardments. - A limited amount of experimental data is now available from the cyclotron bombardment of beryllium carbide specimens at Washington University and the University of California. A description of the experimental conditions under which these bombardments were conducted is shown in Table 14. The earlier bombardments carried out in the Ohio State University cyclotron are also included in this table to illustrate relative beam intensities and the radiation effects encountered under somewhat different conditions.

A preliminary bombardment program using the Washington University cyclotron has been completed. The initial objective has been the measurement of the changes in modulus of elasticity and thermal conductivity of beryllium carbide produced by irradiation. After irradiation, many of the specimens were broken (indicating brittleness) and only a limited number of physical tests could be made. The deterioration of the samples may have resulted from the high power density in the beam (see Table 14) since the power density was greater than that required to rupture unirradiated specimens in thermal stress experiments. It is too early to ascribe the brittleness encountered in bombarded specimens to radiation effects alone.

"Before-and-after" testing to date consists of various tests carried out on the three of the sixteen specimens bombarded at the University of California and one of the Washington University samples which was intact after a deuteron bombardment.

The primary objective of the University of California tests was to observe the chemical changes produced in beryllium carbide by alpha bombardment in air at high temperatures. These tests were characterized by limited oxidation which was neither expected nor obtained in the Washington University bombardments. In both cases, however, temperatures above 1800°F were attained during bombardments. The control and knowledge of the temperatures attained in the bombardments at the University of California were rather complete. This will be of great importance in analyzing all experimental data obtained from cyclotron bombardments. To rule out the changes which may have been produced by temperature alone, control samples of the same dimensions and composition as those bombarded at California were heated in air to similar temperatures, for equivalent times, and then tested in the same manner as the irradiated specimens.

The results of the physical testing to date may be summarized as follows:

The elastic modulus in flexure of the University of California specimens decreased approximately 30 per cent, whereas the elastic modulus of the Washington University specimen was

TABLE 14

CYCLOTRON BOMBARDMENTS OF BERYLLIUM CARBIDE AS OF JUNE 1, 1950

NO.	DATE	SPECIMEN DESCRIPTION: Dimensions (inches)	Total: Area (sq. in.)	Total: Vol. (cu. in.)	Irradiated: Area (sq. in.)	Irradiated: Vol. (cu. in.)	ACCELERATOR DESCRIPTION: Bombarding Particles	Description of Beam (Microamperes): Max.	Av.	Intercepted by Specimen	EXPERIMENTAL CONDITIONS DURING BOMBARDMENTS: Irradiation Atmosphere	Length of Irradiation	Max. Temp. During Bombardment	Inst. Particle Flux	Micro-amp. Hours	Integrated Particle Flux	Power Density in Irradiated Section of Sample (Btu/in^3)	REMARKS
Ohio State University — Beam Shape (Approx.) — Length 3/4 inch, Width 1/8 inch																		
1.	3-1-1950	.010 x .500 x .875	.437	.00437	.0625	6.25×10^{-4}	10 Mev deuterons	Unk.	Est. 10	Est. 10	Bombarded internally in vacuum	15 min.	Est. 1830°F by color	1.6×10^{14}	2.5	1.4×10^{17}	82	Specimen were cracked when inspected after irradiation. Prolific yield of 10-minute N^{13} necessitated care in handling during first hour after bombardment. Metallic Be deposited on water-cooled copper plate to which sample was clamped; cracks were probably due to the rigidity of the mounting during thermal expansion of sample in course of bombardment.
2.	3-1-1950	.010 x .500 x .875	.437	.00437	.0625	6.25×10^{-4}	10 Mev deuterons	Unk.	Est. 10	Est. 10	Bombarded internally in vacuum	30 min.	Est. 1830°F by color	1.6×10^{14}	5.0	2.8×10^{17}	82	Specimen was cracked when inspected after irradiation. Prolific yield of 10-minute N^{13} necessitated care in handling during first hour after bombardment. Metallic Be deposited on water-cooled copper plate to which sample was clamped; cracks were probably due to the rigidity of the mounting during thermal expansion of sample in course of bombardment.
3.	3-8-1950	.030 x .500 x .275	.137	.00411	.0625	6×10^{-4}	20 Mev alphas	Unk.	Est. ~1	Est. ~1	Bombarded internally in vacuum	15 min.	Unk.	8×10^{12}	.25	7.2×10^{15}	66	Inconclusive results. Beam could not be consistently focused on specimen. Slight darkening noted over irradiated area. Induced activity negligible. No cracks observed in specimen.
4.	3-8-1950	.030 x .500 x .275	.137	.00411	.0625	1×10^{-3}	10 Mev deuterons	Unk.	Est. 10	Est. 10	Bombarded internally in vacuum	30 min.	Est. 2000°F using optical pyrometer	1.6×10^{14}	5.0	2.8×10^{17}	100	Sample mounted to permit thermal expansion; no cracks visible. Observable temperatures of 1750°F obtained during bombardment as determined by optical pyrometer.
5.	3-8-1950	.030 x .500 x .275	.137	.00411	.0625	1×10^{-3}	10 Mev deuterons	Unk.	Est. 10	Est. 10	Bombarded internally in vacuum	30 min.	Est. 2000°F using optical pyrometer	1.6×10^{14}	5.0	2.8×10^{17}	100	Specimen coated on exposed side by fused silica coating several mils thick. Temperatures as high as 2000°F were observed as above. Specimen was darkened slightly in area of beam but no cracks were observed.
Washington University — Beam Shape (Approx.) — Length 2-1/16 inches, Width 1/8 inch																		
1.	3/15-4/15-1950	.040 x .250 x 2.25	.563	.0225	.25	.004	9 Mev deuterons	130	109	95	Bombarded in external chamber using dry helium atmosphere	6 hrs. each side	~1830°F	3.7×10^{14}	570	8×10^{18}	200	Sample darkened in bombardment in a similar manner to but not as pronounced as the OSU samples. Sample broke in target probably due to method of mounting.
2.	3/15-4/15-1950	.020 x .250 x 2.25	.563	.0133	.25	.004	9 Mev deuterons	120	116	100	Bombarded in external chamber using dry helium atmosphere	6 hrs.	~1830°F	3.9×10^{14}	600	8.5×10^{18}	212	Sample darkened; broke during post-irradiation inspection.
3.	3/15-4/15-1950	.020 x .250 x 2.25	.563	.0113	.25	.004	9 Mev deuterons	140	133	120	Bombarded in external chamber using dry helium atmosphere	6 hrs.	~1830°F	4.7×10^{14}	720	1.02×10^{19}	254	Sample darkened; broke during removal from target holder.
4.	3/15-4/15-1950	.020 x .250 x 2.25	.563	.0133	.25	.004	9 Mev deuterons	140	126	113	Bombarded in external chamber using dry helium atmosphere	6 hrs.	> 1830°F	4.4×10^{14}	678	9.5×10^{18}	240	Sample darkened; broke during post-irradiation inspection.
5.	3/15-4/15-1950	.040 x .250 x 2.25	.563	.0225	.25	.004	9 Mev deuterons	140	136	121	Bombarded in external chamber using dry helium atmosphere	6 hrs. each side	> 1830°F	4.8×10^{14}	726	1.04×10^{19}	260	Unbroken.
6.	3/15-4/15-1950	.040 x .250 x 2.25	.563	.0225	.25	.004	9 Mev deuterons	140		125	Bombarded in external chamber using dry helium atmosphere	1-2 hrs.	> 1830°F	5.4×10^{14}	210	3.8×10^{18}	270	Unbroken.
University of California — Beam Shape — *Length 1 inch, Width 1/2 inch																		
1.	4/17-4/22-1950	.030 x .200 x .400 (.9 of this area exposed to beam)	.08	2.4×10^{-3}	.072	2.2×10^{-3}	38 Mev alphas	7	1	1	Bombarded in external chamber in presence of atmospheric air	5 hrs.	2340°F	1×10^{13}	7.5	1.8×10^{17}	17	Coating observed on face exposed to beam probably BeO - darkening noticed over beam area. Sample otherwise intact - temperature measured by vacuum thermocouple and focusing lens system.
2.	4/17-4/22-1950	.030 x .200 x .400 (.9 of this area exposed to beam)	.08	2.4×10^{-3}	.072	2.2×10^{-3}	38 Mev alphas	7	1	1	Bombarded in external chamber in presence of atmospheric air	5 hrs.	2340°F	1×10^{13}	7.5	1.8×10^{17}	17	Coating observed on face exposed to beam probably BeO - darkening noticed over beam area. Sample otherwise intact - temperature measured by vacuum thermocouple and focusing lens system.
3.	4/17-4/22-1950	.030 x .200 x .400 (.9 of this area exposed to beam)	.08	2.4×10^{-3}	.072	2.2×10^{-3}	38 Mev alphas	7	1	1	Bombarded in external chamber in presence of atmospheric air	15 hrs.	2340°F	1×10^{13}	22.5	5.4×10^{17}	17	Coating observed on face exposed to beam probably BeO - darkening noticed over beam area. Sample otherwise intact - temperature measured by vacuum thermocouple and focusing lens system.

* Reproduction of autoradiograph taken from a platinum foil 0.00025 inch by 2.75 inches by 1.00 inch which was 2.5 cm. in front of, and parallel to, the sample.

lowered by a factor of 90 per cent. Electrical resistivities ranging from 1 to 2 ohm-centimeters in the unirradiated beryllium carbide body fabricated at NEPA increased to several thousand ohm-centimeters in the samples bombarded at California as compared to 25 to 30 ohm-centimeters in the irradiated Washington University specimen. In the control samples for the University of California bombardments, the thermal treatment in air raised the resistivities to 10 to 20 ohm-centimeters, probably due to oxide formation. The elastic moduli of these controls were not materially changed, indicating that the decreases noted above were probably radiation-induced. No dimensional or extensive weight changes were observed as resulting from radiation. No changes in lattice parameters or chemical composition were observed in the X-ray studies made of the irradiated samples. The microhardness of one of the University of California samples changed from $K_{0.1}$ of 2690 to $K_{0.1}$ of 2208, whereas no change was observed in the corresponding control sample "before-and-after" thermal treatment in air.

2.42 Radiation Damage

Chemical. - As the counterpart of the preceding physical-effects experiments, investigations are being made of the chemical changes that nuclear radiations produce in moderator, coating and coolant materials, hydrogenous shield materials, and lubricants. Tests have been carried out using the radiations inside the ORNL reactor and using the alpha-particle beam from the 60-inch cyclotron at the University of California. Tests are being started using the electron beam from the NEPA 2-Mev Van de Graaff accelerator. The radiation from the cyclotron and from the Van de Graaff accelerator produce ionization intensities comparable to those expected in an aircraft reactor.

Berkeley cyclotron. - Sixteen specimens of beryllium carbide and silicon carbide were held for 5 hours at 1832°F and 2282°F in air while being bombarded by the alpha-particle beam of the 60-inch cyclotron at Berkeley, California. Power was released by the irradiation at the rate of 1 kilowatt per cubic centimeter. The irradiated specimens are being subjected to chemical analysis for comparison with specimens having an identical history in the absence of radiation. The results of this analysis will show whether the radiation has induced appreciable decomposition or reaction with air. Physical tests were performed on the specimens both before and after irradiation. The results of these tests are reported in the preceding section. No gross changes in the appearance of the specimens were observed, although in some cases there was a slight discoloration not observed in the control samples. The target holders illustrated in Fig. 42 and Fig. 43 were used. This apparatus accurately positions the small target specimen, controls the atmosphere to which the target is exposed, measures the amount of exposure of the target specimen to the alpha-particle beam, and controls and measures the temperature of the target material.

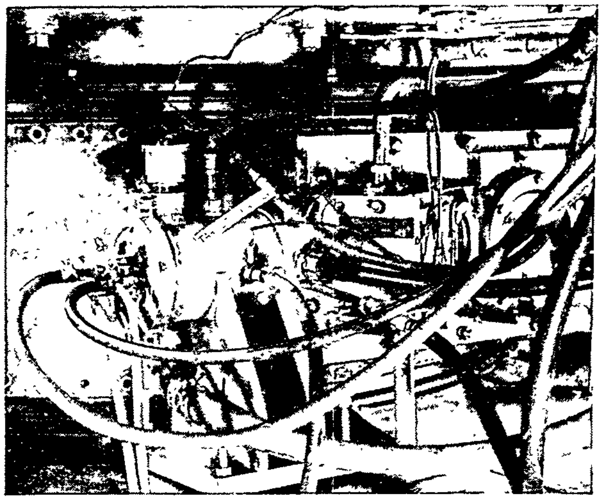

Fig. 42 - CYCLOTRON TARGET CHAMBER INSTALLED FOR TEST

Reactor tests. - Chemical analyses are being continued on beryllium carbide and silicon carbide specimens previously irradiated in the ORNL reactor, and on control samples which were not irradiated. This series of experiments is expected to show whether neutrons and gamma radiation produce any chemical effects on these materials at the relatively low flux level of this reactor.

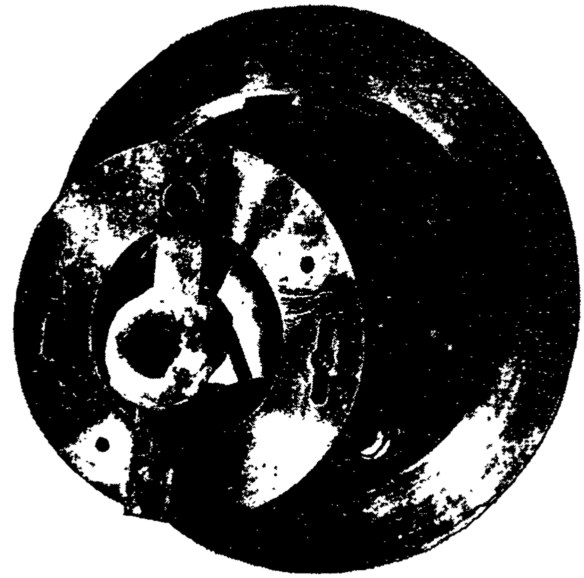

Fig. 43 - CYCLOTRON TARGET HOLDER

Van de Graaff accelerator. - The NEPA 2-Mev Van de Graaff electron accelerator is now in operation. A specially designed holder for thin metal windows was fabricated and put into operation, the purpose of the window being to prevent air from entering the evacuated accelerator tube and yet to permit the electron beam to pass through. The assembly is illustrated in an exploded view in Fig. 44. The flange in the foreground is screwed on to the extension tube of the accelerator. The rest of the illustrated assembly is bolted to this flange with appropriate vacuum-tight gaskets. Features of the assembly include water-cooling of flanges and air-cooling of windows to prevent overheating when high-temperature targets are being irradiated. The strength of thin duralumin windows was investigated as a function of window diameter and thickness over the thickness range from 0.0002 inch to 0.001 inch. Using the result of this investigation, one can minimize losses of electrons due to scattering by the window without risking damage to the accelerator by window rupture.

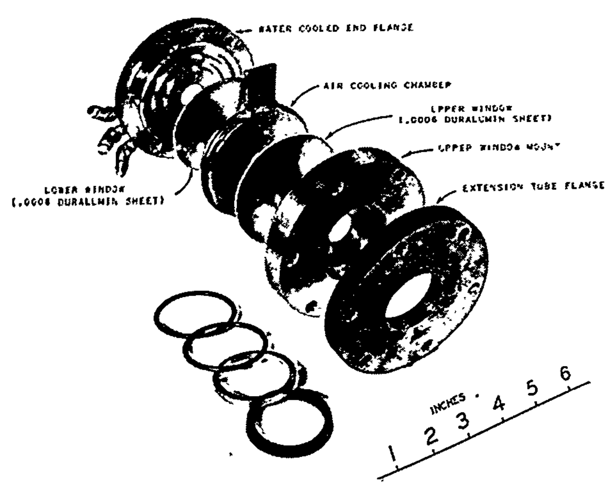

Fig. 44 - TARGET CHAMBER WINDOW ASSEMBLY

A remotely operated device for manipulating a small target or probe in the beam has been constructed. Provision has been made for remotely observing the position of the target or probe by the use of a variable-reluctance transformer. The principal application of this device is in measurements of dosage distribution over the target region. An assembly has been designed for maintaining a solid target at high temperatures in a controlled atmosphere or vacuum during bombardment by the electron beam.

Specimens of beryllium carbide and silicon carbide are being irradiated in air using the cyclotron target chamber shown in Figs. 42 and 43 modified for use on the Van de Graaff machine.

Core coolants. - During the past quarter, considerable emphasis has been given to the determination of the radiation stability of fused sodium hydroxide. This material is being considered as a possible coolant and moderating fluid for the aircraft reactor. It is of particular interest because its pronounced moderating effect due to its hydrogen content permits an extensive reduction of uranium investment. Tests of molten compounds, including sodium hydroxide, are planned first at temperatures of approximately 1300°F and then 1832°F, using the beam from the 2-Mev Van de Graaff electron accelerator.

The problem of design of an apparatus for exposing sodium hydroxide to the electron beam while protecting the compound from the atmosphere reduces to a search for container materials which will withstand the extremely corrosive effects of sodium hydroxide at 1300°F and higher temperatures. One of the walls of the container, which must be thin enough to admit the electron beam, should be approximately 0.0003-inch to 0.001-inch thick. This places severe corrosion resistance requirements on the container material.

Corrosion tests of materials which may be satisfactory are in progress. Other fused salts of interest include mixed melts of lithium chloride and potassium chloride. A sample of this material was irradiated for one week in the ORNL nuclear reactor at a temperature of 1202°F. No significant change in melting point (670°F) was observed.

Lubricants - California Research Corporation. - Research on the development of radiation-resistant lubricants was continued at the California Research Corporation. The first phase of this research consists of irradiating organic fluids to determine the nature of changes induced by nuclear radiations and the types of organic materials which resist such changes. Over 105 combinations of base oils and inhibitors have been irradiated in the ORNL reactor at temperatures ranging from 129°F to 297°F for periods of one to four weeks. From static tests, a number of effective combinations of base oil and inhibitor have been developed. The three most promising base oils are octadecylbenzene, polypropene oxide, and di-2-ethyl-hexyl sebacate. The three inhibitors – iodobenzene, dialkyl selenide saturated with quinizarin, and 1-methylanphthalene – are effective in improving the resistance of these base oils to radiation and oxidation.

Three samples of organic fluids were exposed in the Berkeley 60-inch cyclotron to 38-Mev deuterons. Two of these samples were didecylterephthalate plus 2 per cent dilauryl selenide, and the third sample was octadecylbenzene with 6 per cent iodobenzene and 5 per cent dialkyl selenide saturated with quinizarin. Final effects of this radiation on the materials are now being evaluated. Visual examination showed some increase in viscosity but no gross discoloration.

The second phase is directed toward the investigation of oxidation stability of these materials during irradiation. Eleven accelerated oxidation tests were carried out at 284°F in the ORNL reactor at 85 per cent of maximum flux. Results of these tests are being analyzed.

The third phase of the lubricant research has as its chief concern the duplication of service conditions for lubricants during irradiation. Six bearing test rigs have been constructed and operated at 284°F in the ORNL reactor at 49 per cent of maximum neutron flux. In three of the units, high-speed bearings were operated for 19 days. In the other three, ball bearings, needle bearings, loaded journal bearings, and gears were operated at low speed for 8 days.

In both high-speed and low-speed tests, three base oils – octadecylbenzene, polypropene oxide, and di-2-ethylhexyl sebacate – were tested separately. Each of the oils contained iodobenzene in varying amounts plus 5 per cent dialkyl selenide saturated with quinizarin. In addition to these additives, the di-2-ethylhexyl sebacate contained 20 per cent 1-methylnaphthalene.

The oils and test rigs are currently being examined for effects of the test. The nature of further investigations of radiation-resistant lubricants depends upon the outcome of the test described above.

Work continued on the investigation of various organic compounds as possible fluid hydrogeneous shield materials. A survey was made of petroleum compounds relating hydrogen content per unit volume with density, and ten of the most promising compounds were irradiated in the ORNL pile for one month at 284°F at 87 per cent of maximum flux.

Compounds which have been irradiated are: (1) didecyl terephthalate plus 2 per cent dialkyl selenide; (2) alkylbenzene (MW = 250) plus 4 per cent polylauryl methacrylate and 2 per cent dialkyl selenide; (3) alkylbenzene (MW = 350) plus 2 per cent dialkyl selenide; (4) di-2-ethylhexyl sebacate plus 2 per cent dialkyl selenide; (5) amylbiphenyl;

(6) cetane; (7) alkylbenzene (MW, = 250); (8) octadecylbenzene plus 5 per cent dialkyl selenide plus 2 per cent iodobenzene saturated with quinizarin; (9) polypropene oxide plus 5 per cent dialkyl selenide plus 2 per cent iodobenzene saturated with quinizarin; (10) di-2-ethylhexyl sebacate plus 5 per cent dialkyl selenide plus 2 per cent iodobenzene plus 20 per cent 1-methylnaphthalene saturated with quinizarin. The results of these tests are now being evaluated.

Jet fuel samples irradiated for one month at 86°F at 75 per cent of maximum flux in the ORNL reactor experienced an increase in radiation resistance, but a decrease in hydrogen concentration. These materials are under consideration as constituents of a hydrogenous shield.

• • • • •

3. SHIELDING

3.1 BULK SHIELD TESTS (10.5 Man-months)

Bulk shielding tests conducted jointly at the Oak Ridge National Laboratory, X-10 site, by ORNL and NEPA, were slowed down this quarter as a result of construction work. A new air-conditioned instrument room is being installed, and it is hoped that this will improve the reliability of the instruments. Heretofore, the majority of delays in the program have been directly attributed to instrument failures.

A recently developed, proton-recoil, fast-neutron spectrometer has been installed in the tank, and spectra close to the source will be measured. The instrument is not sufficiently sensitive to measure highly attenuated apectra in the lid tank. All neutron detectors are now fitted with new-type waterproof cases and individual preamplifiers; it is believed that the latter may improve the internal consistency of measurements.

The monitor, which records the incoming flux from the pile, has been replaced with a much larger B^{10} ionization chamber. The new monitor will run a recorder directly, thus eliminating the necessity of an intermediate amplifier and its corresponding uncertainties and servicing requirements. Much attention has been given to the calibration of instruments, with emphasis on the gamma ionization chambers.

The contract for construction of the new bulk-shield testing facility at ORNL has been negotiated, and work was begun on May 25. The facility is to be completed within 150 days.

The free-escape neutron spectrum emerging from a water shield was computed, assuming an incident fission neutron spectrum of the form $e^{-0.72\,E}$, and a total molecular water cross-section given by the relation:

$$\sigma(E) = 11.6\,E^{1/2}\text{ barns.}$$

The emerging neutron spectrum has a maximum which moves toward higher energies with increasing shield thickness.

Similarly, the free-escape neutron spectrum emerging from an iron-water shield was computed. It was found that, for two-thirds iron—one-third water by volume, as used in the iron-water experiments, the emerging spectrum had a peak at about 1 Mev.

The attenuation measurements on 27 per cent and 18 per cent lead by volume in water have been completed. However, due to instrument trouble it became necessary to re-evaluate the results, and hence the results are not as yet available. The same is true for the iron-water-lead measurements.

Measurements of 33 per cent lead – 67 per cent water have been started. No data are yet available, but extensive foil measurements have been made for the first 10 inches of shield.

3.2 NEUTRON SOURCES, SHIELDING NUCLEAR CONSTANT MEASUREMENTS, AND INSTRUMENT DEVELOPMENT (28.6 Man-months)

Because the Oak Ridge National Laboratory has been declared responsible for the nuclear phases of the ANP program, the existing and proposed NEPA subcontracts and activities in this field were reviewed during the quarter with ORNL personnel and agreements were reached. It was decided that the Bartol Research Foundation Van de Graaff and the University of Kentucky Van de Graaff subcontract on scattering of neutrons by shield materials would be continued. It was decided that the Westinghouse Electric Corporation Van de Graaff subcontract on the same subject would not be renewed at the end of fiscal year 1950. It was decided that the continuous cloud chamber subcontract with Mr. F. Forrest Pease would be renewed in June 1950, and that a contract

R-236-2

with the University of Chicago for the development of a neutron spectrometer for use in shield experiments would be initiated. It was also agreed that instrumentation development at NEPA would be essentially limited to those instruments specifically requested by ORNL for the "swimming pool" reactor installation, and for sensory instrumentation for the control of the ARE and the test-stand reactor.

Data continued to be received from Bartol, modifications to the University of Kentucky machine were almost completed, and construction of the NEPA 5-Mev Van de Graaff, to be installed at ORNL on delivery, was still progressing according to schedule. Further details follow.

Bartol Research Foundation. Inelastic scattering of neutrons by shield materials. - Neutron scattering experiments are continuing, a bombardment of lead by fast neutrons has been completed, and the photographic plates are being measured. Measurement and analysis of plates employed in the similar bismuth scattering experiment is also continuing. Thus far, 1150 tracks have been accumulated from experiments with the scatterer in place, and 1431 tracks have been read from experiments with the scatterer removed. Although no evidence for an excited state (indicated by increased number of tracks at a lower energy) has been found, results cannot be considered significant until they can be compared with the results from the experiments with lead. Measurement is now being concentrated at energies below the main group of neutrons in order to improve statistical accuracy in the region where inelastic groups might be expected to appear.

University of Kentucky. Inelastic scattering of neutrons by shield materials. - Modifications to the Van de Graaff proper have been completed and test runs of the machine are about to start. Effort during the quarter was expended in doing such miscellaneous and time-consuming jobs as designing and building the control panels, installation of the ion-source cooling system, fabrication of the platform inside the dome and mounting equipment on it, relocating a charging belt, leak testing, and installing various other electrical and mechanical components. A sketch of completed arrangement is shown in Fig. 45. It is expected that instrumentation will be worked on during the next quarter, and it is hoped that some data, from experiments involving inelastically scattered neutrons, will be obtained.

Westinghouse Electric Corporation. Inelastic scattering of neutrons by shield materials. - The subcontract with Westinghouse Electric Corporation for the use of their Van de Graaff will not be renewed at the end of the fiscal year, June 15, 1950, since the Bartol and Kentucky subcontracts now seem likely to produce all needed data. The Bartol Van de Graaff is already producing data; the University of Kentucky Van de Graaff is expected to do so shortly. The Westinghouse Van de Graaff subcontract is still in the initial stages, because it was initiated at a later date. It would be necessary to go through many of the same modifications as were found necessary for the University of Kentucky machine – increase the beam strength, install a more powerful beam bending magnet, and construct a new target room. There was also some possibility that the beam current would not be increased by merely installing a more powerful ion source, and that the whole accelerating tube system might have to be modified. It might have been possible to utilize the extremely low beam current (approximately 0.15 microamperes) if, like Bartol, data were obtained by the exposure of photographic plates. This would not have entirely served the purpose of the subcontract, since one of the original reasons for the Westinghouse subcontract was to attempt to develop new types of instrumentation, which would reduce the time and manpower requirements by the measurement program. This can now be taken care of by ORNL.

5-Mev Van de Graaff. - Construction of the 5-Mev Van de Graaff by the High Voltage Engineering Corporation is progressing approximately according to schedule. The manufacturer has received the main pressure tank from the vendor. During a test run without the accelerating and pumping tubes in place, and without the equipotential shields, the

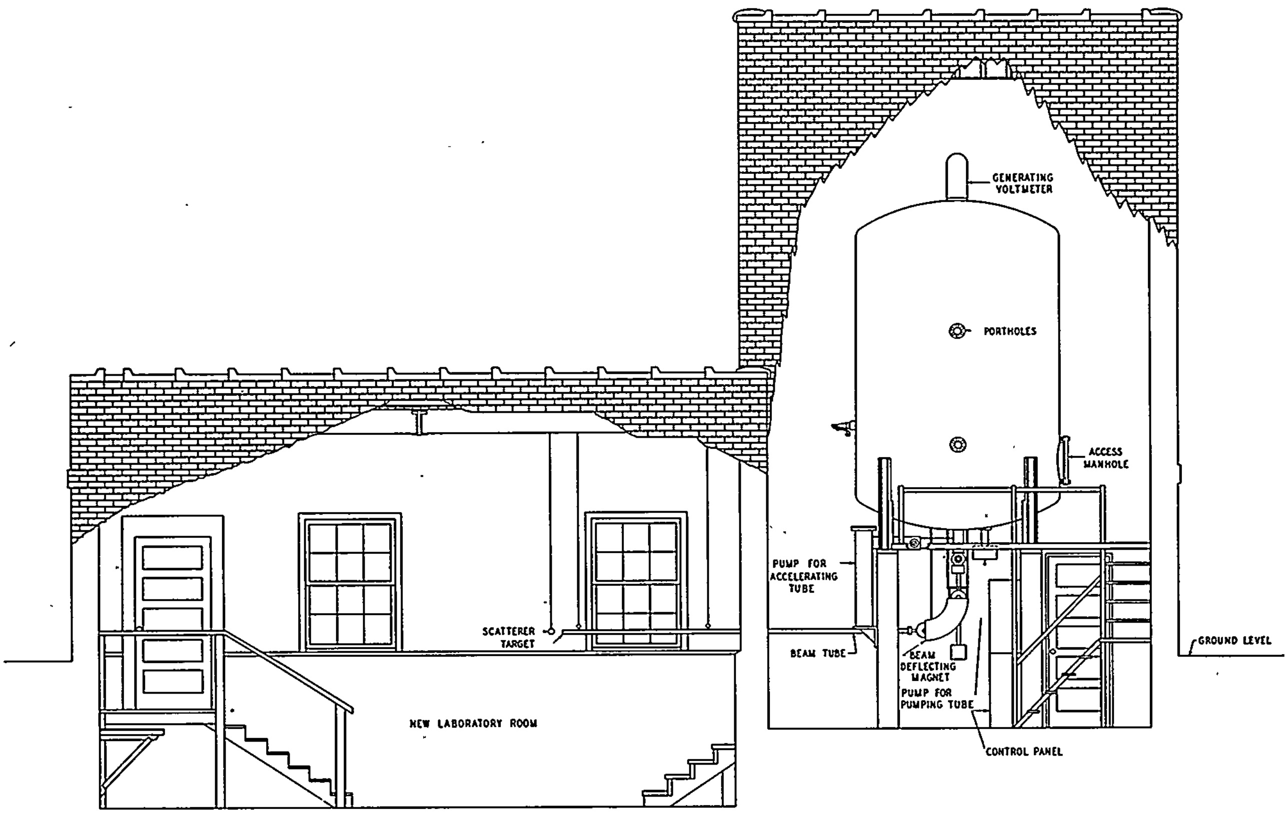

Fig. 45 - ARRANGEMENT OF VAN DE GRAAFF AT UNIVERSITY OF KENTUCKY

machine successfully reached approximately 6.5 Mev. It now seems possible that the machine may not be moved to Oak Ridge at the date originally scheduled; the machine will be eventually installed at the ORNL X-10 site. There has been some delay in initiating work on the ORNL building which will house it and it is now expected that this building will not be completed for perhaps a year. It has not yet been decided by ORNL whether it would be possible and desirable to house it temporarily in the Y-12 area.

Cockroft-Walton accelerator. - The Cockroft-Walton accelerator has been completely assembled and successfully vacuum tested. The capillary arc type ion source has been successfully operated. During a test of the 0.25 Mev voltage source, a flashover and fire occurred, at about 0.21 Mev. The transformer was shipped to the manufacturer for examination, but was ruined in shipping. The manufacturer has rewound it and will send a representative to ensure the proper functioning of the power supply. The entire machine will be put into operating condition and made ready for use when a controlled source of neutrons is needed for instrumentation work.

Instrumentation. - In addition to building some more-or-less standard instruments for critical experimentation, NEPA was involved during the quarter in building, or developing, a beta-ray spectrometer, a Compton-recoil coincidence counter, a single-crystal scintillation spectrometer, a multiple-crystal spectrometer, a proton-recoil neutron-energy spectrometer, and lithium-loaded emulsions. A start was also made in growing or mixing various crystals and liquids which scintillate when exposed to gammas or neutrons.

R-236-4

Late in the quarter, a meeting was held with the ORNL personnel responsible for the shielding reactor installation (swimming pool), and its instrumentation. Recommendations were obtained for instruments needed for the bulk shielding experiments with the shielding reactor. Special interest centers in the beta-ray spectrometer, the Compton-recoil coincidence counter, the multiple-crystal spectrometer, and the proton-recoil neutron spectrometer. Accordingly, work on these instruments will be emphasized and work on the other instruments will only be carried forward at such times as it is impractical to work on the instruments of primary interest.

Beta-ray spectrometer. - During the quarter, attempts to obtain a suitable current regulator for the focusing electromagnets of the beta-ray spectrometer were abondoned through commercial sources, and a satisfactory current regulator was built at NEPA. Other work during the past quarter consisted of improving the resolution by determining optimum positions for the two magnetic lenses and the proper alignment for the baffle system. Batteries were used for magnet current at the low energies and the generator and regulator were used at the higher energies. Fig. 46 shows a picture of the machine. ORNL personnel responsible for instrumenting the shielding reactor facility have shown interest in a modification to the machine suggested by NEPA. It was proposed that by means of a suitable arrangement of baffles, magnets, and counters-in-coincidence the machine could be used as a positron-electron pair spectrometer. Electrons and positrons are emitted as a result of gammas striking a radiator at one end of the spectrometer tube. These electrons spiral down the tube in opposite sense due to the influence of the first magnet, go into a reverse spiral at the second magnet, and are counted in coincidence at the other end of the spectrometer tube. Baffles have been made and special counting tubes will be constructed in order to test the feasibility of this idea.

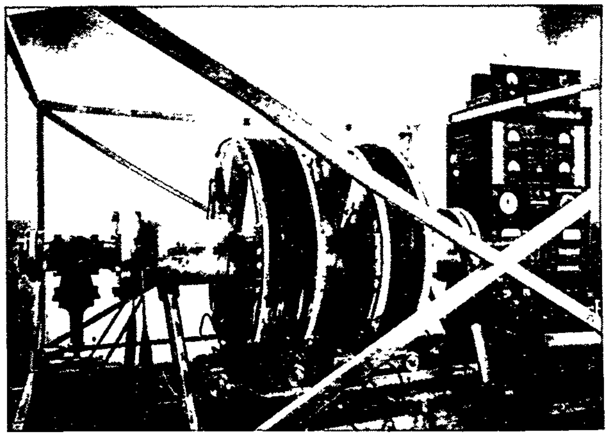

Fig. 46 - BETA-RAY SPECTROMETER

Compton-Recoil coincidence counter. - A Compton-recoil coincidence counter is being constructed for making rough gamma-ray energy measurements in either the lid tank or the shielding reactor facility. In this apparatus, Compton recoil electrons are ejected from a suitable target by the incoming gamma radiation of unknown energy. The electrons traverse two GM tubes which are connected in such a way as to give counts only when both tubes are tripped within a given short period of time. Absorbers are inserted between the two tubes and counts are taken with various thicknesses of absorber screening out the electrons of lower energy. While this instrument will not give complete spectral measurements, it may operate as a variable-energy threshold detector. The necessary electronic equipment was already available from the polonium-beryllium source (n,γ) experiments reported in the *Quarterly Progress Report for the period September 1 - December 31, 1949*, and has been assembled and modified for use. Special GM counters are being constructed at X-10. As soon as they are available, the equipment will be tested in the lid tank.

Crystal scintillation counting. - Scintillation counting offers one possibility of measuring the energies of neutrons which have traversed a shield or escaped from a reactor. Tests on available crystals to determine their relative response to heavy and light ionizing particles were completed during this quarter. This was done in order to determine the feasibility of using them, with lithium included, for neutron spectroscopy, in this type of counting.

R-236-5

The energy of the alpha and tritium particles resulting from the absorption of a neutron by a Li^6 nucleus is dependent on the energy of the incident neutron and would be measured by the intensity of the scintillation. Scintillation from lighter particles represents an undesired background. None of the tests completed have shown a desirable ratio of pulse size from the heavy particles to the pulse size from the light particles. The ORNL work with lithium silicate activated with titanium oxide is being followed; a physically good crystal is still unavailable. A dozen melts of related materials have been prepared and tested for response to alpha particles with encouraging results. A clear glassy melt of 17.3 per cent lithium oxide, 69.63 per cent silica, 4.35 per cent zirconia, and 8.70 per cent lithium chloride–sodium chloride appeared to be most promising. Additional samples of similar compounds with different activating agents are now available. An attempt will be made to grow crystals from the more promising of these melts. It is well known that sodium iodide–thorium iodide is of considerable interest as a possible neutron measuring device. Past attempts to procure such a crystal commercially have been unsuccessful, but it may be possible to grow such a crystal in NEPA's crystal-growing apparatus which is now getting into operation.

Following an announcement from outside sources that certain solutions would act as scintillation counters, such solutions were prepared. These counting liquids are particularly interesting for neutron work in view of the possibility of easily incorporating the lithium compounds desirable for neutron energy determinations. Recoil protons will present a problem. The solutions currently available consist of p-diphenylbenzene in m-xylene and in benzene. Others are being procured.

Multiple-crystal spectrometer. - During the quarter, C. P. Baker (NEPA consultant) brought to the attention of NEPA personnel a method of measuring gamma ray spectra using two crystal counters in coincidence. One crystal measures the energy of the Compton electron produced by the gamma ray in the crystal, and the second measures the presence and direction of the coincident degraded gamma ray. The intensity of the visible light pulse from each crystal is proportional to particle energy. Thus, with collimated gamma rays one can determine the gamma-ray energy uniquely. The reported resolution was sufficient for bulk shield tests and the sensitivity was high. It was believed that such an instrument might be suitable for shield measurements provided sufficient gamma-ray collimation could be provided.

Further thought indicated the possibility of using a three-crystal device so collimated that gamma rays would be unnecessary. In this arrangement (see Fig. 47), a gamma ray is scattered in crystal No. 1 and the degraded gamma ray enters crystal No. 2. The Compton electron generated in crystal No. 1 leaves it and its path ends in crystal No. 3. The coincident sum of the energies in No. 1 and No. 3 gives the electron energy. The presence of the degraded gamma going from 1 to 2 and the location of the crystals then define the angle between the degraded gamma and the Compton electron. This information is sufficient to determine the original gamma-ray energy even though its direction was originally unknown.

A two-crystal spectrometer is almost complete and a three-crystal model is planned to test its feasibility.

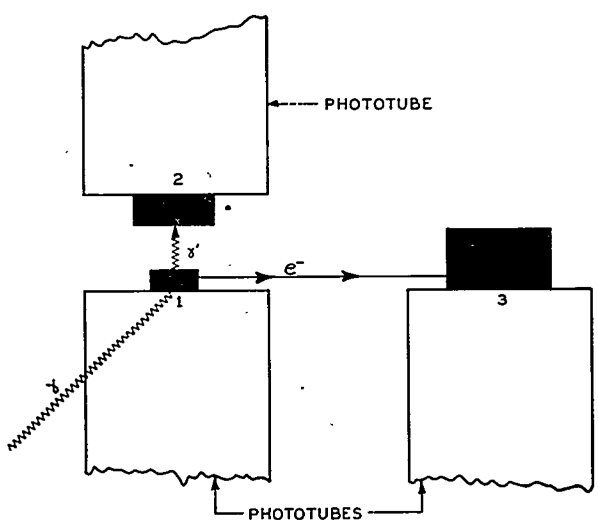

Fig. 47 - PROPOSED MULTIPLE-CRYSTAL GAMMA-RAY SPECTROMETER

R-236-6

Proton-recoil neutron spectrometer. - During the past quarter, the proton-recoil fast-neutron spectrometer was tested at Bartol Research Foundation and at Massachusetts Institute of Technology. The electrostatic generator at Bartol was used to obtain 4.4-Mev neutrons from the d(d,n) helium reaction. Points at 1.9 Mev and 14 Mev using the lithium (p,n) beryllium and tritium (d,n) helium reactions respectively were obtained on the Rockefeller generator at MIT. The resolution checked with design calculations giving a root-mean-square error of ±9.8 per cent. After the foregoing tests, the spectrometer was installed in the lid-tank facility. Some difficulty was encountered, however, in operating this instrument successfully in the lid tank because neither the very large background nor the neutrons to be measured originated at a point source. A coincidence tube and a coincidence circuit are on order and will be used to improve the performance with nonpoint sources.

Lithium-loaded emulsions. - Following the decision that ORNL will have basic responsibility for developing a low-hydrogen-content nuclear emulsion, NEPA subcontract negotiations were terminated with the Ansco Division, General Aniline and Film Corporation. The information regarding this proposed subcontract has been turned over to ORNL. Eastman is continuing work on an emulsion-lithium-emulsion "sandwich" type plate. No further Eastman samples were received during the quarter. A small amount of local work was continued on the technique of evaporating lithium on the emulsions. Along similar lines, Eastman attempted to evaporate lithium fluoride on an NTA emulsion (a special type of emulsion for nuclear track observation) but found that the required high filament temperature caused fogging of the plate.

Continuous cloud chamber. - Work continued on the subcontract investigation of the feasibility of constructing a continuously sensitive cloud chamber. This type of instrument, with no "dead" time, may prove useful for photographing the tracks of charged particles when used in conjunction with a "pulsed" cyclotron or Van de Graaff. With the concurrence of ORNL, the subcontract was renewed for a second six-month period as of June 15, 1950.

Some success was reported in obtaining continuous supersaturation by steam injection into an air nozzle; however conditions suitable for track formation were not obtained. The investigation of this approach will be continued with lower air velocities, if possible. A device is being constructed which will give an absolute measurement of the degree of supersaturation.

Standard pile. - Work on calibrating the standard or sigma pile has been completed. A report, for internal distribution, NEPA 1446-SER-10, has been written to assist in use of the pile. It is not expected that more work will be done with this tool until it is needed for calibration purposes after the start of critical experiments.

University of Chicago. - Acting with ORNL concurrence, a subcontract was negotiated with the University of Chicago. The objective of this subcontract is to investigate the feasibility of various means of measuring the energy of neutrons and construct equipment to perform such measurements.

3.3 MATHEMATICS OF SHIELDING
(18.5 Man-months)

Idealized shield calculations. - During this quarter the calculations of the minimum weight of an idealized shield have been extended, taking into account two new factors. First, the ideal shield has been changed by adding a plenum chamber to each end of the reactor. This is shown in Fig. 48. The second factor, the addition of side walls to the crew shield, will be discussed separately. This ideal shield is in essence a rounded-off cylinder of several layers around the reactor plus a shadow disc placed somewhere between the reactor and the crew position. The radius R_o includes the two inner layers.

The fundamental mass equation for this shield is:

$$M = \frac{4}{3}\pi(\rho_m - \rho_\omega)3\Big[(R_m - R_o)^3 + \frac{3}{2}(1 + \frac{\pi}{2} + \alpha)R_o (R_m - R_o)^2 + \frac{3}{2}(3 + 2\alpha)\, R_o^2\, (R_m - R_o)\Big] + \frac{4}{3}\pi\rho_\omega$$

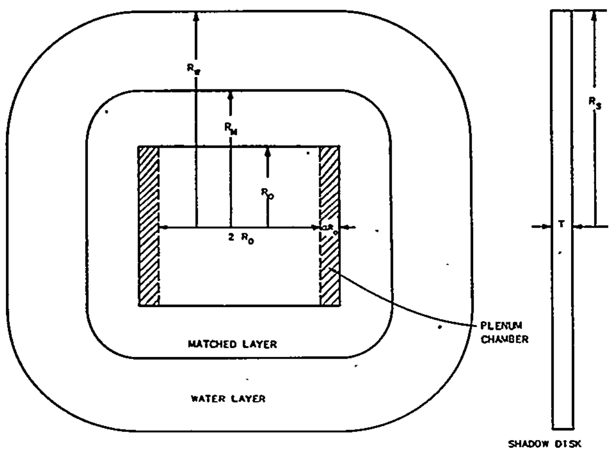

Fig. 48 - IDEALIZED SHIELD

$$\left[(R_w - R_o)^3 + \frac{3}{2}\left(1 + \frac{\pi}{2} + \alpha\right) R_o \, (R_w - R_o)^2 + \right.$$

$$\left. \frac{3}{2}(3 + 2\alpha) \, R_o^2 \, (R_w - R_o)\right] + \pi \rho_s R_s^2 \, T.$$

This neglects the two innermost layers which do not enter into the minimization problem. The relationship between R_m, R_o, R_w, and T is given by the basic attenuation equations

$$\frac{R_m - R_o}{\lambda_m} + \frac{R_w - R_m}{\lambda_{wn}} = 2.3 \, \delta_n + \ln\left(\frac{R_o}{D}\right)^2 = K_1,$$

$$\frac{R_m - R_o}{\lambda_m} + \frac{R_w - R_m}{\lambda_w} + \frac{T}{\lambda_s} = 2\ 3 \, \delta_\gamma + \ln\left(\frac{R_o}{D}\right)^2 = K_2,$$

where δ_n and δ_γ are the necessary powers of 10 to reduce the initial gamma and neutron flux to tolerance.

The factors on the right side of each of the attenuation equations are known, and when computed for a reactor-crew separation distance D, of 100 feet, give 16.1 for K_1, and 13.8 for K_2. Therefore, R_m and R_w may be solved in terms of T. When this is done, then the mass equation becomes a function of one independent variable, T. λ_m, λ_{wn}, λ_w, and λ_s are respectively the relaxation length in the matched layer, the neutron relaxation length in water, the gamma relaxation length in water, and the gamma relaxation length in the shadow shield, and are known for any given substances. R_m, R_w, R_o, and T are shown in Fig. 48; R_s is the radius of the shadow disc taken as four feet, αR_o is the thickness of the plenum chamber; ρ_m, ρ_w, and ρ_s are the densities of the matched layer, outer layer, and shadow shield, respectively.

Computations were made using this relation for a shield using wolfram carbide and boron carbide in the matched layer, water in the outer layer, and lead as the shadow shield. Fig. 49 shows these results and gives a minimum weight M_s for a shadow shield thickness of about 10.5 centimeters. These computations did not take into account the fact that scattered gamma rays would add to the radiation intensity at the crew position, and computations showed that the additional intensity due to the scattered gamma rays is considerable.

This brought up the second new factor, namely the question of adding side wall shielding at the crew position. Accordingly, a factor for the side walls was added to the mass equation; the equation then reads:

$$M = \frac{4}{3}\pi (\rho_m - \rho_w) \left[(R_m - R_o)^3 + \frac{3}{2}\left(1 + \frac{\pi}{2} + \alpha\right)\right.$$

$$\left. R_o (R_m - R_o)^2 + \frac{3}{2}(3 + 2\alpha) R_o^2 \, (R_m - R_o)\right] + \frac{4}{3}\pi \, \rho_\omega$$

153 079

R-236-8

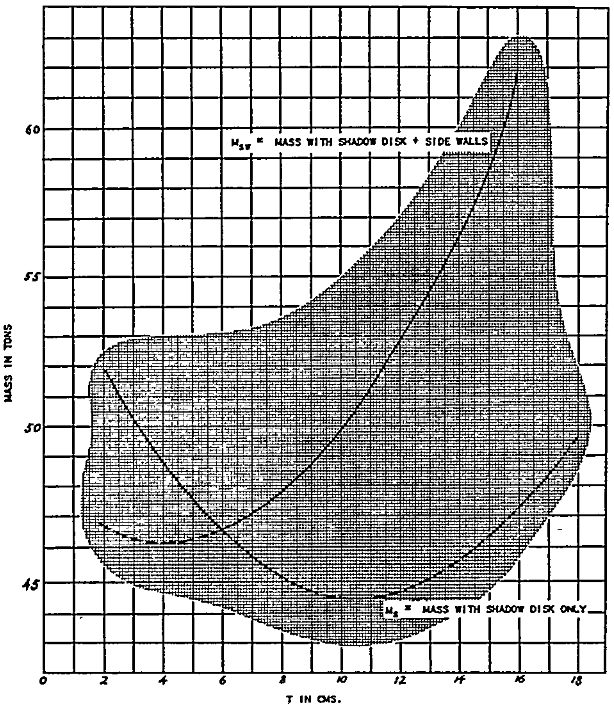

Fig. 49 - WEIGHT OF AN IDEALIZED SHIELD AS A FUNCTION OF SHADOW-DISC THICKNESS

$$\Big[(R_w - R_0)^3 + \frac{3}{2}(1 + \frac{\pi}{2} + \alpha)\, R_0\, (R_w - R_0)^2 +$$

$$\frac{3}{2}(3 + 2\alpha)\; R_0^{\,2}\; (R_m - R_0) \quad + \pi\rho_S R_S^{\,2} T +$$

$$2\pi\rho_S R_S h\beta\,(T - T_0).$$

T_0, here, is the shadow-disc thickness necessary to reduce the direct gamma radiation from the reactor at the crew position to a value equal to the scattered gamma radiation at the crew position at sea level air density, i.e., when the shadow disk has a thickness T_0, addition of sidewall shielding would not greatly reduce the crew-position radiation, and the proper thickness of the side-wall shield is zero. For T greater than T_0 the side-wall thickness is taken to be $\beta\,(T - T_0)$ where $\beta\,(T - T_0)$ is the thickness of the side walls as a function of T (the thickness of the shadow disk), and h is the length of the crew quarters.

Computations of the total shield mass, M_{sw}, using this new formula, were made, and the results are also plotted in Fig. 49. The intersection of the M_S and M_{sw} curves evidently is at the lowest shield weight for the conditions of the computation. Thus, although both the M_S and M_{sw} curves continue on to lower masses, the M_{sw} curve is meaningless to the left of the intersection since the intersection is at zero side-wall thickness, and the lower masses on this curve, therefore, correspond to "negative", i.e., imaginary, side-wall thickness; the M_S curve is meaningless to the right of the M_S - M_{sw} intersection because air-scattering in this region is large enough to require side walls, which have not been accounted for in the weight M_S. It must be noted that theoretical densities are used in computing weights and that the accuracy of relaxation lengths used are still in some doubt. Hence the weights quoted in Fig. 49 are not to be taken as serious estimates of the weight of an aircraft shield. Errors in weight, resulting from experimental inaccuracy, have been calculated (NEPA 1365 STR-25, *A Method for Optimizing an Aircraft Shield*).

The results show that the minimum weight is achieved without side walls, but the shield weight is somewhat greater when due allowance is made for the scattered gamma rays. This conclusion may not be true for a practical shield, for reasons given elsewhere in this report.

Air-scattering. - Studies are being continued on the air-scattering of gamma rays and are being

153 080

R-236-9

extended to the scattering of neutrons. The new studies will determine, for varying crew-shield thicknesses, the intensities of scattered gamma rays and neutrons at the crew position of a nuclear-powered aircraft.

The principal objectives of these studies are: (1) a determination of the intensity of the scattered gammas as a function of the angle at which they strike the crew, unprotected by side shielding; (2) a determination of the scattered-gamma intensity at the center of the crew compartment as a function of the side-wall thickness; (3) a comparison of the gamma intensity with the neutron intensity at the crew position. The first two of these objectives will provide an insight into the problem of shadow-shielding the crew from those regions from which the scattered gammas contribute a large fraction of the total intensity. It will also be possible to estimate crew-shield weight with a fair degree of accuracy.

The comparison of relative neutron and gamma intensities will permit an estimate to be made of the relative contributions from each component necessary to bring the total intensity, at the crew position, to biological tolerance.

Accurate results can not as yet be predicted, but from the preliminary calculations on Objective 2 it was found that, for a crew reactor separation distance of 30 meters and zero side-wall thickness, the primary gamma rays needed to be attenuated by about 6 centimeters of lead in order to contribute an intensity equal to that due to scattered gamma rays. The intensity of once-scattered neutrons reaching the crew position was also calculated. Using the same separation distance and assuming that scattering in air is isotropic and absorption is negligible, it was found that for S_0 fast neutrons per second produced at the reactor the once-scattered flux at the crew position was 6.6×10^{-9} S_0 neutrons per square centimeter. In order to compare this with scattered-gamma intensity, the gamma intensity must be converted to a flux. From an assumption of 1 Mev as the average energy of the gamma rays arriving at the crew position and from the calculated intensity (5.1×10^{-22} N_0), it was found that the ratio was $2.1\ S_0/N_0$ where N_0 is the number of 3-Mev gammas emitted per second from the reactor. The assumption of 1 Mev as the average gamma energy is an artificial one and serves merely as a basis for comparison with results to be achieved through further study.

Transmission calculations. - During the past report period, two transmission problems have been worked on. One is a Monte Carlo type problem and is now being computed on the I.B.M. equipment at the ORNL Y-12 site in order to determine the neutron energy spectrum in carbon resulting from a fission source. The results will be used to check on analytical approach to the problem, reported in NEPA 1162-STR-15, *Neutron Energy Spectrum in Carbon.* Two thousand neutron life histories have been computed, but the results have not been analyzed. The other is a matrix problem for a wolfram carbide and boron carbide system and is being set up to be run through the NEPA computer.

Extensive alterations have been made on the method of determining probabilities of "free state-to-free state" and "free state-to-trap" transmissions; this has resulted in greater accuracy with a correspondingly greater expenditure of labor and time. However, since this problem is the most ambitious yet undertaken, it is believed that a physically meaningful result will be of more value than a quick mathematical answer. Therefore, the increase in computing time will not be wasted.

Physically the problem involves a mixture of wolfram carbide (26.4 per cent by volume) and boron carbide (73.6 per cent by volume) and follows the life histories of neutrons having initial energies of approximately 1 ev to 6 Mev as they are degraded in energy to lower energies.

Currently in the process of solution is a mono-energetic pilot problem involving the solutions of 82 sets, each set containing 20 equations in 20 unknowns.

Preliminary results of the Northrop Monte Carlo attenuation computations for 2000 neutrons through slabs of boron carbide indicate that if boron ^{10} were substituted for natural boron the neutron relaxation length of 6.1 Mev neutrons would be decreased by 21 per cent. A further calculation on 10,000 additional neutron life histories was made using the assumption that boron ^{10} has no inelastic cross-section in order to determine the relative importance of the inelastic cross-section. These calculations indicate that such a fictitious substance (i.e., $B_4{}^{10}C$ with σ in = 0) would have a 6.6 per cent longer relaxation length than using natural boron.

For purposes of comparison, if a shield is constructed with a matched layer of boron carbide and wolfram carbide and the outer layer is made of water, the 21 per cent decrease in neutron relaxation length means a 10 per cent decrease in shield weight. Similarly, the 6.6 per cent increase in relaxation length means an increase in weight of 4.3 per cent. Table 15 summarizes these results.

TABLE 15

SHIELD WEIGHTS CALCULATED BY MONTE CARLO METHOD

Shield Material	Monte Carlo Neutron Relaxation Length (cm)	Experimental Neutron Relaxation Length (cm)	Normalized Neutron Relaxation Length (cm)	Shield Weight of 3 ft. Reactor (tons)
B_4C	6.1	5.5	5.5	48.7
$B_4{}^{10}C$	4.8		4.4	43.6
$B_4{}^{10}C$ (with σ in. = 0)	6.5		5.9	50.8

Duct leakage. - An attempt is being made to analyze the neutron and gamma ducting problem by dividing the duct into sections and thereby finding out what properties are important. This approach is from the viewpoint of calculating how much weight must be added to the outside of a shield to compensate for the leakage of neutrons and gammas through each section of the duct. Preliminary results indicate that the cross-section diameter of the duct is an important parameter; the added weight increasing by a factor of about 1.75 for every increase in duct diameter by one relaxation length. In designing a duct, it is believed to be important to have the angle formed by the axis of the duct and the radius vector as large as can be reasonably obtained. In order to obtain this large angle, use should be made of all three dimensions; the ideal shape for the duct is, perhaps, an extended Archimedean spiral.

The ducting problem is also being studied from the view point of applying the transport equation to it. However, the transport equation must first be solved, and it is believed this may be achieved through use of the NEPA computing machine.

Digital computer. - The electronic computer mentioned in previous reports has now been completed and put into operation (see Fig. 50). The machine is capable of solving problems in distribution of radiation in shields, thermodynamics, heat diffusion, nuclear reactivity, aircraft stress and possibly logistics using the Gauss-Von Seidel method for solving simultaneous liner equations. The machine can solve equations in as many as 300 unknowns by a series of converging iterations.

Problems are fed to the machine on punch-coded, standard, teletype tape, transcribed and recorded by a single electronic recording head, solved, and stored on a magnetic tape for future use. The system is unique in that it uses tape synchronization to achieve a fixed memory sequence, avoiding the characteristic and time consuming search for stored data.

Although the machine is much smaller, slower, and less flexible than machines like the SSEC, it is well adapted to the fairly rapid solution of problems peculiar to NEPA's work. Its relatively low cost and easy accessibility to NEPA are also important characteristics in its favor.

Fig. 50 - NEPA DIGITAL COMPUTER

3.4 SHIELD MATERIALS
(3.6 Man-months)

The continuing investigation of possible hydrogenous materials now embraces work on uranium hydrides. Metal Hydrides Incorporated, has been charged with preparing a uranium hydride that is nonpyrophoric and has good thermal stability and high hydrogen density; such properties would facilitate compaction of the compound. Some properties of the material have been determined; it has been found that the dissociation pressure below 570°F is much higher than reported by the Iowa State College.

Attempts have been made to cast lithium borohydride in molds, to obtain densities nearer to theoretical. Other investigations comprise attempts to obtain the eutectic of the system and to dissolve the material in an organic solvent. On a weight basis, lithium borohydride at 77°F is 60 per cent better than water as a hydrogenous shield material.

Preliminary results of a study begun on a wolfram borohydride indicate that the material is stable and nonpyrophoric. The borohydrides of heavy elements are to be thoroughly investigated during the coming year.

The effect of boron on the formation and dissociation of typical hydrides, such as those of titanium and zirconium, is being examined. The borides of titanium and zirconium have shown no evidence of hydrogen absorption in a hydrogen atmosphere.

A survey completed at the California Research Corporation on organic compounds showed that N_H, the number of hydrogen atoms per unit volume, varies directly with chemical structure - more in the case of paraffins and less for aromatics. Several promising compounds were placed in the ORNL pile for 4 weeks at 87 per cent maximum flux at 285°F in standing air, with and without radiation inhibitors. The results are now being evaluated.

Consideration has been given to incorporating boron long-chain paraffinic compounds, such as lauryl borate, into the organic fluids that appear hopeful.

The investigation of materials of nonhydrogenous nature has continued.

An investigation of the practicality of rolling Boral slabs is continuing, in cooperation with ORNL, at the plant of the Lukens Steel Corporation. A mock-up boron carbide plate for bulk-shielding tests at the ORNL pile was successfully made. Other such plates will be made during the coming quarter.

The successful fusion-welding of thin wolfram sheets was further demonstrated by Fansteel Metallurgical Corporation. Comparison with riveted sections indicates that welding is superior to riveting as a means of joining wolfram. Kennametal, Incorporated, delivered some pieces of wolfram, approximately 0.2-inch by 8 inches by 8 inches, which had been compacted from powder at 25,000 pounds per square inch and subsequently

R-236-12

sintered in vacuum. Larger sections can be produced by the same method with an improvement in density. However, the program for fabrication of wolfram sheets for bulk-shield testing has been put aside pending investigation of a wolfram-alloy system. A wolfram-iron alloy appears promising, and a survey of possible fabricators is in progress. Some experimentation is under-way at ORNL to form sheets from wolfram powder bonded by Tygon, a plastic. A survey of possible uranium alloys and combinations has started. In addition, work is in progress on manufacturing wolfram carbide and boron carbide, singly or in combination, as practical shield material.

3.5 GENERAL SHIELD STUDIES AND DESIGN (2.5 Man-months)

A program has been started to obtain fairly complete designs of several possible shields, which will include all the practical aspects of an aircraft shield as well as the most recent theoretical considerations. Preliminary designs will first be prepared by the design engineers. These will then be analyzed by the best available theoretical methods, taking into account the effects of supporting structure, ducts, and arrangement of the shield components in the aircraft. Following the theoretical analysis, final drawings will be made. These should be completed during the next quarter.

Three types of divided shields will be studied simultaneously in the proposed program:

1. Matched layer of wolfram carbide or equivalent and boron carbide, followed by hydrogenous neutron shielding material (probably water); crew shield to be a lead disk. Both the matched layer and hydrogenous material will completely surround the reactor, though it is expected that the matched layer will be somewhat thinner at the rear.

2. Matched layer of lead and water in the front portion of the shield, with only water adjacent to the reactor in the rear portion; more hydrogenous material (probably gasoline) to surround the water; crew shield is to be made of lead, having thicker rear section than sides.

3. Similar to (1) except that the matched layer will be made of lead and water instead of wolfram carbide and boron carbide.

The type (2) shield described briefly above depends upon shadow-shielding of gammas. Analysis indicates that a considerable reduction in the reactor-shield high-density layer is possible at the rear and sides of the reactor. Thus, in this shield, the materials used solely for gamma-shielding will be concentrated in heavy plates in front of the reactor and again, as part of the crew shield, behind the crew. The heavy plates in the forward portion of the reactor shield may extend for some distance around the sides of the reactor. Preliminary analytical results indicate that thin lead sides are required around the crew compartment to achieve minimum weight for this type of shield.

Analysis of shadow-shielding of neutrons showed that scattering by the aircraft structure limited the reduction in neutron shielding-material thickness at the aft end of reactor shield to only a few inches, if that portion of the shield were clean. However, since it is planned to bring all ducts and several control rods through this part of the shield, any gain which may have been anticipated will most likely be more than offset by the detrimental effect of these passages through the shield. Some of the neutron shielding may be placed around the crew because: (1) the material remains at a low temperature; (2) there is no loss of efficiency due to ducts (this is especially important in the air cycle); (3) nonuniform neutron leakage from the reactor shield is more readily compensated for; (4) there is a weight-saving if the reactor shield outside diameter tends to become larger than the crew shield.

3.51 **Open Cycle.** - A preliminary drawing of a shield section showing the intake and outlet annular air ducts for the IO-2 aircraft was completed and nuclear shielding analysis was started. It was originally planned to test this section in

R-236-13

the ORNL lid-tank shield-testing facility. For this reason, a model of a section of the outlet duct was made to illustrate the shape of the duct and adjacent heavy layer (see Fig. 51). The section is hollow and filled with air.

The section was based on a shield designed for a split-flow type of reactor having a core diameter of 3.54 feet and a free-flow ratio of 0.3/1. The total free-flow areas of the inlet and outlet air ducts are 5.86 and 11.04 square feet, respectively. Two ducts are used for inlet and two for outlet, hence the area of each duct is half of the value given above. However, the ducts within the shield will have to be insulated, adding substantially to the already large volume of void within the shield.

3.52 **Compound Liquid-Coolant Cycle.**

Shield design studies. - The initial shield design work described under section 3.5 is to be carried out for the reactor described in section 2.2 (sodium-cooled, 2.5-foot core diameter, and 3.33-foot reflector outside diameter). The shield is to be of the divided type, with a 50-foot separation between the center of the core and the rear face of the crew shield. The coolant will flow through the shield through 16 ducts, eight inlet and eight outlet, each having an inside diameter of 3 inches. Each duct, however, is double-walled with a 0.5-inch space provided between walls for insulating material and expansion. Hence, the outside diameter of each duct is about 4.25 inches. All ducts and control rods will be brought out through the

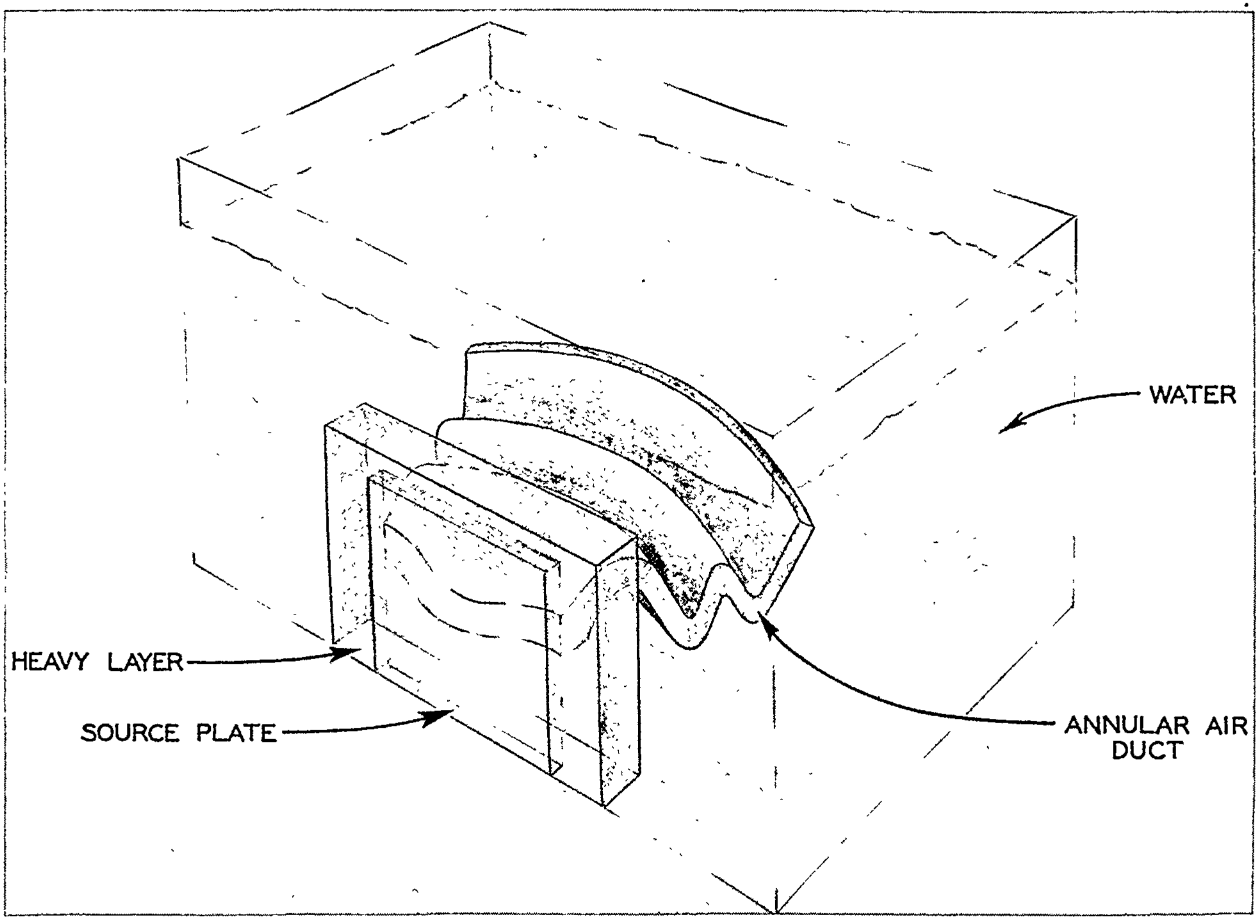

Fig. 51 - PROPOSED ASSEMBLY FOR RESTING SHIELD SECTION IN ORNL LID-TANK FACILITY

R-236-14

rear face of the reactor so that any increased leakage of radiation that they may cause will not be directed initially toward the crew.

Comparative effects of sodium and bismuth on shield weight. - The total weights were determined for a complete reactor-shield assembly when a bismuth cooling system was used and when a sodium cooling system was used. The chief differences in the two systems are:

1. In the bismuth system, bismuth may be passed all around the core to form a heavy gamma-shielding layer, whereas, for the same shielding effects, a separate heavy layer (lead or wolfram carbide) must be used with the sodium system. This results in a weight penalty for the sodium system, because the heavy shielding layer must be at a greater radius than the bismuth gamma-shielding layer in the bismuth system. However, if it is found that no heavy layer is required along the sides and rear of the reactor, this weight advantage for the bismuth system will be removed.

2. The weight of the coolant is much greater in the bismuth system. This results in an over-all weight advantage for the sodium system. The comparison is described in more detail in section 2.22 of this report.

Liquid-metal ducting study. - The manner in which liquid-metal ducts should be brought through the shield so as to cause the least increase in shield weight was studied. A line-of-sight method was used in which the distances through the various materials were weighted by the total macroscopic cross-sections of the respective materials; i.e., if the macroscopic cross-section of a given material was one-fourth that of water, t inches of the material was considered to be as effective as $t/4$ inches of water.

First to be investigated in this way was an 8.5-inch diameter bismuth duct having two-dimensional curvature. It was assumed that a total of four ducts would be required to cool a reactor consisting of a 1.98-foot diameter core with a 2.5-inch reflector; two of the ducts would come into the header at the intake end of the reactor, and two would come out of the exit header. The plane of the duct axis was perpendicular to the axis of the reactor core and passed through the header at either end of the reactor. An allowance was made of 0.5 inch around the outside of the duct for insulation and expansion. Several bending arrangements were tried until the most satisfactory configuration was found (see Fig. 52). It was estimated that an increase in the hydrogenous shield thickness of a few inches in the vicinity of the ducts would be sufficient to offset the detrimental effect of the ducts on the shield.

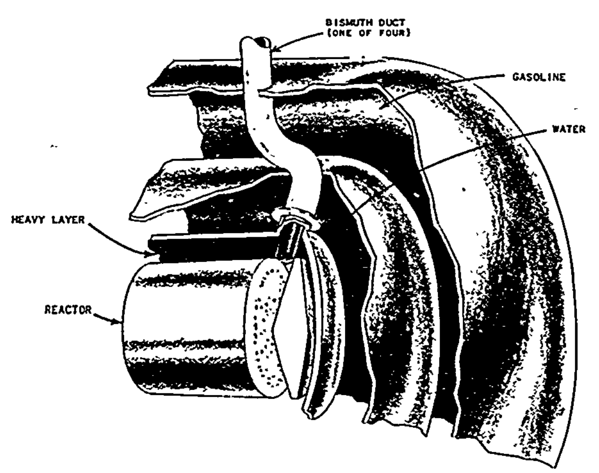

Fig. 52 - BISMUTH DUCT THROUGH SHIELD

Next to be studied was a grouping of 2-inch diameter sodium ducts. Sixteen ducts (eight intake and eight outlet), extending from the rear periphery of the reactor to the rear of the shield, were considered necessary. It was intended that this first study of sodium ducts would involve only two-dimensional curvature, but it was found that much could be gained by incorporating one slight bend in the third dimension. The duct configura-

R-236-15

tion which evolved is shown in Fig. 53. Again it was estimated that a few inches more of hydrogenous shielding would offset the effect of the ducts.

The last study to be undertaken was that of spiral sodium ducts. Though preliminary work indicated that these should cause the least increase in shield thickness, the investigation was interrupted by work of higher priority.

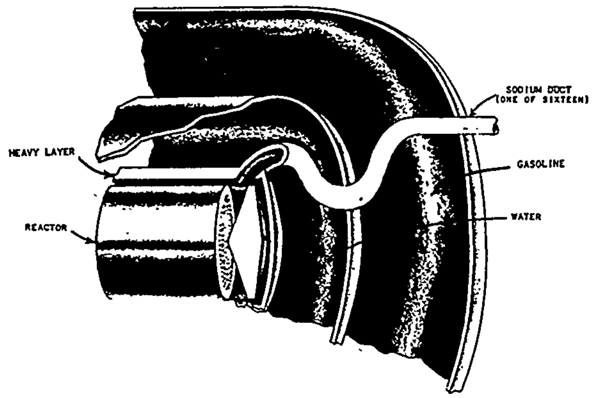

Fig. 53 - SODIUM DUCT THROUGH SHIELD

• • • • •

R-236-16

4. ENGINE COMPONENTS

4.1 ENGINE COMPONENT DESIGN AND ANALYSIS (25.0 Man-months)

4.11 **Open Cycle.** - Work on the open cycle during this quarter has consisted of the following:

1. Design work on the adaptation of the J-57 to the air cycle. A layout is in progress for replacing the engine burners with air inlet and outlet scrolls. Present indications are that no increase in engine length will be necessary, but an increase of 15 per cent in engine weight is anticipated in order to connect the turbine and compressor rigidly through an adequate outer shell.

2. Subcontract work at Westinghouse Electric Corporation on the feasibility of using two J-34 engines as a nuclear test-stand power plant has been completed. No further work is anticipated.

The Westinghouse work has shown that a test setup with two J-34 engines operating from a single heat source is feasible although considerable space, time, and money would be involved. A large heat source with 20-inch diameter ducts and numerous valves and expansion joints is necessary. However, there is some question about the desired pressure drop through the heat source and associated piping. Analysis indicates that a pressure drop of 20 to 30 per cent will be encountered in the proposed full-scale power plants. The test setup proposed by Westinghouse has a pressure drop of only about 11 per cent. It is thought that the full pressure drop should be used in a proper test of starting, control, and operational problems. This, of course, would require redesign of the J-34 turbine section, which is not necessary with the 11 per cent loss. On the other hand, the large ducts and valves could be made smaller, and this would simplify the test installation.

In view of the fact that operation of two jet engines from a single heat source, on a smaller scale, should be achieved fairly soon at NEPA with the Boeing turbo-jets, no further action on the Westinghouse program will be taken at this time.

4.12 **Compound Liquid-Coolant Cycle.**

Core circuit. - Studies of sodium as a core coolant were made, using the same basis as the bismuth studies: i.e., based on the power plant for IL-1 aircraft at Mach 0.8 and 45,000 feet. It has been shown that, besides the direct weight-saving (see section 2.22), the sodium system has some other advantages. Line sizes can be smaller, fluid velocities higher, and pressure drops still not excessive, since the density of sodium is about 1/20 that of bismuth. The intermediate heat exchanger can be smaller because of the greater specific heat of the sodium. The total volume of the core circuit is reduced by about 25 per cent. Table 16 gives a comparison of some of the actual design values.

TABLE 16

COMPARISON OF CORE-CIRCUIT DESIGN DATA FOR Bi-Li AND Na-Li SYSTEMS

Characteristic	Bismuth-Lithium	Sodium-Lithium
Core-coolant flow:		
lb./sec.	6974	845
gpm.	5305	7899
Heat-exchanger core frontal area (sq. ft.)	5.13	3.03
Heat-exchanger tube length (ft.)	3.0	3.0
Coolant line through shield:		
In	2@ 8.6 in. dia.	2@ 3 in. dia.
Out	2@ 12.7 in. dia.	2@ 3 in. dia.
Total line area through shield (sq. in.)	369	112
Total core circuit pressure		
drop: ft.	23.96	295.1
drop: psi.	98.3	98.4
Volume of core coolant (cu. ft.)	47.0	35.9

Fig. 7, section 2.2, shows the proposed sodium core circuit. In this design the reactor and heat exchanger are both horizontal. The heat exchanger and pumps are placed outside the shield and the shield thickness increased somewhat on that end to compensate for the ducting.

Entry into the reactor at the near end makes the lines short and provides a coolant for the outer shell. The sodium flows through an annular passage to the entrance of the core at a velocity

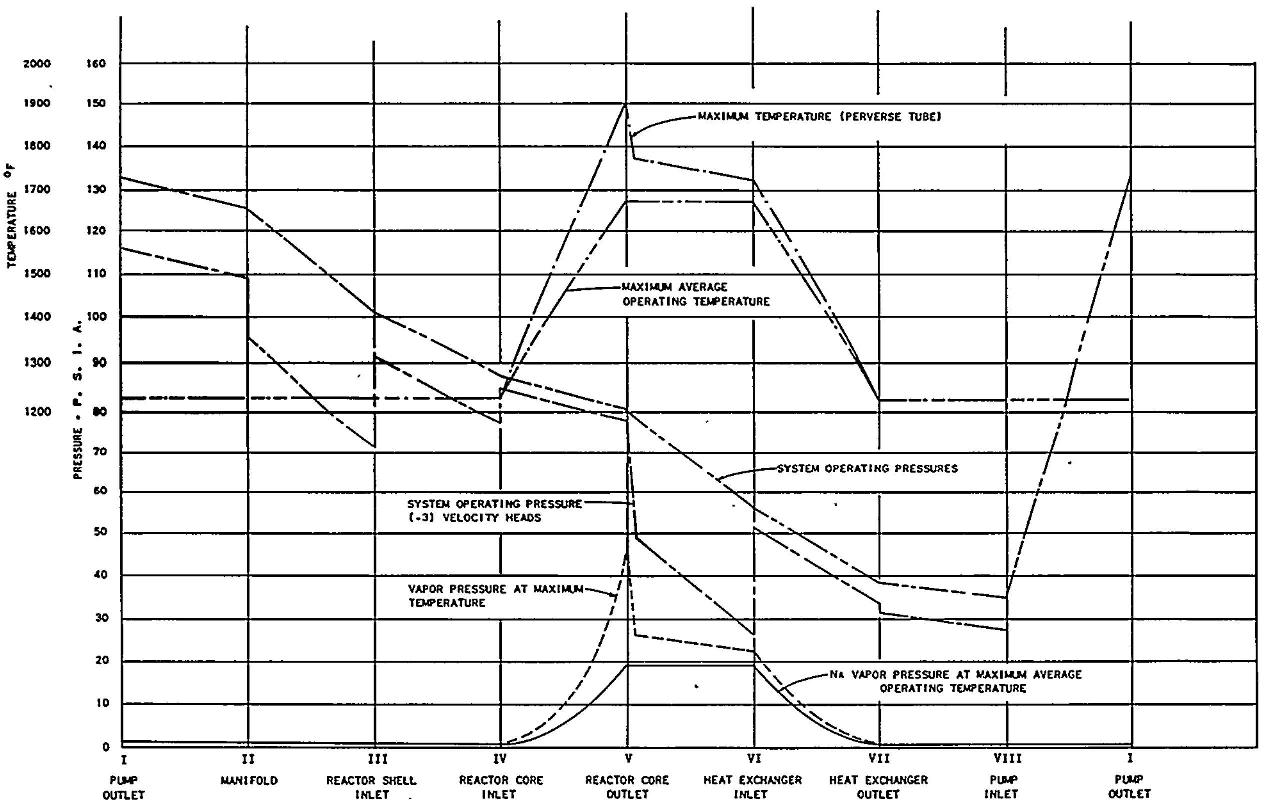

Fig. 54 - SODIUM CORE-CIRCUIT PRESSURE AND TEMPERATURE - TWO PUMP OPERATION

The liquid sodium flows from each pump through single lines at 33 feet per second. A cross-over line is provided at the check valve exits to allow for single pump operation. Just outside the shield, the pump outlet lines enter short headers, and the flow is then divided in four lines on each side. These eight 3-inch lines then curve through the shield to the near end of the reactor. The curvature serves the dual purpose of decreasing neutron streaming and allowing for line expansion. Each line has one-quarter inch of insulation around it, plus a one-quarter inch air gap, and is enclosed by a 4-inch tube. The air gap allows sufficient room for free expansion of the coolant line. The fluid velocity in these lines is 45 feet per second.

of 25 feet per second. After flowing through the core, the coolant is taken out through eight 3-inch lines arranged in two groups of four at 90° to the plane of the entering lines. These also curve through the shield and have insulation and an enclosing shell. The fluid velocity is again 45 feet per second.

Entrance into the heat exchanger header is radial at low velocity to obtain good distribution. The velocity through the core is 18 feet per second. Entrance into the two pumps is at 22 feet per second.

The major problem in the use of liquid sodium as a coolant is to prevent boiling. At one atmosphere, sodium boils at approximately 1616°F. It is therefore necessary to maintain the pressure above that of the sodium vapor pressure at all times. A plot of temperatures, vapor pressures, and system pressures can be seen in Fig. 54.

For a more conservative approach, a plot was made of the system pressure minus 3 velocity heads (3q). This assumes that some local disturbance causes an instantaneous pressure loss of 3 q. Comparing this curve with the perverse tube vapor pressure line shows that there is still no danger of boiling. The critical point comes just

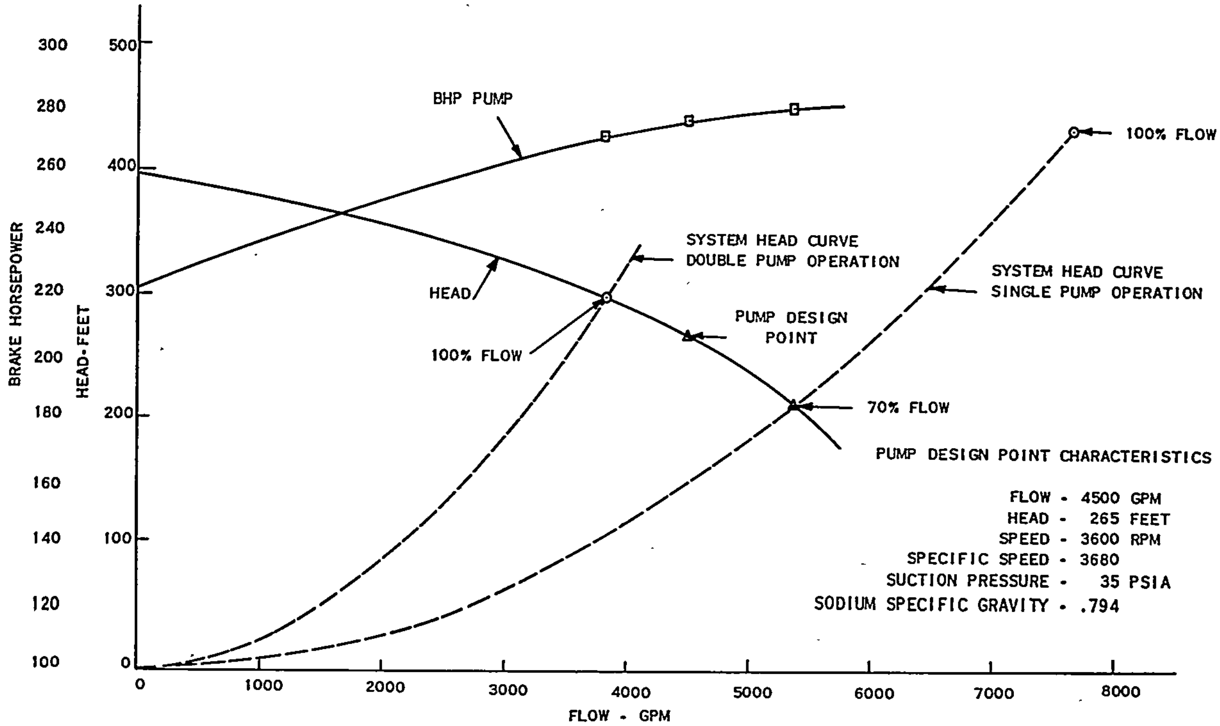

Fig. 55 - ESTIMATED CONSTANT SPEED PERFORMANCE CURVE FOR PHASE I CORE-CIRCUIT SODIUM PUMPS. DOUBLE PUMP INSTALLATION

The system pressure at the pump outlet is 133 pounds per square inch, absolute; at the pump inlet 35 pounds per square inch, absolute. Based on the maximum average temperatures, the sodium vapor pressure reaches a peak of only 19 pounds per square inch, absolute, between the reactor outlet and heat exchanger inlet. The perverse tube-coolant temperature, however, must also be considered. This could reach a peak of 1900°F at the reactor outlet. At this temperature, the sodium vapor pressure is 47 pounds per square inch, absolute; while the system pressure is 81 pounds per square inch, absolute.

before the entrance to the heat exchanger where the velocity is quite high (45 feet per second). The figures shown are conservative, however, as it was assumed that the hot flow from the perverse tube would still be 50°F above the average; while in actuality it would be well mixed by that stage. In addition, the entrance to the heat exchanger provides for gradual diffusion to the header velocity which would raise the bottom of the (pressure – 3q) curve, providing an even greater safety factor.

Pumps. - A design was made of a constant speed, double pump system for use with sodium as a core-circuit fluid, based on the following altitude-system head requirements (see Fig. 55).

	Single Pump Operation	Double Pump Operation
Flow	845 lb./sec. (7660 gpm.)	422.5 lb./sec. (3830 gpm.)
Head	430 ft.	295 ft.

In order to obtain small size pumps with stable performance during parallel operation, it was found necessary to limit the emergency single pump operation to 70 per cent of the required total flow, or 591.5 pounds per second at 210 feet.

The approximate pump dimensions are 9 1/2 inches impeller diameter and 18 inches maximum over-all casing diameter. The brake horsepower required is about the same as for bismuth, since higher heads have resulted from the higher velocities in the sodium system.

Concern over the basic problems of bearings and leakage from a pump seal have led to consideration of several special designs. Negotiations are under way with several subcontractors to do design work followed by testing to help solve some of the difficulties. The design of a seal test rig and a bearing test rig is also nearing completion at NEPA.

One proposed solution is an electromagnetic pump having the rotor completely "canned" or sealed. All indications are that such a pump would not only be a very large development job but that it would result in a very much heavier unit than can be tolerated for aircraft.

A more favored proposal is a sump type pump with a vertical shaft (see Fig. 56). Such a pump has been designed for a bismuth application, and all liquid-metal coolant pumps now being considered are of this type. In this design, the vertical pump shaft has an inert pressurized gas, balancing the pressure of the liquid in a labyrinth around the pump shaft. The labyrinth must be an estimated 20 inches long to prevent leakage during rapid aerial maneuvers. A conventional carbon face type seal operating out of contact with the liquid-metal coolant and at relatively low surface speeds is used to hold the gas leakage to a minimum. It is necessary to have one guide bearing immersed in the liquid metal, and this can possibly be made of ceramic or graphite materials. Since the shaft is vertical, a right angle gear drive is required at the top. However, this right-angle drive can also constitute the necessary reduction gear.

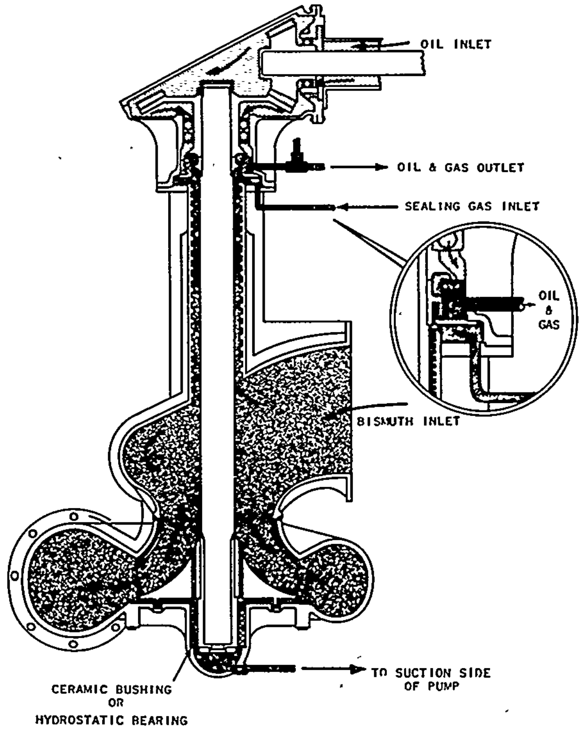

Fig. 56 - LIQUID-METAL-COOLANT PUMP

Heat exchanger. - The test program for development of aircraft type heat exchangers, which was started during the previous quarter and described in the last report, is continuing satisfactorily. NEPA design work has been temporarily finished on liquid-to-liquid and liquid-to-air test units. A subcontract has been negotiated with A. O. Smith

Corporation of Milwaukee, and purchase orders have been placed with Harrison Radiator Division of General Motors Corporation for delivery of the first NEPA designs. Technical contact has been maintained with both corporations, and it is expected that the first units will be delivered for test in September, 1950.

It is planned that this program will indicate satisfactory methods of welding large numbers of small tubes into tube sheets, and develop a method of metal joining suitable for high-temperature operation of a plate-and-fin type compact radiator.

This may prove a serious problem as has already been indicated by Harrison Radiator Division. Development of a brazing alloy strong enough at high temperatures and resistant enough to coolants now under consideration has not yet been accomplished. Considerable development has already been done by one manufacturer using Colmonoy No. 6, but this is a very high nickel alloy soluble in all coolants being considered. Furthermore, it is difficult to keep the alloy from melting through thin sheets of the radiator. However, the work is successful in its present application and encouraging enough to make the NEPA brazing requirement look quite possible. Consideration is also being given to methods of welding the compact plate-and-fin design. Efforts are being made to accelerate all this work since insurmountable difficulties in joining development would undoubtedly lead to heavier and larger radiator designs for the full scale aircraft. This would affect the frontal area of the jet engines and could seriously affect the feasibility of the entire compound liquid-coolant cycle.

4.13 **Compound Helium Cycle.** - Design work has continued on the compound helium cycle engine for the IH-3 aircraft during this quarter with particular attention to engine radiator design, valves, and the circulating unit. Serious problems arise at every point, which make the feasibility of the helium system from the mechanical and operational standpoint much less promising than that of the air or liquid-metal systems. Chief among these problems are the combination of high temperatures and high pressures and the high rate of helium leakage through small holes.

Radiator. - The studies have indicated that the pressures contemplated in the helium cycle were much too high for any type of radiator except tubular. Round tubes can stand considerably higher pressures than flat tubes or flat plates. However, a round tube design tends to be large unless pressures around 650 pounds per square inch are used at the radiator. A design study has been completed on a radiator with helium flowing outside of round tubes at this pressure, and it appears that the stress can be kept below the desired maximum of 5000 pounds per square inch. The tubes are 0.143 inch in diameter, with 0.012-inch wall, and 29 inches long. There would be about 40,000 of them in each radiator. (Six radiators for six engines per airplane.) Stresses in the headers still remain a serious problem and are partially responsible for the large radiator section diameter of 73 inches for a basic 44-inch diameter engine. This large diameter has contributed to a decision to place the engines for the helium cycle in the fuselage rather than in nacelles.

TABLE 17

COMPARISON OF TUBULAR RADIATOR (FOR HELIUM) AND PLATE-AND-FIN INVOLUTE RADIATOR (FOR LIQUID-COOLANT CYCLE)

Characteristic	Helium Radiator	Lithium Radiator
Inlet pressure (psi.)	650	105 (Li)
Inlet temperature (°F)	1650 (40,000 ft.)	1600 (45,000 ft.)
Flow (lb./sec.)	38 (S.L.)	37 (S.L.)
Frontal area (sq. ft.)	12.35	12.35
Max. outside diameter (in.)	73	59.75
Tube length (in.)	28.8	12
Dry weight (lb.)	2827	955
Tubes/engine	40,365	
Total length of tubing per engine (ft.)	96,876	

A comparison is made between the tubular type helium radiator and the plate and fin involute radiator for the compound liquid-coolant cycle in Table 17.

Valves. - In the helium circuit, individual helium ducts run to each engine or engine pod. In case of battle damage or other difficulties, it is felt that shutoff valves must be provided in the fuselage for each of these lines. These valves must operate very quickly, must have very low pressure drop when open, and must have no stem leakage. But, most important, they must have practically zero leakage when closed. The latter requirement suggests the use of a poppet valve. However, zero leakage is a serious problem in a 10-inch diameter duct at 1650°F.

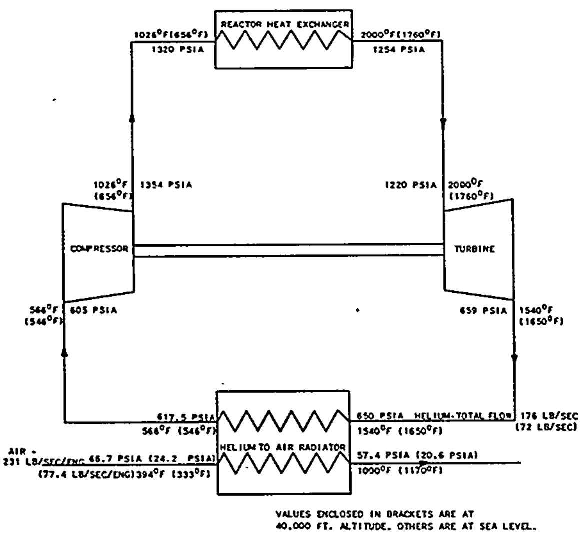

Fig. 57 - HELIUM CIRCUIT DIAGRAM

Calculations showed that a hole with an area of one-half square inch would leak 1.77 pounds of helium per second at a pressure of 520 pounds per square inch. This means that a reserve supply of 500 pounds, occupying a 54.5-cubic foot space, would be gone in less than 5 minutes. There are about 100 pounds of helium in the circulating system. Leakage around a valve equivalent to that through a hole with an area one-half square inch does not seem unreasonable. This is equivalent to an average clearance at the valve seat of only 0.008 inch.

Circulating unit. - Considerable effort has been expended during the past quarter, both at NEPA and at Wright Aeronautical Corporation, on the design of a helium compressor and turbine to circulate the helium through the reactor and radiators. Currently considered pressures and temperatures in the circuit are indicated on the diagram (see Fig. 57). The compressor outlet pressure is 1354

TABLE 18

SPECIFICATIONS FOR HELIUM COMPRESSOR-TURBINE CIRCULATING UNIT

Compressor	
Stages	17
Compression ratio	2.4/1
Speed (rpm.)	6500
Tip velocity (ft./sec.)	800
Inlet hub-tip ratio	0.825/1
Over-all efficiency	0.85
Blade tip diameter (in.)	28.0
Length (in.)	54
Maximum Mach No.	0.39
Turbine	
Stages	8
Expansion ratio	0.54
Speed (rpm.)	6500
Blade tip diameter (in.)	30.8
Axial gas velocity (ft./sec.)	1900
First rotor blade height (in.)	2.22
Max. stress in blade (psi.)	10,000
Max. blade temperature (°F) (50°F nozzle drop; 150°F cooling)	1800
Nozzle discharge angles	40-50°
Efficiency including mechanical losses and cooling losses	0.86
Length (in.)	36

pounds per square inch, and turbine inlet conditions are 1220 pounds per square inch and 2000°F.

The design of the turbine-compressor unit presents difficult and unique problems. The high temperatures and high pressures are serious in themselves, but fundamental questions arise due to the difference in properties between helium and air, which can be answered only by experimental tests. Since the speed of sound in helium (7140 feet per second at 2000°F) is high compared to air, it appears that stress limitations rather than Mach-number limitations will be controlling. Conventional air velocities result in an excessive number of stages so that high helium velocities appear reasonable, but only testing will show whether the required efficiencies can be obtained at these high velocities. The subcontractor is now proceeding with layout work with a unit based upon estimated analysis given in Table 18.

The final helium compressor and turbine unit is expected to be about 36 inches in diameter and 12 feet long. The weight will be much higher than expected from normal jet engine practice because of the high pressures. It should be noted that the internal power of the unit for a Phase I aircraft is approximately 143,000 horse power. This results in high bending loads on all the blades, large shaft size, and large thrust loads.

4.2 ENGINE COMPONENT EXPERIMENTATION (18.9 Man-months)

Preliminary handling tests of liquid metals continued as a preliminary to starting construction of the large-scale model circulating system.

Bismuth circulating rig. - This test rig, which was described in the last quarterly report, was modified by replacing the 7.5-kilowatt muffle furnace with a 60-kilowatt box furnace and adding a cooler of the falling water film type. Satisfactory operation was obtained with this equipment.

The over-all heat-transfer characteristics of the furnace and the cooler were obtained. Of the 60-kilowatt input to the furnace, it was found that 24 kilowatts, or 40 per cent, was transferred to the bismuth as an increased heat content. This roughly checks the design calculations of the radiant-type gas-fired box furnace being procured for the scale-model system, in which it is expected that 42 per cent of the available energy will be transferred to the bismuth.

The cooler has a heat-transfer area of 1.85 square feet and, using this figure, the tests indicate over-all heat-transfer rates of 20 to 40 Btu. per square foot per hour per degree Fahrenheit. It is quite probable that in this type of heat exchanger the effective heat-transfer area increases with heat load and, for the present test conditions, only a small part of the available area is effective, thus indicating that the cooler has adequate capacity for the test work planned.

Fig. 58 - BISMUTH BENCH TEST RIG

Fig. 58 shows the test loop, including the cooler, flow-measuring tank, sump (pump immersed), and the end of the heater coil. Fig. 59 shows the heater coil installed in the furnace.

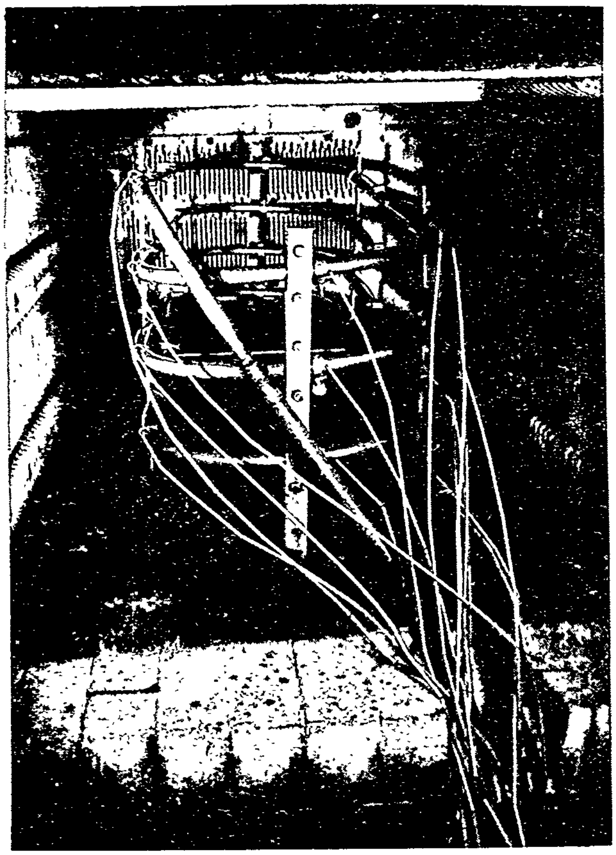

Fig. 59 - HEATING ELEMENT IN 60-KW FURNACES (BISMUTH BENCH TEST RIG)

The maximum bismuth temperature reached to date was 1640°F. This temperature was maintained in a test section between the heater outlet and cooler inlet.

After 12 hours of operation, of which 3/4-hour was above 1600°F, a leak developed in the outlet section of the heater coil. The cause of the failure is being investigated.

Lithium pressure-temperature rig. - A test chamber was built to parallel the static bismuth tests that were described in the last quarterly report.

Because of the formation of surface oxides and nitrides on lithium at room temperature, a special test arrangement was devised to obtain pure lithium. This is shown in Fig. 60 and is briefly described as follows:

> The lower chamber is first loaded with lithium blocks, as received, but cleaned with petroleum ether. This chamber is evacuated as it is heated and is purged repeatedly with argon. After the lithium is melted, an argon atmosphere is maintained. The upper chamber is also evacuated at the same time. A tube from this tank connects through a valve to a standpipe in the lower tank. The upper tank is filled with essentially pure lithium by using a differential pressure to force liquid from the center portion of the lower tank up into the one above. Two ports in the side of the upper

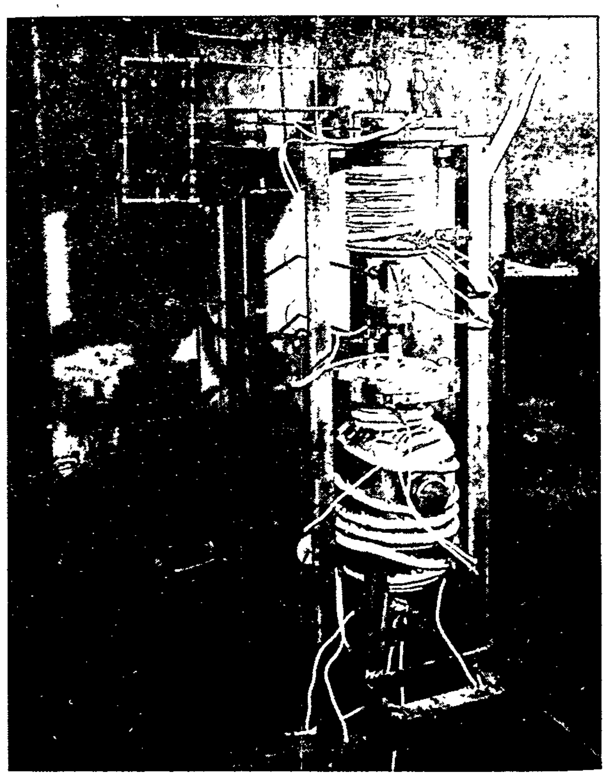

Fig. 60 - LITHIUM VARIABLE TEMPERATURE-PRESSURE STATIC-TEST RIG (REAR VIEW)

chamber allow test specimens to be inserted in a container and later examined for corrosion effects.

The entire system, including an electric light and exhaust fan, is installed in a sheet-steel box approximately the size of a telephone booth.

The first tests were concerned primarily with determining the effect of lithium leaks in air on insulation and construction materials. Good thermal insulators such as mica, asbestos, and Superex were rapidly consumed due to their high silicon content. A slab of JM-3000 Block showed severe erosion. A plate of 0.064-inch aluminum (type 24 ST) was penetrated by a 1000°F lithium stream in 5 seconds. Masonite and Formica were slightly charred after 5 seconds.

A small simulated lithium radiator was tested to determine the effects of a hole developing between the lithium and the air side of the radiator. Compressed air was passed through the tube bundle at 150 feet per second; while lithium at 1375°F and 100 pounds per square inch filled the interstices and was allowed to escape through a No. 60-drill hole into the air stream. Lithium fumes issued from the air duct on the discharge side for 3 minutes, until the duct became clogged with lithium compounds, and the air flow stopped. About 1 minute later the lithium in the duct reacted with the air to bring the steel-pipe duct to incandescence. Ten minutes later the pipe cooled below the glowing temperature (approximately 1300°F). No violent reactions were noted. The heat exchanger appeared to be in good condition after the assembly was cleaned (lithium compounds dissolved).

In another test a stream of lithium 0.060-inch in diameter at a temperature of 1510°F was made to impinge on a sample of ordinary concrete for approximately 3 seconds. A violent reaction took place, scattering lithium and concrete particles with considerable force and giving a brilliant white light and large quantities of fumes. Upon examination, the concrete surface was found to have been attacked over an area 1 1/2 inches in diameter to a depth of 1/8-inch.

• • • • •

5. HEAT TRANSFER AND FLUID FLOW

Heat-transfer work this quarter includes basic studies of heat transfer and pressure drop in reactor and radiator passages, studies of pressure drop in shield ducts, flow distribution studies, and development work on reactor and radiator headers.

The experimental work at United Aircraft Corporation on open cycle ducting and header problems has produced a suitable inlet and discharge header configuration. The summary report on the helical duct studies has been issued as NEPA-1470, *Fluid Flow in Helical Ducts of Rectangular Cross Section.* (See section 5.12.)

The experimental work being done at Massachusetts Institute of Technology on heat transfer and pressure drop for air flowing in small-bore tubes has been completed. (See section 5.11.)

The work at Babcock and Wilcox Company on the determination of heat transfer and pressure drop for lithium is progressing favorably. The rig is scheduled for operation during the next quarter. (See section 5.21.)

Discussions were held regarding plans for liquid-metal ducting and header tests. No definite action has been taken on this work as yet. (See section 5.22.)

5.1 OPEN CYCLE (37.6 Man-months)

5.11 Heat Transfer. - Initial tests were made with the NEPA heat-transfer rig during the quarter. The operating panel for this rig is shown in Fig. 61.

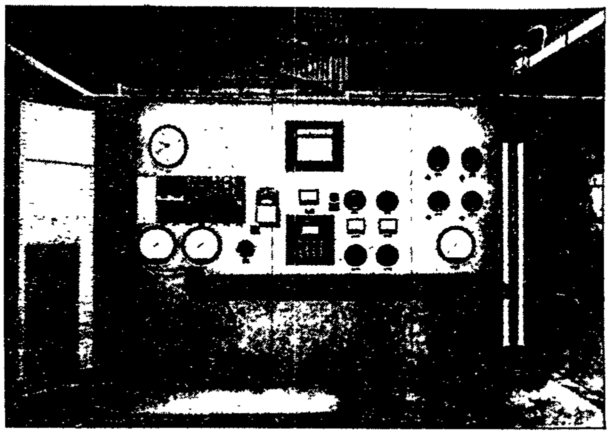

Fig. 61 - CONTROL PANEL, NEPA HEAT-TRANSFER RIG

During the run, it was obvious that several of the static pressure measurements and temperature measurements being taken along the tube wall were in error. The rig was, therefore, disassembled. Six pressure leads and an equal number of thermocouples were found to have broken away from the wall. Also, the ceramic nozzle block had broken. These failures are attributed to the fact that lack of experience in manipulating the power input to the test section led to too rapid changes in tube temperature and hence high thermal stresses in the instrumentation leads. The rig is now being repaired, and it is expected that a full series of tests will be made during the next quarter.

The experimental work being done at MIT, for NEPA, on heat transfer and pressure drop for air flowing in small-bore tubes has been completed. Considerable work remains to be done in correlating and analyzing the data; however, the final report on the work is expected next quarter.

Reasons for the lack of satisfactory correlation of the MIT data obtained during the previous quarter were investigated. It was found that flow measurements were somewhat in error, and also that the radiation shielding on the thermocouples measuring the inlet and outlet air temperatures was not effective at low Reynolds numbers. These items were corrected before the final runs were made. The present data, therefore, should be more reliable.

The survey of the literature on heat transfer and pressure drop during flow with turbulence promotion, being performed for NEPA by the Armour Research Foundation, has been completed. An annotated bibliography covering work done in this field is in preparation, and will be issued as a special report when completed. Topics to be covered include: (1) flow in roughened tubes; (2) effect of tube shape on the heat transfer-friction relationship; (3) the effect of turbulence promoters such as fins, dimples, and louvres.

Analytical studies at Armour Research Foundation on the heat-transfer process in roughened tubes were continued, in order to find favorable roughness configurations for use in design. No definite conclusions may be drawn from this work as yet. All work under this subcontract will be completed during the next quarter.

5.12 **Ducts and Headers.** - Experimental work at the United Aircraft Corporation on ducting and header problems continued during the quarter. The testing of discharge headers was also completed during that period. Starting with the assumption that a full annulus would be required, as was found in the inlet header program, a flat header plate and a number of conical arrangements were tested. The best performance obtained was an average deviation of 2.6 per cent from the average Mach number of 0.39 for all flow passages with a header plate spacing of 2.0 inches. This performance was obtained with a discharge header plate having a peak, the contour of which is formed by the revolution of a circular arc as shown in Fig. 62.

Other configurations tested were a flat header plate, a plate with a conical cavity, one with a spherical cavity, and one with a conical protrusion. The flat plate and plate with a conical cavity gave performance close to that mentioned above for the optimum configuration.

Partial surveys of flow distributions were run on combinations of the most promising inlet and discharge headers. The inlet header chosen was type S-3, an annular header, the outer plate of which has a cone of 8-inch base diameter and 8-degree base angle protruding inward toward the core face. The discharge headers chosen were the ones having a flat outer plate and a concave conical outer plate. Tests on the peaked discharge header plate had not been run yet, so it was not included in the combinations tested. Satisfactory performance was obtained with the configuration shown in Fig. 62b, which had an average deviation of 3.6 per cent from the average Mach number of 0.42 for all flow passages.

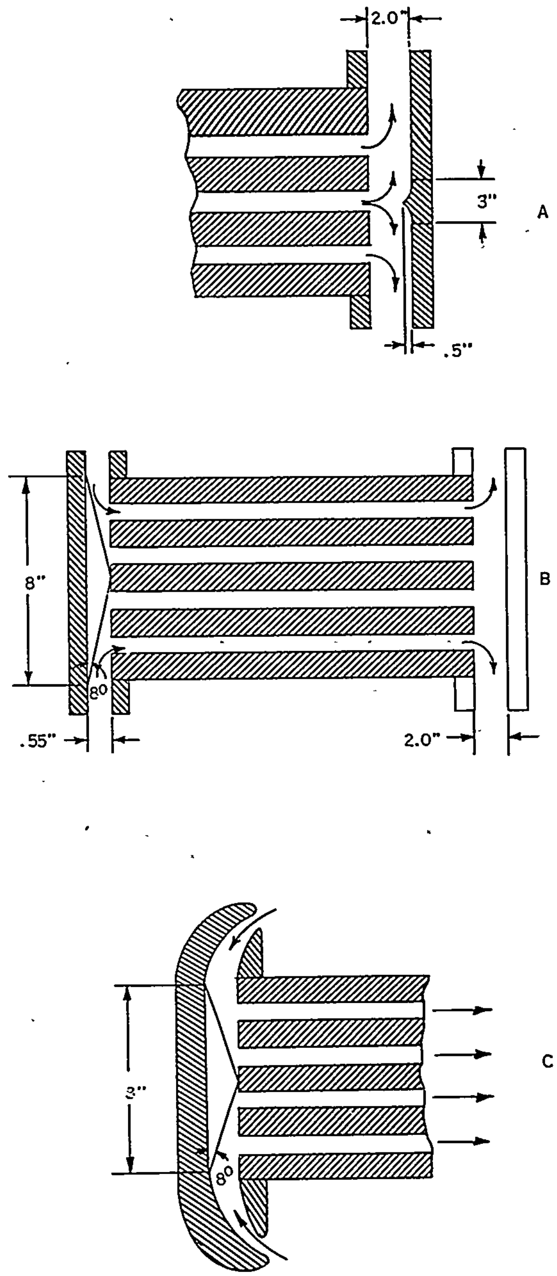

Fig. 62 - INLET DISCHARGE HEADERS

The values of average deviation from average Mach number, for the combination of inlet and discharge headers, are as much as 1 per cent higher than those obtained from tests on either the inlet or discharge headers alone. The distribution plots indicate that the deviations from average Mach number caused by the inlet and discharge headers were additive. Initial pressure loss calculations for these tests indicate that the loss in total pressure through the inlet header and through the discharge header are each about 0.75 of the kinetic energy at the entrance of the core tubes.

Tests were run on an annular inlet header preceded by a single bend as shown in Fig. 62c. Results indicate that, at a header spacing of 0.55-inch (Fig. 62c), choking occurred in the bend. The single bend contour is now being modified, and testing will continue.

All tests on the measurement of frictional pressure drop in cylindrical helical and conical helical ducts have been completed and are reported in NEPA-1470. The results of these tests are summarized in Fig. 63.

Testing of the small wavy and helical ducts will begin during the next quarter. Also, when the tests of the inlet header preceded by a single bend are completed, testing will commence on inlet and discharge headers preceded by annular wavy ducts. Design work is continuing on the model of one half of a split-core reactor, and fabrication and initial testing should be completed during the next quarter.

5.2 COMPOUND LIQUID-COOLANT CYCLE (11.5 Man-months)

5.21 Heat Transfer. - Work continued at the Babcock and Wilcox Company on the experimental determination of heat transfer and pressure drop for liquid lithium. The initial objective of this work is to obtain average lengthwise coefficients with a regenerative type of heat exchanger. In this type of rig, only the end temperatures are measured. From these data, only over-all heat-transfer coefficients can be computed. These include the resistance of the tube wall, and the combined resistances of the two liquids separated by the tube wall. The individual resistance of each liquid must be determined by analysis.

The isometric drawing, shown in Fig. 64, represents the heat-transfer apparatus which is being built. It embodies a simple figure-of-eight circuit, which was chosen because of its simplicity. Basically, the circuit consists of three electric heaters, two regenerative exchangers, and two forced-air coolers. The second regenerative exchanger (labeled "auxiliary") has been included in the circuit, primarily, to reduce the temperature to which the pump check-valves and the flow meter must be exposed. The interior of the cooler is utilized both as a pressurizing chamber and sump. A "pulsafeeder" reciprocating type pump is used. In this pump, no bearings, shaft seals, or moving parts (except check valves) are exposed to the molten lithium.

Methods for making ducting and header tests applicable to the compound liquid-coolant cycle were investigated. It appears that before any three-dimensional work is done, which at best will involve a number of moderately expensive and inflexible models, a two-dimensional-flow water rig should be built. The inlet and discharge headers would be tested together, and the principal objective would be to gain familiarity with the response of the pressure pattern, at the faces of the two tube sheets, to various changes in shapes of the headers. The use of transparent materials and controlled water temperatures, approaching boiling, would permit checking the susceptibility of various configurations to cavitation.

In the three-dimensional tests, the most important things to match are the length-diameter ratio of the tubes and the over-all geometric similarity. Any elbows and special piping configurations which are to be a part of the final system should be simulated in the rig. The margin by which the lowest wall static pressures exceed the vapor pressure of the fluid, and the Reynolds number, will be important parameters.

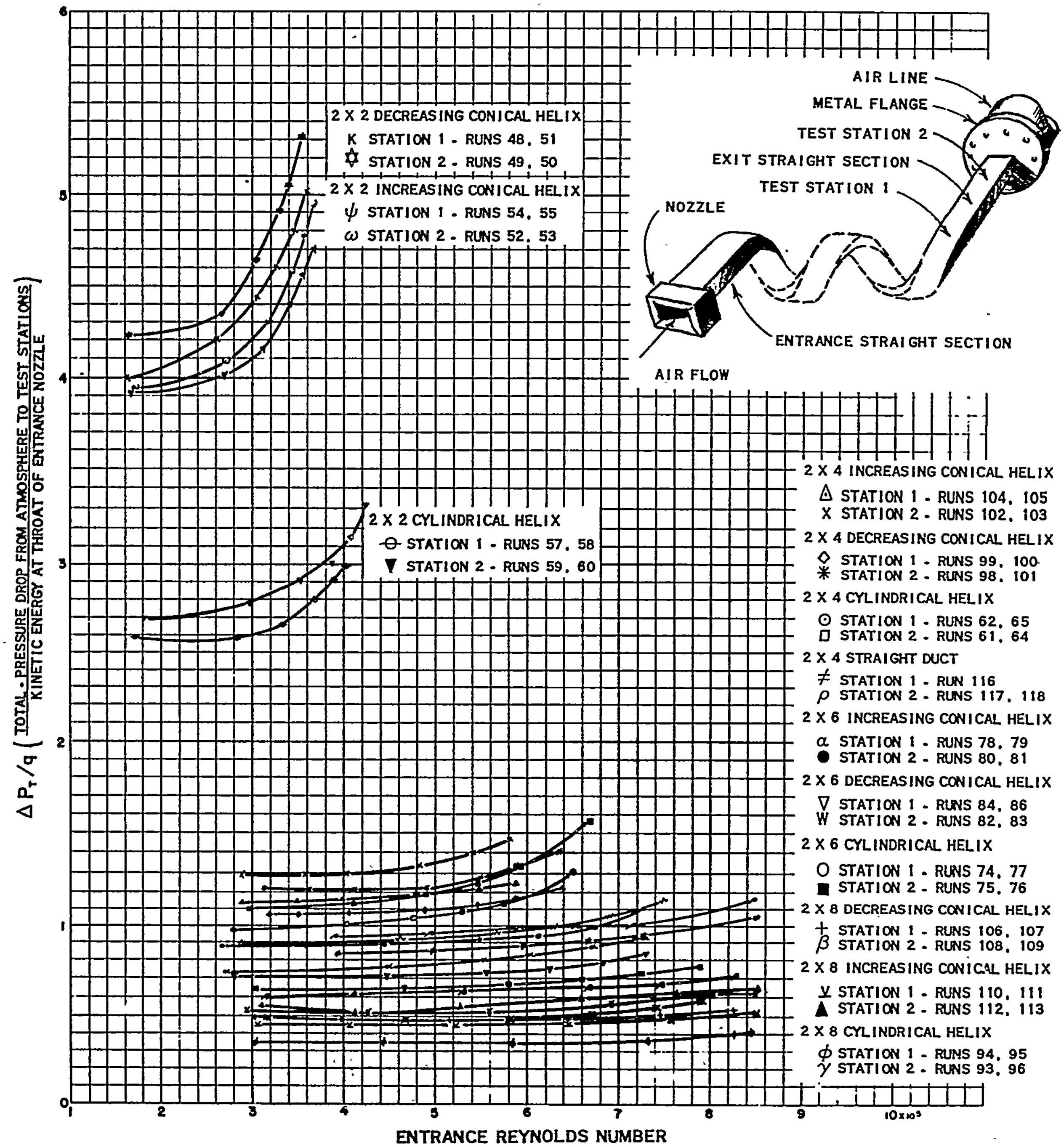

Fig. 63 - SUMMARY OF RESULTS FOR FRICTIONAL PRESSURE DROP IN CYLINDRICAL HELICAL AND CONICAL HELICAL DUCTS

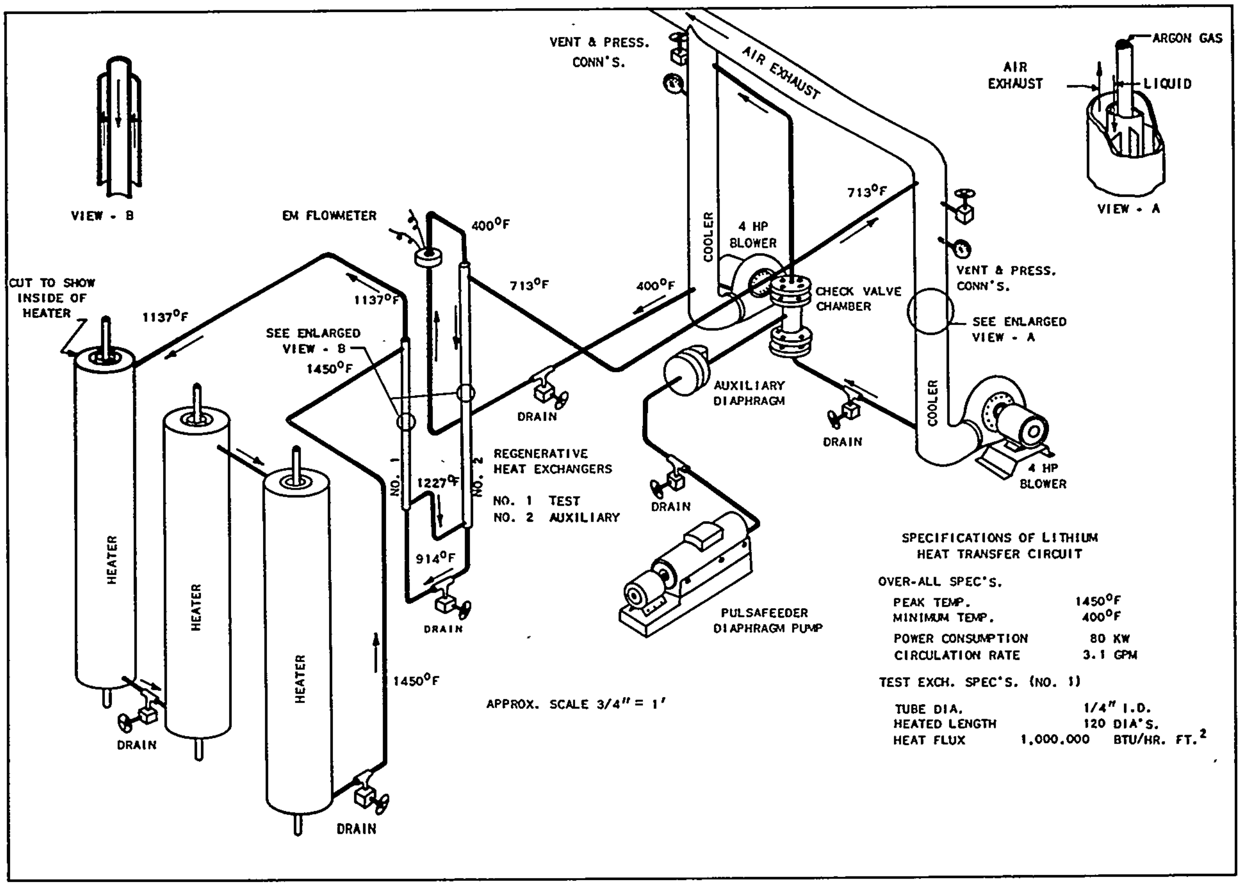

Fig. 64 - SCHEMATIC DIAGRAM OF LITHIUM HEAT-TRANSFER CIRCUIT

• • • • •

6. OVER-ALL POWER PLANT

6.1 POWER PLANT CYCLE ANALYSIS
(48.6 Man-months)

a. Air Cycle. - During this quarter, study continued on the effects of nonuniform reactor power distribution in the radial direction. Considering variations which might occur at different control rod positions, it was calculated that the maximum-to-average power ratio could be reduced to 1.04 without increasing the uranium investment considerably. It was estimated that the minimum-to-average flow-rate ratio which might occur in any heated passage would be 0.89. By applying safety factors, the radial power ratio was raised to 1.07 and the flow deviation to 0.85, for cycle calculation purposes, while the locations of the maximum power and minimum flow were assumed to coincide in the so-called "perverse tube."

Using the above assumptions, it was found that, for similar reactor entrance conditions and pressure ratios, and with 1900°F discharge temperature, the reactor free-flow area required would be 40 per cent larger than that calculated for uniform radial power and flow distribution. At lower reactor discharge temperatures, the area increase is not as severe. When the reactor characteristics were combined with those of the turbo-jet propulsive system for the Phase I flight condition of M = 0.8, 35,000 feet altitude, the peak thrust per square foot of reactor free-flow area was found to occur at 1650°F reactor discharge temperature. At this point, however, the thrust per turbo-jet engine is reduced to about 0.8 of what it would be at the maximum allowable turbine inlet temperature of 1900°F. Investigation of the landing approach condition indicates that a thrust of about 1.7 times the design point thrust can be obtained without exceeding the maximum reactor wall temperature limitation.

Phase II. - Power plant performance has been calculated for the Phase II flight conditions of M = 0.9 and M = 1.2 at sea level, assuming XJ-57 turbo-jet engines with a compressor pressure ratio of 16/1 at these flight conditions. However, a subsequent conference with the engine manufacturer indicates that this engine would have an expected pressure ratio of 16/1 at sea-level static rating. This means that at the ram temperature of the M=0.9 flight condition, the pressure ratio will be reduced to approximately 15/1. The analysis work for the M = 0.9 flight condition is being corrected for the reduced compressor pressure ratio.

b. Compound Liquid-Coolant Cycle. - Cycle analysis effort during this report period has been concentrated on the Phase II power plants. Design point performance calculations were revised for the M = 0.9, 60,000–feet altitude flight condition and tentatively selected for the M-1.5, 45,000–foot condition. Calculations for the thrust available during landing approach are nearly completed for both design points.

The landing approach proves to be more strenuous for the high-altitude airplane than for the high-speed type. This is primarily due to the fact that the high-altitude engine air capacity is roughly eight times that required for sea-level low-speed operation. Consequently, at reactor powers which are not unreasonably higher than at the design point, the engine efficiency is very low. This low efficiency requires special provisions, such as part engine operation and chemical fuel assist, for low-altitude flight. On the other hand, the landing approach thrust demand for the high-speed airplane appears to be well within the capability of the power plant.

c. Compound Helium Cycle. - Preliminary cycle calculations were revised for the Phase I compound helium turbo-jet cycle. As a result of this work, the altitude design point was lowered from 45,000 feet to 40,000 feet, and the pressures were increased to a peak value of 1350 pounds per square inch absolute. The radiator configuration was also changed from a flat tube-and-fin design to a shell-and-tube type to avoid fabrication and stress difficulties. The same radial power ratio and flow perversity which were assumed for the air cycle were also taken into account in calculations relative to the required reactor flow area.

6.2 POWER PLANT CONTROL AND INSTRUMENTATION (24.1 Man-months)

6.21 **Air Cycle.** - The work, during this quarter, on the simulated power plant control test apparatus, at the Y-12 site, has consisted primarily of testing and studying the responses of the heat exchanger to transient power demands.

It was reported in the previous quarterly report that a high percentage of the Globar units of the heat exchanger, was fractured in the initial tests. These fractures were found to be due to differential thermal expansions of the Alundum liners. A quarter section of the heat exchanger was redesigned so that this differential expansion could not fracture the Globar elements.

During the latter part of April, tests were run with the new quarter section. The temperature was first brought up slowly over a period of several hours. After this, step changes in power were applied to the heat exchanger. The heat exchanger was examined after these 2/1 step changes in power, and it was found that the Globar units were intact. However, it was also discovered that the Alundum liners had shattered. The cracking of the Alundum liners was thought to be due both to thermal stresses and mechanical stresses. Certain modifications of this quarter section were made with the aim of eliminating most of the mechanical stresses.

Test runs on the twice-modified quarter section were carried out during the latter part of May. The temperature of the unit was brought up slowly over a period of several hours, after which power level demand transients were studied. The step changes in power level demand were as high as 3/1. Inspection of this quarter section of the heat exchanger showed that the Alundum liners had once again cracked, although not as seriously as had been the case when both mechanical and thermal stresses were present. The step changes in power used in all these tests were such that, with the air flow set at approximately 0.75 pounds per second, the exit air temperature from the heat exchanger rose approximately from 500°F to 1000°F. This change in exit air temperature occurred in approximately 30 seconds.

The experiments with the heat exchanger to date lead to the conclusion that, although the Globar heat elements appear satisfactory, the Alundum material cannot be used as a liner for the heat exchanger. Accordingly, it is proposed to make quarter section tests with liners made of Johns Manville 3000, coated to prevent disintegration in the air stream, Crystalon, and Stuplith. All three materials are high-temperature ceramics which are commercially available.

6.22 **Compound Liquid-Coolant Cycle.** - Analysis of power change and emergency transients for the control schematics presented in the previous quarterly report are in progress. Response times for the radiator, heat exchanger, and reactor are being calculated. Servo actuator response times are being assumed from the best information available. Transit lags are taken from engineering layouts.

These data are intended to illustrate the actions of various components during typical transients.

6.23 **Compound Helium Cycle.** - The Phase I helium cycle power plant control system for the IH 3 airplane is shown in Fig. 65. The control system analysis indicates that the basic thrust control must be handled by reactor power level, with the turbo-jets being controlled dependently. This system is unlike the control for the liquid-coolant cycle due to the fact that: (1) valving for power control is impractical; (2) the circulation time of the helium circuit is exceedingly short; and (3) the minimization of pressure drops in the pipes presents many problems.

The helium turbo-compressor unit is designed to be inherently self-controlled, and therefore no control system is contemplated for it.

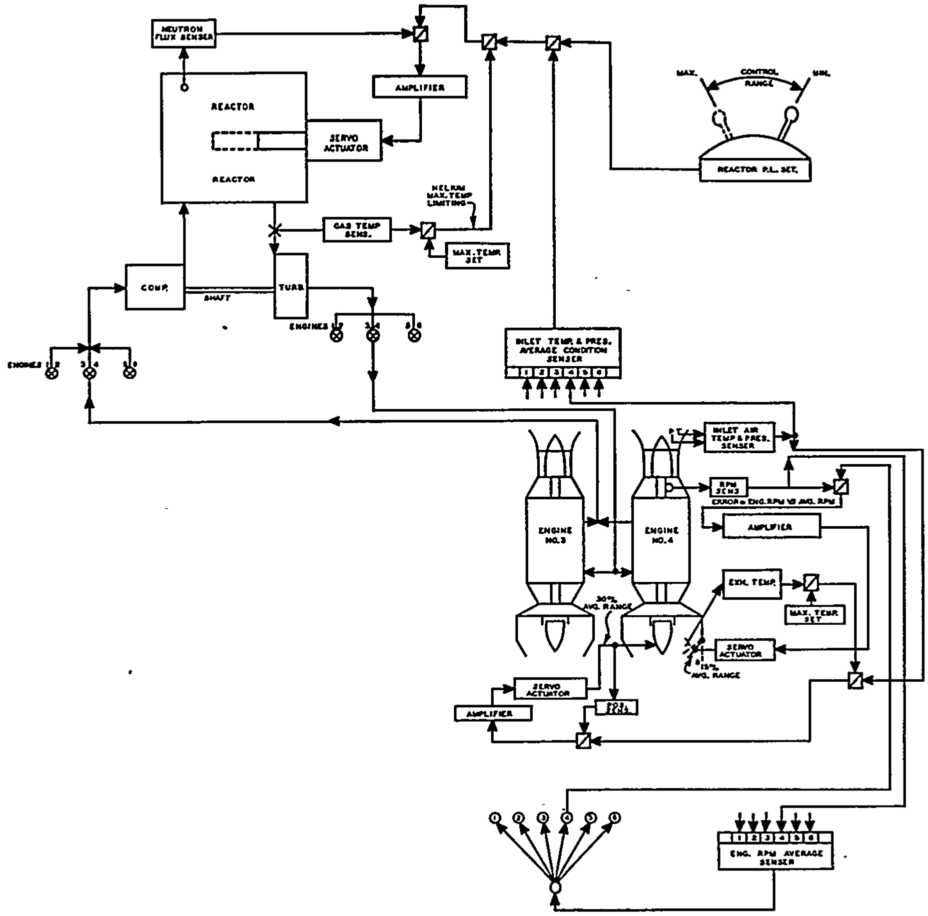

Fig. 65 - PHASE I CONTROL SCHEMATIC FOR HELIUM CYCLE XB-52 AIRPLANE

In the major control loop, reactor power is the controlled process; the pilot's power lever, the set variable; and neutron flux, the sensed variable. Neutron flux is a direct measure of reactor fission rate. Another configuration now being analyzed uses thermometry to measure helium temperature rise through the reactor for power level sensing, and rate of change in neutron flux for indicating rapid power changes. This method may have advantages from the viewpoint of the neutron sensory instrumentation, but presents the difficult problem of correctly measuring gas temperatures.

A maximum-temperature limiter circuit which senses the reactor outlet temperature and depresses the reactor power level in the event of excessive temperature is included in the major control loop. This safety circuit is especially necessary in the helium cycle to protect the helium turbine.

Inlet air pressure and temperature will be sensed at each engine as a measure of available capacity to absorb power, and the average of all engines will allow the pilot's power lever to be calibrated in per cent of available power, regardless of flight condition. Thus, a maximum setting on the power lever will enter the comparator section as a signal systematically controlled not to exceed the heat utilization capacity of the engines at any altitude or aircraft speed.

The adjustment of the engines to varying flight conditions will be achieved by a tail cone area change, which will utilize the inlet pressure and temperature senser previously mentioned, and will vary cone area as a positioning control. Excessive exhaust-gas temperature will operate as a limiter control to open core area in case of high-temperature transients.

Engine speed will be controlled by sensing engine revolutions per minute and comparing the individual revolutions per minute to the average revolutions per minute of all operating engines. The error signal will be amplified and applied to the tail cone tab control actuator. The cone area tab will have limited area control and will be only sufficient to accurately synchronize all engines. This system has the disadvantage of inflexibility, since all engines must operate at the same power level; however, any flexible control circuit leads to valves, by-passes, etc., with attendant pressure losses in the helium ducting.

6.3 POWER PLANT LAYOUT AND INSTALLATION (6.9 Man-months)

6.31 **Open Cycle.** - No significant power plant layout or installation work has been done on the open cycle during the quarter, awaiting cycle analysis of the landing approach condition.

6.32 **Compound Liquid-Coolant Cycle.** - The report, NEPA No. 1447-EPR-1, *Arrangements for the Compound Liquid-Coolant Cycle Components Installed in a IL-1 Airplane* was completed.

Auxiliary Power. - This report compares three types of auxiliary power units:

1. Bleeding the turbo-jets downstream of the compressor, routing this bleed air through a radiator and then to a turbine.
2. Bleeding the turbo-jets downstream of the radiator, then routing this bleed air to a turbine.
3. Utilizing a turbo-prop type engine with the burner replaced by a radiator, similar to the nuclear turbo-jet engines.

Weights of types 1 and 3 were almost identical when some allowance was made for the thrust loss due to bleeding. The weight of type 2 was about twice that of types 1 or 3.

It was concluded that type 3 would be used if there was an available turbo-prop of the desired power, and type 1 if there was no engine available. As the power requirement for the IL-1 installation can be met by two modified XT-38 engines, these will be used.

The report compares intermediate-coolant pumps driven by the turbo-jet engines to pumps driven by the auxiliary power unit. It also considers constant flow vs. variable flow in the core-coolant circuit and in the intermediate-coolant circuit; the relative merits of valving and the effect of valve location on engine operation and maintenance; and the over-all power plant control problem.

Coolant Circuit. - An informal report was begun, analyzing the coolant circuit presented in the previous report in more complete detail. The methods of system charging, starting, operation, and maintenance will be discussed.

Intermediate-Coolant Lines. - The problems of mounting and provisions for expansion of the intermediate-coolant lines have been studied further.

The linear thermal expansion for a typical material which could be used in the lines was found to be about 1.5 per cent at 1600°F. Approximately 25 per cent of the intermediate-coolant lines would have to be expansion bellows to compensate for 1.5 per cent expansion using existing bellows designed to operate at 700°F. This percentage will no doubt increase with an increase in temperature.

Expansion joints can be provided for all lines except the long lines to and from the turbo-jet engine radiators. The proposed method for handling the expansion in the lines to and from the radiators is to permit the lines to move laterally. Flexible bellows are to be placed at the pivot points. An analysis of this approach in the IL-1 airplane produced fairly complex line supports, but a minimum of expansion joint length.

The lines are fixed at their origins in the fuselage, and at the connections to the turbo-jet radiators. There is also a pinned support, halfway out, within the wing. In expanding, the line moves like a nutcracker. Flexible bellows are provided at each point where angularity is expected. External provision will be made across the flexible joint to take the thrust loads. This system requires approximately 12 per cent of the line length as bellows. A small scale model of this proposed line arrangement was built to verify the motion.

Only incomplete data on the aircraft structure and its motion relative to the intermediate fluid lines were available; therefore, these factors were not considered. All supports, other than the pinned support mentioned above, will be hangers supporting the pipe but allowing for motion.

Computations of line sizes, gauges, insulation, and system weights were completed and are shown as Table 19.

TABLE 19

XB-52 AIRPLANE LIQUID-METAL CYCLE
LINE AND WEIGHT SUMMARY INTERMEDIATE COOLANT

	I.D. (in.)	Wall Thickness (in.)	Insul. Thickness (in.)	Over-all O.D. (in.)	Line Length (ft.)	Line (wt.lb.)	Insul. (wt.lb.)	Li (wt.lb.)	Expansion System (lb.)	Supports (lb.)	Totals (lb.)
1. Pump to shield manifold	7.95	0.235	1.0	10.42	6.0	130	7.38	64.2	75.0	4.0	280.58
2. Shield manifold	15.0	0.391	1.0	17.78	3.0	204	5.50	114.0	----	2.0	325.50
3. Shield manifold to IHE* inlet header	2.75	0.112	1.0	4.97	4.0	6 Lines 85.32	6 Lines 12.48	6 Lines 30.78	6 Lines 35.0	6 Lines 6.0	169.58
4. IHE* outlet header to shield attachment	2.75	0.107	1.0	4.96	4.0	6 Lines 85.32	6 Lines 12.48	6 Lines 27.78	6 Lines 35.0	6 Lines 6.0	166.58
Shield Attachment (inboard)	3.22	0.110	1.0	5.44	115.0	4 Lines 1948.00	4 Lines 267.20	4 Lines 726.00	4 Lines 650.0	4 Lines 184.0	3775.20
5. to Engine radiator, (outboard)	3.22	0.110	1.0	5.44	140.0	2 Lines 1184.00	2 Lines 162.40	2 Lines 442.00	2 Lines 325.0	2 Lines 112.0	2225.40
Engine radiator (inboard)	3.16	0.007	1.0	5.31	115.0	4 Lines 1292.00	4 Lines 259.20	4 Lines 776.00	4 Lines 650.0	4 Lines 184.0	3161.20
6. to Pump manifold (outboard)	3.16	0.007	1.0	5.31	140.0	2 Lines 786.00	2 Lines 157.40	2 Lines 472.00	2 Lines 325.0	2 Lines 112.0	1852.40
7. Pump manifold	15.0	0.107	1.0	17.21	3.0	53.60	6.40	144.00	----	4.0	178.00
8. Manifold to pumps	7.95	0.079	1.0	10.11	8.0	58.00	9.50	85.70	80.0	6.0	239.20
9. Shield attachment to APU** radiator	1.0	0.070	1.0	3.14	20.0	2 Lines 26.00	2 Lines 11.20	2 Lines 6.12	2 Lines 5.0	2 Lines 12.0	60.32
10. APU** radiator to pump manifold	1.0	0.070	1.0	3.14	20.0	2 Lines 26.00	2 Lines 11.2	2 Lines 6.80	2 Lines 5.0	2 Lines 12.0	61.00
					SUBTOTAL lb.	5878.24	922.34	2865.38	2185.00	644.00	----
										GRAND TOTAL	12,494.96

*IHE = Intermediate Heat Exchanger
**APU = Auxiliary Power Unit

DECLASSIFIED

SECRET

An isometric drawing (see Fig. 66) showing the XB-52 (IL-1) liquid metal cycle-power plant installation was completed. The weight breakdown and line sizes shown in Fig. 66 are based upon using bismuth as the core-circuit coolant, and lithium as the intermediate-circuit coolant. The weight breakdown shown in Fig. 66 differs somewhat from the weight breakdown for the IL-1 aircraft given in section 1.1, "Design Data," which was based upon preliminary analytical shield estimates.

6.33 **Compound Helium Cycle.** - The latest design study of the helium coolant cycle IH-3 aircraft calls for six XJ-53 engines, instead of eight XJ-53 engines as was shown in the previous quarterly report. A revised schematic diagram, showing six engines instead of eight, and with the engines relocated from the wing to a position aft of the reactor within the fuselage is being prepared.

An analysis was made comparing the duct weights of engines installed in pods and within the fuselage. This study revealed that ducting to and from the engine radiators weighed approximately 25,200 pounds for the engines installed on the wings. For engines installed within the fuselage, such ducting weighs approximately 3,000 pounds. These figures, however, do not include the weights for the ducting to and from the helium turbo-compressor. .For the effect of this weight saving, see section 7.3.

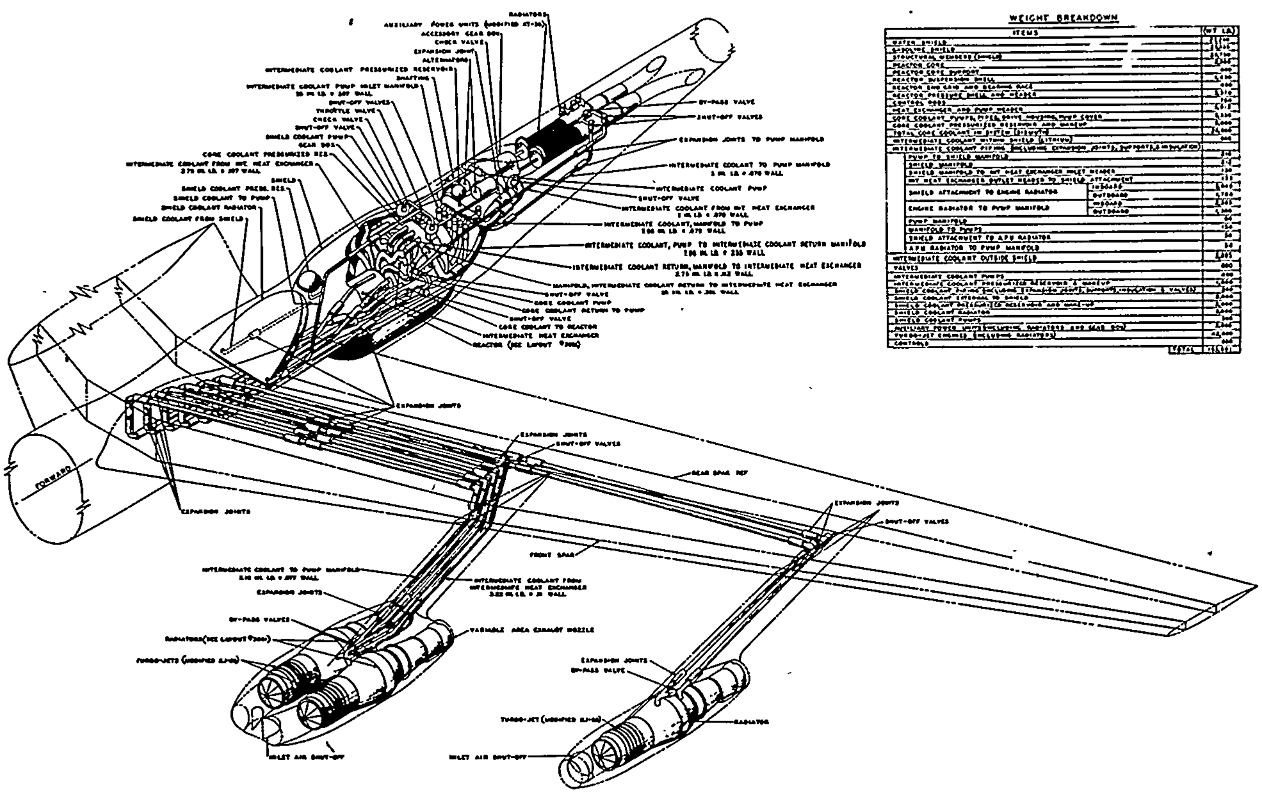

Fig. 66 - XB-52 (IL-1) LIQUID-METAL CYCLE POWER PLANT INSTALLATION

• • • • •

SECRET

DECLASSIFIED

7. AIRCRAFT ANALYSIS

7.1 AERODYNAMICS
(22.5 Man-months)

Aerodynamics work, during this quarter, included the analysis of aircraft configurations for the airframe – power plant combination studies described in section 1, as well as the continued collection and organization of aerodynamic data. The aircraft configuration studies during the quarter were made for Phase II design points: Mach 0.9 at 60,000 feet altitude, Mach 0.9 at sea level, and M = 1.5 at 45,000 feet altitude. Preliminary performance analysis of the IILF-6 aircraft (M = 1.5 at 45,000 feet) and the IILF-7 aircraft (M = 0.9 at sea level) have been completed.

Results of an optimization analysis for a IILF-6 aircraft are presented in Figs. 67-69, for an unswept wing configuration. Swept-wing aircraft configurations will be considered in later studies. Eighty wings were considered in the study to arrive at optimum wing loadings and aspect ratios for wing thickness ratios of 3, 4, 5, and 6 per cent. The wing taper ratio was taken to be 0.25 with zero degree angle of sweep at the 50 per cent chord. A gross weight of 500,000 pounds and a fuselage 15 feet in diameter and 170 feet in length were used. The combined vertical and horizontal tail area was taken to be 30 per cent of the wing area. Power requirements for both the landing condition and the design point were considered in the optimization. Employing power plant and shielding data available at the time, the following configurations were obtained.

Gross Weight	Max. Wing Thickness to Chord Ratio (t/c)	Aspect Ratio	Wing Loading (w/s)	Margin of Feasibility
500,000 lb.	3%	3.0	102 lb./ft.^{2}	18.4%
500,000 lb.	4%	2.25	100 lb./ft.^{2}	18.3%
500,000 lb.	5%	2.0	103 lb./ft.^{2}	17.5%
500,000 lb.	6%	2.15	111 lb./ft.^{2}	13.5%

The margin of feasibility was the percentage of the 500,000 pounds gross weight remaining after all the airplane component weights were summed up.

The configuration showing the largest feasibility was selected for an off-design-point performance study. A schematic drawing of the aircraft is presented in Fig. 67 and the results of the performance analysis are presented in Fig. 68. The power available for the rates of climb and the stall limitation is obtained by arbitrarily assuming that the reactor may be operated at 2.3 times the design–point power. Fig. 68 also indicates a flight plan for accelerating to speed and climbing to the design point. The time to climb from takeoff to M = 1.5 at 45,000 feet along the indicated flight path is in the order of nine minutes.

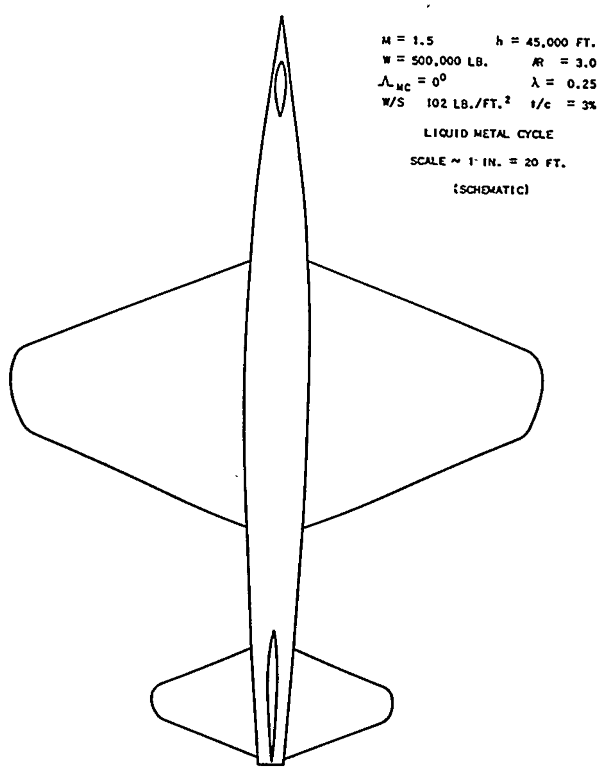

Fig. 67 - AIRPLANE CONFIGURATION FOR MACH 1.5 AT 45,000 FEET ALTIDUDE

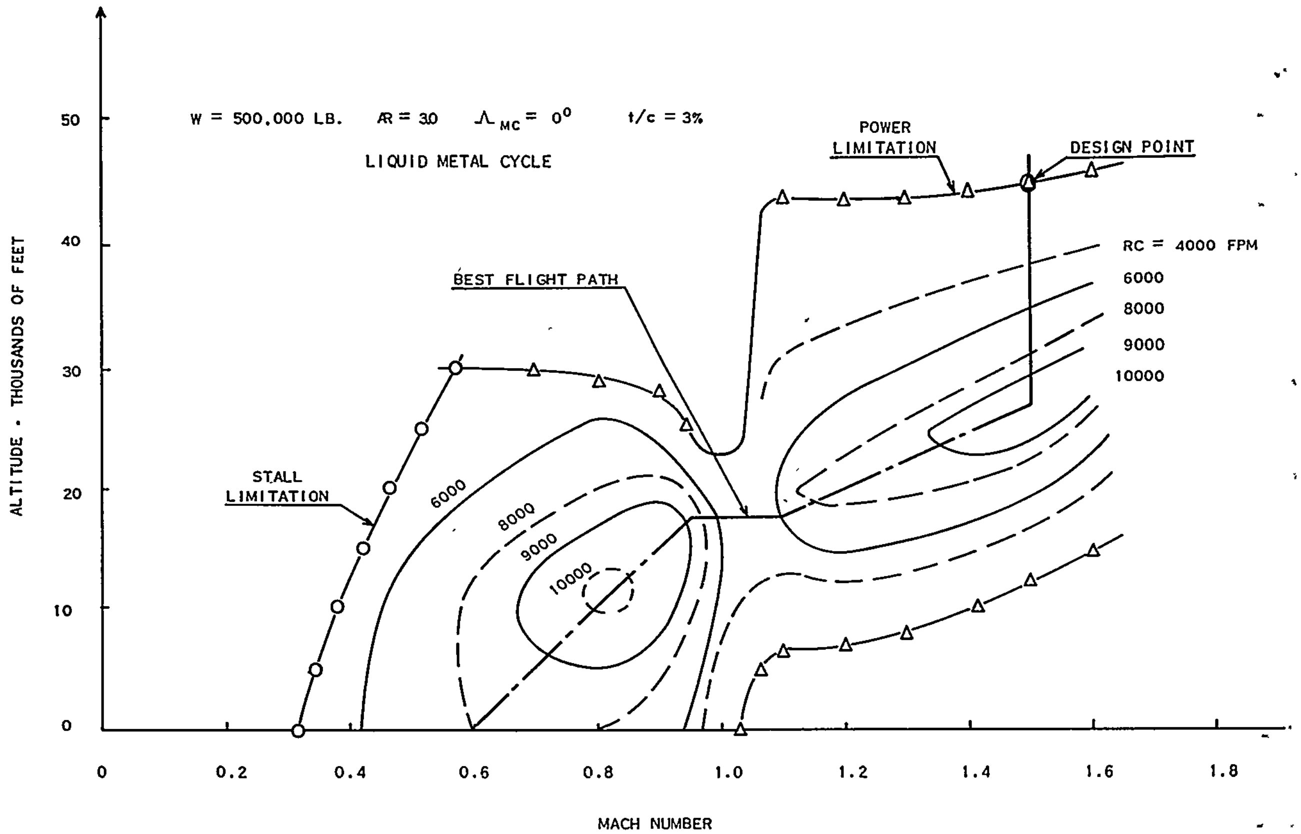

Fig. 68 - MACH NUMBER–FLIGHT SPECTRUM FOR A 500,000 POUND LIQUID-METAL CYCLE AIRPLANE

The effect of decreased lift-drag ratio is shown in Fig. 69. The airplane lift-drag ratio can be decreased to about 5.0 before the weight margin is used up by additional engine and shield weight. The effect of increasing the design-point altitude is also shown in Fig. 69. It can be seen that additional engine and reactor-shield weight rapidly consumes the weight margin for small gains in altitude.

The effect of decreasing airplane gross weight as a function of weight margin is shown in Fig. 69. An airplane of the order of 290,000 pounds gross weight is obtained for 0.0 per cent weight margin.

A performance study was conducted during the past quarter for an aircraft to fly M = 0.9 at sea level (110L-7), with a ceiling of 30,000 to 35,000 feet altitude. Thirty-six wings were considered in the study, and a configuration was selected embodying a 30-degree swept-back wing of aspect ratio 4, thickness ratio of 8 per cent. With this wing, the airplane had a gross weight of 295,000 pounds. The estimated performance spectrum is shown in Fig. 70. Fig. 71 shows the effect of increasing the operating altitude of the airplane on the gross weight and the number of engines required. Geometric characteristics of this design are given in section 1.

At the present time, a standardized drag estimation procedure, which is to be incorporated into NEPA No. EDR-13, *Aerodynamics Handbook*, is being checked against experimental data. The estimation procedure will cover the subsonic, transonic, and supersonic regimes of flight.

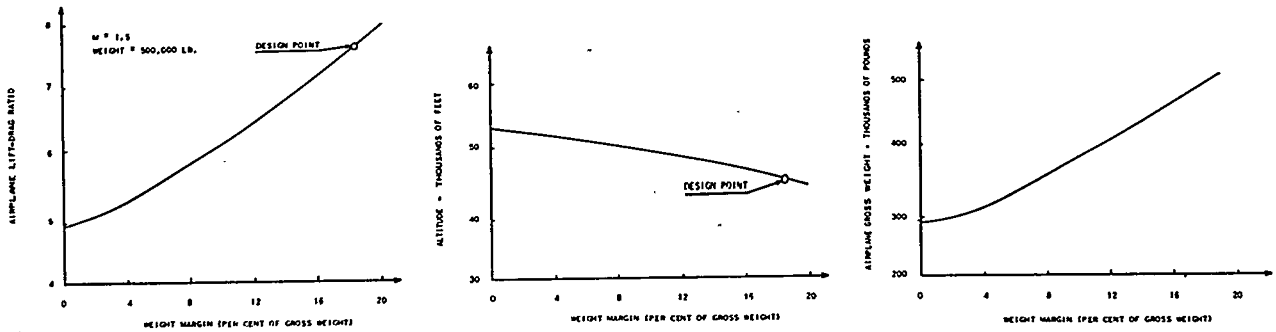

Fig. 69 - VARIATION OF WEIGHT MARGIN WITH L/D AND ALTITUDE

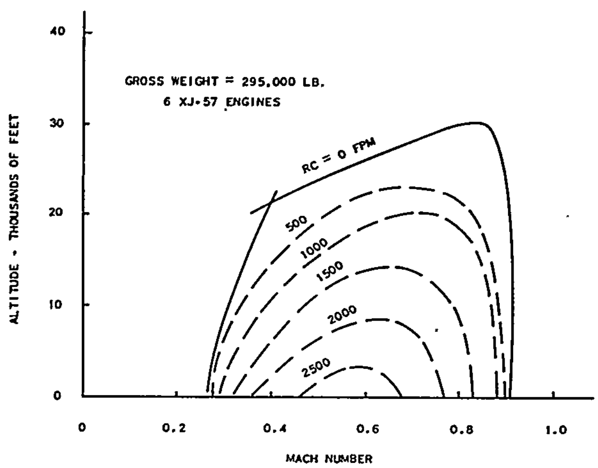

Fig. 70 - PERFORMANCE SPECTRUM FOR A SEA LEVEL AIR CYCLE AIRPLANE (GROSS WEIGHT 295,000 POUNDS)

Tug-Tow Investigation. - Instrumentation of the T-33 tow airplane was completed at Wright-Patterson Air Force Base during the quarter, and flight checking of the installed equipment is in progress. All the data taken during the tests will be fed into an automatic synchronous recording oscillograph which is radio-triggered to assure simultaneous readings in both the tug and the tow planes. Engineer observers will be located in both planes to check the functioning of the recording oscillographs and other equipment. The signals obtained from the measuring instruments are fed into bridge balance circuits, which will in turn transmit them to the channels of the recording oscillograph.

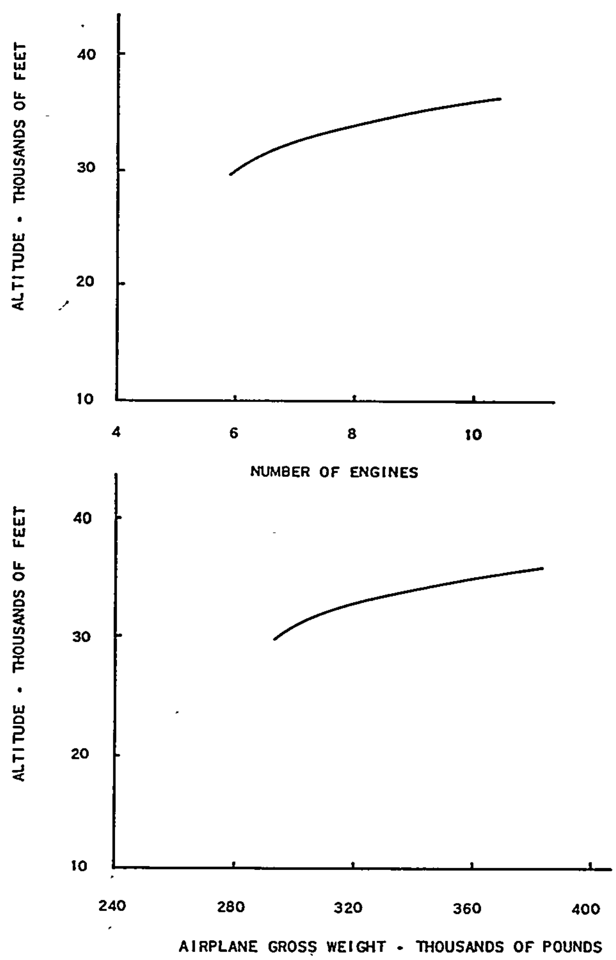

Fig. 71 - ABSOLUTE CEILING FOR AN AIR CYCLE SEA LEVEL AIRPLANE

Delivery of the B-50D tug airplane in May completes procurement of the major items of equipment for the tests. The airplane has undergone the acceptance checks of the Flight Test Division at Wright-Patterson Air Force Base. It is currently in the shops for modifications and installation of the test equipment. The B-50D airplane will carry the same instrumentation as the T-33 airplane, and the data will be recorded in the same manner. The master radio transmitter which will control the recording of data in both planes will also be located in the B-50D.

It is tentatively planned that one photo F-80 airplane and one photo B-43 airplane will be used to photograph the tug-tow combination in flight.

During the quarter, an analysis was made of the flight test data obtained by the United States Air Force and the United States Navy during the development of the Chance Vought high-speed target glider, which has been towed at speeds of 450 miles per hour, 37,000 feet altitude, and 12,000 feet of cable. No accurate quantitative results were obtained because of the incomplete information recorded during the tests. However, the qualitative value of these tests in showing the feasibility of high-speed, long-line towing is important.

7.2 AIRFRAME STRUCTURAL ANALYSIS (22.8 Man-months)

Structures work during this quarter included the development of generalized formulas for estimating structural weight and deformations of thin unswept supersonic wings, investigation of torsional stiffness requirements for supersonic wings, detailed weight calculations of two wing configurations, additional weight calculations for the nose section of an extended-fuselage configuration to include a shield in the crew compartment, and a study of the shielding afforded by the structure of a delta-winged airplane.

Generalized Wing Weight Formulas. - Generalized formulas for estimating deflections and structural component weights of supersonic unswept wings have been derived and summarized in a report, NEPA No. 1393-EDR-22, entitled *Generalized Formulas for the Estimation of the Structural Weight and Deformations of Thin Unswept Supersonic Wings.* The formulas are based on the elementary theories of stress and distortion and are primarily applicable to thin wings of low aspect ratio containing no concentrated or distributed loads. An approximation for swept planforms which neglects local bending effects near the root has also been included in the report.

Torsional Rigidity. - An important factor in the design of thin high-speed wings is the torsional rigidity necessary to meet the requirements for roll control and to preclude wing divergence and flutter. In the case of large subsonic airplanes, roll control is usually the critical requirement. In the case of large supersonic airplanes it is not known which requirement will predominate; however, it appears that consideration of the roll control requirement will be the most direct approach to the problem. NACA Technical Note 1890, entitled *The Effect of Torsional Flexibility on the Rolling Characteristics at Supersonic Speeds of Tapered Unswept Wings,* analyzes the effect of torsional flexibility on the rolling characteristics, at supersonic speeds, of tapered unswept wings with partial span constant-per-cent-chord ailerons extending inboard from the wing tip. This method is being studied with a view toward incorporating an assumed roll control effectiveness in the procedure for estimating supersonic wing weights. This will insure that adequate skin weight is included to provide the desired torsional rigidity.

Detailed Wing Weight Calculations. - Work has continued on detailed weight calculations for two wing configurations, one a subsonic and the other a supersonic configuration. These calculations are being carried out as a check on present wing weight estimation procedures. The subsonic wing configuration would be suitable for an airplane such as the 0.9 Mach number, 60,000-foot altitude airplane. Characteristics of this wing are: A sweep angle of 50°, a thickness ratio of 10 per cent in a streamwise direction, aspect ratio of 5.15, and a wing area of 8750 square feet. The supersonic wing configuration would be suitable for an airplane such as the 1.5 Mach number, 45,000-foot altitude airplane. The characteristics of this wing include an aspect ratio of 3, a thickness of 3 per cent, a ratio of tip chord to root chord of 0.25, and a wing area of 4900 square feet. The wing has no sweep.

Extended Fuselage Weights. - In NEPA 1374-IPR-52, a method of estimating the weight of extended fuselages was discussed. It was reported that, as a check on the accuracy of this method, a typical extended fuselage had been selected, and that a detailed weight estimate of the nose section of that fuselage had been made, without including a shield in the crew compartment. During the past quarter, this detailed weight estimate has been extended to include a shield in the crew compartment. For this condition, a crew compartment weight of 55,000 pounds including shield was assumed. Ultimate design load factors of +4 and −2 at the center of gravity of the airplane were used, and an approximation for the elastic effects of the extension was made. The structural weight of a 100-foot nose section was estimated to be 7250 pounds for no shielding in the crew compartment and 17,500 pounds with shielding. These weights are approximately 9 per cent and 24 per cent, respectively, under those predicted by the method mentioned in the last quarterly report. This variation may be due to an overestimation of the weight by the one method or to an insufficient allowance for such items as joint inefficiencies, use of standard gauges, use of nontapered skin and stringers, etc., in the more detailed analysis. This work is summarized in a report, NEPA No. 1396-EDR-23, entitled *Weight Estimation, Under Two Loading Conditions, of Fuselage Extensions 12 Feet in Diameter up to 150 Feet in Length.*

Structural Shielding. - A brief study was made of the possibility of considering the primary structure of an airplane as shielding material. It was thought that, by this procedure, the reactor shield weight might be reduced to some extent. A delta-winged airplane was selected for this study. A structurally efficient design for the primary structure was assumed and the thickness of material along a number of lines radiating from the reactor was estimated. These thicknesses were of the order of 1 inch or less, and the minimum thickness occurred on the line toward the crew compartment. This resulted from the use of a shell-type fuselage reinforced by stringers and circular rings. The possibility of using materials less structurally efficient but affording better shielding was also considered. It was found, however, that a structurally efficient design provided an insignificant amount of shielding, and that even a compromise of the structural efficiency in favor of better shielding materials or a better shielding arrangement gave little improvement. This results primarily from the fact that, to avoid scattered radiation, the reactor must be completely surrounded by shielding material, and, consequently, any shielding disposed at a distance from the reactor is very inefficient from the shield weight point of view. Further work along these lines is anticipated.

7.3 GENERALIZED AIRCRAFT STUDIES (2.1 Man-months)

Lockheed Aircraft Corporation

Crew Separation. - The study of bombardment aircraft utilizing large crew-reactor separation distances has progressed during the quarter. Considerable time has been spent in discussions between the staffs of the Lockheed Aircraft Corporation and NEPA to arrive at suitable power plant data for use in the study. Nuclear power plant data consistent with those shown in section 1 were transmitted to Lockheed, and further information is being compiled. While awaiting basic power plant data, Lockheed has made a layout study of six airplanes, primarily to get a configuration which could serve as a starting point for the discussion of various weight, balance, and arrangement problems. The results are presented in Lockheed Report No. 7385, *Study of Six Airplanes.* These results are considered relative at best and are meant only as a guide for more thorough future investigations. Three altitudes were considered in this study. These were sea level, 35,000 feet, and 50,000 feet. Speed range covered was from Mach No. 0.8 to 1.5 at each altitude. A conventional wing-tail configuration, and a single value for crew-reactor separation distance were utilized in these studies. The general arrangement is shown in Fig. 72. The summary of the airplane characteristics as reported in the Lockheed report are shown in Table 20.

Landing Gear. - A study of relationships between landing gear arrangements and available airport strengths for very heavy aircraft has been completed, and Lockheed Report No. 7437, *Landing Gear–Airport Relationships for Very Large Aircraft,* was issued.

The report concludes that airplanes weighing 400,000 to 500,000 pounds will encounter severe restrictions in the number of existing airports from which they can operate. The strength requirements for the runways coupled with the runway lengths anticipated for the nuclear powered airplane will, in all likelihood, call for construction of new, extra-heavy-duty airports.

Wings. - A broad survey of the weights of a series of wings whose characteristics are defined by all possible permutations of three wing loads, sweep angles, thickness ratios, taper ratios, and aspect ratios is under way for a 600,000-pound airplane in order to establish trends for external wing optimization. A study of the effects of all possible wing shape parameters and auxiliary devices on the maximum lift of any wing has been initiated.

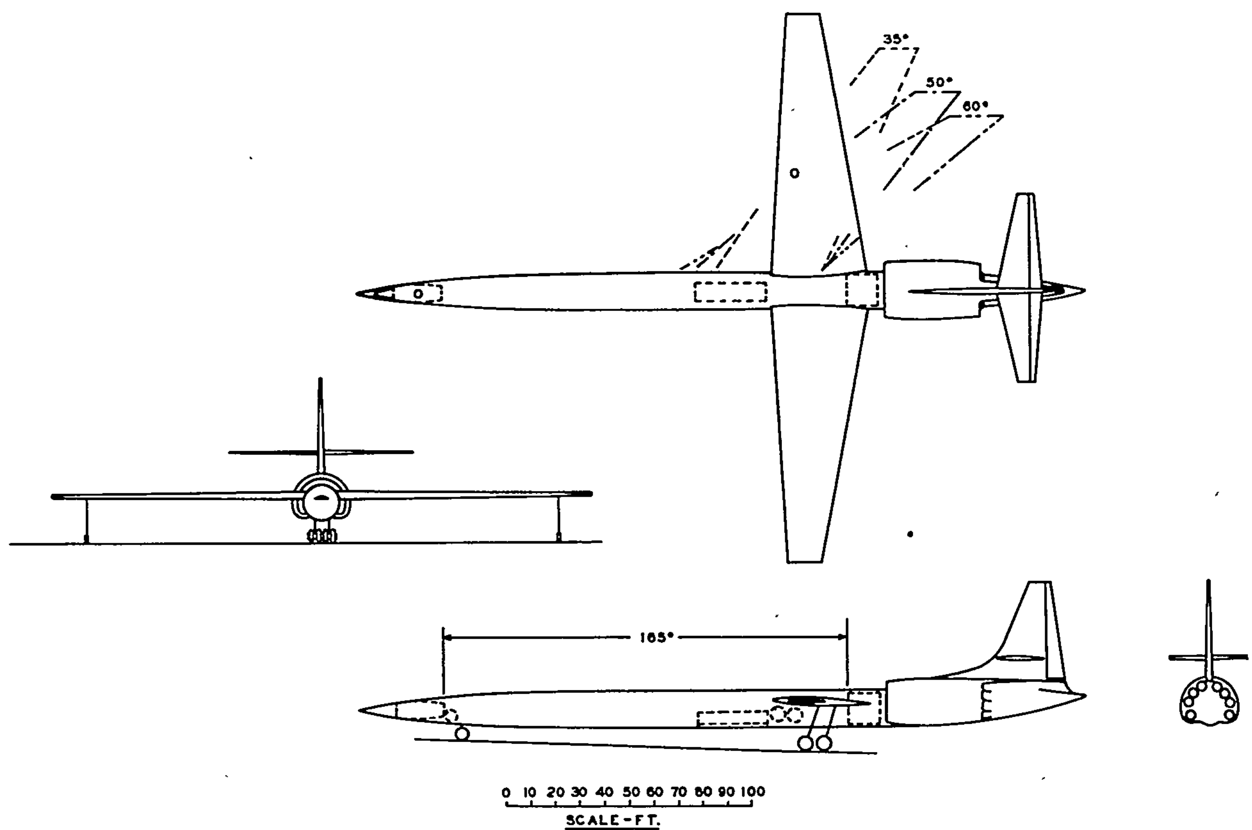

Fig. 72 - GENERAL ARRANGEMENT OF AIRPLANE USED IN LOCKHEED AIRCRAFT CORPORATION STUDIES

TABLE 20

SUMMARY OF AIRPLANE CHARACTERISTICS
(Lockheed Aircraft Corporation Designs)

Airplane type	A-5	A-6	A-7	A-8	A-9	A-10
Designed for	Reasonable landing and take-off characteristics	Reasonable landing characteristics and ceiling above 50,000 ft.	Reasonable landing characteristics and high speed at 50,000 ft.	High speed at medium altitudes	High speed at low altitudes	High speed at 50,000 ft.
Gross weight	600,000 lb.	475,000 lb.	550,000 lb.	540,000 lb.	520,000 lb.	514,000 lb.
Wing loading	100 lb/sq.ft.	100 lb/sq.ft.	100 lb/sq.ft.	200 lb/sq.ft.	400 lb/sq.ft.	200 lb/sq.ft.
Wing area	6000 sq.ft.	4750 sq.ft.	5500 sq.ft.	2700 sq.ft.	1300 sq.ft.	2570 sq.ft.
Maximum thrust output	200,000 lb. (sea level)	55,000 lb. (50,000 ft.)	82,500 lb. (50,000 ft.)	200,000 lb. (sea level)	200,000 lb. (sea level)	82,500 lb. (50,000 ft.)
Number of engines	8	8	12	8	8	12
Sea level maximum Mach No.	1.055	0.905(0.902)	0.970	1.250(1.103)	1.500(1.120)	1.000(0.965)
Wing sweep	60°	25°(35°)	60°	60°(50°)	45°(15°)	60°(45°)
Maximum Mach No. at 35,000 ft.	1.080	1.050(0.952)	1.120	above 1.500	above 1.500	1.450(1.245)
Wing sweep	60°	60°(35°)	60°	50°	15°	60°(45°)
Mach No.* at 50,000 ft.	----	0.880	1.020	----	----	above 1.500
Wing sweep*	----	35°	60°	----	----	45°

* Ceilings less than 50,000 feet.

Brakes. - An investigation of brake design which is to be combined with landing gear study has been initiated recently.

Fuselage Weight Investigation. - Another investigation which is under way is a preliminary analysis of the effect of forward fuselage length (crew reactor spacing, roughly) on the total weight of the forward fuselage, including the crew shield.

Consolidated-Vultee Aircraft Corporation. - A study of nuclear bombardment aircraft, designed over a weight range of speed and altitude requirements, has been started this quarter by the Fort Worth Division of the Consolidated-Vultee Aircraft Corporation. Members of Convair's staff and NEPA's staff have conferred several times during the quarter, and a number of questions concerning the airframe, power plant, reactor shielding operations, and other items were clarified. Basic power plant data which will be required have been agreed upon and are in process of being compiled.

United Aircraft Corporation. - United Aircraft Corporation has undertaken an investigation of the performance aspects of nuclear powered aircraft. A study is under way to determine the interrelationships between volume, drag, and weight when the aircraft and power plant size are minimized. The first phase of the study consists of the analysis of a series of all-wing aircraft of varying aspect ratios and thicknesses. The engine parameters used to determine the effects of these geometric variations on the choice of the smallest aircraft and smallest power plant for 45,000 feet and Mach 1.5 are: (1) the thrust required to fly a unit volume, and (2) the allowable installed weight for a pound of thrust. The work on this phase has been finished, and a draft of the first performance and design report on the method of analysis and its application is complete. However, certain questions have arisen regarding the validity of the analysis which have delayed its release. There has been no apparent, simple way to clear up the continued difficulty which centers on the repeated occurrence of designs which do not utilize their maximum lift-to-drag ratios. By rather lengthy explorations of the basic factors entering into the aircraft designs, a fairly clear explanation has been developed and will be made part of the delayed report. A study of delta planform all-wing aircraft similar in nature to the rectangular all-wing aircraft study is under way. The results of this study so far indicate that the delta wing design is superior to the rectangular wing designs, since it gives lower gross weights, lower over-all drags, and smaller wing areas.

Maneuvering load factors have been under investigation, and a report containing the results of this study will be published. A chart is also being prepared which can be utilized to determine attainable maneuvering load factors. This chart is intended to be used as an aid in the rapid calculation of load factors.

Structural design and weight investigation of wings used in the aerodynamic studies has continued. A report is in preparation which discusses a method for wing-weight estimation.

NEPA. - During the quarter, airframe work at NEPA has revolved around the development of new configurations for the air- and helium–cooled Phase I aircraft, and the development of very preliminary layouts of the following Phase II aircraft: Mach 0.9 at 60,000 feet, Mach 1.5 at 45,000 feet, and Mach 0.9 at sea level. A summary of this work follows.

Phase I Aircraft Air Cycle. - A nuclear powered air-cycle aircraft design based on the XB-52 which will cruise at Mach 0.8 at 35,000 feet was developed during the quarter.

The large air ducting requirements for this cycle prohibited the use of engine pods such as those used on the chemically fueled XB-52. The engines have been relocated in the fuselage, increasing the fuselage cross–sectional area considerably beyond that of the original XB-52 fuselage. Engine air is supplied by wing leading edge intake. The landing gear has been relocated fore and aft, and requires a complete redesign. Because of the absence of the relieving loads of the chemical fuel and the engine pods on the wing-bending moments, the wing weight for this configuration is approximately 45 per cent greater than that of the original XB-52. The leading edge air intakes also cause design changes. The airplane is structurally close to a complete new design rather than an XB-52 modification. The airplane gross weight at take-off would be 350,000 pounds. A three-view drawing of the airplane is shown in Fig. 73.

Phase I Aircraft Helium Cycle. - Since the last quarter, the compound helium cycle nuclear version of the XB-52 airplane has been completely revamped. The previous configuration corresponded very closely to the chemically fueled XB-52 airplane, which featured jet pods underslung on a sweptback wing. A careful analysis of the ducting weight required for such a configuration indicated that an installation of the engines in the fuselage might be more favorable. This is reported in section 6.33.

An investigation was made of a modified XB-52 airplane with the six XJ-53 engines installed in the fuselage behind the reactor. The engine air was introduced through wing leading edge inlets and ejected through nozzles placed in a step on the lower surface of the fuselage.

A comparison between this configuration and the original showed the following pertinent differences:

GROSS WEIGHT		350,000 LB.
ALTITUDE		35,000 FT.
MACH NUMBER		0.8
AIRCRAFT:		
WING		
WING LOADING		87.5 LB/FT^2
WING AREA		4000 FT^2
ASPECT RATIO		8.55
TAPER RATIO		0.4
THICKNESS RATIO - ROOT		16%
TIP		8%
SWEEP ANGLE AT 1/4 CHORD		35°
POWER PLANT		
ENGINES & NUMBER		(6) XJ-57
TURBINE INLET TEMPERATURE		1685°F
DESIGN POINT THRUST		18,500 LB.
AIR FLOW/ENGINE (MAXIMUM)		150 LB/SEC
URANIUM INVESTMENT		160 LB.
(MAY BE REDUCED TO ~ 100 LB. FOR TACTICAL VEHICLE)		
AERODYNAMICS		
C_l (TAKE-OFF)		1.00
L/D DESIGN POINT		18.9
L/D MAXIMUM		20.5
DRAG BASED ON WING AREA		
WING PROFILE DRAG	C_{D_0} = 0.0060	
WING DRAG DUE TO LIFT	C_{D_i} = 0.0132	
FUSELAGE DRAG	C_{D_f} = 0.0046	
TAIL DRAG	C_{D_t} = 0.0020	
INTERFERENCE DRAG	C_{D_I} = 0.0006	

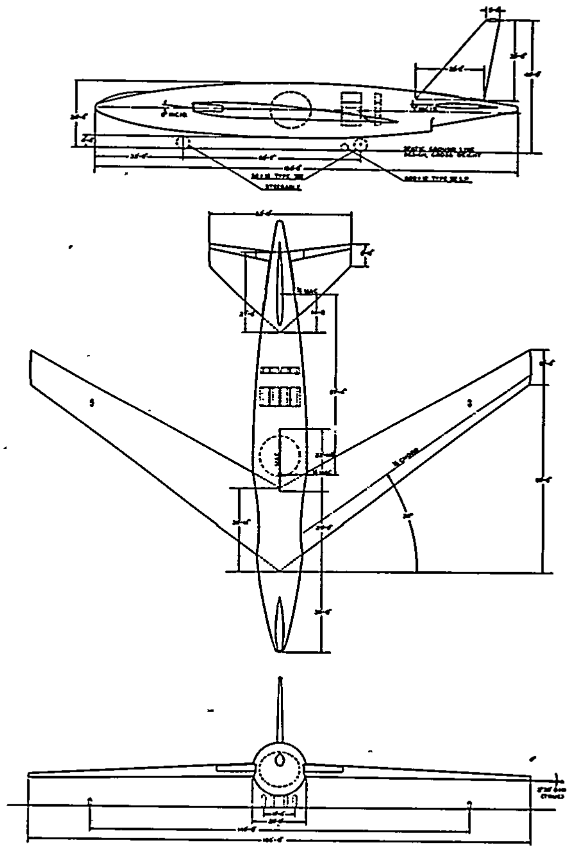

Fig. 73 - GENERAL ARRANGEMENT OF PHASE I AIR CYCLE AIRPLANE

1. The flyable gross weight of the aircraft type having the engines in the fuselage is 20,000 pounds higher than that of the conventional configuration. This is due to the higher lift-to-drag ratio obtained by removing the nacelle.

2. The wing weight increased approximately 35 per cent when the engines were moved to the fuselage. This is due to the concentration of this weight at the center line of the wing as opposed to weight distribution along the wing.

3. The landing gear weight increased with the 20,000-pound increase in gross weight.

4. The engine ducting weight decreased to approximately one-tenth of its original value when the engines were moved close to the reactor. The net result of these and other minor factors was that the aircraft having the engines in the fuselage could carry a heavier reactor-shield assembly. This is reflected in the reduction of the uranium investment from over 300 pounds to approximately 80 pounds. A three-view drawing of this airplane is shown in Fig. 74.

Phase II Liquid-cooled Cycle. - Analysis by the aerodynamic and structures groups of various wings, during the quarter, has revealed certain optimum combinations of aspect ratio, thickness-to-chord ratio, taper ratio, and sweep angles for the design Mach numbers of 0.9 at 60,000 feet and

GROSS WEIGHT		340,000 LB.
ALTITUDE		40,000 FT.
MACH NUMBER		0.8
AIRCRAFT:		
WING		
WING LOADING		85.0 LB/FT^2
WING AREA		4000 FT^2
ASPECT RATIO		8.55
TAPER RATIO		0.4
THICKNESS RATIO - ROOT		16%
TIP		8%
SWEEP ANGLE AT 1/4 CHORD		35°
POWER PLANT		
ENGINES AND NUMBER		(6) XJ-53 MOD.
TURBINE INLET TEMPERATURE		1170°F
DESIGN POINT THRUST		17,000 LB.
AIR FLOW/ENGINE (MAXIMUM)		231 LB/SEC
URANIUM INVESTMENT		80 LB.
AERODYNAMICS		
C_l (TAKE-OFF)		1.0
L/D DESIGN POINT		20.1
L/D MAXIMUM		21.0
DRAG BASED ON WING AREA		
WING PROFILE DRAG	$C_{D_o} = 0.0060$	
WING DRAG DUE TO LIFT	$C_{D_i} = 0.0125$	
FUSELAGE DRAG	$C_{D_f} = 0.0039$	
TAIL DRAG	$C_{D_t} = 0.0020$	
INTERFERENCE DRAG	$C_{D_I} = 0.0006$	

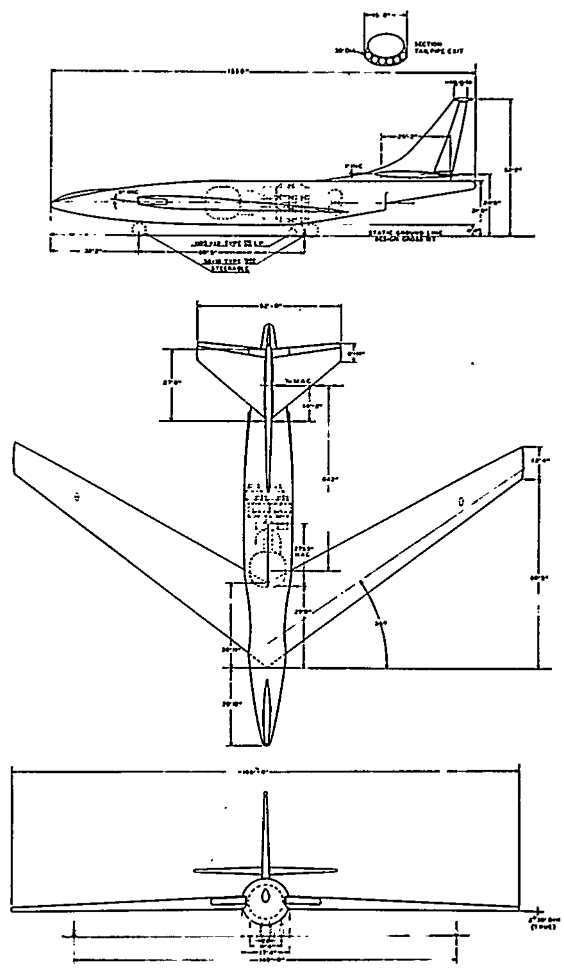

Fig. 74 - GENERAL ARRANGEMENT OF MODIFIED PHASE I HELIUM CYCLE XB-52 AIRPLANE

1.5 at 45,000 feet. Using the optimum combination of wing variables, preliminary layouts of Phase II liquid-coolant cycle airplanes have been drawn up. The results of these layouts are shown in Figs. 75 and 76. It should be realized that more extensive studies of configurations will be made to determine optimum over-all airplane designs.

Phase II Air Cycle. - A study of the sea-level high-speed airplane was initiated during the quarter, and preliminary results are available at this time. Analysis of various wings by the aerodynamics and structures groups has revealed a combination of wing variables suited for the design flight speed and altitude. An explanation of this study will be found in section 7.1. Using this wing, a preliminary layout of an airplane has been made, and is shown in Fig. 77.

Further work is planned on the sea-level airplane in which the altitude requirement will be abandoned, and higher wing loadings, variable swept wings, and variable area wings will be

GROSS WEIGHT		460,000 LB.
ALTITUDE		60,000 FT.
MACH NUMBER		0.9
AIRCRAFT:		
WING		
WING LOADING (LB/FT^2)		43 LB/FT^2
WING AREA		10,700 FT^2
ASPECT RATIO		4.4
TAPER RATIO		0.4
THICKNESS/CHORD RATIO		0.09
SWEEP ANGLE (0.25 CHORDLINE)		50.8°
POWER PLANT		
ENGINES AND NUMBER		12 NEPA NO. 7 ENGINES
TURBINE INLET TEMPERATURE		1550°F
DESIGN POINT THRUST		31,000 LB.
AIR FLOW/ENGINE (MAXIMUM)		400 LB/SEC
COMPRESSOR PRESSURE RATIO AT D. P.		7.0
URANIUM INVESTMENT		~ 100 LB.
AERODYNAMICS		
C_l (TAKE-OFF)	(V_{TO} ~ 180 MPH)	0.5
L/D DESIGN POINT		17.0
L/D MAXIMUM		18.7 AT C_L = 0.35
DRAG BASED ON WING AREA		
WING PROFILE DRAG	C_{D_o} =	0.0062 AT C_L = 0.2
WING DRAG DUE TO LIFT	C_{D_i} =	
FUSELAGE DRAG	C_{D_f} = 0.0011	
TAIL DRAG	C_{D_t} = 0.0018	
NACELLE DRAG	C_{D_I} = 0.0013	

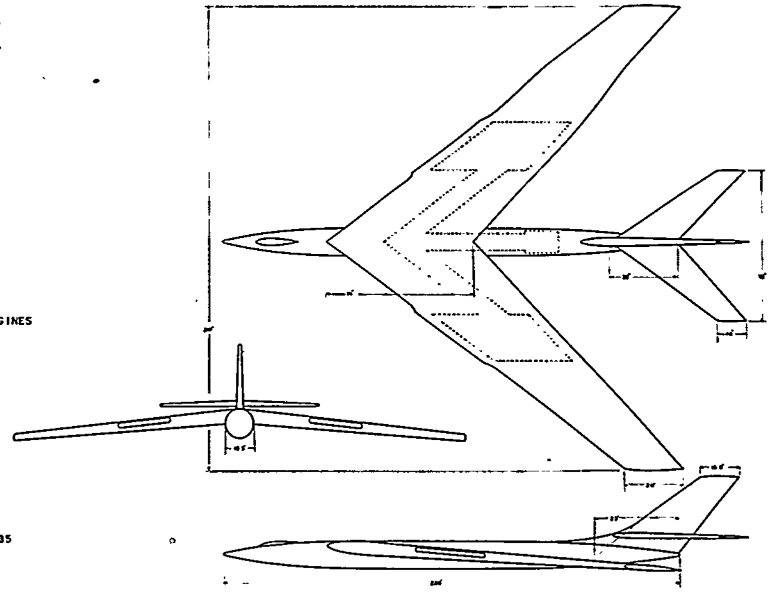

Fig. 75 - LAYOUT FOR A PHASE II LIQUID-METAL-COOLED AIRPLANE (GROSS WEIGHT 460,000 POUNDS)

studied to determine the effects of the results on the airplane design.

Crew Shield Weights. - To obtain lower crew shield weights for the air-, helium-, and ternary-liquid-coolant cycle aircraft, several geometric shapes are being investigated for use as crew compartments. Compartments for both the single- and twin-reactor installations were examined. The single-reactor aircraft was assumed to be of conventional design having a fuselage, while the twin-reactor aircraft was always assumed to be an all-wing type aircraft with the reactors being housed in two nacelles. A prolate spheroid was selected as an optimum for the single-reactor configuration. This resulted in a considerable shield weight reduction over compartments of the type presently used for aircraft design studies. A triangular compartment with elliptical front and profile views appears most desirable for the twin-reactor configuration. Since twin-reactor configurations are now being dropped from further study in the over-all airplane analysis, the calculations on this shield compartment were stopped.

Shield weight design charts are being prepared as a function of the size of crew compartment and the crew shield thickness requirements. The thicknesses, in turn, are given for the air and helium cycle as a function of reactor power, crew-reactor separation distance, and altitude. Shield thickness requirements will soon be made available for the ternary–liquid-coolant cycle; then shield weight design charts for this cycle will also be constructed.

(Figs. 76 and 77 are shown on following pages)

GROSS WEIGHT		400,000 LB.
ALTITUDE		45,000 FT.
MACH NUMBER		1.5
AIRCRAFT:		
WING		
WING LOADING (LB/FT^2)		102 LB/FT^2
WING AREA		3920 FT^2
ASPECT RATIO		3.0
TAPER RATIO		0.25
THICKNESS/CHORD RATIO		3%
SWEEP ANGLE (.50 CHORDLINE)		0°
POWER PLANT		
ENGINES AND NUMBER	(9)	NEPA NO. 7 ENGINES
TURBINE INLET TEMPERATURE		1500°F
DESIGN POINT THRUST		60,500 LB.
AIR FLOW/ENGINE (MAXIMUM)		400 LB/SEC
URANIUM INVESTMENT		~ 110 LB.
AERODYNAMICS		
C_l (TAKE-OFF) (V_{TO} = 174 KTS.)		1.0
L/D DESIGN POINT		6.6
DRAG BASED ON WING AREA		
WING WAVE DRAG	C_{D_w} = 0.0033	
WING DRAG DUE TO LIFT	C_{D_l} = 0.0128	
WING FRICTION DRAG	$C_{D_{fr}}$ = 0.0043	
FUSELAGE DRAG	C_{D_f} = 0.0087	
TAIL DRAG	C_{D_t} = 0.0026	

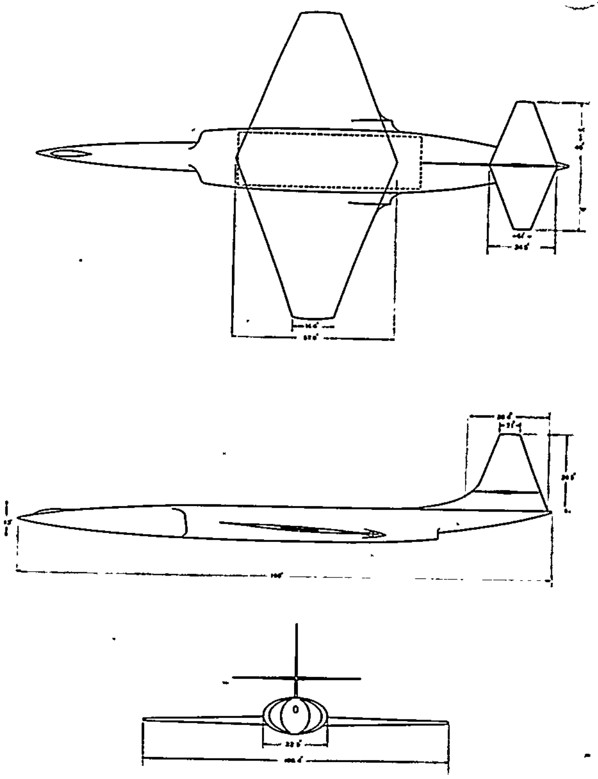

Fig. 76 - LAYOUT FOR A PHASE II LIQUID-METAL-COOLED AIRPLANE (GROSS WEIGHT 400,000 POUNDS)

GROSS WEIGHT		300,000 LB.
ALTITUDE		SEA LEVEL
MACH NUMBER		0.9
AIRCRAFT:		
WING		
WING LOADING (LB/FT^2)		96 LB/FT^2
WING AREA		3100 FT^2
ASPECT RATIO		4.0
TAPER RATIO		0.25
THICKNESS/CHORD RATIO		0.08
SWEEP ANGLE (0.25 CHORDLINE)		30°
AIRFOIL - NACA 65 SERIES WITH 0.10 CAMBER		
POWER PLANT		
ENGINES AND NUMBER		(6) XJ-57
TURBINE INLET TEMPERATURE		1900°F
DESIGN POINT THRUST		47,600
AIR FLOW/ENGINE AT S.L.S. THRUST		150 LB/SEC
URANIUM INVESTMENT		180 LB.
AERODYNAMICS		
C_l (TAKE-OFF)		0.95
L/D DESIGN POINT		6.46
L/D MAXIMUM		15.20
DRAG BASED ON WING AREA		
WING PROFILE DRAG	C_{D_o} = 0.00540	
WING DRAG DUE TO LIFT	C_{D_i} = 0.00057	
FUSELAGE DRAG	C_{D_f} = 0.00380	
TAIL DRAG	C_{D_t} = 0.00202	
INTERFERENCE DRAG	C_{D_I} = 0.00059	

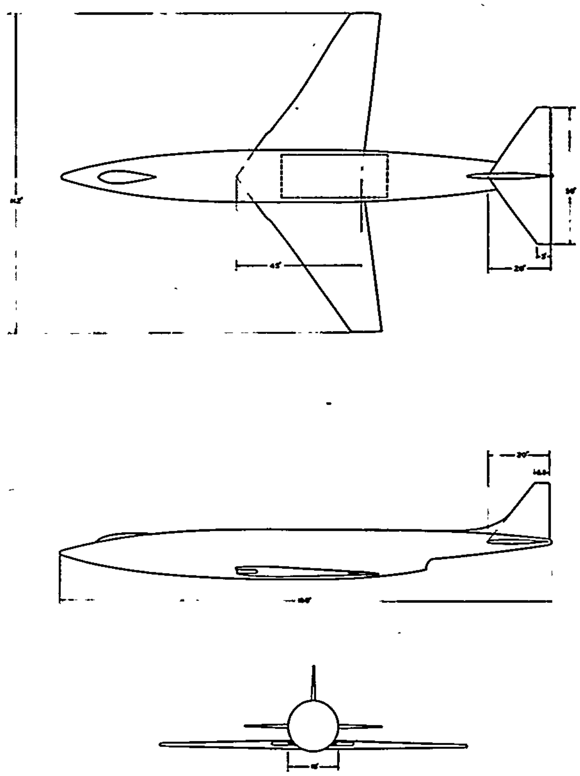

Fig. 77 - PHASE II AIR CYCLE AIRCRAFT

8. TACTICAL CONSIDERATIONS

(0.3 Man-months)

The outstanding development in tactical considerations during this quarter has been the conclusion that the uranium content of the reactors has a very great influence on nearly all other design variables. This conclusion has been arrived at by considering preliminary results of an operational analysis of nuclear powered aircraft made by the Weapons Systems Evaluation Group (WSEG). NEPA provided data on three versions of tactical airplanes having design speeds of Mach 0.9 at 60,000 feet, Mach 0.9 at sea level, and Mach 1.5 at 45,000 feet. WSEG made a systems analysis (in a fashion similar to that developed by the Rand Corporation) of such aircraft delivering multiple strikes onto enemy territory. Although the detailed results of this analysis are subject to revision, and it is difficult, if not impossible, to take all factors properly into account in such an analysis, they clearly indicate the very strong influence of uranium investment on the over-all desirability of nuclear airplanes.

The cost, in fissionable material, of dropping an atomic bomb on a defended target can be expressed in terms of a delivery efficiency. This efficiency may be defined as the ratio of fissionable material dropped on the target to the total fissionable material expended (dropped and lost). If Z is the number of atomic bombs represented by the uranium investment in the airplane power plant, and a the attrition rate, i.e. the ratio of aircraft lost to aircraft sortied, and it is assumed that half the aircraft are lost before the bomb is dropped, then the delivery efficiency is:

$$N = \frac{1 - a/2}{1 + aZ}$$

Two airplanes having the same delivery efficiency will cause the same amount of target damage per pound of fissionable material expended if possible differences in bombing accuracy between them are neglected. For a chemically fueled airplane $Z = 0$, and the delivery efficiency is $1 - a/2$. The nuclear airplane, with $Z > 0$, must obviously have a lower attrition in order to equal the efficiency of the chemical airplane.

If a is small compared to unity, as it obviously has to be, then the above expression can be simplified, and the airplanes can be compared with sufficient accuracy on the basis of the fissionable material lost for a given number of atomic bombs sortied. On this basis, it can be shown that, in comparison with chemically fueled aircraft, the attrition of nuclear powered aircraft must be of the order of $1/(1 + 2Z)$ for an equal loss of fissionable material. Thus, even for an optimistic case where Z is equal to 2, the attrition of the nuclear powered aircraft must be one-fifth that of the chemically fueled aircraft. This must come about by superior altitude-speed capabilities of the nuclear powered aircraft. The overriding importance of keeping the uranium investment of each reactor to a bare minimum thus becomes apparent. Since the use of twin reactors will increase the uranium investment per airplane, by a factor greater than two, over the single reactor airplane, studies of twin-reactor airplanes have been dropped. Reliance is being placed on the use of standby chemical fuel to provide multiengine reliability, at least at take-off and landing and in the vicinity of the home base.

The three design points considered were rated by WSEG in the following order of decreasing desirability: Mach 0.9 at sea level, Mach 0.9 at 60,000 feet, and Mach 1.5 at 45,000 feet. As mentioned previously, no firm conclusions other than the importance of minimum uranium investment can be derived from this analysis at the present time, since some of the assumptions going into the analysis should be revised. It might also be pointed out that all comparisons with chemically fueled aircraft make the tacit assumption that chemically fueled aircraft will be able to reach all the desired targets from available bases. This will not always hold true. This factor may in itself be of determining importance.

Included in the work for this quarter was a familiarization study of the problems associated with vulnerability. This study resulted in a preliminary report, NEPA 1405-EDR-24, *Vulnerability-Size Relations for Nuclear Powered Aircraft,* issued May 9, 1950. It was not intended that this work should define the vulnerability problem in an absolute sense. The express purpose was threefold:

1) To become familiar with the subject of vulnerability;

2) To attempt to determine what factors are pertinent in vulnerability as applied to nuclear powered aircraft;

3) To determine, if possible, the qualitative effects of vulnerability on the ultimate configuration of the nuclear powered aircraft.

It is not intended actively to pursue the problem of vulnerability further. However, efforts will be made to keep abreast of this problem so that any future developments by other agencies in vulnerability studies, which have bearing on the nuclear powered aircraft design, will not go unnoticed.

• • • • •

9. OPERATIONAL PROBLEMS AND TEST FACILITIES

9.1 FULL SCALE REACTOR TEST STAND (2.25 Man-months)

A preliminary layout of the Phase I test stand facility, showing a tentative disposition of the major items of test equipment and a possible building arrangement, has been completed. This drawing was prepared to furnish a rough idea of the scope of the engineering and design work required, and to serve as a guide for cost and man power estimates.

The facility planning has been based on the compound liquid-metal cycle, because a facility capable of accommodating the requirements of this cycle is expected to present the greatest number of novel and difficult engineering problems. The test stand proper is planned as a modest facility with all possible supporting services located outside the maximum hazard area, some five miles from the test stand. This would reduce the number of operating personnel permanently stationed at the test facility to a minimum.

9.2 FLIGHT TEST SITES (2.25 Man-months)

Though the Snake River Plain adjacent to Arco is considered a possible location for Phase I flight testing, studies are being conducted on other potentially suitable sites, both inland and coastal.

Inland Sites. - Cursory study of potential inland sites indicates that the arid regions of Utah, Nevada, and California between the Sierra Nevada and the Rocky Mountains are well adapted for nuclear flight testing. A broad area approximately 125 miles wide, extending from the Great Salt Lake Desert in Utah to the Mojave Desert in California, appears to be the most suitable within the continental United States, when the special probelms of nuclear powered flight are considered. It is unique geologically in that it is a very large catchment area and has no open drainage to the sea. Further, the area would provide access to Edwards Air Force Base at Muroc, and Wendover Air Force Base in Utah.

The area is sufficiently large to permit turning radii up to 50 miles, and straight runs of 250 to 400 miles. Though it is generally mountainous, there exist a number of dry lake beds and valleys which appear suitable for emergency landing strips. While comprehensive studies of the area have not been made, locating the flight-test-base facilities at either Arco, Muroc Air Force Base, or Wendover Air Force Base appears to be a possibility. Of these, Wendover would possibly be superior in meeting the technical requirements for the air base.

Coastal Sites. - Preliminary studies of coastal areas indicates that three potentially acceptable sites exist, all in the state of Florida. These are the Eglin Air Force Base area, the Banana River area and, southwest of Tallahassee, the Liberty-Franklin Counties area. Of these, the Liberty-Franklin Counties area appears, from preliminary studies, to be the most suitable.

Additional information on these areas is being obtained in order that a sound appraisal of the sites may eventually be made.

The coastal base, as contemplated, would be situated as near the shore line as practicable, and all flight testing would be conducted over water.

• • • • •

10. RADIATION MEDICINE AND BIOLOGY

(1.5 Man-months)

During the quarter, preparations continued for subcontract activity on the radiation medicine and biology tasks proposed by the NEPA Advisory Committee on Radiation Tolerance of Military Personnel (cf. *NEPA Project Quarterly Progress Report,* second quarter, fiscal year 1950). Programs which will be started in the near future include experimental study of physical fitness following total-body irradiation (at both the Naval Radiological Defense Laboratory, sponsored by NEPA, and the University of California at Los Angeles, under a NEPA subcontract), and a program of compiling and publishing data on the biological effects of radiation (at the University of California at Los Angeles). Procedures for these studies have been outlined. In addition to its physical fitness studies, the Naval Radiological Defense Laboratory is proposing an investigation of the long-term effects of ionizing radiations. Quarters and personnel have been obtained for the UCLA work, and sources of equipment and animals for the studies are being investigated.

Having completed its functions of surveying available data on the biological effects of ionizing radiations and recommending specific fields of research, the NEPA Medical Advisory Committee was dissolved during this period. In its place, the NEPA Research Guidance Committee was established to assist in the initiation and prosecution of the proposed tasks. Members of the new medical panel are: Dr. Simeon Cantril; Dr. Andrew Dowdy; Dr. Robley Evans; Dr. W. A. Selle; Dr. Robert Stone; and Colonel John Talbot (USAF liaison). The Research Guidance Committee will hold its first meeting in San Francisco in September 1950.

Further discussions of the effects of radiation on physical fitness were held with Wright-Patterson Air Force Base personnel during the quarter. The possibility of obtaining foreign literature on radiation effects is being investigated. Plans have been made to contact scientists engaged in radiological research in the western zone of Germany, requesting reports of past and current investigations.

A survey was made of equipment and procedures used at Wright-Patterson for quantitative measurement of behavior-decrement under conditions related to flight. It was apparent that similar techniques can be used in NEPA's projected psychomotor studies.

A four-day conference on radiation effects, held in Atlantic City, New Jersey, was attended. Discussions were held with representatives of the AEC, the USAF, the Naval Radiological Defense Laboratory, the Office of Naval Research, the Naval Medical Research Institute, atomic energy projects at the University of Rochester and the University of California, and the AEC national laboratories. Papers presented at the conference showed that marked progress is being made in the field of radiation biology. The need for a satisfactory medium summarizing work in the field was emphasized.

Work in process at the Scripps Metabolic Institute on the prevention of radiation effects by rutin and related pharmacological agents was discussed with institute members during this period. Similar discussions were held with pharmacologists and toxicologists of the University of California's Atomic Energy Project. In additional conferences with UCLA representatives, recent developments in radiation biology and techniques of use in NEPA's research program were outlined.

Information on the physiological stress of aircraft crews was obtained from members of the California Aero Medical Association, and from Dr. Craig Taylor of UCLA, USAF consultant and authority on aviation physiology.

The recent meeting of the Aero Medical Association in Chicago was attended. Papers presented treated quantitative measurements of behavior-decrement under stress related to aircraft flight. Techniques useful in NEPA's studies were described.

Data on radiation effects have been collected in continuing literature surveys. A report is being prepared to summarize available information on the biochemical effects of radiation.

Several members of the NEPA Research Guidance Committee attended a symposium at Oberlin College on "The Basic Aspects of Radiation Effects on Living Systems." Papers were presented.

• • • • •

11. REPORTS ISSUED

RELEVANT NEPA NUMBERED REPORTS ISSUED DURING THE QUARTER
(April, May, June, 1950)

NEPA NO.	TITLE
1363-STR-24	A Diffusion Solution for the Cylindrical Ducting Problem of Infinite Geometry. By D. Whitcombe.
1365-STR-25	A Method for Optimizing an Aircraft Shield. By J. Carnes, W. E. White, and R. L. Echols.
1369-EXR-7	Thermal Stress Tests on Five Per Cent Uranium-Impregnated Graphite. By A. R. Crocker.
1370-SCR-58	Enthalpy, Mean Heat Capacity, and Absolute Heat Capacity of Solid and Liquid Lithium. By A. M. Cabbage.
1371-BRF-4	Monthly Progress Report for April 1950; Bartol Research Foundation. By W. F. G. Swann.
1372-MIT-53	Twenty-second Informal Monthly Report for the Project on "Heat Transfer and Pressure Drop of Air Flowing in Small Tubes"; Massachusetts Institute of Technology. By W. H. McAdams, J. N. Addoms, and C. L. Kroll.
1373-LAC-4	Study of Six Airplanes (In Lieu of Progress Report No. 4, for the Period March 1 - March 31, 1950); Lockheed Aircraft Corporation. By W. M. Hawkins, Jr.
1374-IPR-52	NEPA Project Progress Report for the Period January 1 - March 31, 1950.
1375-CIN-1	Monthly Report of the University of Cincinnati. By J. W. Sausville.
1376-OSU-34	Monthly Progress Report for the Period March 15 to April 15, 1950; Ohio State University. By F. H. McRitchie, and W. J. Wilson.
1377-BW-4	Erosion and Heat Transfer with Liquid Metals, Progress Report No. 4, for the Period March 16 to April 15, 1950; Babcock and Wilcox Company. By H. G. Elrod, Jr., and R. R. Fouse.
1378-FAN-36	Informal Monthly Progress Report for the Period March 10 to April 10, 1950; Fansteel Metallurgical Corporation. By Ralph Wehrmann.

1379-UAC-69	Analytical and Design Investigations of Various Aircraft Power Plants, for the Period March 11 to April 10, 1950; United Aircraft Corporation. By K. K. Klingensmith, and J. P. Grandfield.
1380-UAC-70	Ducting and Header Tests Report for Period March 11 to April 10, 1950; United Aircraft Corporation. By W. G. Kennedy.
1381-CRC-31	Survey of Possible Fluid Hydrogenous Shield Materials and Summary of Work Performed to Date on the Development of Such Materials; California Research Corporation. By R. O. Bolt, J. G. Carroll, F. A. Christiansen, B. A. Fries, J. W. Kent, E. G. Lindstrom, and C. D. Newman.
1382-CRC-32	Monthly Progress Report Covering Period March 10 to April 15, 1950; California Research Corporation. By J. G. Carroll, and F. A. Christiansen.
1383-BAT-41	Apparatus for Modulus of Rupture Determinations at Elevated Temperatures; Battelle Memorial Institute. By C. G. Harman, J. F. Quirk, and E. C. Hoeman.
1384-AOS-27	Report on NEPA Project at A. O. Smith Corporation for Month Ending April 15, 1950. By M. K. Blanchard, C. A. Marcowka, and W. E. Stearns.
1385-UM-24	Progress Report No. 24 on Beryllium-Carbon Equilibria; University of Minnesota. By R. L. Dowdell.
1386-WU-18	Monthly Report on "The Effect of Charged Particles on the Physico-Mechanical Properties of Materials," Covering the Period March 15 to April 15, 1950; Washington University. By W. P. Armstrong.
1387-MHI-22	Informal Progress Report No. 20 for the Period March 16 to April 15, 1950; Metal Hydrides Incorporated. By T. R. P. Gibb, Jr.
1388-BAT-42	Report for the Month of April 1950; Battelle Memorial Institute. By H. W. Russell.
1389-MIC-21	Twenty-first Progress Report on "Development of Apparatus and Methods for Measurement of Creep at Temperatures to 3500°F," Covering Period March 15 to April 14, 1950; University of Michigan. By M. J. Sinnott.
1390-ARM-32	The Mechanical Protection of the Wolfram-Iridium Thermocouple; Armour Research Foundation. By Gary Steven, and W. C. Troy.
1391-MIT-54	Eighth Informal Monthly Report on "Development of Metal-Ceramic Compositions Suitable for Service at Elevated Temperatures," for

	the Period March 1 to March 31, 1950; Massachusetts Institute of Technology. By W. D. Kingery, G. Economos, M. Humenik, Jr., and M. Berg.
1392-NBS-16	Creep Tests on Graphite; National Bureau of Standards. By M. D. Burdick.
1393-EDR-22	Generalized Formulae for the Estimation of a Structural Weight and Deformations of Thin Unswept Supersonic Wings. By R. G. Noel.
1394-NOR-96	Monthly Progress Report for April 1950; Northrop Aircraft, Incorporated. By H. E. Metcalf and L. A. Ohlinger.
1395-WGT-13	Monthly Progress Report for April 1950; Westinghouse Electric Corporation, Aviation Gas Turbine Division. By H. S. Jordan.
1396-EDR-23	Weight Estimation Under Two Loading Conditions of Fuselage Extensions 12 Feet in Diameter up to 150 Feet in Length. By R. Q. Boyles, Jr.
1397-EMR-69	Properties of High-Beryllium-Content Alloys. By Helen Lee.
1398-NOR-97	Utilization of Monte Carlo Techniques for Reactor Problems; Northrop Aircraft, Incorporated. By B. A. Shoor.
1399-ARM-33	Report No. 4 on "Study of Effects of Turbulence Promoters on Heat Transfer"; Armour Research Foundation. By Aaron Shaffer and O. E. Teichmann.
1402-FAN-37	Topical Progress Report on "Coatings on Graphite," Covering Period September 1948 to March 1950; Fansteel Metallurgical Corporation. By Ralph Wehrmann.
1403-FFP-3	Progress Report for March 1950; F. Forrest Pease. By F. Forrest Pease.
1404-FFP-4	Progress Report for April 1950; F. Forrest Pease. By F. Forrest Pease.
1406-EMR-70	The Present Status of the Art of Molybdenum Fabrication. By C. E. Schwartz.
1409-CRC-33	Monthly Progress Report for the Period April 15 to May 15, 1950; California Research Corporation. By R. O. Bolt, J. G. Carroll, and F. A. Christiansen.
1410-BRF-5	Progress Report for May 1950; Bartol Research Foundation. By W. F. G. Swann.

1411-MIT-55	Twenty-third Informal Monthly Report for the Project on "Heat Transfer and Pressure Drop of Air Flowing in Small Tubes," for the Period April 1 to May 1, 1950; Massachusetts Institute of Technology. By W. H. McAdams, J. N. Addoms, and C. L. Kroll.
1412-CIN-2	Progress Report for May 1950; University of Cincinnati. By J. W. Sausville.
1413-BAT-43	Progress Report for May 1950; Battelle Memorial Institute. By H. W. Russell.
1414-ARM-34	Report No. 29 on "The Mechanical Protection of the Wolfram-Iridium Thermocouple"; Armour Research Foundation. By Gary Steven and W. C. Troy.
1415-LAC-5	Progress Report No. 5 Covering Period April 1 to May 1, 1950; Lockheed Aircraft Corporation. By W. M. Hawkins, Jr.
1416-LAC-6	Landing Gear-Airport Relationships for Very Large Aircraft; Lockheed Aircraft Corporation. By W. M. Hawkins, Jr.
1417-WU-19	Monthly Report on "The Effect of Charged Particles on the Physico-Mechanical Properties of Materials," Covering the Period April 16 to May 15, 1950; Washington University. By W. P. Armstrong.
1418-AOS-28	Report on NEPA Project at A. O. Smith Corporation for Month Ending May 15, 1950. By M. K. Blanchard, C. A. Marcowka, and W. E. Stearns.
1419-MHI-23	Informal Monthly Report No. 21 to NEPA, for Period April 16 to May 16, 1950; Metal Hydrides Incorporated. By T. R. P. Gibb, Jr.
1420-UM-25	Progress Report No. 25 on Beryllium-Carbon Equilibria; University of Minnesota. By R. L. Dowdell.
1421-UAC-71	Analytical and Design Investigations of Various Aircraft Power Plants, Report for the Period April 11 to May 10, 1950; United Aircraft Corporation. By K. K. Klingensmith and J. P. Grandfield.
1422-UAC-72	Ducting and Header Tests Report for the Period April 11 to May 10, 1950; United Aircraft Corporation. By W. G. Kennedy.
1423-BW-5	Progress Report No. 5 on "Erosion and Heat Transfer with Liquid Metals," Covering Period April 16 to May 17, 1950; Babcock and Wilcox Company. By W. G. Elrod, Jr., and R. R. Fouse.
1426-MIC-22	Twenty-second Progress Report on "Development of Apparatus and Methods for Measurement of Creep to Temperatures of 3500°F,"

	for the Period April 15 to May 15, 1950; University of Michigan. By M. J. Sinnott and J. C. Johnson.
1427-NBS-17	Creep Tests on Graphite, Report for May 1950; National Bureau of Standards. By R. F. Geller.
1428-FAN-38	Informal Monthly Progress Report for May 1950; Fansteel Metallurgical Corporation. By Alex Bartok and Ralph Wehrmann.
1431-ARM-35	Report No. 5 on "Study of Effects of Turbulence Promoters on Heat Transfer"; Armour Research Foundation. By A. Shaffer and O. E. Teichmann.
1432-WRL-4	Status Letter No. 4, April 1 to May 1, 1950; Westinghouse Research Laboratories. By B. Jennings.
1433-NOR-98	Monthly Progress Report for May 1950; Northrop Aircraft, Incorporated. By L. A. Ohlinger.
1435-MIT-36	Ninth Informal Monthly Report on "Development of Metal-Ceramic Compositions Suitable for Service at Elevated Temperatures"; Massachusetts Institute of Technology. By W. D. Kingery, G. Economos, M. Humenik, Jr., and M. Berg.
1436-WGT-14	NEPA Summary Report; Westinghouse Electric Corporation, Aviation Gas Turbine Division. By C. A. Meyer.
1437-WGT-15	Design of Installation for Operation of Twin 24-C (J-34-WE-30) Engines with External Heat Source; Westinghouse Electric Corporation, Aviation Gas Turbine Division. By E. F. Drewniany.
1438-WGT-16	Engine Model J-34-WE-30 Modified for an External Heat Source-Internal Performance; Westinghouse Electric Corporation, Aviation Gas Turbine Division. By H. S. Jordan.
1440-NOR-99	Summary Report on Monte Carlo Techniques; Northrop Aircraft, Incorporated. By B. A. Shoor.
1441-NOR-100	Summary Report on the Program for Analytical Design Studies of Total and Shadow Shielding for Aircraft; Northrop Aircraft, Incorporated. By B. A. Shoor and J. S. Stewart.
1444	Minutes of the First ANP Liquid Coolants Conference, April 26, 1950.

• • • • •

DO NOT PHOTOSTAT

~~SECRET~~ ~~CONFIDENTIAL~~

NEPA PROJECT PROGRESS REPORT

UNCLASSIFIED

DISTRIBUTION LIST

UNITED STATES AIR FORCE

Major General S. R. Brentnall
Director of Research and Development (MCR)
Air Materiel Command
Wright-Patterson Air Force Base
Dayton, Ohio

Colonel M. C. Demler
Power Plant Laboratory
Engineering Division (MCREXP)
Air Materiel Command
Wright-Patterson Air Force Base
Dayton, Ohio

Colonel J. A. Gibbs
Chief, Aircraft Laboratory
Engineering Division (MCREXA)
Air Materiel Command
Wright-Patterson Air Force Base
Dayton, Ohio

Colonel Walter A. Carlson
Chief, Aero-Medical Laboratory
Engineering Division (MCREXD)
Air Materiel Command
Wright-Patterson Air Force Base
Dayton, Ohio

Lt. Colonel N. C. Appold
Acting Chief, Propulsion Branch
Director of Research and Development (MEN-5)
Office, Deputy Chief of Staff, Materiel
Headquarters, United States Air Force
Washington 25, D. C.

Mr. Robert E. Hage
Weapons Systems Evaluation Group
Office of the Secretary of Defense
Washington 25, D. C.

Mr. D. Z. Beckler
Executive Secretary
R.D.B. Committee on Atomic Energy
Office of the Secretary of Defense
Washington 25, D. C.

Lt. Colonel J. R. Hood, Jr.
AMC Engineering Field Officer
Post Office Box E
Oak Ridge, Tennessee

Major J. L. Steele
AF Plant Representative
NEPA Division
Fairchild Engine and Airplane Corporation
Oak Ridge, Tennessee

Mr. M. R. Whitmore
Materials Laboratory
Engineering Division (MCREXM)
Air Materiel Command
Wright-Patterson Air Force Base
Dayton, Ohio

Mr. J. B. Johnson (MCREXM)
Air Materiel Command
Wright-Patterson Air Force Base
Dayton, Ohio

Mr. R. H. Best, Librarian
RAND Corporation
1500 Fourth Street
Santa Monica, California

MILITARY LIAISON COMMITTEE

Mr. Robert LeBaron, Chairman
Military Liaison Committee
U. S. Atomic Energy Commission
1901 Constitution Avenue
Washington 25, D. C.

UNITED STATES ATOMIC ENERGY COMMISSION

Mr. R. A. Anderson
U. S. Atomic Energy Commission
1901 Constitution Avenue
Washington 25, D. C.

Dr. Kenneth S. Pitzer
Director, Division of Research
U. S. Atomic Energy Commission
1901 Constitution Avenue
Washington 25, D. C.

Mr. Walter J. Williams
U. S. Atomic Energy Commission
1901 Constitution Avenue
Washington 25, D. C.

Dr. L. R. Hafstad
Director, Division of Reactor Development
U. S. Atomic Energy Commission
1901 Constitution Avenue
Washington 25, D. C.

Mr. Robert Williams
Office, Director, Division of Reactor Development
U. S. Atomic Energy Commission
1901 Constitution Avenue
Washington 25, D. C.

Colonel W. S. Barksdale
Office, Director, Division of Reactor Development
U. S. Atomic Energy Commission
1901 Constitution Avenue
Washington 25, D. C.

Captain H. G. Rickover
Office, Director, Division of Reactor Development
U. S. Atomic Energy Commission
1901 Constitution Avenue
Washington 25, D. C.

A. H. Holland, Jr., M. D.
Office, Research and Medicine
Oak Ridge Operations
U. S. Atomic Energy Commission
Oak Ridge, Tennessee

Mr. Stuart Scott
Patent Adviser
U. S. Atomic Energy Commission
Oak Ridge, Tennessee

Document Room
U. S. Atomic Energy Commission
1901 Constitution Avenue
Washington 25, D. C.

United States Atomic Energy Commission
Chicago Operations Office
P. O. Box 6140-A
Chicago 80, Illinois
(Attention: Research Service Division)

United States Atomic Energy Commission
Hanford Operations Office
P. O. Box 550
Richland, Washington
(Attention: Technical Information Library)

Knolls Atomic Power Laboratory
P. O. Box 1072
Schenectady, New York
(Attention: Document Librarian)

United States Atomic Energy Commission
New York Operations Office
P. O. Box 30, Ansonia Station
New York 23, New York
(Attention: Division of Technical Information and Declassification Service)

United States Atomic Energy Commission
Library Branch
Technical Information Division, ORE
Post Office Box E
Oak Ridge, Tennessee

Brookhaven National Laboratory
Information and Publications Division
Documents Section
Upton, New York
(Attention: Mary E. Waisman)

General Electric Company
Metallurgy and Control Division
Technical Information Group
P. O. Box 100
Richland, Washington
(Attention: M. G. Friedank)

Los Alamos Scientific Laboratory
P. O. Box 1663
Los Alamos, New Mexico
(Attention: Document Custodian)

Westinghouse Electric Corporation
Atomic Power Division
P. O. Box 1468
Pittsburgh 30, Pennsylvania
(Attention: Librarian)

NATIONAL ADVISORY COMMITTEE FOR AERONAUTICS

Dr. Hugh L. Dryden (Attention: Dr. A. M. Rothrock)
National Advisory Committee for Aeronautics
1724 F. Street N. W.
Washington 25, D. C.

National Advisory Committee for Aeronautics (2 copies)
Aircraft Engineer Research Laboratory
Cleveland Airport
Cleveland, Ohio
(Attention: Dr. R. F. Selden)

UNITED STATES NAVY

Rear Admiral C. M. Bolster
Assistant Chief for Research and Development
Bureau of Aeronautics
Room 2W 65 Navy Building
Washington 25, D. C.

Rear Admiral T. A. Solberg
Chief of Naval Research
Navy Department
Washington 25, D. C.

OAK RIDGE NATIONAL LABORATORY, OAK RIDGE, TENNESSEE

Dr. A. M. Weinberg
Research Director

Oak Ridge National Laboratory (15 copies)
P. O. Box P
Oak Ridge, Tennessee
(Attention: Central Files)

Technical Advisory Board Reports Office (10 copies)
Carbide and Carbon Chemicals Division (Y-12)
P. O. Box P
Oak Ridge, Tennessee

ARGONNE NATIONAL LABORATORY, CHICAGO, ILLINOIS

Dr. Harold Etherington
Director of the Naval Reactor Division

Argonne National Laboratory
P. O. Box 5207
Chicago 80, Illinois
(Attention: Dr. Hoylande D. Young)

FAIRCHILD ENGINE AND AIRPLANE CORPORATION

Mr. L. B. Richardson
Director of Research
Hagerstown, Maryland

Mr. F. B. Kauffman
Assistant to the General Manager, NEPA Division
1025 Connecticut Avenue N. W.
Washington, D. C.

NEPA PROJECT, OAK RIDGE, TENNESSEE

Mr. Turner A. Sims
General Manager

Dr. Miles C. Leverett
Technical Director

Mr. Charles Wandel
Comptroller

Mr. C. W. Cole
Director, Industrial Relations

Mr. Andrew Kalitinsky
Associate Technical Director

Dr. A. J. Miller
Acting Head, Physics Department

Mr. D. D. Cowen
Head, Technical Information Department

~~SECRET~~ UNCLASSIFIED

~~CONFIDENTIAL~~

CONSULTANTS

Mr. C. F. Bachle
Vice President in Charge of Research
Continental Aviation and Engineering Corporation
12801 East Jefferson Avenue
Detroit 14, Michigan

Mr. Fredric Flader
President and General Manager
Fredric Flader, Incorporated
583 Division Street
North Tonawanda, New York

Mr. B. R. Prentice
Manager, Nucleonics Department
General Electric Company
1 River Road
Schenectady, New York

Mr. H. E. Metcalf
Chief, Nuclear Energy Research
Northrop Aircraft, Incorporated
Hawthorne, California

Mr. F. W. Caldwell
Director of Research
United Aircraft Corporation
400 Main Street
East Hartford 8, Connecticut

Mr. R. P. Kroon
Manager of Engineering
Westinghouse Electric Corporation
Aviation Gas Turbine Division
Lester Branch Post Office
Philadelphia 13, Pennsylvania

Mr. W. G. Lundquist
Chief Engineer
Wright Aeronautical Corporation
Wood-Ridge, New Jersey

Mr. C. H. Wiegman
Chief Engineer
Lycoming Division
AVCO Manufacturing Corporation
Williamsport 38, Pennsylvania

Mr. R. M. Hazen
Director of Engineering
Allison Division
General Motors Corporation
Indianapolis 6, Indiana

Dr. Hans A. Bethe
Laboratory of Nuclear Studies
Cornell University
Ithaca, New York

Mr. Kenneth A. Browne
Research Consultant
Chesapeake & Ohio Railroad
Terminal Tower
Cleveland, Ohio

Dr. Clark Goodman
Physics Department
Massachusetts Institute of Technology
Cambridge, Massachusetts

Dr. Morris Kolodney
Associate Professor of Chemical Engineering
School of Technology
The City College
New York 31, New York

Professor W. H. McAdams
Professor of Chemical Engineering
Massachusetts Institute of Technology
Cambridge, Massachusetts

Professor A. C. G. Mitchell
Physics Department
Indiana University
Bloomington, Indiana

Brookhaven National Laboratory
Information and Publications Division
Document Section
Upton, New York
(Attention: Mary E. Waisman for Dr. Charles P. Baker)

Internal Distribution

NEPA PROJECT, OAK RIDGE, TENNESSEE

Dr. Robert L. Echols

Dr. V. P. Calkins

Mr. J. F. Coneybear

Mr. Mason W. Nesbitt

Mr. Kenneth Miles

Mr. W. B. Seaver

Dr. W. B. Lewis

Dr. R. S. Anderson

Mr. Lyle Martin

Dr. E. R. Mann

Mr. E. S. Bettis

Mr. D. M. Poole

Mr. Walter J. Koshuba

Mr. Richard E. Adams

Mr. Angus N. MacDonald

Mr. P. M. Reyling (4 copies)

Main Library

SECRET

UNCLASSIFIED

RESTRICTED DATA
ATOMIC ENERGY ACT OF 1946
SPECIFIC RESTRICTED DATA CLEARANCE REQUIRED

UNCLASSIFIED

SECRET

45

DTI – EXTENSION INTERNAL CHANGE NOTICE

Date: Sept. 14, 1970

NATURE OF CHANGE:

REPORTS LISTED BELOW has been declassified w/out deletions

☐ ________ has been downgraded to: ________

☐ ________ has been upgraded to: ________

☐ Duplicates, Retain ________ as prime and ________ as secondary.

☐ Report No. correction. Change ________ to ________.

☐ ________ has been recalled.

☐ ________ has been cancelled.

☐ Errata for ________

☐ Other ________

AUTHORITY FOR CHANGE: ANP DOCUMENT REVIEW BY DECLASSIFICATION BR. MAY 1970
COPY OF REVIEW FORM IN MASTER

LOCATION OF RECORDS THAT MAY REQUIRE CHANGE:

Computer Section 1
Card Catalog 8
Descriptive Cataloging
Distribution & Central Services
Microcard Corporation 7*
Systems Control
Science & Technology Branch
INFORMATION SERVICES SECT. 11

INSTRUCTIONS:

1. ☒ Correct IBM accountability and /or availability records, including Holdings List
2. ☐ Make physical change on extra copies.
3. ☐ Distribute TI–FL–14 to ________
4. ☐ Make revised cards
5. ☐ Make revised – errata – negatives. DTIE should – should not – be charged.
6. ☐ Correct –Remove from Computer Files
7. ☒ Destroy ~~(Full size copies)~~ Class. (Micronegative)
8. ☒ Correct catalog cards and /or prepare information cards as required.
9. ☐ Return all copies to: ________
10. ☐ Stop all processing immediately. Return the master and/or all negative copies to Regulation & Appraisal Section.
11. ☒ Other For Info.

APEX-325	C-RD	NEPA-391	C-RD	NEPA-1388	C-RD*
DCL-59-7-42	C-RD	NEPA-663	C-DI	NEPA-1429	C-RD
DCL-59-7-63	C-RD	NEPA-823	S-RD	NEPA-1436	C
DCL-59-7-214	C-RD	NEPA-916	S-RD*	NEPA-1444	C-DI
DCL-59-8-1	C-RD	NEPA-920	C *	NEPA-1458	C-DI
DCL-59-8-176	C-RD*	NEPA-921	C	NEPA-1475	C-DI
DCL-59-9-32	C-RD	NEPA-969	C-RD*	NEPA-1478	C-DI
DCL-59-9-61	C-RD	NEPA-977	C-RD	NEPA-1484	C-RD
NDA-57-24	S-RD*	NEPA-981	C-RD*	NEPA-1501	C-DI*
NDA-57-38	S-RD*	NEPA-998	C-RD*	NEPA-1502	C-DI
NDA-73-4	S-RD*	NEPA-1034	C *	NEPA-1574	C-DI
NDA-2057-4-3	S-RD*	NEPA-1264(Supp.4)	S-RD	NEPA-1583	C-RD
NDA-2092-7	S-RD*	NEPA-1264(Supp.5)	S-RD	NEPA-1608	C-DI
NEPA-147	C	NEPA-1264(Supp.6)	S-RD	NEPA-1646	C-RD
NEPA-389	S-RD	NEPA-1365	S-RD*	NEPA-1653	S-RD*

NEPA 1484
(Report Number)

ANP CLASSIFICATION REVIEW FORM

Report Title: ______________________

____

Author: ______________________

Please indicate in square below classification determination

/__/ Classification confirmed as ______________________

in accordance with CG-RAN-4 topic __________ __________

/__/ Classification downgraded to ______________________

in accordance with CG-RAN-4 topic __________ __________

/__/ Declassification is contingent on (Explain)

____

____

____

/✓/ Contains no Restricted Data nor other Defense Information

and may be declassified in accordance with CG-RAN-4 Guide

Topic 5.1.1 ~~OK.~~

HRG

J. K. Dicker
Signature

May 5, 1970
Date